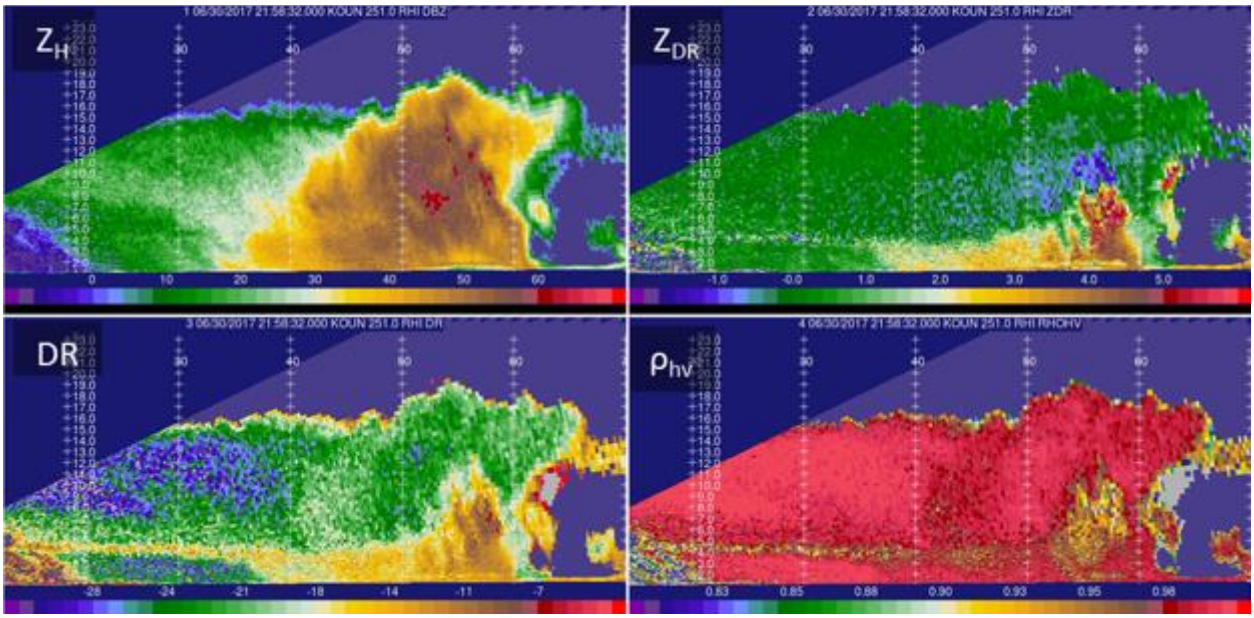

Cooperative Institute for Mesoscale Meteorological Studies

Annual Report

Prepared for the
National Oceanic and Atmospheric Administration
Office of Oceanic and Atmospheric Research

Cooperative Agreement NA11OAR4320072

Fiscal Year – 2017

Cover image – *Z_H, Z_{DR}, Depolarization Ratio (DR), and ρ_{hv} from a high-resolution RHI collected by KOUN on the afternoon of 30 June 2017. A deep Z_{DR} column is seen extending to ~8 km AGL, above which a ~2-3 km deep region of negative Z_{DR} (as low as approximately -2 dB). Associated with these Z_{DR} features is reduced ρ_{hv}, and the combined influences of ρ_{hv} and Z_{DR} led to a prominent DR column. For more on this project, "Identifying Characteristics of Hail Growth Aloft", involving Jeffrey Snyder (CIMMS at NSSL), see pages 46-47.*

Table of Contents

COOPERATIVE INSTITUTE FOR MESOSCALE METEOROLOGICAL STUDIES
THE UNIVERSITY OF OKLAHOMA

Annual Report of Research Progress Under
Cooperative Agreement NA11OAR4320072
During the 2017 Fiscal Year: July 1, 2016-June 30, 2017

Randy A. Peppler, Interim Director
Tracy L. Reinke, Executive Director of Finance and Operations
Sebastian Torres, Assistant Director for NOAA Relations

INTRODUCTION

General Description of CIMMS and its Core Activities

The Cooperative Institute for Mesoscale Meteorological Studies (CIMMS) was established in 1978 as a cooperative program between the National Oceanic and Atmospheric Administration (NOAA) and The University of Oklahoma (OU). CIMMS provides a mechanism to link the scientific and technical resources of OU and NOAA to create a center of research excellence in weather radar, stormscale meteorological phenomena, regional climate variations, and related subject areas – all with the goal of helping to produce better forecasts and warnings that save lives and protect property.

CIMMS promotes cooperation and collaboration on problems of mutual interest among university researchers and the NOAA Office of Oceanic and Atmospheric Research (OAR) National Severe Storms Laboratory (NSSL), National Weather Service (NWS) Radar Operations Center (ROC) for the WSR-88D (NEXRAD) Program, NWS NCEP (National Centers for Environmental Prediction) Storm Prediction Center (SPC), NWS Warning Decision Training Division (WDTD), NWS Norman Forecast Office (OUN), NWS Training Center (NWSTC) in Kansas City, Missouri, NOAA Air Resources Laboratory's Atmospheric Turbulence and Diffusion Division (ATDD) in Oak Ridge, Tennessee.

CIMMS research contributes to the NOAA mission through improvement of the observation, analysis, understanding, and prediction of weather elements and systems and climate anomalies ranging in size from cloud nuclei to multi-state areas. Advances in observational and analytical techniques lead to improvements in understanding of the evolution and structure of these phenomena. Understanding provides the foundation for more accurate prediction of hazardous weather and anomalous regional climate. Better prediction contributes to improved social and economic welfare. Because small-, meso-, and regional-scale phenomena are also important causes and manifestations of climate, CIMMS research is contributing to improved understanding of the global climate system and regional climate variability and change. CIMMS promotes research collaboration between scientists at OU and NOAA by providing a center where government and academic scientists may work together to learn about and apply their knowledge of stormscale weather and regional-scale climate processes.

CIMMS is part of the National Weather Center, a unique confederation of federal, state, and OU organizations that work together in partnership to improve understanding of the Earth's atmosphere. Recognized for its collective expertise in severe weather, many of the research and development activities of the Center have served society by improving weather observing and forecasting, and thus have contributed to reductions in loss of life and property.

In addition to CIMMS, National Weather Center organizations include:

- NOAA OAR National Severe Storms Laboratory (NSSL)
- NOAA NWS Warning Decision Training Division (WDTD)
- NOAA NWS NCEP Storm Prediction Center (SPC)
- NOAA NWS Radar Operations Center (ROC)
- NOAA NWS Norman Forecast Office (OUN)
- Oklahoma Climatological Survey (OCS)
- OU Center for Analysis and Prediction of Storms (CAPS)
- OU Advanced Radar Research Center (ARRC)
- OU College of Atmospheric and Geographic Sciences
- OU School of Meteorology
- OU Department of Geography and Environmental Sustainability

CIMMS concentrates its research and outreach efforts and resources on the following principal themes: (1) weather radar research and development, (2) stormscale and mesoscale modeling research and development, (3) forecast and warning improvements research and development, (4) impacts of climate change related to extreme weather events, and (5) societal and socioeconomic impacts of high impact weather systems.

This report describes NOAA-funded research and outreach progress made by CIMMS scientists at OU and those assigned to our collaborating NOAA units under cooperative agreement NA11OAR4320072 during 1 July 2016 through 30 June 2017. Publications written, awards received, and employee and funding statistics are presented in Appendices.

Management of CIMMS, including Mission and Vision Statements, and Organizational Structure

An Executive Board and Council of Fellows help advise CIMMS.

The CIMMS Executive Board is to meet quarterly to provide advice and recommendations to the Director of CIMMS regarding appointments, procedures, and policies; to review and adopt bylaws; and to periodically review the accomplishments and progress of the technical and scientific programs and projects of the CIMMS.

The Council of Fellows meets as needed and is composed of a cross-section of local and national scientists who have expertise relevant to the research themes of CIMMS and are actively involved in the programs and projects of CIMMS. Appointment as a Fellow, by the CIMMS Executive Board, is normally for a two-year term, and reappointment is possible. Appointments may be made for a shorter period of time or on a part-time basis with the concurrence of the appointee and the CIMMS Executive Board. Fellows will review and suggest modifications of bylaws, participate in reviews of CIMMS activities, and elect two of their number to serve on the Executive Board. The Executive Board appoints Fellows.

The Mission and Vision Statements of CIMMS are as follows:

Mission *– To promote collaborative research among University and NOAA scientists on problems of mutual interest to improve basic understanding and to help produce better forecasts and warnings that save lives and property*

Vision *– A center of research excellence in mesoscale meteorology and related topics, fostering vibrant University-NOAA collaborations*

The organizational structure of CIMMS during FY17 included: Interim Director (Randy Peppler), Executive Director of Finance and Operations Director (Tracy Reinke), Assistant Director for NOAA Relations (Sebastian Torres), Account and Budget Representative (Jamie Foucher), and Staff Assistant (Tanya Riley). Scientists, students, and post-docs are housed on the OU campus in its National Weather Center (NWC), at the NWSTC in Kansas City, and at ATDD in Oak Ridge. Some CIMMS undergraduate students have duty stations off-campus at ROC in Norman.

Executive Summary Listing of Activities during FY2017

Theme 1 – Weather Radar Research and Development

At the very center of NOAA's mission are the objectives of achieving a "reduced loss of life, property, and disruption from high-impact weather events", "improved transportation efficiency and safety", and "improved freshwater resource management" (*NOAA' s Next Generation Strategic Plan,* Long-Term Goal: Weather Ready Nation, pp. 10-14*,* December 2010). The weather systems involved include severe thunderstorms, tornadoes, tropical storms and hurricanes, and winter cyclones. Those systems produce the high intensity precipitation, strong winds, flooding, lightning strikes, freezing rain, and large snow accumulations that damage property, cost lives, disrupt transportation, and cause other economic dislocation. Reduction of these adverse impacts can result from the availability and use of accurate forecasts of the above weather systems and their associated phenomena, for future periods ranging from several days down to a few minutes. One of the essential starting points for developing those forecasts is the detailed observation of the present state of the atmosphere.

For almost 60 years, remote sensing via weather radar has been a vital source of the necessary observations. The present national weather radar system (WSR-88D) uses reflectivity and Doppler velocity measurements to document the location and movement of the above weather systems, and indicate the time evolution of their precipitation intensity and wind strength. However, this radar system soon will be as old (30 years) as the chronologically and technologically ancient system (WSR-57) that it replaced in 1988. This situation has two crucial implications for NOAA's continued pursuit of its above objectives to achieve a "reduced loss of life, property, and disruption from high impact weather events", "improved transportation efficiency and safety", and "improved freshwater management". First, NOAA and its partners must complete the recently initiated development of the new Multi-Function Phased Array Radar (MPAR) system that will replace the WSR-88D and is incorporating all relevant technological advances during the last 20+ years. Second, since completion of this development activity will require another 7-12 years at its current rate of progression, the ongoing current WSR-88D upgrades (especially Dual-Polarization) must be brought to fruition as soon as possible.

During the past year, research was conducted on:

- ***NSSL Project 1 – Advancements in Weather Radar***
  - WSR-88D Improvements
  - Dual-Polarization
  - MPAR Meteorology
  - MPAR Engineering

- ***CIMMS Task III Projects***
  - ARRC R&D Activities for the Multi-Mission Phased Array Radar Program
  - Polarimetric Phased Array Radar Research in Support of MPAR Strategy

Theme 2 – Stormscale and Mesoscale Modeling Research and Development

Research and development for stormscale and mesoscale modeling are essential for NOAA's aforementioned objectives. Use of stormscale and mesoscale models is a major ingredient of the forecasting and nowcasting procedures for high impact weather events, and is expected to grow in the future. The initialization of those prediction models is depending increasingly on wind and other observations from the current weather radar systems. This dependence also is anticipated to expand and therefore is a principal motivation for the weather radar research and development proposed above -- to improve the initialization and hence performance of the prediction models. At the center of this radar-modeling interface is the manner in which radar data are ingested into the models, especially in combination with measurements from other platforms (e.g., satellite, rawinsonde, surface) via "assimilation" procedures. In addition to their predictive roles, stormscale and mesoscale models also are used extensively in a research mode to understand better the behavior of weather systems on those scales. The atmospheric processes that receive particular attention in these simulations include mesoscale dynamics, convective initiation, cloud dynamics and microphysics, and the

precipitation process. Also investigated is the sensitivity of the simulation results to the data assimilation procedures. The ultimate goal of such stormscale and mesoscale simulation research is to improve the performance of the operational forecasting models.

During the past year, research was conducted on:

- ***NSSL Project 7 – Synoptic, Mesoscale and Stormscale Processes Associated with Hazardous Weather***

- ***CIMMS Task III Projects***
    - Lightning Mapper Array Operation in Oklahoma to Aid in Preparation for GOES-R GLM

Theme 3 – Forecast and Warning Improvements Research and Development

It is under this theme that the results of the research and development from the two preceding themes are integrated and converted into improved weather forecasts and warnings disseminated to the U.S. public. The ultimate outcome is to provide NWS forecasters routinely with enhanced information on which to base their forecasts. Two areas of highly innovative activity, anchored within the Hazardous Weather Testbed (HWT), dominate this effort – the Experimental Forecasting Program and the Experimental Warning Program. Activity within this theme also is dominated by the training activities of CIMMS scientists at the Warning Decision Training Branch.

During the past year, research and training were conducted on:

- ***NSSL Project 5 – Hazardous Weather Testbed***

- ***SPC Project 11 – Advancing Science to Improve Knowledge of Mesoscale Hazardous Weather***

- ***NWSTC Project 14 – Forecast Systems Optimization and Decision Support Services Research Simulation and Training***

- ***CIMMS Task III Projects***
    - The GOES-R GLM Lightning Jump Algorithm: A National Field Test for Operational Readiness
    - National Sea Grant Weather & Climate Extension Specialist Activities
    - Prototyping and Evaluating Key Network-of-Networks Technologies

Theme 4 – Impacts of Climate Change Related to Extreme Weather Events

Here, we are concerned with the regional and global climate system context of mesoscale and stormscale weather variability, and especially the functioning of what now is termed the weather-climate interface. The genesis and trends of extreme events

are of particular interest, given society's current concerns about climate maintenance and change. The optimum path forward will require an appropriate combination of observational (using fine resolution data) and modeling (emphasizing convection) research. This theme also addresses the NOAA objective of achieving "improved scientific understanding of the changing climate system and its impacts" and "assessments of current and future states of the climate system that identify potential impacts and inform science, services, and stewardship decisions" (*NOAA's Next Generation Strategic Plan*, Long-Term Goal: Climate Adaptation and Mitigation, pp. 5-10, December 2010).

During the past year, research and outreach were conducted on:

- ***CIMMS Task III Project***
    - The Assimilation, Analysis, and Dissemination of Pacific Rain Gauge Data (PACRAIN)

Theme 5 – Societal and Socioeconomic Impacts of High Impact Weather Systems

This theme contributes to several of NOAA's objectives - - providing "mitigation and adaptation choices supported by sustained, reliable, and timely climate services"; achieving "a climate-literate public that understands its vulnerabilities to a changing climate and makes informed decisions"; and furnishing "services meeting the evolving demands of regional stakeholders" (*NOAA's Next-Generation Strategic Plan,* Long-Term Goal: Climate Adaptation and Mitigation, pp. 5-10, December 2010). Much of the effort here is motivated and fed by results obtained under the Forecast and Warning Improvements and Extreme Weather-Climate Change Impacts themes that, in turn, are built around the core of the more basic Weather Radar and Stormscale/Mesoscale Modeling Research and Development. The goal here is to facilitate the mitigation (enhancement) of the adverse (beneficial) social and socioeconomic impacts of high-impact weather systems and regional/seasonal-scale climate variations. Thus, our contributions to this theme are part of NOAA's crucial ultimate interface with society, and therefore will reflect the continuing and increasing involvement of OU social scientists.

During the past year, research and outreach were conducted on:

- ***NSSL Project 8 – Warning Process Evolution and Effective Communication to the Public***

- ***NSSL Project 9 – Evaluating the Impact of New Technologies, Data, and Information in the Operational Forecasting Environment***

- ***CIMMS Task III Projects***
    - Collaborative Research: Understanding the Current Flow of Weather Information and Associated Uncertainty, and Their Effect on Emergency Managers and the General Public

- Implementation of a Drought App for Mobile Devices
- Drought Risk Management for the United States

Public Affairs and Outreach

CIMMS education and outreach activities help NOAA achieve its objectives of providing "an engaged and educated public with an improved capacity to make scientifically informed environmental decisions" and making "full and effective use of international partnerships and policy leadership to achieve NOAA's mission objectives" (*NOAA's Next Generation Strategic Plan*, Engagement Enterprise Objective, pp. 30-32, December 2010). CIMMS location and role within the OU-NOAA National Weather Center (NWC) has embedded it within a wide-ranging and ongoing set of education and outreach activities that will draw continuously on the knowledge developed within the five above research themes. Those activities (a) involve local and national outreach to the general public, (b) extend across all levels of formal education, and (c) provide post-doctoral and professional development opportunities for individuals in careers related to the atmospheric sciences.

During the past year, public affairs and outreach activities included:

- NOAA Partners Communications, Public Affairs, and Outreach

Awards and Honors

See Appendix A.

Distribution of NOAA Funding by CIMMS Task and Research Theme

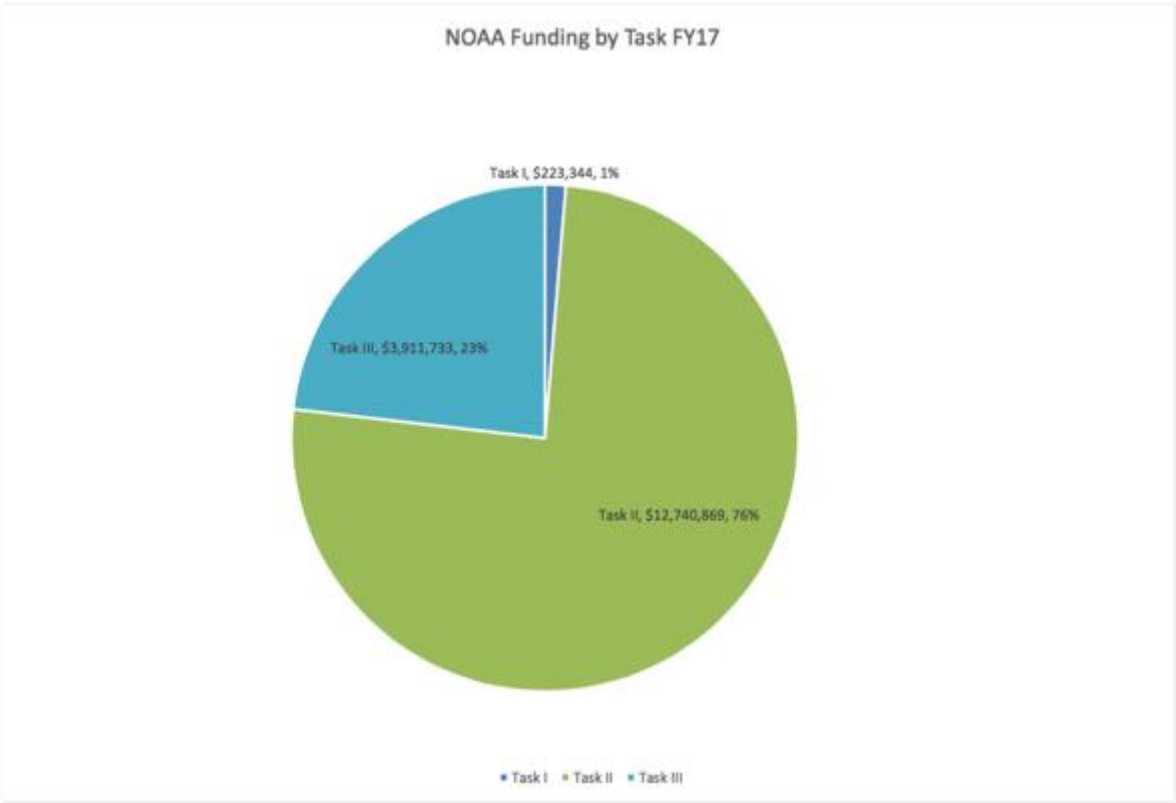

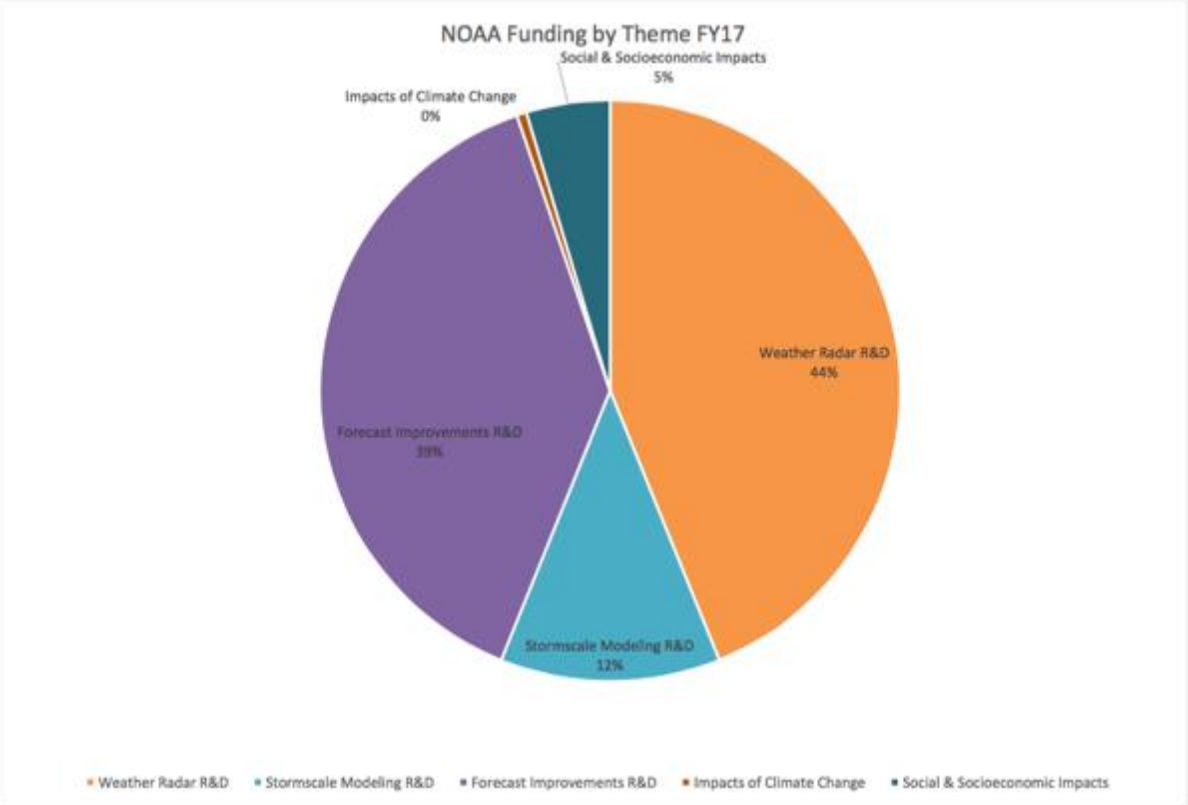

CIMMS Executive Board and Council of Fellows Meeting Dates and Membership

Executive Board meetings were held on September 12, 2016 and April 27, 2017. Membership was as follows:

- Dr. Randy Peppler (Chair), Interim Director, CIMMS, and Lecturer, Department of Geography and Environmental Sustainability, OU
- Dr. Robert Palmer, Associate Vice President for Research, Executive Director, ARRC, and Professor and Tommy C. Craighead Chair, School of Meteorology, OU (Provost designated)
- Dr. Carol Silva, Director, CRCM, and Associate Professor of Political Science, OU (Provost designated)
- Dr. Kirsten de Beurs, Chair and Associate Professor, Department of Geography and Environmental Sustainability, OU (Provost designated)
- Mr. Lans Rothfusz, Deputy Director, NSSL (OAR designated)
- Dr. Jack Kain, Chief, Forecast Research and Development Division, NSSL (OAR designated)
- Mr. Richard Murnan, Radar Operations Center Applications Branch (NWS designated)
- Dr. Steven Weiss, Chief, Science Support Branch, SPC (NWS designated)
- Dr. Boon Leng Cheong, Research Scientist, ARRC (Elected from Assembly of Fellows)
- Dr. David Turner, Research Meteorologist, NSSL (Elected from Assembly of Fellows)
- Dr. Ming Xue, Director, CAPS (Elected from Assembly of Fellows in spring 2017 to replace David Turner)
- Mr. David Andra, Meteorologist-in-Charge, Norman NWS WFO (*ex-officio* member)
- Dr. Steven Koch, Director, NSSL (*ex-officio* member)
- Mr. Ed Mahoney, Director, WDTD (*ex-officio* member)
- Dr. Russell Schneider, Director, SPC (*ex-officio* member)
- Mr. Terry Clark, Director, ROC (*ex-officio* member)
- Mr. John Ogren, Director, NWSTC, and Chief Learning Officer, NWS (*ex-officio* member)
- Dr. David Parsons, Chair, OU School of Meteorology, Associate Director, CAPS, and Mark and Kandi McCasland Professor of Meteorology (*ex-officio* member)
- Dr. Berrien Moore, Dean, OU College of Atmospheric and Geographic Sciences, OU Vice President, Weather & Climate Programs, School of Meteorology Chesapeake Energy Corporation Chair in Climate Studies, and Director, National Weather Center (*ex-officio* member)

No Council of Fellows meetings took place during the fiscal year. Membership was as follows:

- Dr. Jeffrey B. Basara, Associate Professor of Meteorology, OU
- Dr. Michael I. Biggerstaff, Professor of Meteorology, OU
- Dr. Howard B. Bluestein, George Lynn Cross Research Professor of Meteorology, OU
- Dr. Keith Brewster, Senior Scientist and Associate Director, CAPS, OU
- Dr. Harold E. Brooks, Research Meteorologist and Team Leader, Mesoscale Applications Group, NSSL, and Adjunct Professor of Meteorology, OU
- Dr. Frederick H. Carr, Professor of Meteorology OU
- Dr. Steven Cavallo, Assistant Professor of Meteorology, OU
- Dr. Boon Leng Cheong, Research Scientist, ARRC, OU
- Dr. Phillip Chilson, Professor of Meteorology, OU
- Dr. Adam J. Clark, Research Meteorologist, NSSL
- Mr. Terrence Clark, Director, ROC
- Dr. Michael Coniglio, Research Scientist, NSSL
- Dr. Kirsten de Beurs, Chair and Associate Professor of Geography and Environmental Sustainability, OU
- Dr. Michael W. Douglas, Retired Research Scientist, NSSL
- Dr. Richard J. Doviak, Senior Engineer, Doppler Radar and Remote Sensing Research Group, NSSL, and Affiliate Professor of Meteorology and of Electrical and Computer Engineering, OU
- Dr. Kelvin K. Droegemeier, Vice President for Research and Regents' Professor, OU
- Dr. Claude E. Duchon, Emeritus Professor of Meteorology, OU
- Dr. Chris Fiebrich, Associate Director, OCS
- Dr. Jack Friedman, Research Scientist, CASR, OU

- Dr. Caleb Fulton, Assistant Professor of Electrical and Computer Engineering, OU
- Dr. Jidong Gao, Research Scientist, NSSL
- Dr. Nathan Goodman, Associate Professor of Electrical and Computer Engineering, and Director of Research, ARRC, OU
- Dr. J.J. Gourley, Research Scientist, NSSL
- Dr. Pamela Heinselman, Research Scientist, NSSL
- Mr. Kurt Hondl, Research Meteorologist, NSSL
- Dr. Yang Hong, Associate Professor of Civil Engineering and Environmental Sciences, OU
- Mr. Ken Howard, Research Meteorologist, NSSL
- Mr. Michael Jain, Acting Chief, Radar Research & Development Division, NSSL
- Dr. Hank Jenkins-Smith, Associate Director, CASR, and Professor of Political Science, OU
- Dr. Israel Jirak, Science and Operations Officer, SPC
- Dr. David P. Jorgensen, Chief, Warning Research & Development Division, NSSL
- Dr. Jack Kain, Chief, Forecasting Research & Development Division, NSSL
- Dr. Petra Klein, E. K. Gaylord Presidential Professor and Associate Professor of Meteorology, OU
- Dr. James F. Kimpel, Director, Emeritus NSSL, and Emeritus Professor of Meteorology, OU
- Dr. Kevin Kloesel, Director, OCS, and Associate Professor of Meteorology, OU
- Dr. Steven Koch, Director, NSSL
- Dr. Fanyou Kong, Research Scientist, CAPS, OU
- Dr. Daphne LaDue, Research Scientist, CAPS, OU
- Dr. S. Lakshmivarahan, George Lynn Cross Research Professor of Computer Science, OU
- Dr. Lance M. Leslie, Robert E. Lowry Chair and George Lynn Cross Professor of Meteorology, OU
- Dr. Donald R. MacGorman, Research Physicist, Convective Weather Research Group, NSSL, and Affiliate Professor of Meteorology and of Physics and Astronomy, OU
- Mr. Ed Mahoney, Chief, WDTD
- Dr. Edward Mansell, Research Scientist, NSSL
- Dr. Patrick Marsh, Techniques Development Meteorologist, SPC
- Dr. Elinor Martin, Assistant Professor of Meteorology, OU
- Dr. Amy McGovern, Associate Professor of Computer Science, OU
- Dr. Renee McPherson, Director of Research, South Central Climate Science Center, and Associate Professor of Geography and Environmental Sustainability, OU
- Dr. Berrien Moore III, Vice President for Weather and Climate Programs, Dean, College of Atmospheric and Geographic Sciences, Director, National Weather Center, and Chesapeake Professor of Meteorology, OU
- Dr. Mark L. Morrissey, Professor of Meteorology, OU
- Mr. Richard Murnan, Radar Meteorologist, ROC
- Mr. John Ogren, Chief Learning Officer, NWS
- Dr. Robert D. Palmer, Associate Vice President for Research, Executive Director, ARRC, and Tommy Craighead Chair and Professor of Meteorology, and OU
- Dr. David Parsons, Director, School of Meteorology, Mark and Kandi McCasland Professor of Meteorology, OU
- Dr. Robert Rabin, Research Scientist, NSSL
- Dr. Michael B. Richman, E. K. Gaylord Presidential Professor of Meteorology, OU
- Mr. Lans Rothfusz, Deputy Director, NSSL
- Dr. Jessica Ruyle, Assistant Professor of Electrical and Computer Engineering, OU
- Dr. Jorge Salazar-Cerreno, Assistant Professor of Electrical and Computer Engineering, OU
- Dr. Russell Schneider, Director, SPC
- Dr. Mark Shafer, Director of Climate Services, OCS, and Assistant Professor of Geography and Environmental Sustainability, OU
- Dr. Alan M. Shapiro, American Airlines Professor and President's Associates Presidential Professor of Meteorology, OU
- Dr. Hjalti Sigmarsson, Assistant Professor of Electrical and Computer Engineering, OU
- Dr. Carol Silva, Director, CRCM, and Professor of Political Science, OU
- Dr. Paul Spicer, Professor of Anthropology, OU
- Dr. Jerry M. Straka, Professor of Meteorology, OU
- Dr. Aondover A. Tarhule, Associate Dean, College of Atmospheric and Geographic Sciences, and Associate Professor, Department of Geography and Environmental Sustainability, OU
- Dr. David Turner, Research Scientist, Global Systems Division, ESRL
- Dr. Xuguang Wang, Associate Professor of Meteorology, and Presidential Research Professor, OU
- Mr. Steven J. Weiss, Chief, Science Support Branch, SPC

- Dr. Louis J. Wicker, Research Meteorologist, Convective Weather Research Group, NSSL, and Affiliate Associate Professor of Meteorology, OU
- Dr. Qin Xu, Research Meteorologist, Models and Assimilation Team, NSSL, and Affiliate Professor of Meteorology, OU
- Dr. Ming Xue, Director, CAPS, and Professor of Meteorology, OU
- Dr. Mark Yeary, Professor of Electrical and Computer Engineering, OU
- Dr. Tian-You Yu, Director of Operations, ARRC, and Professor of Electrical and Computer Engineering, OU
- Dr. Guifu Zhang, Professor of Meteorology, OU
- Dr. Jian Zhang, Research Hydrometeorologist, NSSL
- Dr. Yan Zhang, Associate Professor of Electrical and Computer Engineering, OU
- Dr. Conrad Ziegler, Research Meteorologist, Models and Assimilation Team, NSSL
- Dr. Dusan S. Zrnic, Senior Engineer and Group Leader, Doppler Radar and Remote Sensing Research Group, NSSL, and Affiliate Professor of Meteorology and of Electrical and Computer Engineering, OU

General Description of Task I Expenditures

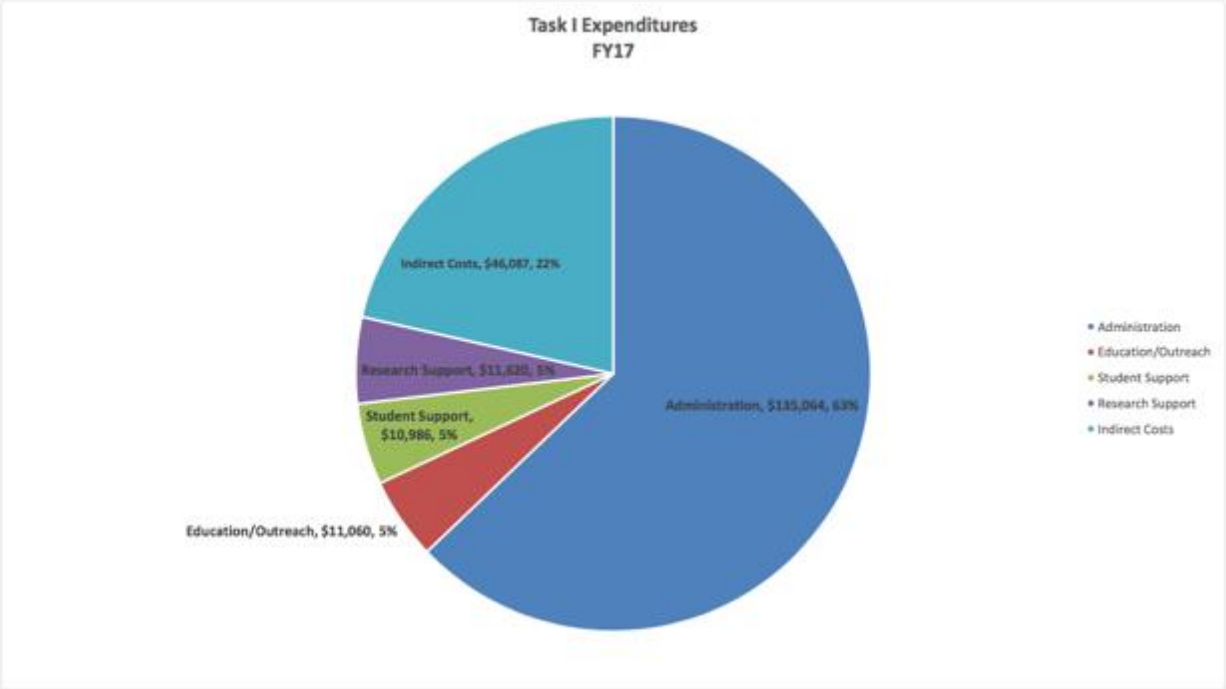

RESEARCH PERFORMANCE

Theme 1 – Weather Radar Research and Development

NSSL Project 1 – Advancements in Weather Radar

NOAA Technical Lead: Michael Jain (NSSL)

NOAA Strategic Goal 2 – *Weather-Ready Nation – Society is Prepared for and Responds to Weather-Related Events*

Funding Type: CIMMS Task II

1. WSR-88D Improvements

Overall Objectives
Conduct research and development to provide improvements to the NWS operational radar (WSR-88D). This research explores ways to improve the detection of hazardous weather and improve the weather radar data quality.

Accomplishments

a. Ground Clutter Mitigation – CLEAN-AP^{TM}/WET

David Warde, Sebastián Torres, David Schvartzman, and Christopher Curtis (CIMMS at NSSL)

A common dilemma in obtaining good-quality meteorological-variable estimates using Doppler weather radar is the application (or misapplication) of ground clutter filters (GCF) to mitigate contamination from ground returns. Typically, weather radars use static clutter maps (i.e., pre-identified clutter contaminated regions) to control the application of the GCF. Ideally, the GCF should only be applied if the ground clutter contamination obscures the weather estimate. However, the problem of applying the GCF becomes very complex considering the dynamic atmospheric effects on radar beam propagation. The goal of this project is to develop efficient techniques that provide both automated detection and application of ground clutter filtering. The Clutter Environment Analysis using Adaptive Processing (CLEAN-AP^{TM}) filter is a spectral technique for automatic detection and mitigation of ground clutter contamination developed by CIMMS personnel. We had previously shown the clutter detection and mitigation performance of the CLEAN-AP^{TM} filter using time-series data from the national network of weather surveillance radars (WSR-88D), the dual-polarized (DP) KOUN and OU Prime radars, and the NWRT PAR.

From FY2012–FY2016, we have optimized, completed performance analysis, and delivered algorithmic descriptions of the CLEAN-AP^{TM} filter for uniform and Staggered PRT implementation into the WSR-88D signal processing chain. We have also

developed the Weather Environment Thresholding (WET) algorithm to identify weather signals, which reduces the ambiguity between low velocity weather signals and ground clutter. The WET algorithm when combined with CLEAN-AP™ was shown to enhance the ground clutter mitigation capability for a snow event where current NEXRAD WSR-88D ground clutter mitigation techniques had failed. We have successfully transferred the CLEAN-AP™ technique to the UK Met Office (UK Met/NSSL MOU) and to a commercial weather radar company (OU licensing to Baron Services). Compared to current technologies used for ground clutter mitigation, the CLEAN-AP™/WET algorithms provide a real-time, integrated clutter mitigation solution with: (a) improved ground clutter suppression, (b) effective ground clutter detection, and (c) dynamic ground clutter suppression characteristics optimally matched to the existing atmospheric environment.

In FY17, we made improvements to the CLEAN-AP™ filter, which allows robust clutter suppression levels for a wide range of weather signal levels. We implemented the filter in the SZ-2 algorithm and analyzed its performance in our offline DSP that includes provisions to process weather signals from multiple radar platforms. We started investigating the use of additional spectral windows and multitaper spectral estimation to improve the variance of estimates. We provided updates to the CLEAN-AP™ filter description by incorporating improvements and integrated WET for expanded ground clutter mitigation with uniform, staggered PRT, and SZ-2 processing modes. We continue to support Radar Operation Center engineers on the implementation, integration, and testing of CLEAN-AP™ in the Staggered PRT (SPRT) processing mode. We are evaluating the merged CLEAN-AP™/WET algorithms for inclusion in the WSR-88D uniform and SZ-2 processing modes. We continue collaboration with the UK Met Office under the UK Met/NSSL MOU and have recently transferred the WET algorithm. We are assisting in a performance evaluation of CLEAN-AP™/WET for inclusion on the UK Met network of weather radars.

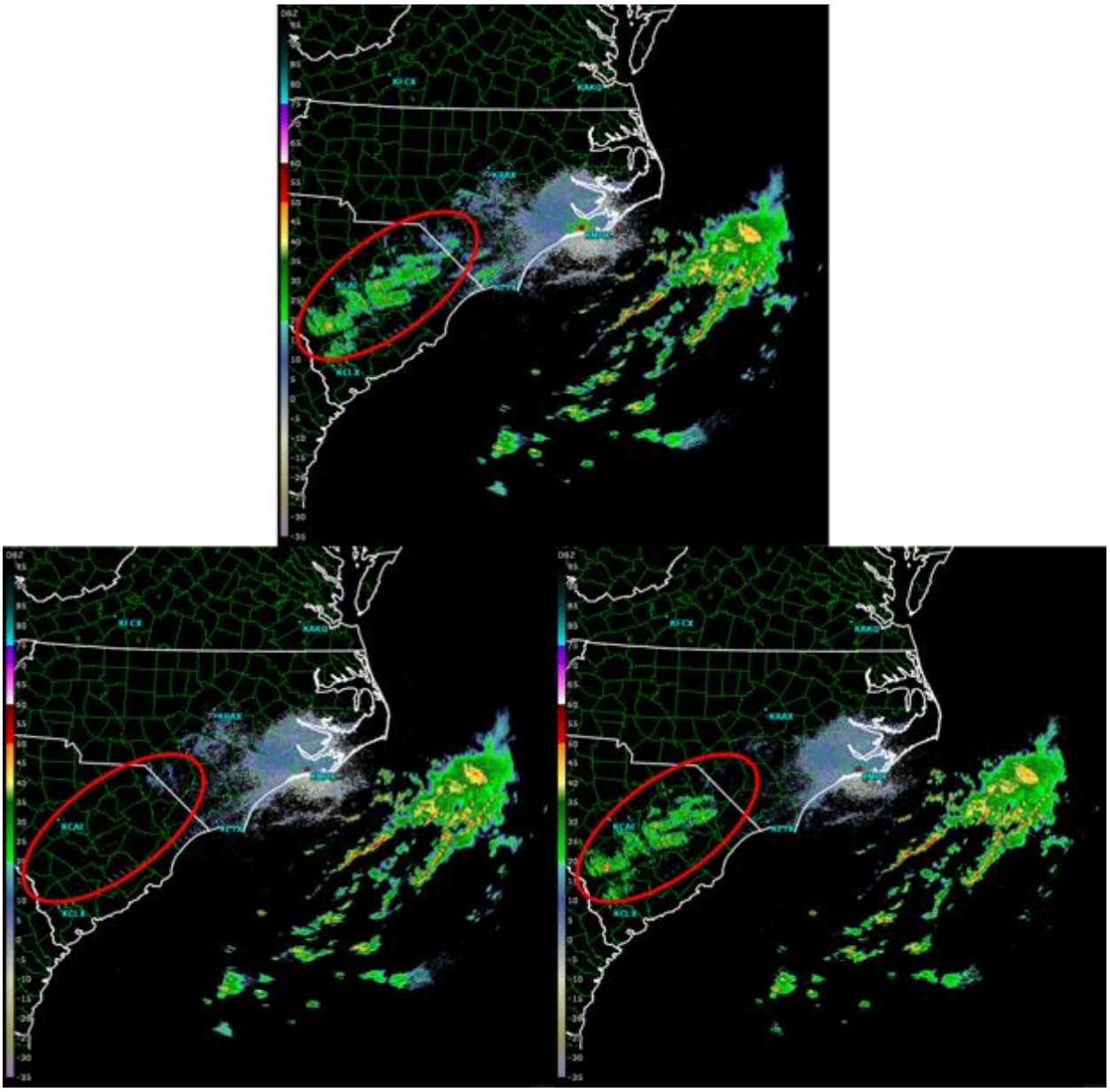

Example of unfiltered (top, from reprocessed level I), CLEAN-AP™/WET filtered (bottom-left, from reprocessed level I) and current WSR-88D filtered (bottom-right, NCDC level II) reflectivity from data collected on the WSR-88D operational radar (KMHX). Red oval shows a region of ground clutter from anomalous propagation that is properly removed by application of the CLEAN-AP™/WET algorithms.

b. Range and Velocity Ambiguity Mitigation – Staggered PRT Algorithm

David Warde and Sebastián Torres (CIMMS at NSSL)

In pulsed Doppler weather radars, the range and Doppler velocity ambiguity problems are coupled so that trying to alleviate one of them worsens the other. Special

techniques are necessary to resolve both range and velocity ambiguities to the levels required for the efficient observation of severe weather. Efforts in this area are expected to culminate in significantly improved WSR-88D data quality when implemented on the Radar Data Acquisition sub-system. The increased data quality will result in an improved ability for the WSR-88D to detect severe weather, flash floods, winter storms, and provide aviation forecasts. Over the last decade, two techniques have emerged as viable candidates to address the mitigation of range and velocity ambiguities in the WSR-88D, thus reducing the amount of purple haze obscuration currently encountered during the observation of severe phenomena. These are: systematic phase coding (SZ-2) and staggered pulse repetition time (SPRT). The two techniques are complementary since they offer advantages at specific elevation angles; hence, they can be simultaneously incorporated into the same volume coverage pattern. The first stage of upgrades that implemented SZ-2 is now complete and has been operational with great success for a number of years. The second stage of NEXRAD upgrades dealing with range and velocity ambiguities involves the operational implementation of SPRT. For ground clutter filtering SPRT data, we developed a novel spectral processing SPRT algorithm that incorporates the mature CLEAN-AP filter, range-overlaid recovery, dual polarization and dual polarization with generalized PRT ratios.

From FY13 to FY16, we provided scientific support to the NWS Radar Operations Center to ease software implementation of Staggered PRT into the NEXRAD software update cycle. We completed an extensive ground clutter filter analysis of the new staggered PRT algorithm and developed optimum acquisition parameters for operational volume coverage patterns (VCPs) that use staggered PRT in place of the Batch waveforms. The largest improvements from staggered PRT are seen in the mid-levels of the VCPs where replacement of batch waveforms with staggered PRT results in reduced error of estimates for reflectivity, differential reflectivity, differential phase, and correlation coefficient, higher maximum unambiguous velocities, reduced range-overlay obscuration, and increased dual polarization coverage.

In FY17, we continue to support ROC engineers on the implementation, integration, and testing of staggered PRT processing mode. The operational use of staggered PRT has stalled due to the unexpected increase in the number of velocity dealiasing errors seen on the WSR-88D testbeds. Our analysis has exposed coherency issues with the WSR-88D system. This analysis has led to changes to the IFDR frequency, which has helped to reduce the number of velocity dealiasing errors. However, further engineering tests are ongoing to address other noise sources. Meanwhile, we are exploring the use of post-processing dealiasing techniques (i.e., 2D-velocity-dealiasing algorithm in the RDA) to mitigate these velocity errors. On a positive note, level II data observed in the SPRT processing mode provides better performance in many aspects such as increased coverage for all fields (both due to no overlaid echoes and increased detectability at range), dual polarization and reflectivity fields with better quality, and, of course, larger maximum unambiguous velocity.

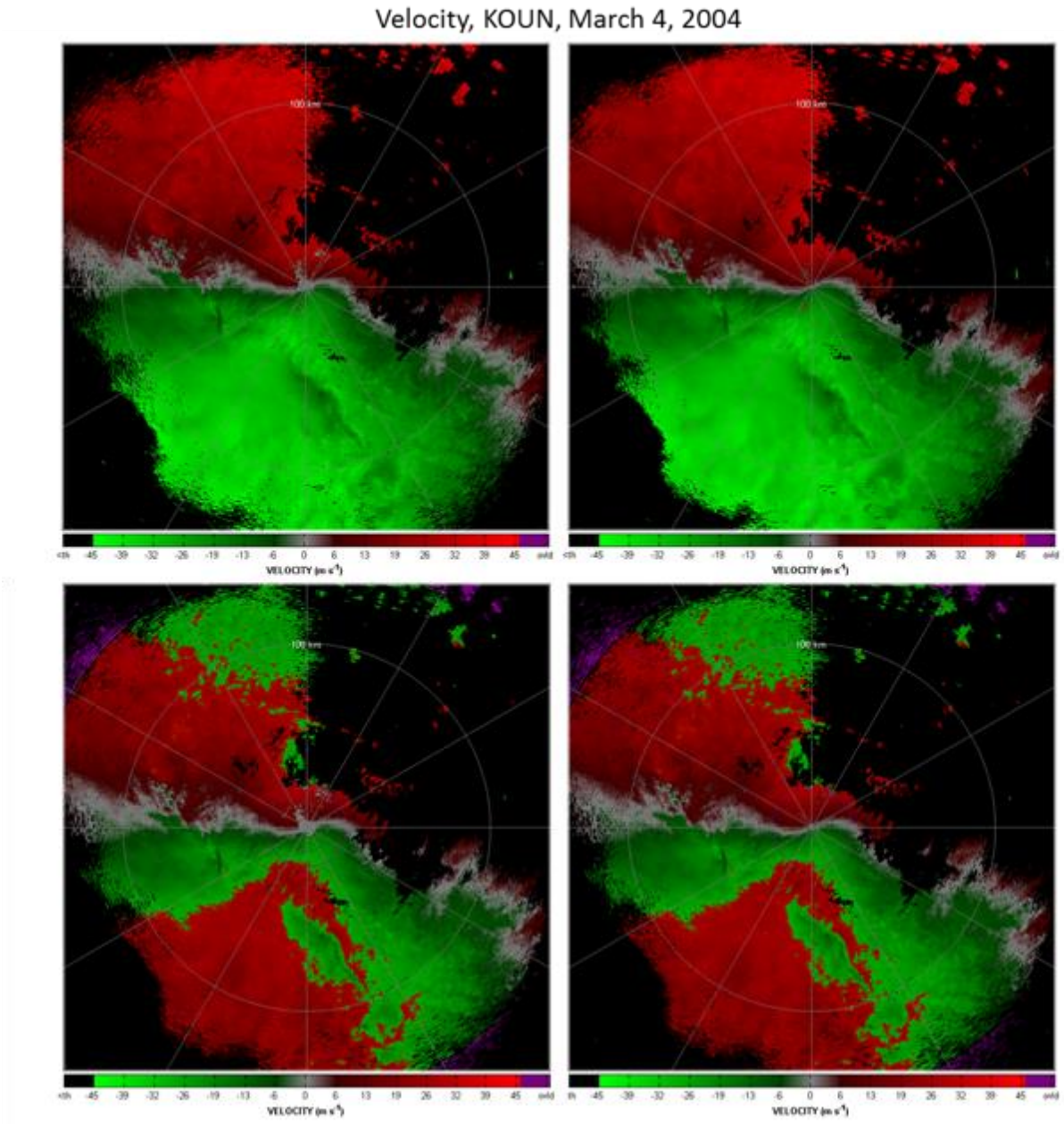

Examples of comparisons of Doppler velocity, unfiltered (left panels) and CLEAN-AP/WET ground clutter mitigation techniques (right panels), using Staggered PRT (top panels) and Batch (bottom panels) processing modes.

c. Range and Velocity Ambiguity Mitigation: SZ-2 Algorithm

Sebastián Torres and David Warde (CIMMS at NSSL)

The goal of range-and-velocity ambiguity mitigation is to reduce obscuration (“purple haze”) and Doppler velocity errors. One technique that has proven effective at addressing this need is the SZ-2 algorithm. The SZ-2 algorithm relies on systematic phase coding of the transmitted pulses to resolve range-overlaid echoes. Thus, shorter

pulse repetition times (PRT) can be used to obtain Doppler velocity estimates in a larger Nyquist co-interval. The SZ-2 algorithm was developed by CIMMS and NSSL scientists in the late 1990's and was transferred to the WSR-88D over a decade ago. Over time, it has gained popularity among National Weather Service forecasters, especially in widespread weather situations where accurate Doppler velocity measurements are needed.

Since then, the WSR-88D signal processor has undergone a series of functional upgrades, some of which required extensive modifications to the original SZ-2 algorithm. For example, the dual-polarization upgrade of the network led to significant changes to the signal processor and required extension of the original single-polarization SZ-2 algorithm to support dual-polarization operations. Other signal processing techniques aimed at improving data quality such as Coherency-Based Thresholding (CBT) and the hybrid spectrum-width estimator also required modifications to the SZ-2 algorithm. Throughout the years, these algorithmic modifications were documented in a differential manner (these were referred to as "delta" documents) to the point that the full algorithm description could only be grasped by looking at three different documents. Because of the current state of the algorithm description, the development of new techniques for improved data quality (e.g., CLEAN-AP^{TM} and Weather Environment Thresholding - WET), and a need to re-validate the operational implementation of SZ-2 (after undergoing a series of updates), we developed a fresh implementation during FY17 and delivered it to the Radar Operations Center. This new implementation includes the algorithmic description of the dual-polarization SZ-2 algorithm with the modifications required to integrate the Hybrid Spectrum Width, WET, and CLEAN-AP algorithms. In addition, in preparation for future signal processing upgrades, we developed and tested a proof-of-concept implementation of the SZ-2 Algorithm that works with the dual-polarization Hybrid-Scan Estimators (HSE) and with range-oversampling processing.

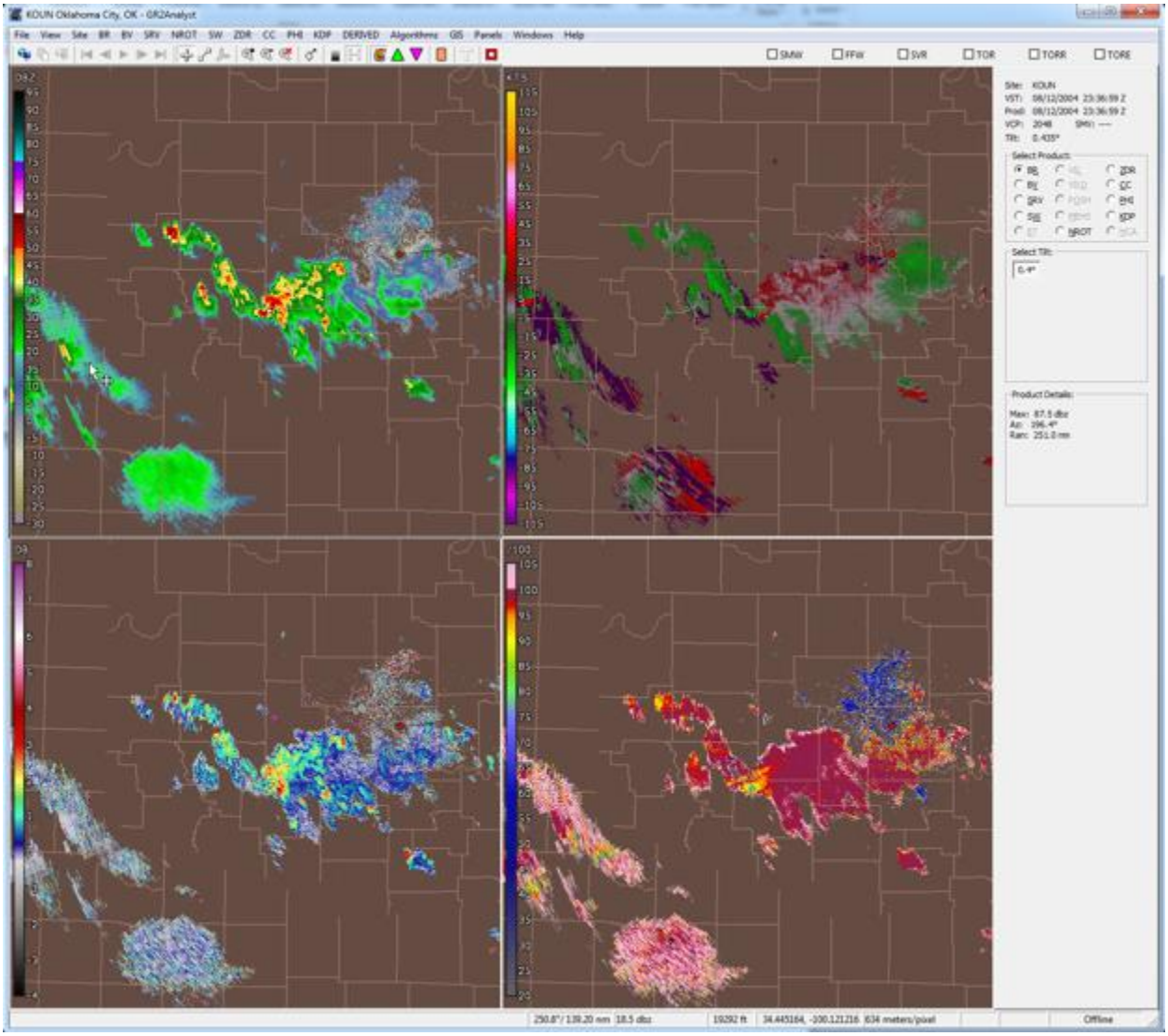

Example of processing with the updated dual-polarimetric SZ-2 algorithm that includes modifications to work with CLEAN-AP™, WET, hybrid spectrum-width, CBT, dual-polarization HSE, and range-oversampling algorithms. Phase-coded, range-oversampled data were collected with the KOUN radar on 8 Aug 2004. The fields shown in this figure correspond to reflectivity (top left), Doppler velocity (top right), differential reflectivity (bottom left), and correlation coefficient (bottom right).

d. Correlation Coefficient Estimation

Igor Ivić (CIMMS at NSSL)

The co-polar correlation coefficient (CC) is one of the three polarimetric variables being produced by the WSR-88D. CC aids in the recognition of types of radar echoes and in separation of returns from rain and snow. The latter requires precise measurements of CC in areas with low and moderate signal-to-noise ratios (SNR). Unfortunately, correlation coefficient estimates are unusable when they become larger than one, which

is common when the number of samples per dwell is small and in areas with SNR less than ~15 dB. In addition, the current CC estimator is positively biased, especially when the number of samples per dwell is small. To mitigate these issues, a novel correlation coefficient estimation technique is being developed that has the potential of producing less biased estimates. Mitigating the CC bias will result in more accurate estimates, which will improve polarimetric recognition of echoes. It will also reduce the number of estimates that cannot be used for classification (i.e., invalid estimates). The improved CC estimator will provide improved accuracy while being computationally viable for easier operational implementation on the WSR-88D. During FY17, details of the algorithm were described in the form of Algorithm Enunciation Language (AEL) and delivered to the ROC.

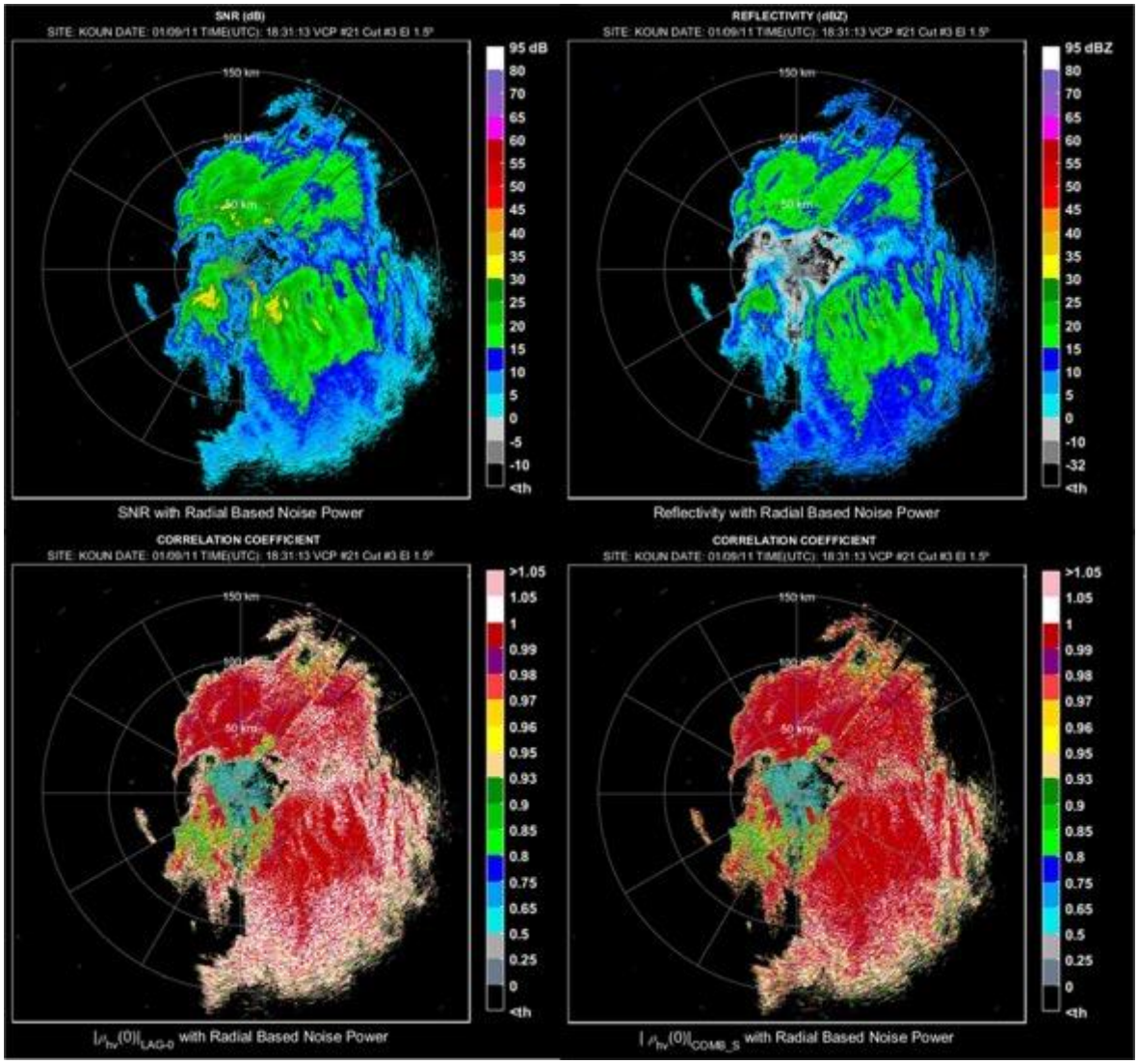

Comparison between CC fields produced using the legacy estimator (bottom left) and the improved CC estimation technique (bottom right) at 1.5° elevation. The field on the right exhibits visibly reduced number of invalid estimates (shown in pink). The top panels show the corresponding SNR (left) and reflectivity (right) fields.

e. Spectrum Width Estimation

David Warde and Sebastián Torres (CIMMS at NSSL)

Improving the quality of spectrum width estimates enhances data assimilation (Warn on Forecast), storm feature identification (rear flank downdrafts, boundaries, tornado genesis, and hail spikes), and downstream algorithms (NEXRAD Turbulence Detection Algorithm, range oversampling, non-uniform beam filling, Bragg scatter identification). On Doppler weather radars, the spectrum width is commonly estimated from a ratio of autocorrelation estimates at two different lags. These estimators have been used for decades on operational weather radars and have well known properties. For example, the R0/R1 estimator, which is based on the ratio of lag-0 to lag-1 autocorrelations, performs best for wide spectrum widths but has poor performance for narrow spectrum widths and relies on accurate noise measurements. The R1/R2 estimator, which is based on the ratio of lag-1 to lag-2 autocorrelations, and other estimators based on higher-lag autocorrelations provide better narrow spectrum-width estimates than the R0/R1 estimator and improve performance when accurate noise measurements are not available. Unfortunately, they are severely biased for wide spectrum widths. Thus, to provide better estimates over a wide range of spectrum widths, a few estimators can be suitably combined. This so-called hybrid spectrum-width estimator can take advantage of the best characteristics of each estimator for different regimes.

We developed improvements to spectrum width estimation by combining ASD and Welch processing to create “matched” autocorrelations. Using Monte Carlo simulations and reprocessed Weather Surveillance Radar-1988 Doppler (WSR-88D) data, the new estimators were shown to provide less biased estimates at narrow spectrum widths and at lower sample sizes, with less variance than standard methods. For wide spectrum widths, the new estimators are unaffected and perform comparably to the standard estimators. The results were presented to the NEXRAD Technical Advisory Committee and were well received. The new estimators were combined into a simple hybrid spectrum width estimator that showed improve performance over the current NEXRAD WSR-88D hybrid spectrum width estimator.

In FY17, we continued working with ROC software engineers to incorporate the Hybrid Spectrum Width Estimator for SPRT into the WSR-88D. Using perturbation analysis on a Gaussian shaped power spectrum, the formulas for the mean and standard deviation of the new estimators were formulated. The theoretical formulas confirmed that when matched autocorrelations are used, spectrum-width estimates exhibit improved statistical performance compared to the conventional estimator. This is particularly evident for narrow spectrum widths and as the SNR increases and/or as the number of samples decreases.

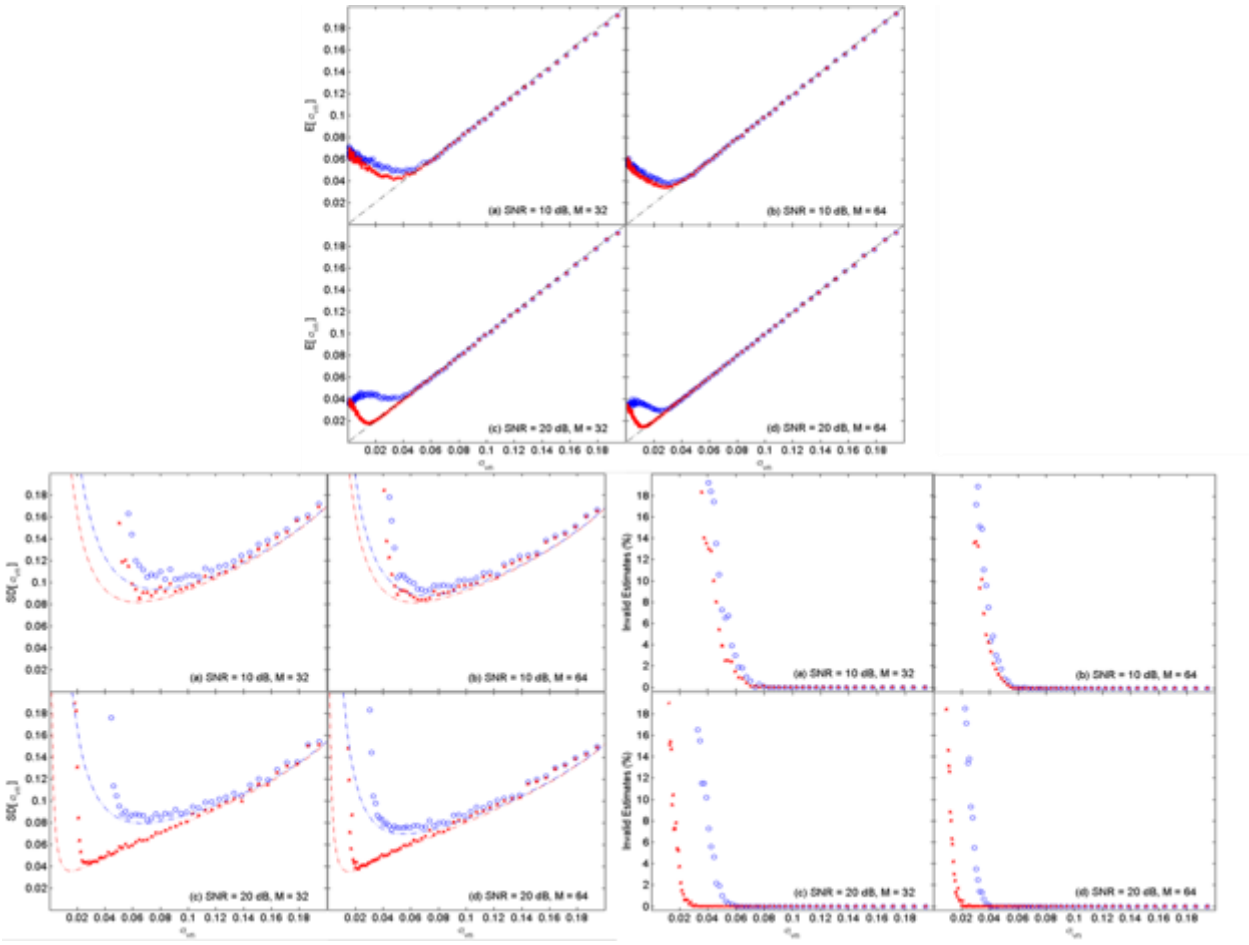

Example of the improvements in mean (top 4 panels), standard deviation (left 4 panels), and percentage of invalid estimates (right 4 panels) using matched autocorrelation (red 'x') compared to using conventional (blue 'o') R0/R1 spectrum-width estimates. Results are a function of the normalized true spectrum width for signal-to-noise ratios of 10 dB (sub-panels a and b) and 20 dB (sub-panels c and d) with 32 samples (subpanels a and c) and 64 samples (subpanels b and d).

f. Improving Radar-Variable Estimates from Ground-Clutter-Filtered Data

Igor Ivić (CIMMS at NSSL)

Radar returns from ground clutter contaminated weather signals can result in biased estimates of meteorological variables if not processed properly. A frequency domain ground-clutter filter (e.g., GMAP or CLEAN-AP) is typically employed to remove this contamination. This usually results in less biased meteorological-variable estimates. However, if spectra of meteorological and ground clutter signals are overlaid (typical in stratiform rain and snow events), removal of the latter also removes a portion of the useful signal. The result is that the estimates of Doppler moments may still be significantly biased in these cases. To mitigate this, an interpolation is typically used to replace the removed spectral coefficients. But, if the overlap of clutter and weather

signal spectra is extensive, the removal of clutter also removes most of the signal which can result in large errors even after interpolation. Such cases occur when the true signal velocity is either close to zero or when it aliases to a value close to zero due to the finite unambiguous velocity (v_a). Consequently, the frequency of severe clutter and signal overlap is higher in data from scans with smaller v_a (e.g., WSR-88D surveillance scans at the lowest elevations).

On the WSR-88D network, radar-variable estimates at the lowest elevations are produced from the surveillance (with small v_a but large unambiguous range) and Doppler (with short unambiguous range but large v_a) scans. Data from the former is used to estimate reflectivity and polarimetric variables while velocity and spectrum width are produced from the latter. Due to this arrangement, fields of reflectivity and polarimetric variables suffer more degradation in the areas where clutter is present (due to a higher frequency of severe signal and clutter overlap). The velocity and spectrum width are plagued by overlaid signals (caused by the multiple trip echoes as a result of short unambiguous range).

Clearly, the current operational arrangement on the WSR-88D network is such that it does not use the information about the reflectivity and polarimetric variables contained in the data from Doppler scans. The proposed Hybrid-Scan Estimators aim to rectify this situation in the case of the polarimetric variables, but these estimators only use polarimetric variable estimates from the Doppler data if they are not contaminated by overlaid echoes. Estimates from the surveillance scans, in the case of extensive clutter and signal overlap, may be significantly more degraded than those from the Doppler scans even if contaminated by overlaid signals. Thus, it is important to explore the possibility of improving the clutter-contaminated reflectivity and polarimetric variable estimates by using data from Doppler scans despite the contamination by overlaid signals.

During FY17, a development of basic principles and software infrastructure for this work was established. This work is ongoing.

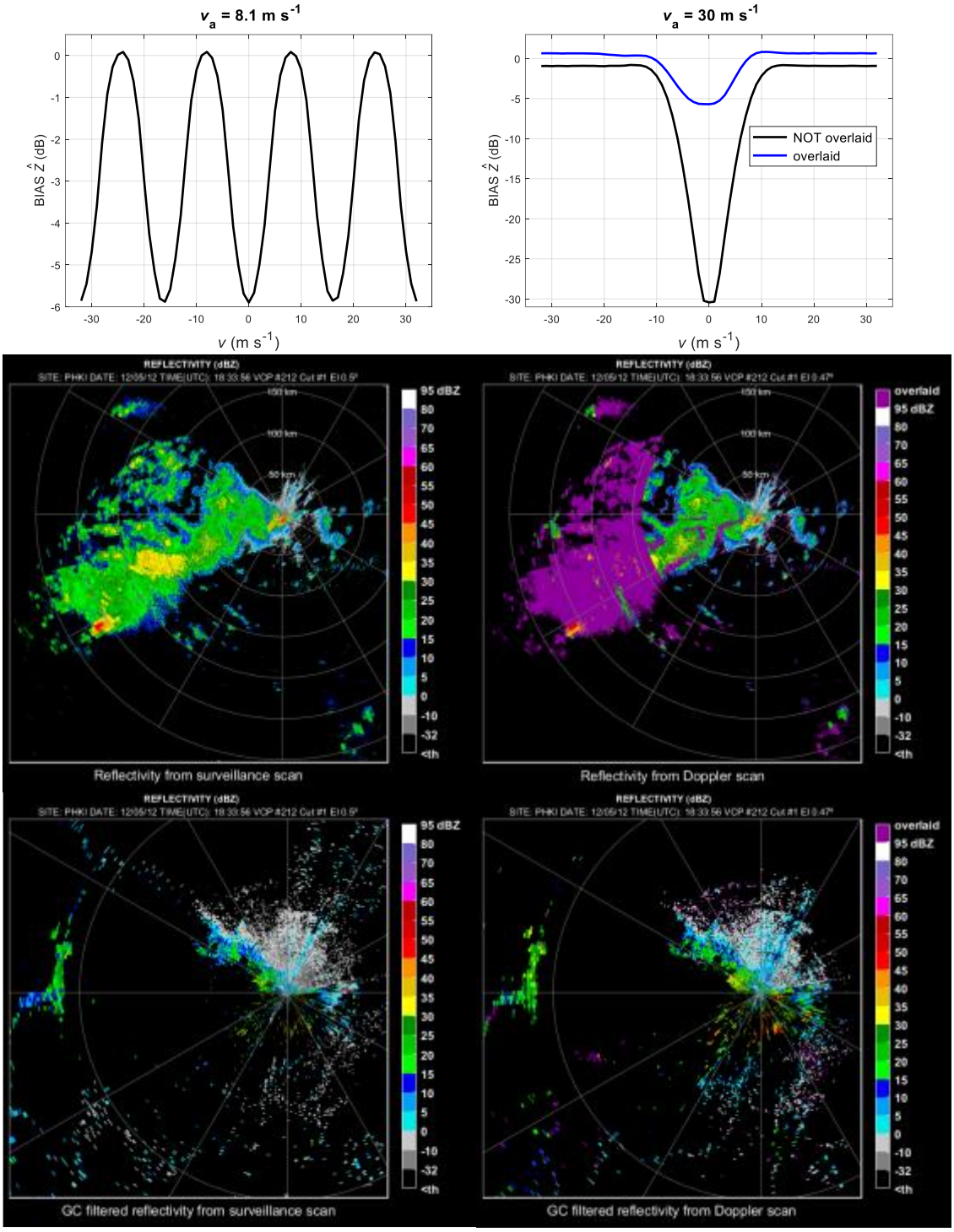

Simulated bias for surveillance (top leftmost panel) and Doppler (top rightmost panel) scan. Signal parameters are: SNR = 35 dB, CSR = 20 dB, σ_v = 2 m s^{-1}, and the overlaid signal is 5 dB smaller than the main signal and located at v = 15 m s^{-1} in the case of the Doppler scan. Surveillance (middle left panel) and Doppler (middle right panel) reflectivity fields. Reflectivity in ground clutter filtered bins for surveillance (bottom left panel) and Doppler (bottom right panel) scans. CLEAN-AP was used for ground clutter (GC) filtering.

g. Hybrid Scan Estimator

David Schvartzman and Sebastián Torres (CIMMS at NSSL)

Since the upgrade of the WSR-88D network with dual-polarization capabilities in 2012, polarimetric variables and their derived Level-III products have been extensively used by meteorologists and NWS forecasters. Information provided by the differential reflectivity (Z_{DR}), differential phase (Φ_{DP}), and correlation coefficient (ρ_{hv}) fields greatly improves our understanding of weather phenomena. However, these variables tend to have lower data quality (i.e., noisier) than spectral moments, which in turn decreases their operational value. Thus, it is important to investigate techniques to improve the data quality of polarimetric variables. This can be done by using data from split cuts, which consist of a surveillance scan followed by a Doppler scan at the same elevation angle. The goal of this project is to develop a technique that chooses the polarimetric-variable estimate with the best data quality from either the surveillance or Doppler scans of a split cut.

Currently, reflectivity and polarimetric variables are obtained from the long-pulse-repetition-time (PRT) surveillance scan, whereas Doppler velocity and spectrum width are obtained from the short-PRT Doppler scan. While not currently used, polarimetric variables estimated from the Doppler scan could result in better estimates than those from the surveillance scan. For example, this could happen under several conditions: (a) when dwell times in the Doppler scan are longer than those in the surveillance scan, (b) at low-to-medium SNRs when the larger number of samples may help reduce statistical fluctuations, (c) for wide spectrum widths, or (d) in the case of ground-clutter contamination for which a larger number of samples typically results in improved mitigation.

In previous years, we simulated dual-polarization data to assess the statistical performance of surveillance and Doppler scan estimates for a wide range of meteorological conditions. Using theoretical equations to compute the expected bias and variance of polarimetric estimates, the Hybrid Scan Estimator (HSE) chooses the estimate with better statistics from either the surveillance or Doppler scan. We processed several real-data cases with and without the HSE estimator and observed significant improvement in data quality. We presented our findings at the ROC/NSSL Data Quality team meeting. We qualitatively analyzed real-data cases processed with the algorithm and quantified the amount of invalid correlation-coefficient estimates reduction obtained when using this technique. Results indicate that the use of hybrid-scan estimators can significantly improve the quality of polarimetric variables.

For FY17, we integrated the HSE algorithm with SZ-2 VCPs that use phase coding techniques to extend the unambiguous range of Doppler variables. The SZ-2 VCP number 212 is often used for severe weather events. Amongst several cases, we processed radar data collected with VCP-212 during the May 20, 2013 severe weather event, using both surveillance and HSE polarimetric estimates. The results show significant improvement in polarimetric estimates (~25% on average) and improved

ground clutter suppression. A comparison of surveillance and HSE estimates is shown in the figure below. Improving the quality of polarimetric-variable estimates, especially in severe weather situations, could be important for saving lives and property.

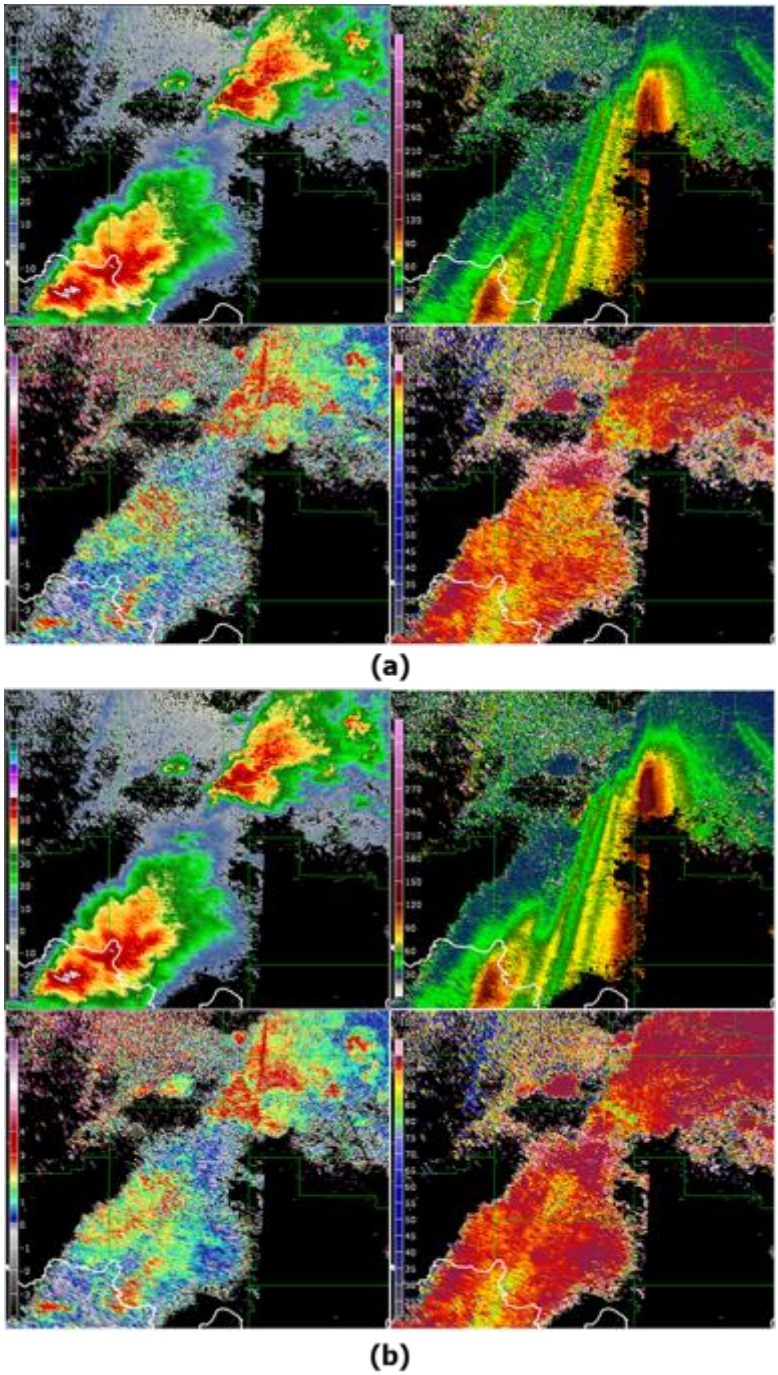

Plan-position-indicator (PPI) displays of (a) conventional and (b) HSE polarimetric-variable estimates from the May 20, 2013 severe weather event. For each panel, the subpanels are as follows: (top left) reflectivity, (top right) differential phase, (bottom left) differential reflectivity, and (bottom right) correlation coefficient estimates. Note that reflectivity estimates are shown only as a reference.

h. Hybrid Differential Reflectivity Estimator

David Schvartzman and David Warde (CIMMS at NSSL)

Initial processing schemes for the polarimetric variables after the implementation of the WSR-88D dual-polarization upgrade were based on the surveillance scan. As a result, polarimetric-variable estimators with relatively large statistical errors at low SNRs are routinely observed. Additionally, uncertainty in the noise estimates for the horizontal and vertical channels can introduce additional bias and standard deviation. Alternative estimators have been suggested to mitigate the influence of noise and improve the accuracy and precision of polarimetric-variable estimates at low SNRs (Lei et al. 2012; Melnikov and Zrnić 2007). Specifically, the differential reflectivity (Z_{DR}) lag-1 estimator estimators discussed by Melnikov and Zrnić (2007) are free from the influence of noise and are therefore more robust at lower SNR values. In this work, we propose a hybrid differential-reflectivity estimator that uses either the lag-1 estimator (at low-to-medium SNRs) or the lag-0 estimator. One of the objectives of this study is to identify criteria to choose the appropriate estimator that leads to the best statistical performance.

To compare the statistical performance of the lag-0 and lag-1 differential reflectivity estimators in a controlled environment, we used a weather-signal simulator. It produces dual-polarization time-series data with pre-determined acquisition parameters (i.e., radar frequency, PRT, and number of samples) based on the true values of all six meteorological variables. We used parameters for the fastest WSR-88D VCP, VCP 12, since it is the most challenging for radar-variable estimation. The simulation results confirm that the performance of these estimators is mostly determined by the signal-to-noise ratio (SNR) and spectrum width. For lower SNRs, the noise introduced in the classic (lag-0) estimator significantly contaminates the signal, which leads to estimates with poor data quality. The lag-1 estimator shows better performance at low SNRs due to the fact that it uses the (noiseless) lag-1 correlation to estimate powers. Initial results revealed that some improvement could be obtained using the proposed hybrid estimator at low-to-medium SNRs.

Using the results from extensive simulations, we derived a set of binary decision tables to choose the best estimator of Z_{DR} based on minimizing the bias and variance. To validate our findings, we processed several real data cases using the hybrid Z_{DR} estimator and qualitatively evaluated improvement compared to the classical lag-0 estimator. The figure below shows a comparison of the discussed differential reflectivity estimators during the May 20, 2013 severe weather event.

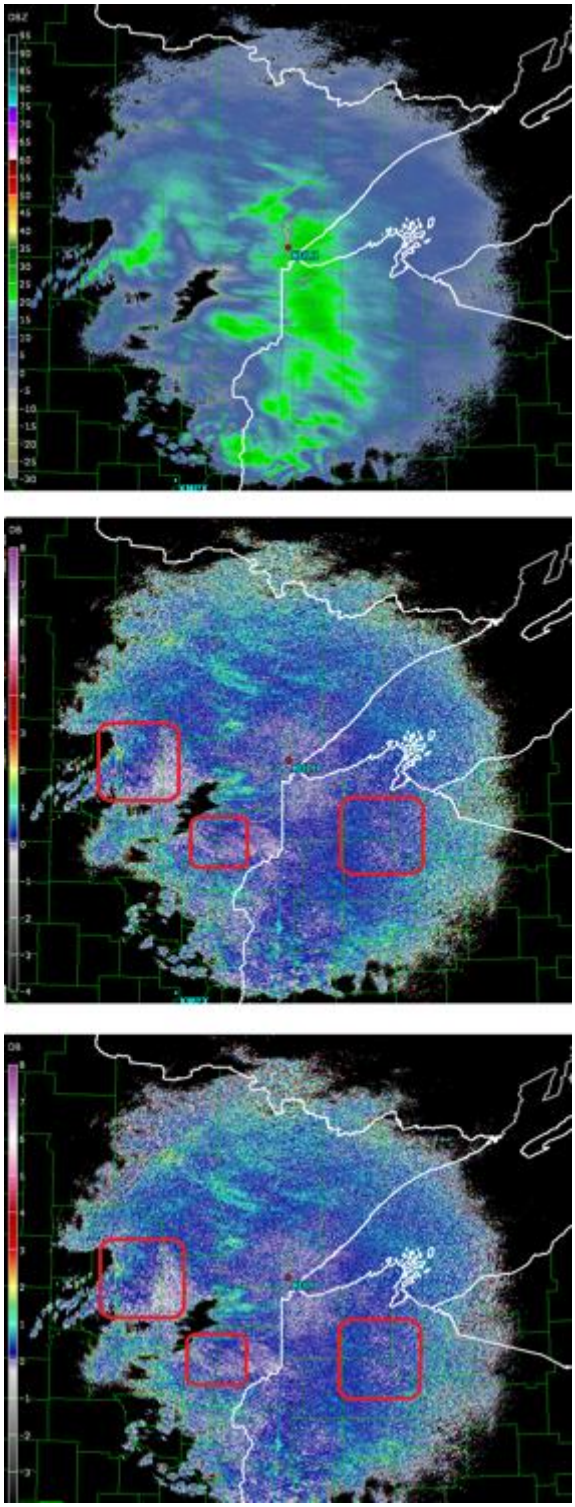

Plan-position-indicator (PPI) displays of reflectivity (top), lag-0 Z_{DR} (middle), and hybrid-Z_{DR} (bottom) estimates from May 20, 2013 severe weather event. Most of the improvement can be seen in the fringes, at ranges far from the radar. In addition, there is some improvement in the areas indicated with the red boxes. Notice that reflectivity estimates are shown only as a reference.

i. Range Oversampling Techniques

Sebastián Torres, Christopher Curtis, and Igor Ivić (CIMMS at NSSL)

Obtaining radar data at faster rates can improve the ability of forecasters to observe rapidly evolving weather phenomena. When increasing data rates, the conventional trade-off involves sacrificing either spatial coverage or data precision. With range oversampling, it is possible to add a new dimension to this trade-off: signal processing. Range oversampling allows us to either obtain data twice as fast with variances similar to conventional processing or improve data quality without sacrificing update time or spatial coverage. This type of processing has been used to significantly reduce update times on the National Weather Radar Testbed (NWRT) Phased Array Radar (PAR) and to improve polarimetric data quality on a NEXRAD research radar (KOUN).

In the original implementation of adaptive pseudowhitening, we used explicit variance expressions for each estimator to choose a transformation that was appropriate for the weather signal characteristics. This worked well for traditional radar-variable estimators, but some of the new non-traditional estimators either do not have an explicit variance expression or have a difficult-to-derive expression. We formulated a lookup-table technique (LUT adaptive pseudowhitening) that uses Monte Carlo simulations to find the proper transformation without utilizing a variance expression. In FY17, we completed the review process for a journal paper that captures this research. We also began to look at integrating range oversampling processing with the new correlation coefficient estimator described in the correlation coefficient estimation subsection (d). Because of this estimator's dependence on tables, the integration is more complicated than with other nontraditional estimators. We also studied the most effective way to implement range oversampling with SZ-2 processing. This research was included as part of the updated SZ-2 mode described in the SZ-2 subsection (c).

In addition to this research work, we also continued to work with Radar Operations Center engineers to determine how best to implement range oversampling processing on the NEXRAD network. This included supporting ROC efforts to find out how many oversampled gates can be collected with the RVP-9 signal processor.

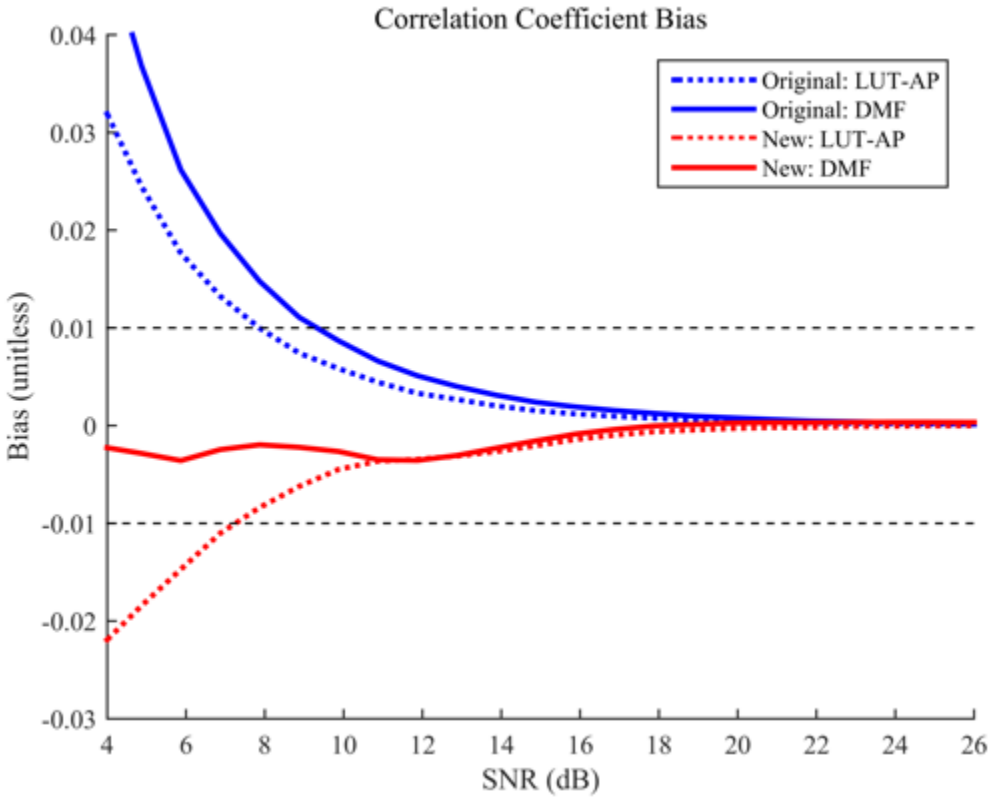

Biases of both the original and new correlation coefficient estimators processed with a digital matched filter and LUT adaptive pseudowhitening. This shows the bias introduced when implementing LUT adaptive pseudowhitening directly without taking into account the special requirements of the new correlation coefficient estimator.

j. Pulsed Interference Filters

Christopher Curtis (CIMMS at NSSL)

Pulsed interference from other radars is a significant problem for the NEXRAD network. In an era when spectrum may become more scarce, dealing with pulsed interference could become even more critical. One way to mitigate pulsed interference is to use a pulsed-interference filter. There are two main parts of a pulsed-interference filter. The first is detecting pulsed interference, and the second is interpolating data to replace the data corrupted by interference.

In FY17, we looked at several different ways to detect pulsed interference and looked for the best way to increase the probability of detection while keeping the false alarm rate low. We evaluated the previously developed Interference Spike Detection Algorithm (ISDA), the median of the powers (computed from the I/Q data), and a special trimmed mean that uses the average of the smallest 2/3 of the powers. The trimmed mean performed the best but only slightly better than the median for interference detection.

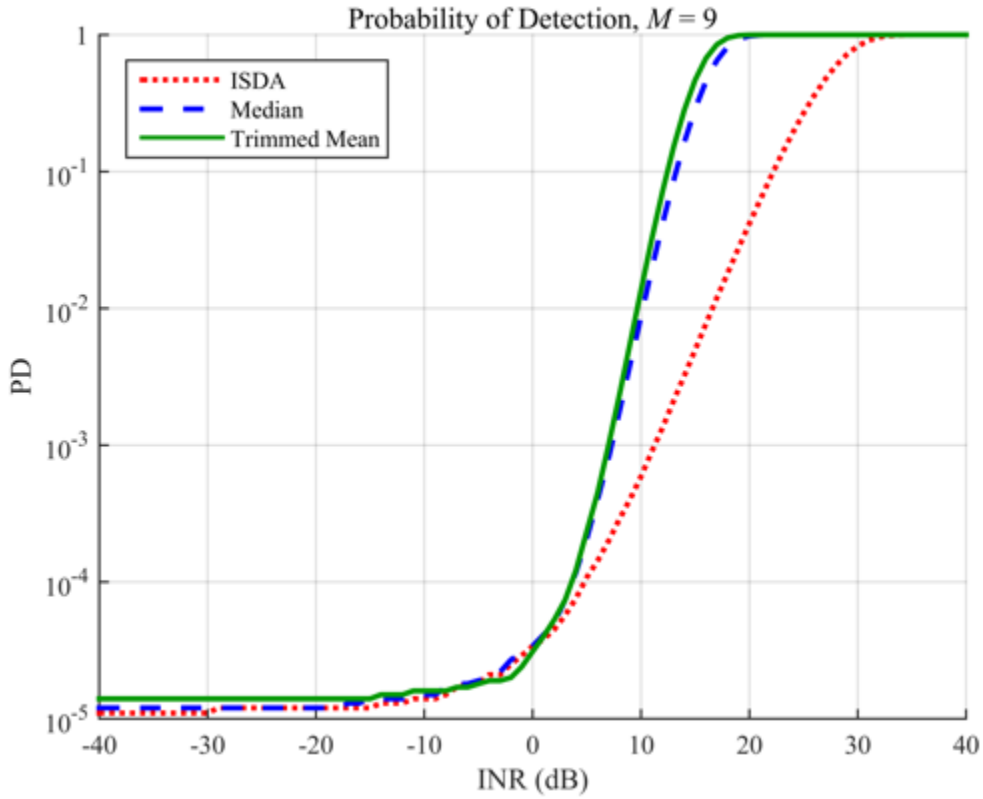

Probability of detection when the number of samples M = 9 for three pulsed-interference filters: ISDA, median, and trimmed mean.

k. Hardware Development and Maintenance for KOUN and Mobile Radars

Danny Wasielewski and Mike Schmidt (CIMMS at NSSL), Mike Shattuck (NSSL)

NSSL maintains several radar assets used by researchers, including both mobile radars and NSSL's research and development WSR-88D, KOUN. In addition to their use as meteorological and hydrological research instruments, these radar assets also serve as testbeds for technological research. Technologies prototyped on KOUN in particular are directly applicable to the WSR-88D network. Maintenance and continual improvement of these assets is essential to providing high quality instruments for new research and for supporting NSSL's commitment to R2O.

l. Creating Software for Presentation of Multiple-Radar Data in a Standard 3D Grid

John Krause (CIMMS at NSSL)

Upgrading our scientific software infrastructure this year will allow us to continue the shift from 2D algorithms and views of radar data to viewing the data and creating algorithms with a 3D perspective. Radar data are normally displayed in the Azimuth, Range, Elevation coordinates, but many applications of the data including model simulations and assimilation techniques require data in Cartesian coordinates of

latitude, longitude, and height. The technique to convert radar data into Cartesian coordinates is well known but has significant challenges, both scientific and technical. Understanding these challenges and designing software that can ingest the multiple radar data and produce grids of them for both scientific study and real time application has been a core achievement of this year.

The Radar3DGrid software can transform multiple-radar data onto a single grid. It has been shown to work for up to 25 radars over the SE United States in real time on a 6km horizontal grid spacing and 500m vertical grid spacing. It can also be used to grid a single-radar data into a 500m grid in both the horizontal and the vertical. The software can use a variety of objective analysis or weighting schemes when combining the data and can utilize virtual volumes or time based cutoffs. This high level control was a key software requirement from the scientists who use the gridded data. The software has been optimized to compute multiple data fields at the same time such as radar reflectivity Z, differential reflectivity Z_{DR}, and cross-correlation coefficient ρ_{hv}. It has been tested extensively on more than 20 cases, including real time operation. This software has already been utilized to study the use of radar reflectivity in the Warn on Forecast system and to compute the location of the Z_{DR} and ρ_{hv} columns. In the future, we plan to compare the output from the Column Vertical Profile technique (CVP) in a time/height format to the results of the gridded data output.

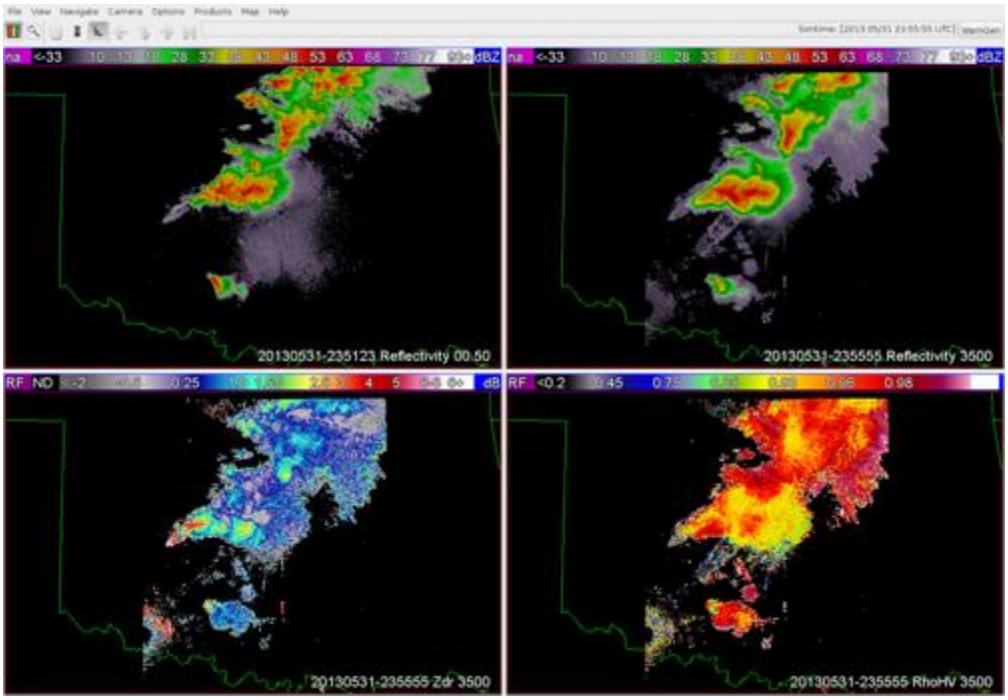

The 0.5 degree measured reflectivity Z from the KTLX radar on May 31, 2013 (upper left panel). The gridded reflectivity Z from multiple radars (KCRI, KTLX, KFDR, KVNX) at 3.5 km AGL (upper right panel), The gridded differential reflectivity Z_{DR} obtained from the same set of radars (lower left panel) and the gridded cross-correlation coefficient ρ_{hv} from the same set of radars. The gridded data have a 500m resolution in the horizontal and vertical directions.

m. Novel Approaches for Calibration of Radar Reflectivity Z and Differential Reflectivity Z_{DR}

Valery Melnikov (CIMMS at NSSL)

Ground clutter can potentially serve as a natural calibrator of Z and Z_{DR}. Radar data from ground clutter have been systematically collected and analyzed. Deviations of Z and ZDR associated with ground clutter from their mean values were analyzed together with the ROCSTAR data on radar parameters. It has been shown that the deviations can be caused by the deflections of antenna pointing from determined/directed elevations, bracketing of transmitted pulses, malfunctions of radar modulator, and wet radome. The ROCSTAR data have been analyzed by ROC personnel (Richard Ice, Robert Macemon, and Alan Free). The data show that ground clutter can be used to continuously monitor Z and ZDR in real time during data collection with the standard VCPs. Such a continuous monitoring is useful to control radar calibration between the standard calibration tests and in the absence of appropriate calibration weather objects such as light rain, snow, and Bragg scatter. Attenuation in wet radome can be estimated from a reduction of the intensity of ground clutter observed during rain on a radar site. This reduction can be used to correct Z from weather objects for the bias caused by a wet radome. Some results of this study were published in the papers by Richardson et al. (2017a, b).

Publications

Ivić, I. R., 2016: A technique to improve copolar correlation coefficient estimation. *IEEE Transactions on Geoscience and Remote Sensing*, **54**, 5776–5800.

Torres, S. M., and D. A. Warde, 2017: Staggered-PRT sequences for Doppler weather radars. Part I: Spectral analysis using the autocorrelation spectral density. *Journal of Atmospheric and Oceanic Technology*, **34**, 51-63.

Warde, D. A., and S. M. Torres, 2017: Staggered-PRT sequences for Doppler weather radars. Part II: Ground Clutter Mitigation on the NEXRAD Network Using the CLEAN-AP Filter. *Journal of Atmospheric and Oceanic Technology*, **34**, 703-716.

Warde, D. A., and S. M. Torres, 2017: Spectrum Width Estimation Using Matched Autocorrelations. *IEEE GRSL*, **PP**, 1-4.

2. Dual-Polarization

Overall Objectives

Use dual-polarization radars for quantitative precipitation estimation, hydrometeor classification, and investigation of microphysical processes in clouds and precipitation.

Accomplishments

a. Development and Testing of New Algorithms for the WSR-88D that Combine Polarimetric Radar data with HRRR Model Output to Determine Melting Layer Coverage and Surface-Based Precipitation Types in Winter Storms

Terry Schuur, Alexander Ryzhkov, and John Krause (CIMMS at NSSL)

In the past year, research-based functional descriptions for the Hybrid Melting Layer Detection Algorithm (HMLDA) and surface Hydrometeor Classification Algorithm (sHCA) have been coded to produce initial operational implementations of each algorithm that allow them to be simultaneously run on a large number of winter weather events. By being able to quickly and efficiently run the algorithms on a much larger number of events than was previously possible, the process by which the algorithms are tested, evaluated, and improved has been accelerated. This important step also moves us closer to the goal of making fully operational versions of the algorithms available to be run and evaluated in real time on the MRMS system.

Twelve events that encompass a broad spectrum of winter weather have been identified, processed and analyzed to evaluate and refine algorithm performance. Since sHCA performance is highly dependent on the accurate detection of melting layer (ML) coverage, much of the initial testing using the newly-developed, quasi-operational code has focused on improving HMLDA performance, which can be negatively impacted by contamination from ground clutter and the dendritic growth layer (DGL), both of which exhibit polarimetric signatures that are similar to that of the ML. Techniques are also being investigated to fill artificial gaps, due to widely spaced elevation angles that are common to many WSR-88D volume coverage patterns (VCPs) used in winter weather events, that occasionally occur with the radar-based ML detection.

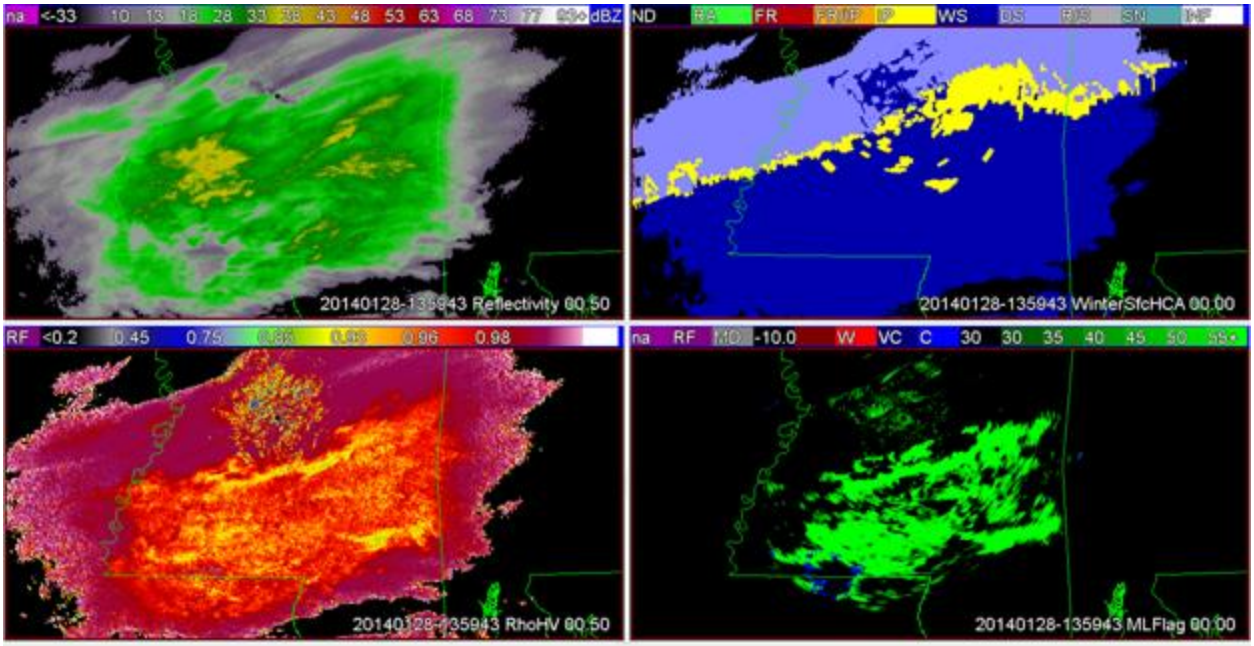

KDGX (Jackson, MS) radar reflectivity (upper left), correlation coefficient (lower left), sHCA (upper right), and radar-based HMLDA detections (lower right) results at 135943 UTC on January 28, 2014.

b. A Polarimetric Analysis of Ice Microphysical Processes in Snow, Using Quasi-Vertical Profiles of Polarimetric Radar Variables

Erica Griffin, Terry Schuur, and Alexander Ryzhkov (CIMMS at NSSL)

A study that uses a new quasi-vertical profile (QVP) methodology to investigate the microphysical evolution and significance of intriguing winter polarimetric signatures and their statistical correlations has been completed. QVPs of a selection of transitional stratiform and pure snow precipitation were analyzed using S-band WSR-88D data, alongside their corresponding environmental thermodynamic HRRR model analyses. The investigation builds upon the work of Ryzhkov et al. (2016) by demonstrating the value of using QVPs of K_{DP} and Z_{DR} to examine the temporal evolution of ice microphysical processes in winter clouds and precipitation. Several fascinating and repetitive signatures were observed in the QVP K_{DP} and Z_{DR} fields, particularly when comparing K_{DP} and Z_{DR} signatures from the dendritic growth layer (DGL; -10 to -20°C) with cloud top temperature. The most striking feature found was that maximum Z_{DR} (up to 6 dB) in the DGL occurred when K_{DP} in the DGL was low and at times of warm cloud top temperatures. Conversely, maximum K_{DP} (up to 0.3° km^{-1}) in the DGL occurred when Z_{DR} was low and at times of cold cloud top temperatures. Z_{DR} and K_{DP} in the DGL were therefore found to essentially be anti-correlated and to strongly depend on cloud top temperature (panels a, b, d). The analyses also show correlations indicating larger Z_{DR} within lower Z_H in the DGL, and larger K_{DP} within greater Z_H in the DGL (panels c, e). The high Z_{DR} regions are likely dominated by growth of a mixture of highly oblate dendrites and/or hexagonal plates, or prolate needles. Regions of high K_{DP} are expected to be overwhelmed with snow aggregates and crystals with irregular or nearly spherical shapes, seeded at cloud tops.

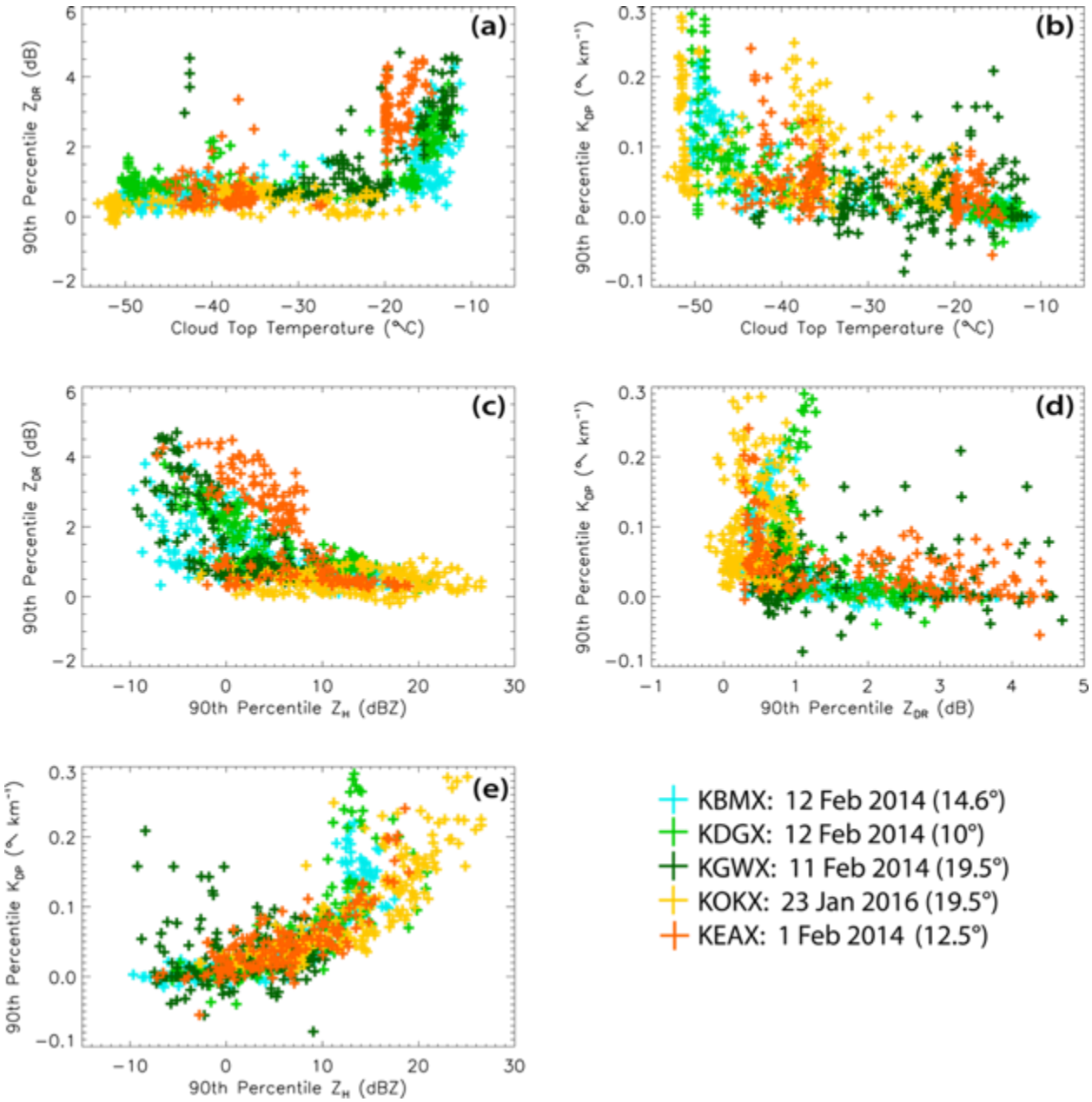

Composite scatterplots of a) CTT (°C) vs. 90th percentile maximum Z_{DR} in the DGL, b) CTT (°C) vs. 90th percentile maximum K_{DP} in the DGL, c) 90th percentile maximum Z_H in the DGL vs. 90th percentile maximum Z_{DR} in the DGL, d) 90th percentile maximum Z_{DR} in the DGL vs. 90th percentile maximum K_{DP} in the DGL, and e) 90th percentile maximum Z_H in the DGL vs. 90th percentile maximum K_{DP} in the DGL. Data from the KBMX, KDGX, KGWX, KOKX, and KEAX events are indicated by the light blue, light green, dark green, yellow, and orange symbols in each plot, respectively.

c. Assimilation of Z_{DR} Columns to Improve Storm-Scale Analyses and Forecasts

Jacob Carlin, Jeff Snyder, and Alexander Ryzhkov (CIMMS at NSSL)

The performance of short-term convective forecasts depends on the accurate specification of storm-scale initial conditions, which are typically unknown. Radar data are frequently assimilated into these models to reduce the model spin-up time. Cloud analysis techniques insert hydrometeors, and, crucially, moisture and buoyancy (to account for latent heating) based on reflectivity (Z) in order to establish observed storms in the model, but rely on general and simplified ideas to do so. Z_{DR} columns are ubiquitous markers of updrafts in deep moist convection and thus represent areas of buoyancy due to latent heating and saturation. We have used this principle to modify the cloud analysis method of radar data assimilation to assimilate polarimetric data.

We implemented a Z_{DR} column detection algorithm based on the work of Snyder et al. (2015) into the cloud analysis routine. As opposed to moistening based on a Z threshold and warming in regions of positive analyzed vertical velocity as is done in the legacy cloud analysis, moisture and warming are added in and immediately surrounding observed Z_{DR} columns. Additionally, a simple drying routine was included to prevent overmoistening in regions of high relative humidity outside of detected Z_{DR} column regions. We have performed two cycled case studies to compare the impact of assimilating Z_{DR} columns to that of the legacy cloud analysis employing only Z using the Advanced Regional Prediction System model. Results indicate notable improvements with improved storm positioning and speed, less spurious convection, and higher quantitative verification scores. These early results are promising and support further study of the assimilation of diabatic heating profiles and moisture derived from observed polarimetric signatures. Further testing is ongoing that includes the use of multiple radar sites, the inclusion of K_{DP} columns, and implementation into the WRF model.

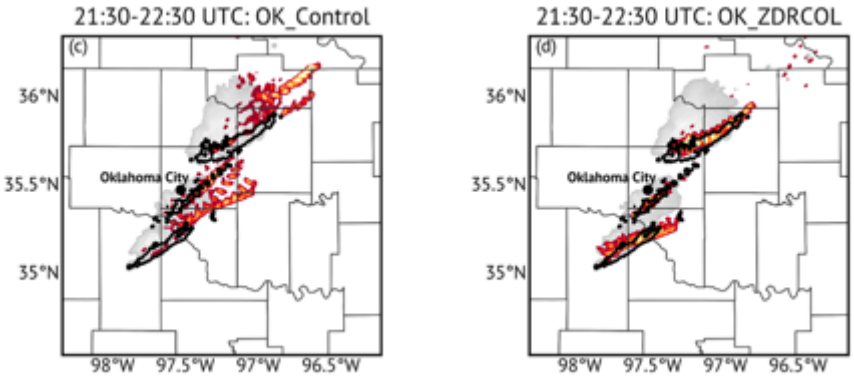

Example comparison of a 0-1 h forecast when assimilating (left) only Z and (right) with the addition of Z_{DR} columns using the cloud analysis for the 19 May 2013 central Oklahoma tornado outbreak. Composites of forecast 1-6 km AGL updraft helicity (red shading), along with observed 1-6 km AGL MRMS-derived rotation tracks for the corresponding period (black contours), are shown. The initial 1-km AGL Z is shown in gray for reference.

d. Thermodynamic Retrievals of the Melting Layer Using a 1-D Spectral Bin Model

Jacob Carlin and Alexander Ryzhkov (CIMMS at NSSL)

The melting layer within precipitation is an important region owing to the diabatic cooling due to melting and evaporation and its associated consequences, including downdraft formation, the formation and modification of cold pools, and the potential for sudden changes in surface precipitation type. As such, many studies have attempted to model these effects, including its representation in observed radar data (i.e., the radar “bright band”). However, models (generally with bulk microphysics) often fail to reproduce these observed melting layer signatures due to deficiencies in the microphysics schemes’ treatment of melting and mixed-phase particles. Operational dual-polarization data, and particularly quasi-vertical profiles (QVPs), have shed new insight into the polarimetric characteristics of the melting process.

We have developed a one-dimensional spectral bin model that explicitly models the sublimation, melting, and evaporation of snow and rain particles and allows for variable riming fraction, and includes environmental temperature and moisture feedbacks. This model is coupled to a polarimetric radar operator that calculates Z, Z_{DR}, and K_{DP}, along with the cooling rate due to various microphysical processes. Results indicate that the model faithfully reproduces observed polarimetric bright band signatures, and can thus be used to study the relationship between the vertical profiles of these signatures and the associated diabatic cooling rate, with future implications for assimilation and diagnosing model deficiencies. The model can also be used as a tool to investigate the cause of so-called “sagging” bright bands, and whether deepening isothermal layers can be a cause in addition to riming.

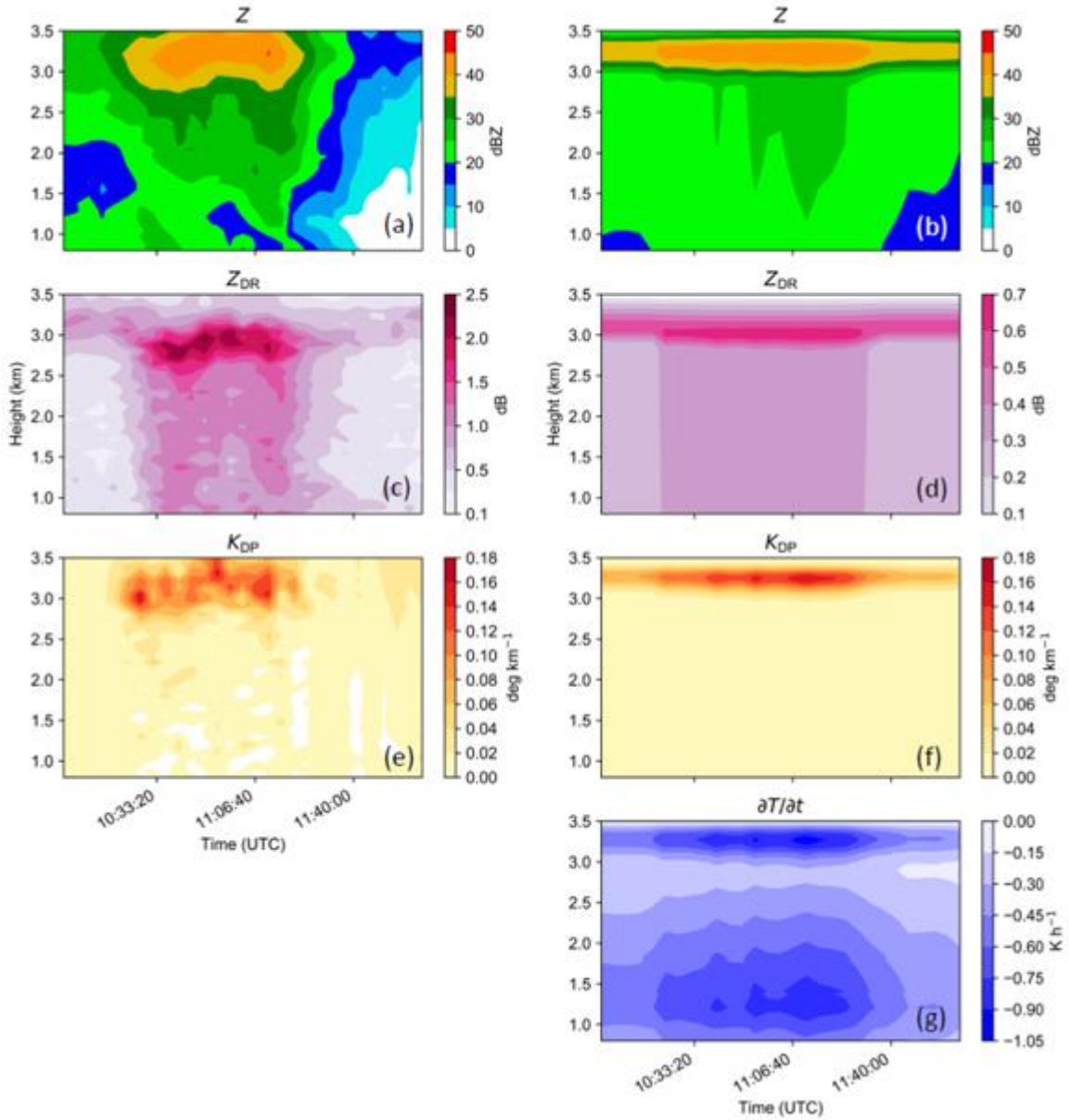

(a,b) Z, (c,d) Z_{DR}, (e,f) K_{DP}, and (g) cooling rate from (left) observed QVP from 20 May 2011 and (right) output from the 1-D model.

e. Development of the Algorithm for Cloud detection with WSR-88D Radar

Valery Melnikov (CIMMS at NSSL)

Convection is one of the sources of the cloud formation. To forecast cloudiness, it is important to obtain information about the intensity of convection. The convective intensity is also important for aviation meteorology because it causes airplane shocks at takeoffs and landings. To help with forecasting of convective clouds and convective turbulence, a study was conducted in 2017 to observe convective thermals, which are the first stage of the development of convective clouds. Convective thermals also cause airplane shocks.

The convective thermals are low reflecting objects. To observe them with the WSR-88D, some signal processing techniques has been tested on KOUN. It has been shown that radar detectability can be enhanced by about 9 dB by utilizing a few signal processing techniques. Enhanced radar detectability allows observations of convective thermals. The height of the thermals, their horizontal sizes, and the rate of growth are characteristics of convection, which can be obtained from radar data. An example of radar observations is shown in the plot obtained from data collected in July 2013. The tops of convective thermals are at heights of about 2.5 km and seen as radar echoes with ZDR less than 1 dB. The source of radar echoes there is Bragg scatter. The lower parts of convective boundary layer exhibit high ZDR and also show patterns in a form of plumes. These parts of thermals are filled with insects producing large ZDR values.

Developing convective clouds are also visible from the satellites. The results of this study are summarized in the article of Melnikov and Zrnic (2017).

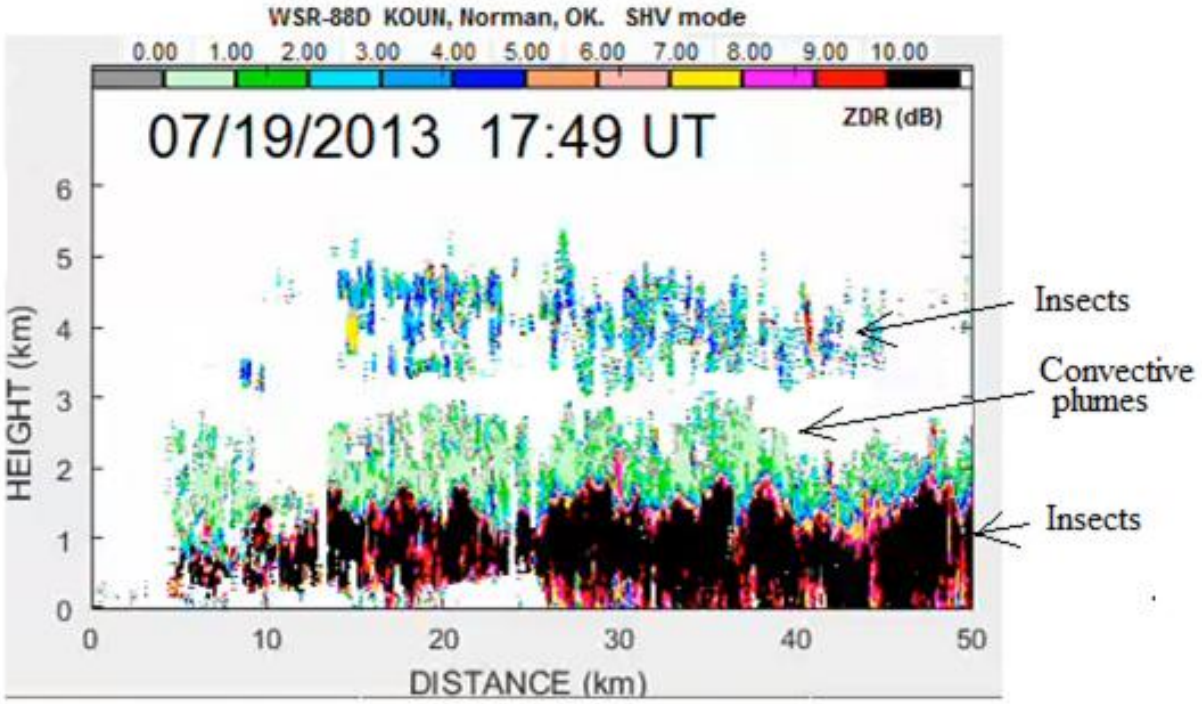

Vertical cross section of ZDR on 19 July 2013 at 1749 UTC at az = 191°.

f. Polarimetric Weather Radar Forward Operator Development

Jeff Snyder (CIMMS at NSSL)

Significant advancements in computing resources and model parameterizations have led to the rise of storm-scale numerical weather prediction in the past couple of decades. Concurrent with the development of high-resolution numerical modeling, the development and deployment of polarimetric weather radar technology (now through

the nationwide WSR-88D radar network) has provided a trove of microphysical information on the scale (in time and space) never before possible. However, numerical models do not explicitly predict the quantities that polarimetric radars measure; a forward operator is used to calculate relevant radar quantities from model fields. The use of a polarimetric radar forward operator enables for a more thorough comparison between and validation of numerical model simulations and weather radar observations. Simulated radar fields in supercells from high-resolution models produce signatures similar to those observed, which allows us to study how signatures relate to unobserved or unobservable quantities (e.g, Snyder et al. 2017a,b). Unfortunately, no microphysics scheme currently provides all of the necessary information needed to calculate the common suite of polarimetric radar measurements (e.g., Z_{DR}, ρ_{hv}, K_{DP}, etc.). Instead, the user must specify at least a few parameters and/or relations, some of which are well founded but others of which have been established using more limited observational and theoretical evidence.

Although it is currently unknown how best to use polarimetric radar information to improve numerical model performance, we want to ensure that the best forward operator is used (since errors of the final simulated quantities are a function of errors in the model microphysics compounded by those in the forward operator itself). Work has continued in the past year to improve the forward operator that was originally developed for use with the Hebrew University Cloud Model (HUCM). This advanced forward operator is being ported into an experimental version of the Weather and Research Forecasting (WRF) model. To provide one example, changes to the forward operator include modifications to the aspect ratios for larger hail and graupel to account for more research observations resulting from field campaigns. In FY17, work also began on a collaboration with colleagues in Germany to add polarimetric radar capabilities forward operator used in the COSMO model.

In addition to improving the forward operator, it is important to quantify the errors that can be associated with choices that a user must make when using a polarimetric radar forward operator. To this end, work continues on examining the differences that are seen when, for example, a user opts to use lookup tables instead of calculating exact T-matrix scattering amplitudes for hydrometeors at all necessary grid points. The examination of errors will provide guidance to cloud modelers and users of simulated radar data, and it will be useful for data assimilation research as well.

g. Improving the Detection of Large Hail Using Polarimetric Weather Radar

Jeff Snyder and John Krause (CIMMS at NSSL)

Much research has been carried out to characterize the polarimetric radar signature of large hail in the past several decades. In general, large hail is associated with higher Z_H, Z_{DR} ~ 0 dB, and reduced ρ_{hv} (e.g., less than 0.95), and the Hail Size Discrimination Algorithm (HSDA; Ryzhkov et al. 2013a,b; Ortega et al. 2015) highlights this part of the parameter space to identify small, large, and giant hail. However, there are situations in which the Hydrometeor Classification Algorithm (HCA; Park et al. 2008) and the HSDA

do not properly identify large and giant hail. In particular, the HSDA fail to identify large hail that may fall along the periphery of a supercell's updraft, where prominent size sorting results in a very low number concentration of very large hail and, as a result, where Z_H may be relatively low (i.e., less than 35 dBZ). This size sorting effects leads the HCA to misclassify as rain some areas where large hail is occurring (e.g., Fig 2g, top). To improve algorithm performance, we are currently looking to expand how the HSDA and HCA work. At this time, the HCA and HSDA work on a bin-by-bin basis, where any given radar bin is essentially independent of the others. Although large hail occasionally falls near supercell updrafts in very low number concentrations (Fig 2g, bottom), it is not possible to inform the current algorithms of storm-based features such as the updraft that would be necessary to adjust membership functions of the algorithms to account for this situation (i.e., large hail with low Z_H).

To improve algorithm performance, we continue to look at ways to modify the HSDA and HCA to include information such as proximity to updraft (as identified by bounded weak echo regions, Z_{DR} columns, etc.) and near-storm environment characteristics. For example, the lower bound of the Z_H membership function for large and giant hail is reduced near strong updrafts to assist in properly identifying hail that may fall near the updraft. Such algorithm modifications are being carefully examined to minimize negative impacts associated with increased false positives.

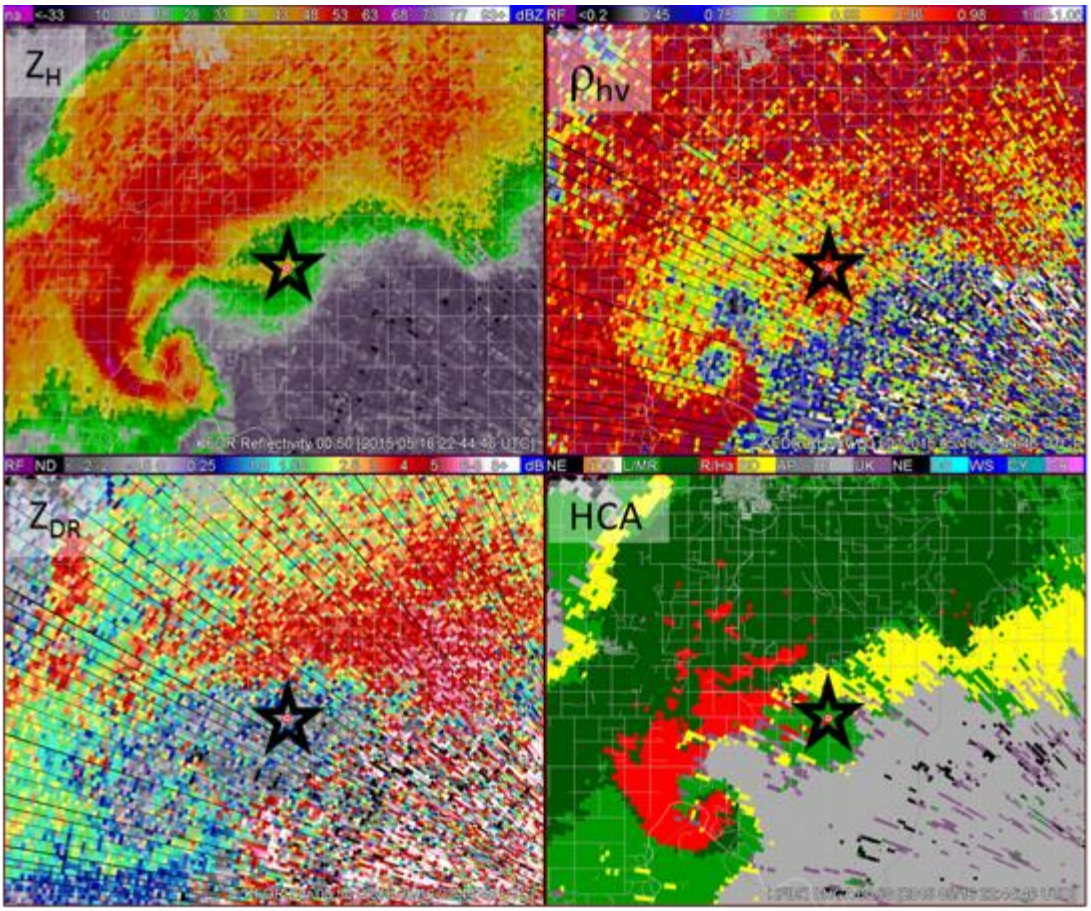

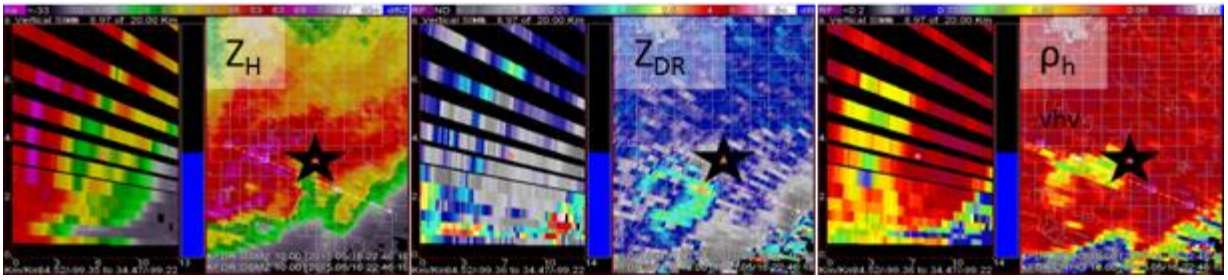

Top figure: Z_H, ρ_{hv}, Z_{DR}, and HCA from a supercell in southwestern Oklahoma on 16 May 2015. The black start indicates the location where hail exceeding 2.5" in diameter was observed. Note that the HCA classifies this area as "light/moderate rain", primarily on account of the modest Z_H (~20-35 dBZ) and low Z_{DR} (~0 dB). Data are from the 0.5° elevation angle. Bottom figure. Reconstructed vertical cross-sections and 10.0° elevation angle data of Z_H, Z_{DR}, and ρ_{hv} from approximately the same time as at top.

h. Identifying Characteristics of Hail Growth Aloft

Jeff Snyder (CIMMS at NSSL)

The results of the HCA and HSDA are purely diagnostic in nature – the algorithm cannot be used to identify where hail may be growing aloft before it reaches large (2.5 cm < D < 5.0 cm) or giant (D > 5.0 cm) sizes. Studies of polarimetric radar observations of large-hail-producing convective storms have shown an enhanced of LDR (e.g., the "LDR cap") or reduction in ρ_{hv} (e.g., the "LoRB"; Snyder et al. 2013) in the mid-levels of such storms. It is hypothesized that these signatures represent areas where wet hail is present and where we growth may be occurring, which means that the identification of these signatures may provide prognostic information to improve warning lead time. In addition, regions of anomalously negative Z_{DR} (sometimes as low as or even lower than -2 dB) have been seen near and above Z_{DR} columns in storms that produce large hail. There are two main possibilities that may explain why this area of negative Z_{DR} (often co-located with reduced ρ_{hv}) is seen near or above Z_{DR} columns (which can be used as reasonable proxy for updraft location in storms with strong updrafts) – (1) it is associated with prolate scatterers (e.g., hydrometeors with a greater vertical dimension than horizontal dimension) or (2) it is a result of resonance scattering. For the former case, unfortunately, very few in situ observations are available in the mid-levels of updrafts in strong supercells, although it is possible that the negative Z_{DR} is associated with conical graupel that may be present near the updraft.

Alternatively, scattering simulations at S-band indicate that hailstones with D ~ 6 cm are associated with Z_{DR} of -2 dB or less (e.g., Ryzhkov et al. 2013a,b), though the net impact on Z_{DR} depends upon the shape and fall behavior (e.g., canting angle characteristics) of the hail. With the updraft where hail is likely, it is reasonable to think that these areas of negative Z_{DR} aloft are associated with giant hail. The reduction in ρ_{hv} often co-located with the regions of negative Z_{DR} indicate that mixed-phase hydrometeors such as wet hail undergoing wet growth and a wide variety of hydrometeor shapes and sizes may be present. We have collected high-resolution RHIs using KOUN to support our effort to examine the relationship hail growth aloft and corresponding polarimetric radar data. In addition, we are examining a series of products (e.g., minimum ρ_{hv} and Z_{DR} between -10 C and -40 C, minimum and average Z_{DR} within 2 km of Z_{DR} columns, etc.) relative to hail observations collected by the SHAVE project to determine how we can best identify where hail is growing aloft in order to allow users to anticipate large hail at the ground before it falls.

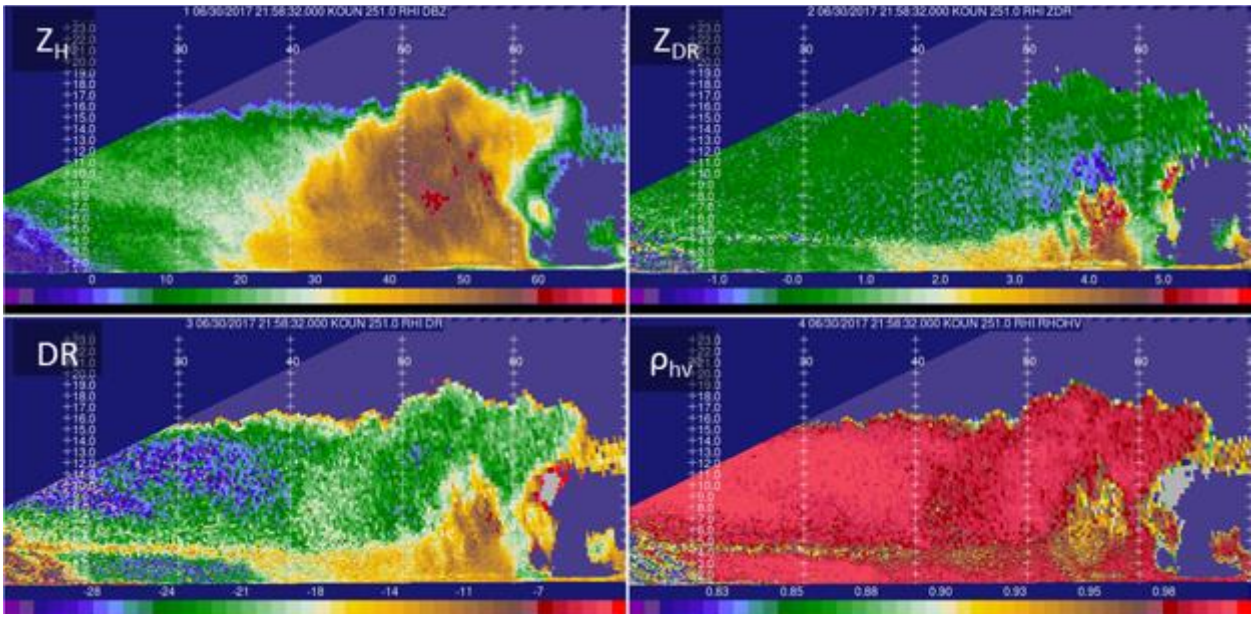

Z_H, Z_{DR}, Depolarization Ratio (DR), and ρ_{hv} from a high-resolution RHI collected by KOUN on the afternoon of 30 June 2017. A deep Z_{DR} column is seen extending to ~8 km AGL, above which a ~2-3 km deep region of negative Z_{DR} (as low as approximately -2 dB). Associated with these Z_{DR} features is reduced ρ_{hv}, and the combined influences of ρ_{hv} and Z_{DR} led to a prominent DR column.

i. A Polarimetric and Microphysical Analysis of the Stratiform Region of MCSs

Amanda Murphy, Pengfei Zhang, and Alexander Ryzhkov (CIMMS at NSSL)

In recent years, the method of quasi-vertical profiles (QVPs; Ryzhkov et al. 2016) has emerged as a novel way to investigate polarimetric radar data in a time-height format. QVPs are created by averaging radar data from a high elevation scan over all 360° around the radar, and assuming typical beam height as a function of range to assign data to a particular height. This process results in radar-centric time-height polarimetric radar data that is conducive for a deeper understanding of polarimetric signatures within different types of precipitation. Accordingly, QVPs have been used in a number of studies to connect observed or modeled microphysical processes with what is observed by radar. Column-vertical profiles (CVPs) are similar to QVPs, but instead focus on only a small analysis sector in range and azimuth instead of the entire region surrounding the radar. CVPs are preferable to QVPs when precipitation is horizontally inhomogeneous, or if the goal of a study is to analyze a specific region of a storm. Both QVPs and CVPs can be (and most commonly are) generated from operational WSR-88D radar data.

Currently we are working on using CVPs in conjunction with aircraft in situ microphysical data to better understand the stratiform region of mesoscale convective systems (MCSs), using data collected during MC3E and PECAN. Of particular interest are strong polarimetric signatures that have been observed by QVPs in the dendritic growth layer

and melting layer (e.g., Griffin et al. 2017). CVPs offer the ability to directly collocate in situ microphysical and operational weather radar data, by having the analysis sector centered on the location of the aircraft as the aircraft moves in time. Fig. 2i shows a CVP from 7/6/2015 that was made following the aircraft, with the aircraft track overlaid. Combined with assuming a linear time offset in radar data collection time from the 0.5° elevation scan time with height, the method of the CVP sector following the aircraft allows for a confident collocation of polarimetric radar and in situ microphysical data.

These collocated data can be used in multiple ways. The first is for improvement of existing ice water content algorithms (e.g., IWC(Z), IWC(Z,K_{DP}), etc.). Such algorithms can be directly tested to see if they can reproduce ice water content values observed by the aircraft, and can be further tuned for accuracy. Additionally, microphysical data can be analyzed within the dendritic growth layer and melting layer to try and determine what microphysical processes are taking place within these layers. In MC3E, flight legs and spirals were made through the melting layer and dendritic growth layer, and were made through the melting layer in PECAN. An analysis of bulk microphysical data, particle size distributions, and even possibly particle imagery and habit classification can be made to facilitate a far deeper understanding of these layers than has been possible in the past. All in all, there exists a rich set of in situ and radar polarimetric data to explore and be analyzed through a variety of means.

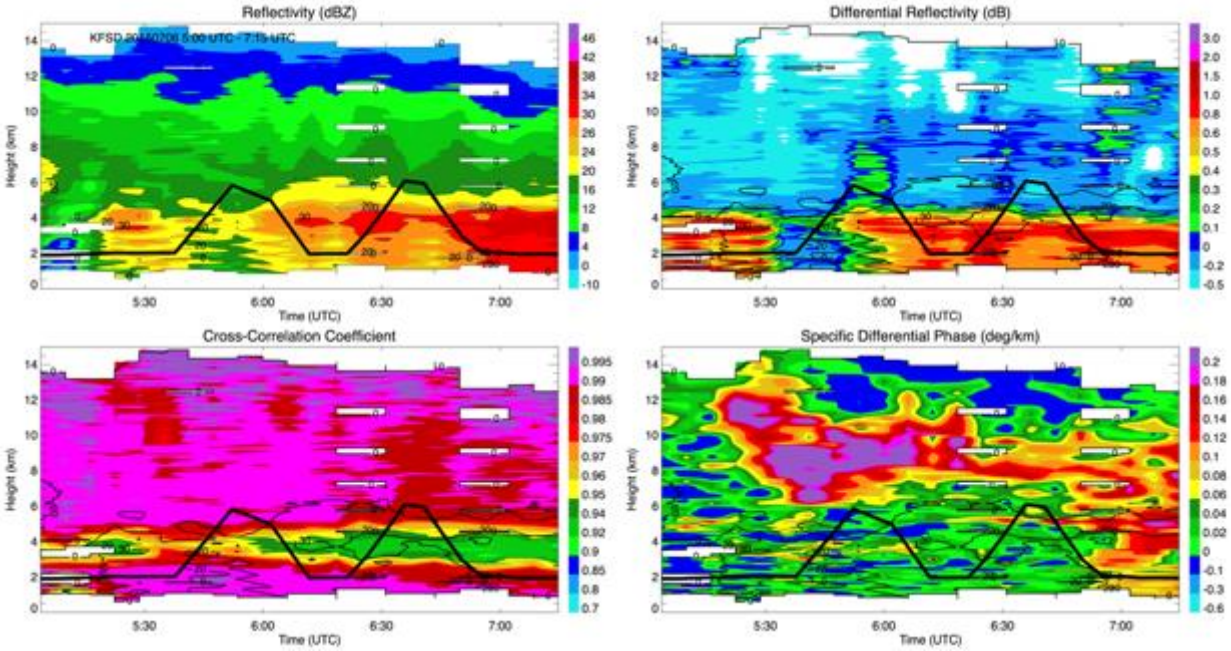

CVP using data from Sioux Falls, SD (KFSD) radar on 7/6/2015 from 5:00-7:15 UTC. The CVP sector has an averaging range/azimuth of 10 km/10°, and follows the aircraft (track overlaid).

j. Developing Polarimetric Radar Relations for Quantification of Snow Based on Disdrometer Data

Petar Bukovčić, Pengfei Zhang, and Alexander Ryzhkov (CIMMS at NSSL)

Accurate measurements of snow amounts by radar are very difficult to achieve. The inherent uncertainty in radar snow estimates based on the radar reflectivity factor Z is caused by the variability of snow particle size distributions and snow particle density as well as large diversity of snow growth habits.

In this study, a novel methodology for snow quantification based on the joint use of radar reflectivity Z and specific differential phase K_{DP} is introduced. An extensive dataset of 2D video disdrometer measurements of snow in central Oklahoma is used to derive polarimetric relations for snow water equivalent rate (S) and ice water content (IWC) in the forms of bivariate power-law relations $S = \gamma_1 K_{DP}^{\alpha_1} Z^{\beta_1}$ and $\mathrm{IWC} = \gamma_2 K_{DP}^{\alpha_2} Z^{\beta_2}$, along with similar relations for the intercept N_{0s} and slope Λ_s of exponential snow size distribution. The polarimetric relations dramatically reduce the impact of the variability of snow particle size distributions on the S and IWC estimates. This is illustrated in Fig. 2j where the scatterplots of S measured by the disdrometer versus their estimates from the S(Z), S(K_{DP}), and S(Z,K_{DP}) relations are displayed. This novel approach is tested against the standard $S(Z)$ relation using snow disdrometer measurements in three geographical regions (Oklahoma, Colorado, and Canada). It demonstrated significant improvement in snow estimates compared to the traditional Z-based methods.

Initial $S(K_{DP}, Z)$ and IWC(K_{DP}, Z) relations were obtained from the disdrometer analysis of 16 snow events in Oklahoma. Besides an excellent performance locally (Oklahoma), these relations perform reasonably well for snowstorms in Colorado and very well in Canada, two distinct climate regions, which attests to a (potentially) universal character of such relations.

The correlation coefficient between the measured and estimated $S(K_{DP}, Z)$ (or IWC(K_{DP}, Z)) is much higher (~0.99) than for $S(Z)$ (or IWC(Z)) estimate (~0.83 to ~0.89), which boosts confidence into the utility of the novel polarimetric relations.

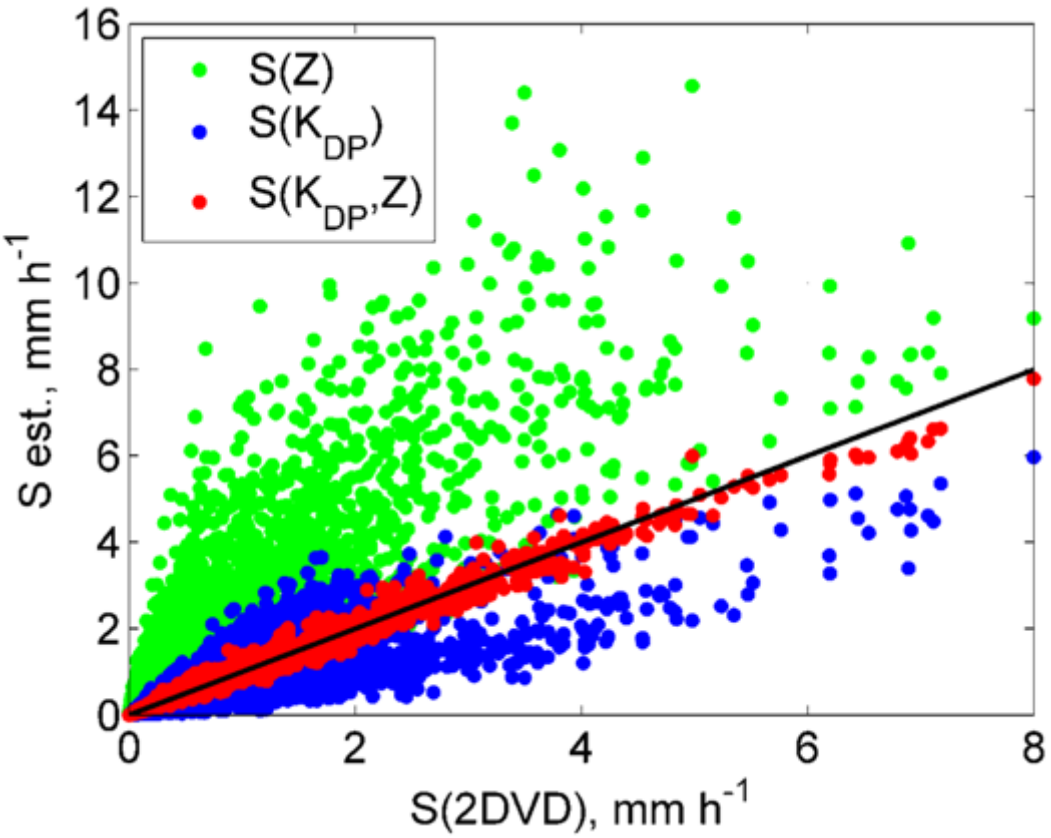

The scatterplots of snow water equivalent rate S measured by the disdrometer versus its estimates from the S(Z), S(K_{DP}), and S(Z,K_{DP}) relations.

Publications

Bluestein, H., M. French, J. Snyder, and J. Houser, 2016: Doppler-radar observations of anticyclonic tornadoes in cyclonically rotating, right-moving supercells. *Monthly Weather Review*, **144**, 1591-1616.

Bluestein, H. B., Z. B. Wienhoff, D. D. Turner, D. W. Reif, J. C. Snyder, K. J. Thiem, and J. B. Houser, 2017: A comparison of the fine-scale structures of a prefrontal wind-shift line and a strong cold front in the Southern Plains of the U.S. *Monthly Weather Review*, In Press.

Bukovcic, P., A. Ryzhkov, D. Zrnic, and G. Zhang, 2017: Polarimetric radar relations for quantification of snow based on the disdrometer data. *Journal of Applied Meteorology and Climatology,* Accepted.

Cao, Q., M. Knight, A. Ryzhkov, P. Zhang, and N. Lawrence, 2016: Differential phase calibration of linearly polarized weather radar for accurate measurements of circular depolarization ratio. *IEEE Transactions in Geosciences Remote Sensing*, **55**, 491-501.

Carlin, J., A. Ryzhkov, J. Snyder, and A. Khain, 2016: Hydrometeor mixing ratio retrievals for storm-scale radar data assimilation: Utility of current equations and potential benefits of polarimetry. *Monthly Weather Review,* **144**, 2981-3001.

Carlin, J., J. Gao, J. Snyder, and A. Ryzhkov, 2017: Assimilation of Z_{DR} columns for improving the spin-up and forecast of convective storms in storm-scale models: Proof-of-concept experiments. *Monthly Weather Review,* Accepted.

Fridlind, A., X. Li, D. Wu, M. van Lier-Walqui, A. Ackerman, W.-K. Tao, G. McFarquhar, W. Wu, X. Dong, J. Wang, A. Ryzhkov, P. Zhang, M. Poellot, A. Neumann, and J. Tomlinson, 2017: Use of observation-based aerosol profiles in simulations of a mid-latitude squall line during MC3E: Similarity of stratiform ice microphysics to tropical conditions. *Atmospheric Chemistry and Physics,* **17**, 5947-5972.

Giangrande, S., T. Toto, A. Bansemer, M. Kumjian, S. Mishra, and A. Ryzhkov, 2016: Insights into riming and aggregation processes as revealed by aircraft, radar, and disdrometer observations for a 27 April 2011 widespread precipitation event. *Journal of Geophysical Research,* **121**, 5846-5863.

Griffin, C. B., C. C. Weiss, A. E. Reinhart, J. C. Snyder, H. B. Bluestein, J. Wurman, and K. A. Kosiba, 2017: In situ and radar observations of the low reflectivity ribbon in supercells during VORTEX2. *Monthly Weather Review*, Accepted.

Griffin, E., T. Schuur, and A. Ryzhkov, 2017: A polarimetric analysis of ice microphysical processes in snow, using quasi-vertical profiles. *Journal of Applied Meteorology and Climatology,* Accepted.

Houser, J. B., H. B. Bluestein, and J. C. Snyder, 2016: A fine-scale radar examination of the tornadic debris signatures and weak reflectivity band associated with a large, violent tornado. *Monthly Weather Review*, **144**, 4101-4130.

Ilotoviz, E., N. Benmoshe, A. Khain, V. Phillips, and A. Ryzhkov, 2016: Effect of aerosols on freezing drops, hail, and precipitation in a mid-latitude storm. *Journal of Atmospheric Science.*, **73**, 109-144.

Kaltenboeck, R., and A. Ryzhkov, 2017: A freezing rain storm explored with a C-band polarimetric weather radar using the QVP methodology. *Meteorologische Zeitschrift*, **26**, 207-222.

Khain, A., E. Ilotoviz, A. Ryzhkov, and J. Snyder, 2017: Relationship between hail microphysics, aerosols, and Z_{DR} columns. *Journal of Atmospheric Science,* Accepted.

Krause, J., 2016: A simple algorithm to discriminate between meteorological and non-meteorological radar echoes. *Journal of Atmospheric and Oceanic Technology*, **33**, 1875-1885.

Kumjian, M., S. Mishra, S. Giangrande, T. Toto, A. Ryzhkov, and A. Bansemer, 2016: Polarimetric radar and aircraft observations of saggy bright band during MC3E. *Journal of Geophysical Research, Atmospheres,* **121**, 3584-3607.

Kuster, C. M., P. L. Heinselman, J. C. Snyder, K. A. Wilson, D. A. Speheger, and J. E. Hocker, 2017: An evaluation of radar-based tornado track estimation products by Oklahoma public safety officials. *Weather and Forecasting*, In Press.

Melnikov, V, and D. Zrnic, 2017: Observations of Convective thermals with weather radar. *Journal of Atmospheric and Oceanic Technol*ogy, **34**, 1585-1590.

Melnikov, V**.,** 2017: Parameters of cloud ice particles retrieved from radar data. *Journal of Atmospheric and Oceanic Technology*, **34**, 717-728.

Ortega, K., J. Krause, and A. Ryzhkov, 2016: Polarimetric radar characteristics of melting hail. Part III: Validation of the algorithm for hail size discrimination. *Journal of Applied Meteorology and Climatology*, **55**, 829 – 848.

Oue, M., M. Galletti, J. Verlinde, A. Ryzhkov, Y. Lu, and N. Bharadwaj, 2016: Use of X-band differential reflectivity measurements to study shallow Arctic mixed-phase clouds. *Journal of Applied Meteorology and Climatology,* **55**, 403-424.

Reeves, H., A. Ryzhkov, and J. Krause, 2016: Discrimination between winter precipitation types based on spectral-bin microphysical modeling. *Journal of Applied Meteorology and Climatology,* **55**, 1747-1761.

Richardson, L., J. Cunningham, W. Zittel, R. Lee, R. Ice, V. Melnikov, N.Hoban, and J. Gebauer, 2017: Bragg scatter detection by the WSR-88D. Part I: Algorithm development. *Journal of Atmospheric and Oceanic Technology*, **34**, 465-478.

Richardson, L., W. Zittel, R. Lee, V. Melnikov, R. Ice, and J. Cunningham, 2017: Bragg scatter detection by the WSR-88D. Part II: Assessment of ZDR bias estimation. *Journal of Atmospheric and Oceanic Technol*ogy, **34**, 479-493.

Ryzhkov, A., P. Zhang, H. Reeves, M. Kumjian, T. Tschallener, C. Simmer, and S. Troemel, 2016: Quasi-vertical profiles – a new way to look at polarimetric radar data. *Journal of Atmospheric and Oceanic Technology,* **33**, 551-562.

Ryzhkov, A., S. Matrosov, V. Melnikov, D. Zrnic, P. Zhang, Q. Cao, M. Knight, C Simmer, and S. Troemel, 2017: Estimation of depolarization ratio using radars with simultaneous transmission / reception. *Journal of. Applied Meteorology and Climatology*, **56**, 1797-1816.

Snyder, J. C., H. B. Bluestein, D. T. Dawson II, and Y. Jung, 2017: Simulations of polarimetric, X-band radar signatures in supercells. Part I: Description of experiment and simulated ρ_{hv} rings. *Journal of Applied Meteorology and Climatology*, **56**, 1977-1999.

Snyder, J. C., H. B. Bluestein, D. T. Dawson II, and Y. Jung, 2017: Simulations of polarimetric, X-band radar signatures in supercells. Part II: Z_{DR} columns and rings and K_{DP} columns. *Journal of Applied Meteorology and Climatology*, **56**, 2001-2026.

Tromel, S., A. Ryzhkov, M. Diederich, K. Muhlbauer, C. Simmer, S. Kneifel, J. Snyder, and C. Simmer, 2017: Multi-sensor characterization of mammatus clouds. *Monthly Weather Review,* **145**, 235-251.

Tromel, S., A. Ryzhkov, T. Bick, K. Muhlbauer, and C. Simmer, 2017: Towards nowcasting of winter precipitation: The Black Ice Event in Berlin 2014. *Meteorologische Zeitschrift,* **26**, 147-160.

Wakimoto, R., N. Atkins, K. Butler, H. Bluestein, K. Theim, J. Snyder, J. Houser, and J. Wurman, 2016: Aerial damage survey of the 2013 El Reno tornado combined with mobile radar data. *Monthly Weather Review*, **144**, 1749-1776.

Xie, X., R. Evaristo, S. Troemel, P. Saavedra, C. Simmer, and A. Ryzhkov, 2016: Radar observation of evaporation and implications for quantitative precipitation and cooling rate estimation. *Journal of Atmospheric and Oceanic Technology*, **33**, 1779-1792.

Patents

Ryzhkov, A., M. Knight, and R. May, 2016: Process for measuring circular depolarization ratios in a weather radar. US patent 9482752 B1, November 1, 2016.

Ryzhkov, A., M. Knight, and R. May, 2016: Apparatus for measuring circular depolarization ratios in a weather radar. US patent 9494681 B1, November 15, 2016.

3. MPAR Meteorology

Accomplishments

a. Examining Benefits of Rapid-Update Radar Data to Emergency Managers and NWS Forecasters

Charles Kuster, Katie Wilson, and Jeff Snyder (CIMMS at NSSL), Pamela Heinselman (NSSL), Doug Speheger (OUN), and James Hocker (OCS)

Emergency managers use weather-radar data to assist them in making decisions ranging from activating and directing storm spotters to guiding first responders around dangerous storms. To engage this important stakeholder in the development of new weather-radar products and technologies, we distributed an online survey and held a focus group to collect feedback about weather radar use, decisions typically made with the support of weather-radar, and perceptions of several developmental products that estimate the location and intensity of a tornado. Analysis of the survey and focus group responses revealed that emergency managers prefer products that are easy to understand and therefore quick to use. Of the five tornado track estimation products shown to survey and focus group participants, the National Weather Service Track was most preferred, because it clearly showed where a tornado may have occurred and was easy to use and interpret (first figure below). Participants indicated that such a product would be useful to them, because it would help them understand the scope of a disaster and thereby aid them in directing first responders, search and rescue teams, and disaster-response resources.

Survey and focus group responses also provided important information about how such a product would be best received by the emergency management community.

Participants indicated that they want a product shared with them via multiple methods (e.g., e mail and text message alert). They also expressed a need for a product they could interact with and add information to, so providing the product in multiple file formats—including a shapefile—would likely be beneficial to emergency managers. Clear communication by product developers of a product's strengths and weaknesses and situations when it is likely to work well and when it is likely to fail is also very important for the successful understanding and application of a product by the emergency management community.

Both emergency managers and National Weather Service (NWS) forecasters indicated that rapid-update data (i.e., volumetric update times of two minutes or less) would be useful to them during severe weather events. During the focus group, emergency mangers stated that tornado track estimation products created using rapid-update data looked more complete and realistic to them than products created using conventional-update data (i.e., volumetric update times of about four minutes). Therefore, participants were more likely to use a tornado track estimation product if it were produced using rapid-update data. For NWS forecasters, analysis of data collected during the Phased Array Radar Innovative Sensing Experiment revealed that severe thunderstorm and tornado warning lead time generally increased with faster radar update times, though this result was dependent on storm mode and threat type (second figure below). Forecasters using rapid-update data were able to better understand storm evolution in the context of their conceptual models and were able to observe signatures earlier, which allowed them to issue warnings sooner than forecasters using data with longer update times. Even though warnings were issued earlier, the basic characteristics of the warning (size, shape, duration, etc.) did not change with changes in radar update time. Therefore, radar update time likely affects when not how a forecaster issues warnings.

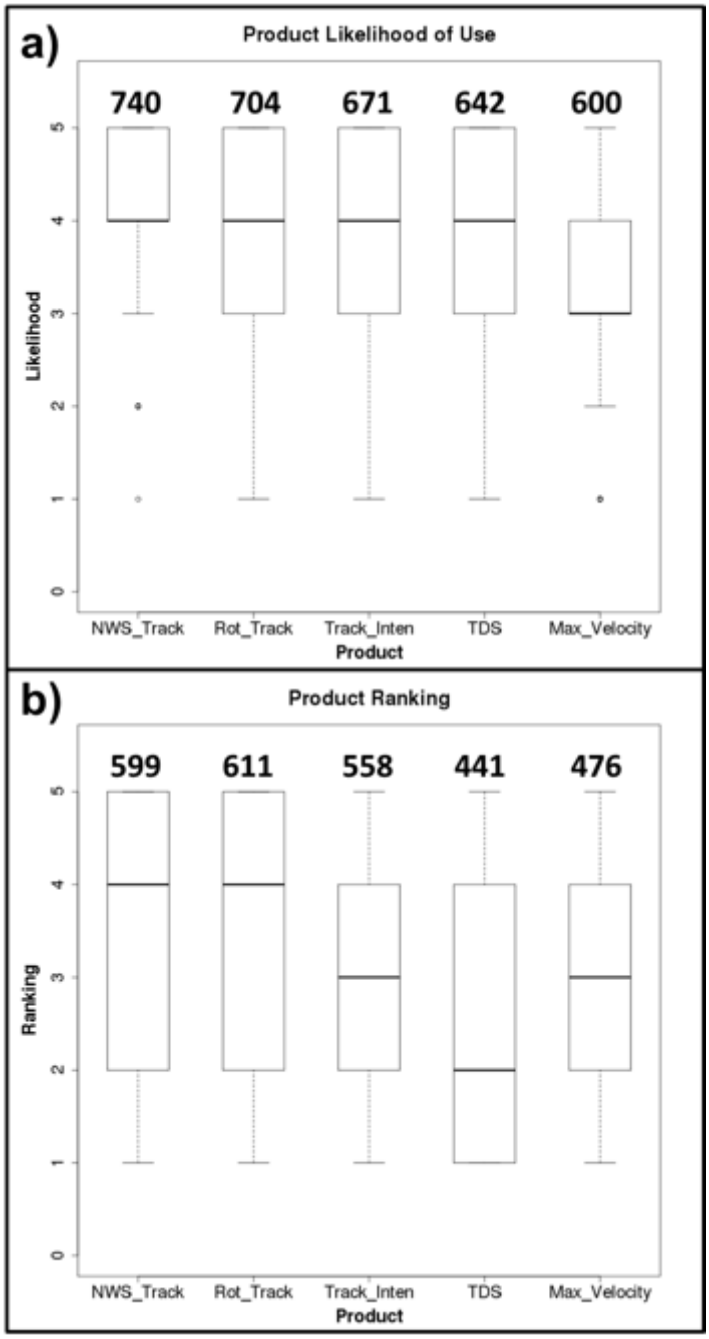

*Box plots showing distribution of survey participants' a) likelihood of using each product from "not at all likely" (1) to "extremely likely" (5) and b) ranking of each product from 1 (worst) to 5 (best). Bold numbers represent each product's score calculated by summing the numeric scores provided by the participants. Higher numbers indicate a greater likelihood of use or higher ranking. Box edges are the lower (Q1) and upper (Q3) quartiles, the horizontal black line is the median, and the lower and upper whiskers represent Q1-1.5*IQR and Q3+1.5*IQR respectively, where IQR is the interquartile range. Outliers are indicated by dots.*

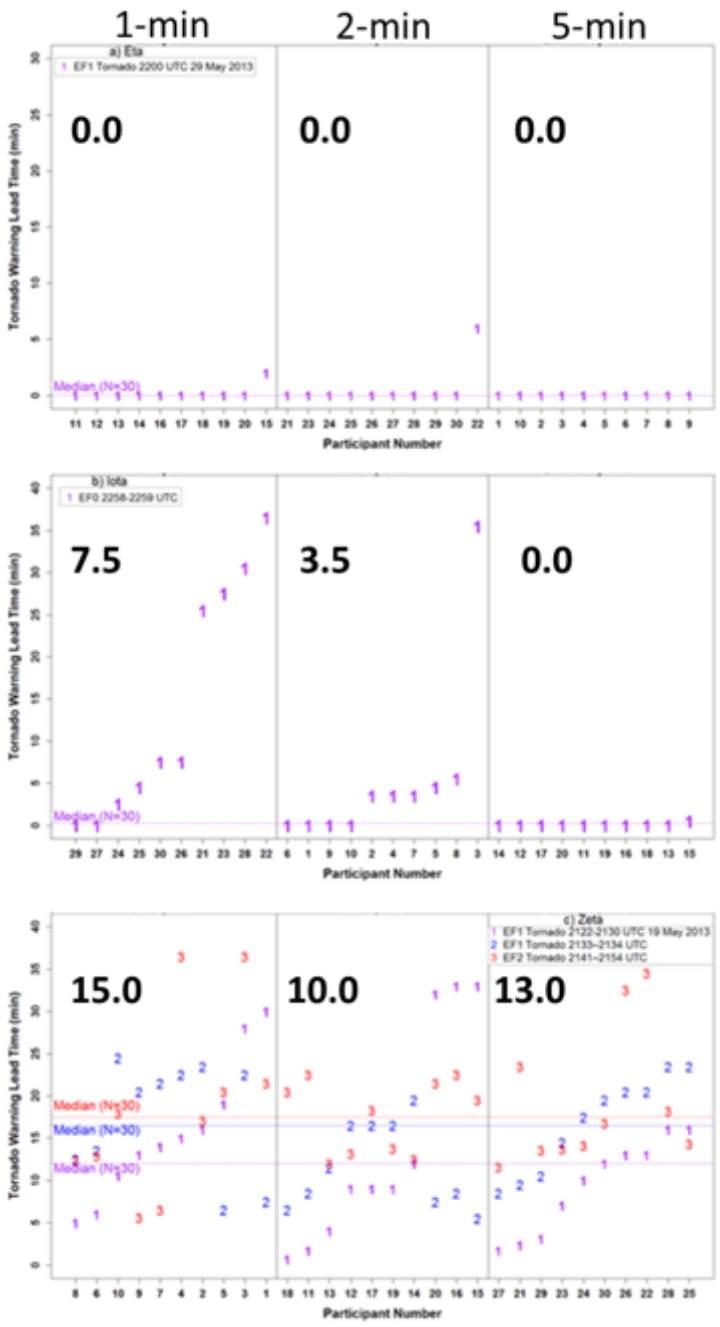

Distribution of forecasters' tornado warning lead time (min) organized by radar update time (1-min, 2-min, and 5-min). Bold numbers indicate median lead time (min) for warnings issued using each radar update time. First, second, and third tornado reports are denoted by numbers 1, 2, and 3 (magenta, blue, and red). For each report, the median severe warning lead time (min) for the full distribution is given by a dotted and annotated line (magenta, red, and blue).

b. Advancing Scientific Understanding of Z_{DR} Column Evolution Relative to Mesocyclones and Upper-Level Reflectivity Cores Through the Use of Rapid-Scan Dual-Polarization Radar Data

Charles Kuster, Jeff Snyder, and Terry Schuur (CIMMS at NSSL), and Pamela Heinselman (NSSL)

With the recent dual-polarization upgrade of the National Weather Service (NWS) radar network, new data is now available to NWS forecasters. One new signature forecasters can see is the Z_{DR} column, which is an indicator of thunderstorm updraft intensity. To examine the evolution of this potentially beneficial signature, we used a research Weather Surveillance Radar-1988 Doppler radar located in Norman, Oklahoma (KOUN) to collect rapid-update volumetric data of severe and nonsevere thunderstorms using 90-degree sector scans. In an ongoing research effort, we are examining the evolution of Z_{DR} columns, mesocyclones, and upper-level reflectivity cores using rapid-update radar data in an effort to integrate Z_{DR} columns into conceptual models typically employed by NWS forecasters during severe weather events. We also aim to identify any useful trends or precursor signatures in Z_{DR} column evolution that might enhance forecaster ability to anticipate certain threats (e.g., hail, tornado, etc.), thereby enhancing their ability to alert the public to impending danger. The analysis thus far has shown clear increases in Z_{DR} column size and magnitude prior to severe hail reports (figure below). Upon completing analysis for all cases, we will conduct an in-depth qualitative and statistical analysis to definitively identify operationally relevant trends in Z_{DR} column evolution.

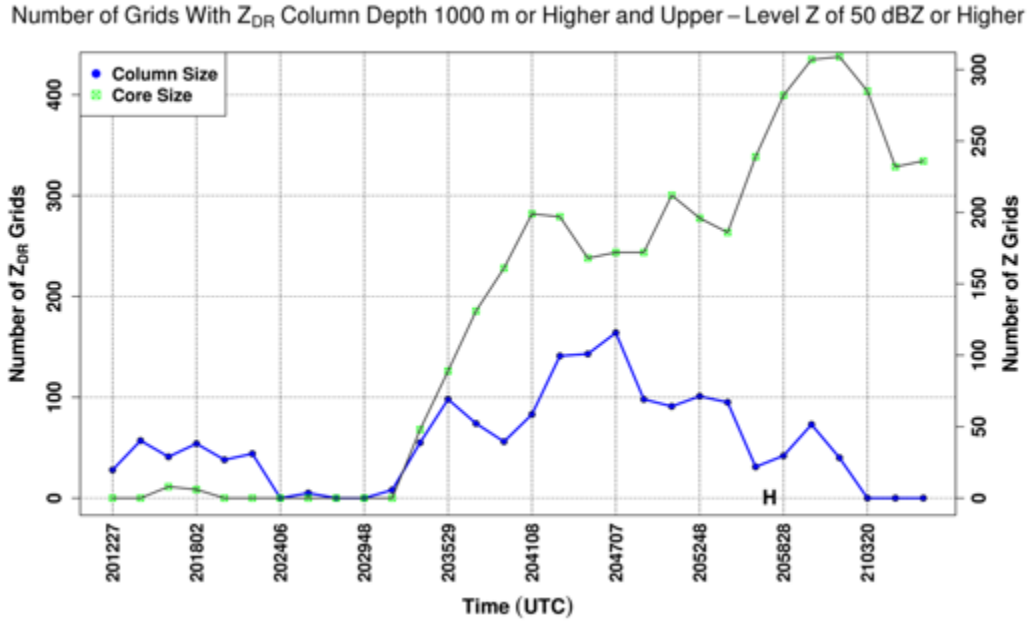

*Z_{DR} column size (blue line) and -20C reflectivity core size (black line with green markers) for a nontornadic supercell that occurred on 9 May 2016 in Oklahoma. Size is approximated by summing the number of 0.0025° by 0.0025° latitude/longitude grids where Z_{DR} column depth is 1000m or higher and -20C reflectivity is 50 dBZ or higher. The **H** represents the time of a severe hail report.*

Publications

Kuster, C. M., P. L. Heinselman, and T. J. Schuur, 2016: Rapid-update radar observations of downbursts occurring within an intense multicell thunderstorm of 14 June 2011. *Weather and Forecasting*, **31**, 827–851.

Kuster, C. M., P. L. Heinselman, J. C. Snyder, K. A. Wilson, D. A. Speheger, and J. E. Hocker, 2017: An evaluation of radar-based tornado track estimation products by Oklahoma public safety officials. *Weather and Forecasting*, In Press.

Wilson, K. A., P. L. Heinselman, C. M. Kuster, D. M. Kingfield, and Z. Khang, 2017: Forecaster performance and workload: Does radar update time matter? *Weather and Forecasting*, **32**, 253-274.

4. MPAR Engineering

Objectives

Continue research and development in collaboration with NSSL and other government, industry, and university partners to determine the usefulness of phased array radars (PAR) for meteorological observations in a multifunction environment. The National Weather Radar Testbed Phased-Array Radar (NWRT/PAR) in Norman, OK was the first of its kind to study meteorological applications of this technology. It is now undergoing engineering upgrades to take advantage of modern PAR technology and to add a dual-polarization capability. Theoretical, simulation, and experimental studies are being conducted to determine the feasibility of dual-polarized phased-array antenna systems along with the applications of using the radar for multiple functions (e.g., aircraft and weather surveillance). Other areas of research and development include the design of fast and adaptive scanning techniques, the refinement of radar functional requirements, the exploration of pulse-compression techniques, and the evaluation and implementation of advanced digital signal processing techniques.

Accomplishments

a. MPAR Advanced Technology Demonstrator

Christopher Curtis, Eddie Forren, Doug Forsyth, Igor Ivić, Rick Rhoton, Montana Rowe, David Schvartzman, Sebastián Torres, Danny Wasielewski, and Allen Zahrai (CIMMS at NSSL); Kurt Hondl, Mark Benner, and Micheal Shattuck (NSSL); and other government, industry, and university collaborators.

The Advanced Technology Demonstrator (ATD) is being developed in support of Multifunction Phased-Array Radar (MPAR) risk reduction. It will replace the current SPY-1A antenna at the NWRT with an S-Band, 4-m diameter, dual-polarization, active phased array. The system's operating capabilities are intended to serve as a basis for ongoing engineering and meteorological research at NSSL. The ATD leverages several prior investments in order to provide a flexible, useful system while striving to keep cost and risk low. The antenna system is based around tile-able array panels developed under the MPAR Government Proof-of-Concept Technology Risk Reduction Program carried out by MIT/Lincoln Laboratory. The receiver and exciter electronics leverage work done by General Dynamics Mission Systems (GD) for the United States Navy in support of the Air and Missile Defense Radar development. The radar control system

leverages the work done by GD for the Office of Naval Research under the Digital Array Radar and Affordable Common Radar Architecture (ACRA) programs. Finally, the weather signal processor (including the inter-process-communication infrastructure, system control and monitoring, techniques, and algorithms) leverages the work done by CIMMS and NSSL for the original SPY-1A-based NWRT/PAR. Accomplishments by CIMMS staff in three main areas are described next: programmatic, application software, and facilities.

Programmatic Support. CIMMS staff supported programmatic ATD efforts by actively participating in planning and design meetings, by providing input to scheduling decisions, outlining and reviewing system requirements and system design documents, and supporting programmatic milestones such as periodic design review meetings. Several team members attended a calibration meeting at MIT/Lincoln Laboratory, which resulted in outlines for scan strategies and processing routines for the necessary array and weather calibrations. In addition, the team continues to support regular conference calls for status updates and coordination of the entire ATD project.

Application Software. CIMMS staff continued to lead the Application Software portion of the ATD, which combines software developers and engineers from CIMMS and GD. The required functionality of the Application Software includes generating weather- and aircraft-surveillance products, providing scan control and high-level radar control, system status monitoring, and archiving and display of data and products. The goal for the design of the Application Software is to maximally leverage legacy NWRT and ACRA software to reduce risk. The figure below shows the functional architecture of the ATD Application Software and delineates responsibilities between the CIMMS/NSSL (blue) and GD (green) teams.

During FY17, we developed the functionality for multifunction scan generation, including the implementation of control and status reporting through the weather Human-Machine Interface (HMI). In preparation to integrate the software developed by CIMMS/NSSL with the one developed by GD, we created a real-time weather-processing thread by integrating the multifunction scan generation function with weather-data-simulation, weather-data-ingest, and weather-signal-processing functions. During this process, we merged the legacy weather-data preprocessor with the weather-data ingest software. This overcame some design problems from the legacy preprocessor and laid the groundwork for supporting the ATD's expected larger number of data channels and higher data rates. The current design can support up to 10 channels or 2.5 Gbit/s of I/Q data, which is ~10 times the data rate of the legacy NWRT. As the first stage of integration, we created a real-time weather-processing thread that included GD's digital-receiver data simulator along with data-routing, pulse-compression, and weather-data-transfer functions. In this first integration phase, we used GD's manual scan generation. The ATD's newly developed multifunction scan generation was included in the second integration phase.

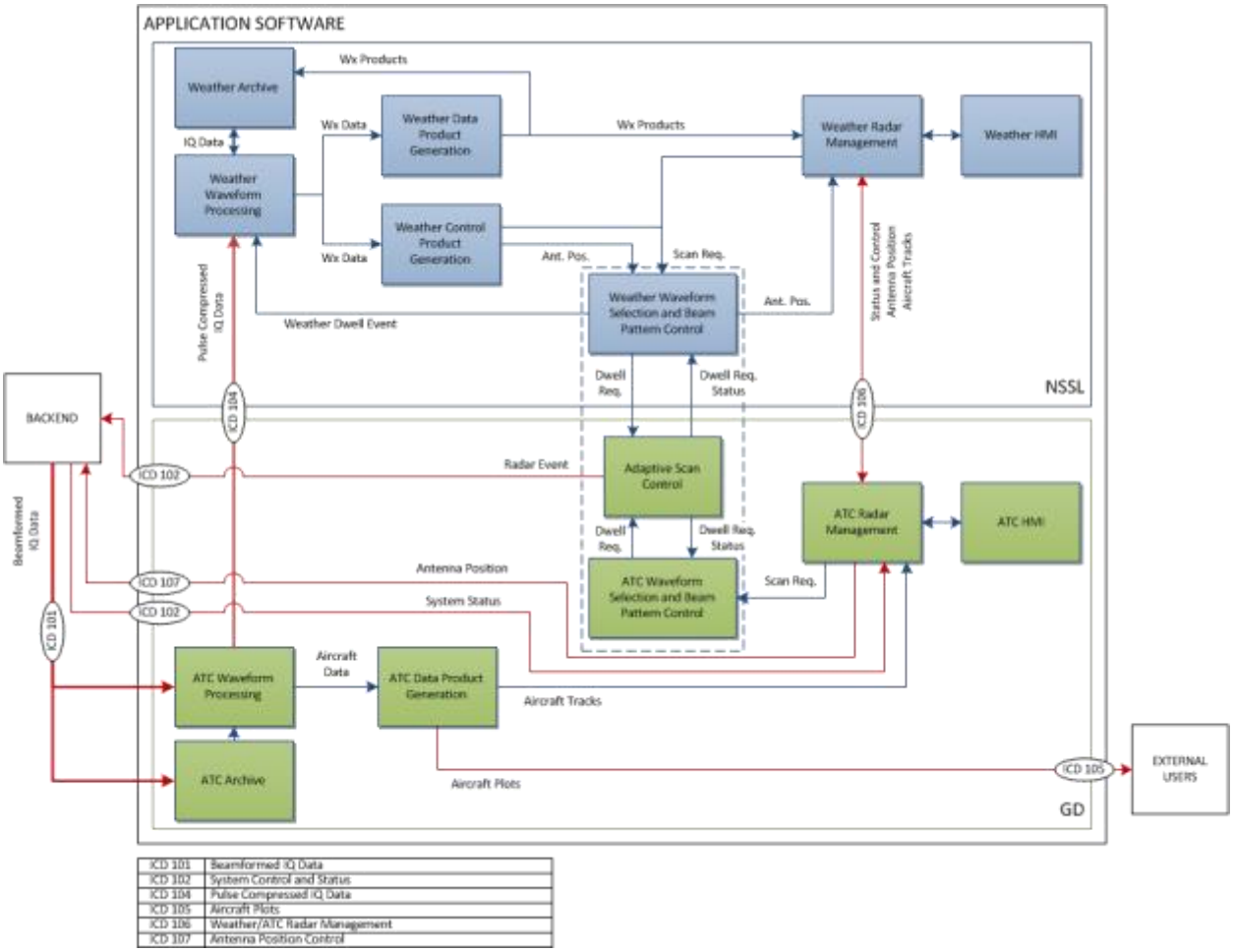

Block diagram of the application software for the ATD. The application software integrates legacy and new software developed by CIMMS/NSSL (blue blocks) and GD (green blocks).

During this reporting period, we also improved and validated the weather signal-processing code. We implemented and tested the triple-PRF function that is needed for the lower tilts of the baseline ATD scanning strategy. Additionally, we validated the real-time weather signal processing implementation against its MATLAB counterpart, which was also developed by CIMMS/NSSL scientists. This involved producing weather I/Q and product data using the real-time software, and iteratively running comparisons of the weather radar variables produced by the real-time and MATLAB applications. Through detailed analyses of these comparisons, we were able to identify and correct several software problems. To facilitate this process, we developed additional tools (example in figure below) on the real-time side to also show intermediate results graphically.

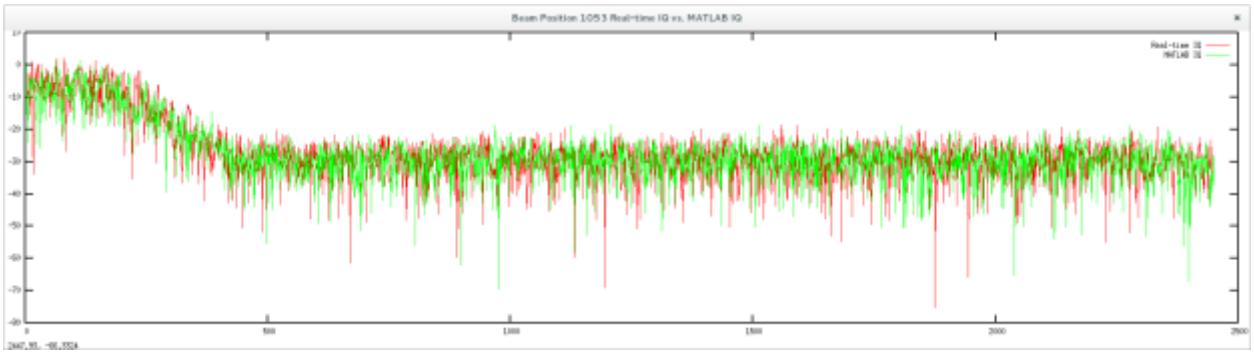

Graphical comparison of intermediate real-time and MATLAB I/Q data used to debug and validate the weather signal-processing functionality of the ATD.

We also devoted significant attention to the weather-radar-management function and the weather HMI since the ACRA radar-management function's treatment of subsystems and status reporting was significantly different from those of the legacy NWRT. In addition, we developed new communication channels between the weather radar manager and the air-traffic-control (ATC) radar manager, and between the weather signal processor and the ATC radar manager. We also added appropriate subsystem buttons for control and status to the weather HMI along with new buttons for pedestal control and status reporting. Since the legacy NWRT radar manager and HMI had been developed over several years by a developer who retired, much of this work involved reverse engineering the legacy NWRT code. In refactoring this code, we developed a re-useable GUI component class hierarchy. This allowed much of the same code to be used for many new parts on the weather HMI, even when the behavior is slightly different across these parts. Much of this work focused on simplifying the application and improving its appearance. A screen capture of the latest system panel of the weather HMI is shown in the figure below.

Throughout this period, we devoted significant efforts to test, report, and fix bugs in the application software. Additionally, we enhanced the CIMMS/NSSL cluster manager to run and monitor the GD portion of the application software. We also addressed system-administration problems, including configuration of 'ssh' to allow no-prompt login, configuration of precision timing protocol (ptp) in software mode, configuration of real-time processing and 'corefile' dumping, and 'nfs' configuration for disk-usage reporting. To simplify future installations of the application software, we developed partially automated CentOS installation scripts and added a required list of third-party tools.

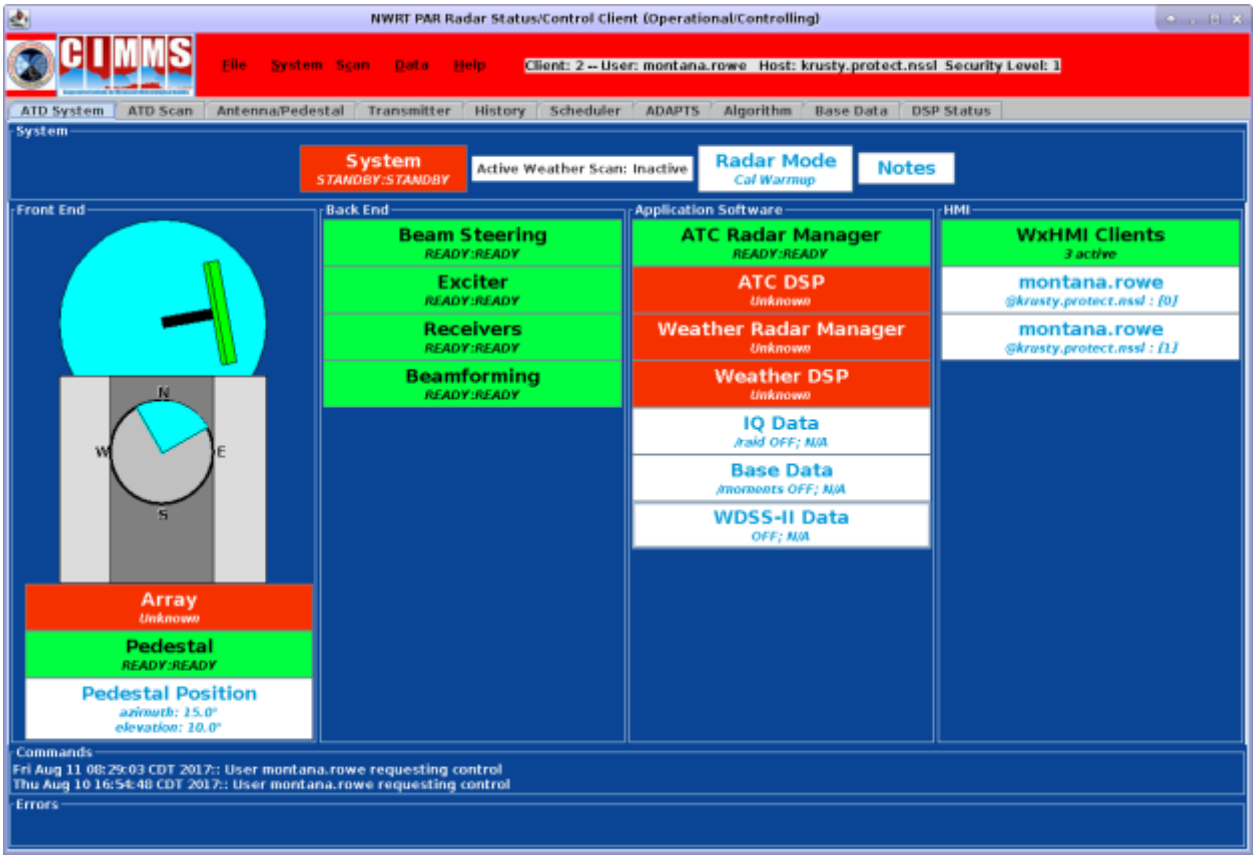

Screen capture of the refactored weather HMI system panel for the ATD as of the end of FY17. This is work in progress.

Facilities. In August of 2016, the SPY-1A antenna and associated radar equipment were removed from the NWRT facility. CIMMS and NSSL employees then began work to prepare the facility for the installation of the ATD radar. Work performed by CIMMS staff include redesigning the electrical power distribution, revising the network layout, updating the safety interlock circuit, planning the physical layout of the equipment and cabling, and working with a contractor to design several mechanical structures to be fabricated. CIMMS engineers also worked on the calibration tower, an integral part of the measurement and calibration infrastructure for the ATD. Contributions include: design of control and RF equipment, progress on land leasing and physical relocation of the tower, and documenting the physical infrastructure and use cases. During April and May 2017, CIMMS employee Daniel Wasielewski was on temporary assignment at MIT Lincoln Laboratory. This assignment provided opportunity to improve the coordination of systems engineering efforts between CIMMS/NSSL and MIT Lincoln Laboratory, reducing risk and timeline for the upcoming functional integration and test phase of the ATD installation. Mr. Wasielewski was also involved in accelerating the testing and troubleshooting of the antenna array.

b. MPAR Dual Polarization Demonstrator

Igor Ivić, Daniel Wasielewski, and Allen Zahrai (CIMMS at NSSL)

One of the main challenges of using PAR technology for weather observations is the implementation of dual polarization with acceptable isolation between horizontal and vertical channels, which is essential for accurate interpretation of polarimetric-variable estimates. Simulations and measurements on phased array antennas have shown that such isolation cannot be achieved only by the antenna hardware alone. Hence, additional modifications to the radar system are required to attain supplementary isolation of orthogonal channels. To achieve this, a pulse-to-pulse (or inter-pulse) phase coding of the transmitted pulses in the horizontal and vertical channels is being evaluated. In previous years, this scheme was investigated using analytical derivations as well as simulated and experimental time-series data. Pulse-to-pulse phase coding was shown to provide additional isolation with a small increase in the standard deviation of estimates (compared to the perfect isolation between orthogonal channels).

To evaluate the performance of polarimetric planar phased array technology with respect to the national weather mission, NSSL and the FAA commissioned the construction of a 10-panel, mobile, polarimetric, phased-array system (referred to as the Ten Panel Demonstrator or TPD) by MIT/Lincoln Laboratory. Previously, a test plan was developed to exercise the capabilities of the demonstration system; the plan focuses on absolute and relative accuracy measurements. Absolute measurements resolve the system's capability to accurately identify hydrometeors, while relative measurements examine the correct calibration of the system as well as off-broadside cross-polarization impacts. An analysis of the performance will play an ongoing important role in defining the expected performance of future systems, including the replacement of the SPY-1A antenna on the NWRT PAR (see previous project).

Having addressed the most pressing reliability issues in FY16, numerous data sets with the antenna pointing at vertical incidence (the so-called 'birdbath mode') were collected in FY17. Due to the lack of proper infrastructure to perform the absolute calibration of copolar powers, the experimental efforts were aimed mainly at characterizing the array behavior and the experimental evaluation of the pulse-to-pulse phase coding (including the associated effects on Doppler moments and polarimetric variables). The latter revealed an unexpected broadening of spectrum-width estimates caused by phase coding. Several methods were devised to mitigate this effect. The array characterization results indicate strong cross coupling between the horizontal (H) and vertical (V) channels, which exceeds the levels predicted by the theory and simulations. This may be due to the significant coupling in the antenna backplane hardware and/or the transmission lines behind the antenna. Application of the pulse-to-pulse phase coding produced results with visible differences compared to those from non-phase coded data. These differences indicated reduction of cross coupling as predicted by the analytical derivations and simulations. Given the subarray architecture of TPD, further efforts have been targeted at improving the amplitude and phase alignment of signals generated by individual subarrays (which affects the quality of the summed receive

signal). To this end, a method using weather data was devised. Additionally, to further improve the performance of pulse-to-pulse phase coding, a spectral domain filtering method is being developed. This method removes the portion of the cross-coupled signal, which is left intact by the original pulse-to-pulse phase coding application (which operates in time domain only). In addition to the weather data collections, experiments using an external far-field continuous-wave (CW) transmitter were conducted. These were aimed at characterizing the system stability as well as the quality of the antenna receive patterns. These experiments also included the measurements of the differences between the H and V received powers as function of the beam steering angle (to prototype calibration measurements that are planned for the ATD). These results were compared to the corresponding results from weather data measurements.

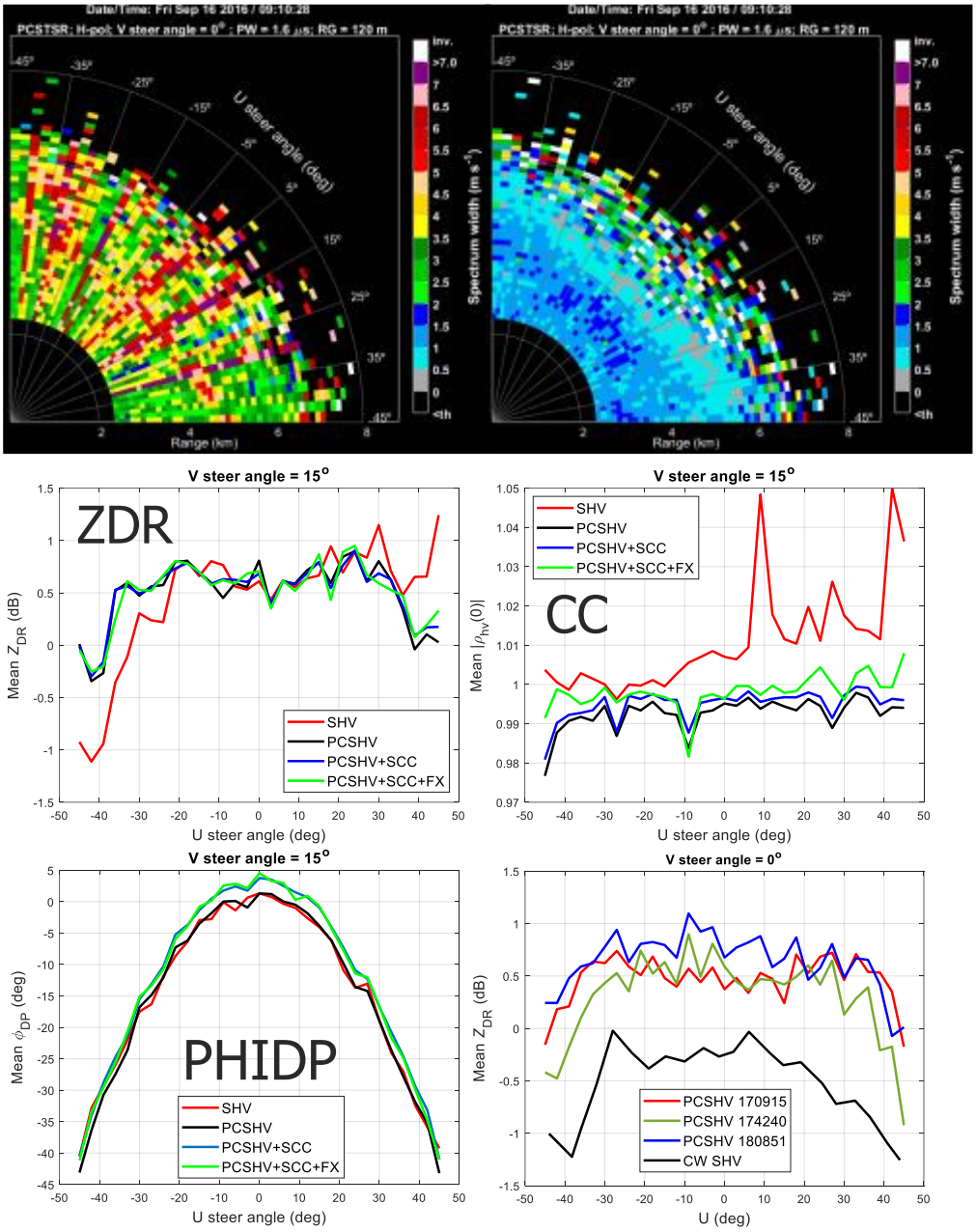

Spectrum width fields from phase-coded data before (top left panel) and after (top right panel) correction. Range-averaged differential reflectivity (middle left panel), correlation coefficient (middle right panel), and differential phase (bottom left panel) from data collected in the 'birdbath mode' as function of electronic beam steering angle. SHV denotes the non-phase coded simultaneous transmit and receive mode, and PCSHV denotes SHV with phase coding processing in time-domain only. PCSHV+SCC denotes PCSHV with the amplitude and phase alignment, and PCSHV+SCC+FX denotes PCSHV+SCC with the spectral domain filtering. The bottom right panel shows the differential reflectivity from multiple weather data collections (time labeled as hour-min-sec) and the differential reflectivity measured using the CW signal (black line labeled as CW SHV).

c. MPAR Program Support

Sebastian Torres, Christopher Curtis, Doug Forsyth, Igor Ivić, Danny Wasielewski, and Allen Zahrai (CIMMS at NSSL)

CIMMS continues to support the MPAR program and the MPAR program manager on several technical and programmatic fronts. Support consists of actively participating in the MPAR Government Engineering Team (GET), giving presentations at meetings with industry and other government organizations, reviewing proposal and technical documents, participating in internal and external technical discussions, and assisting the program manager as needed.

d. PAR Dual Polarization

Igor Ivić and Djordje Mirković (CIMMS at NSSL), and Dusan Zrnić (NSSL)

Search for novel methods to improve the polarimetric performance of phased array radars (PAR) is an important part of the effort to determine their usefulness for meteorological observations. In that regard, creating controlled realistic environments in which these methods can be tested is essential. The first step towards this goal is obtaining realistic antenna radiation patterns. The patterns alone, however, do not provide direct information about the ensuing errors in radar measurements. Hence, in previous years, a method using analytical formulas was developed to compute the biases of polarimetric variable estimates from radiation patterns. Also, a method to produce simulated weather-like time series that account for polarimetric PAR (PPAR) effects (i.e., cross coupling and antenna gain variations with beam steering) was developed. Both methods, however, depend on the accuracy of computed (see next project) or measured radiation patterns to produce valid results. Due to modeling and computational complexity, obtaining radiation patterns of large arrays using computational electromagnetics (CEM) tools is extremely difficult. A simpler (and less accurate) approach is to combine single-element radiation patterns computed using CEM with the array factor. The convenience of this approach is that repeated CEM computations to produce patterns for each electronic beam steering direction are not required. Thus, due to the lack of full array models, the array-factor based patterns were used to produce preliminary antenna patterns for the TPD and the ATD radars. Such approach does not consider array effects (e.g., mutual coupling, diffractions, array impedance as well as the hardware effects behind the antenna). Nonetheless, it proved to be extremely useful in investigation of PPAR aspects.

In FY17, the array-factor based radiation patterns were used to investigate the effects of array tilt on the polarimetric performance of PAR. The results indicated that positive antenna tilt may increase cross coupling. These patterns were also used to test the performance of pulse-to-pulse phase coding as well as to predict, investigate, and verify effects observed in experimental data.

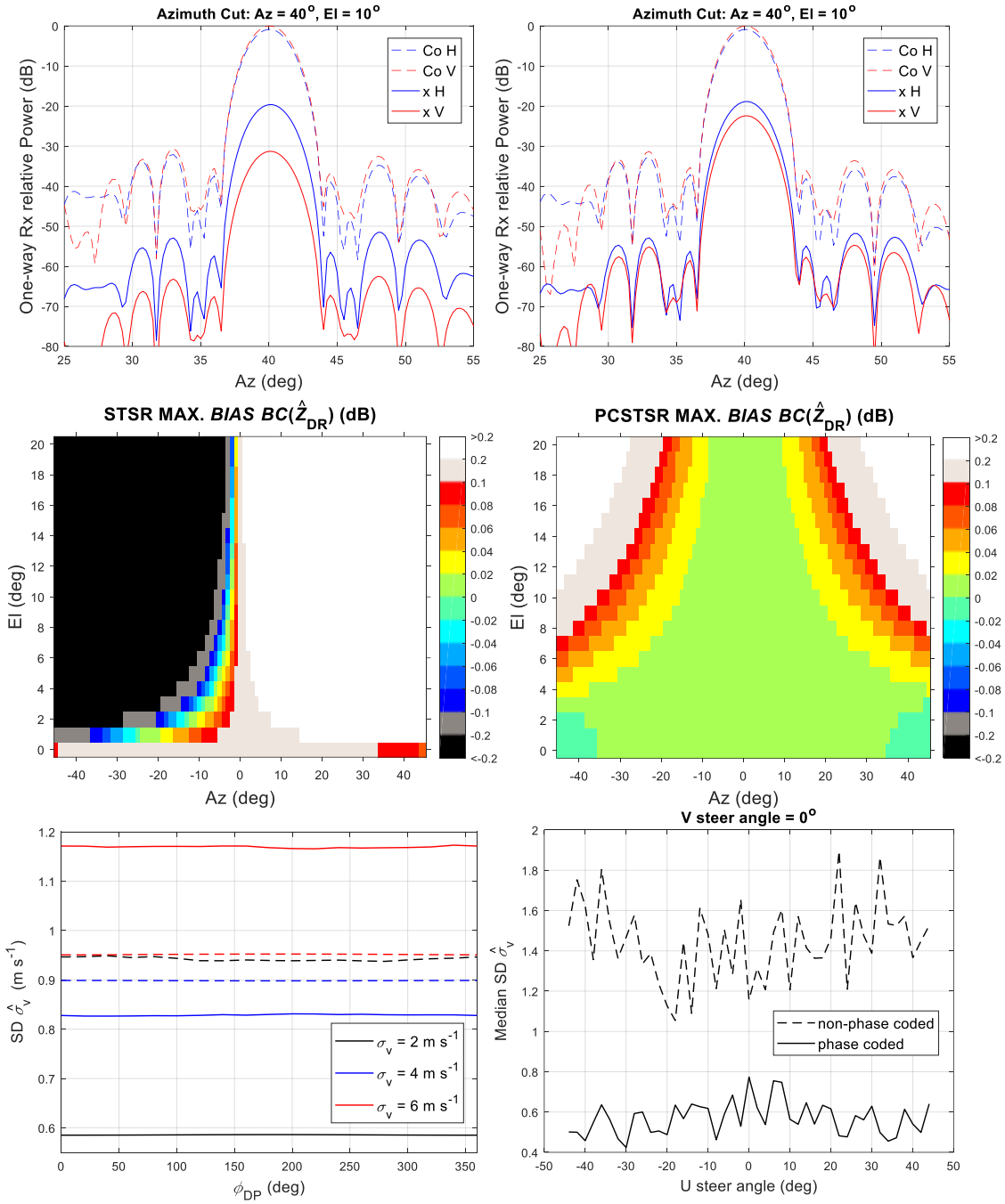

Copolar (Co) and cross-polar (x) array-factor-based receive patterns of the non-tilted (top left) and 5° tilted (top right) ATD antenna. Cross-coupling Z_{DR} bias before (middle left) and after the application of pulse-to-pulse phase coding (middle right). Spectrum width (σ_v) standard deviation (SD) for non-phase-coded (dashed lines) and phase-coded filtered data (full lines) produced via simulations (bottom left). Results predict SD reduction via filtering at σ_v = 2 m s^{-1}. Spectrum width SDs measured from TPD data corroborate the simulation results (bottom right).

e. PAR CEM Modeling

Djordje Mirković and Igor Ivić (CIMMS at NSSL), and Dusan Zrnić (NSSL)

Computational electromagnetics (CEM) tools can be used to facilitate the evaluation of dual-polarization performance on PAR using simulations and analytical considerations, where the goal is to produce realistic antenna radiation patterns. To produce accurate patterns for the Ten Panel Demonstrator (TPD), the first and the most important step was to produce an accurate model of the three-layer stacked patch antenna. In FY17, an ambiguity in the radiation element topology was observed: the radiation-element blueprints received from engineers at the Georgia Tech Research Institute (GTRI) and Lincoln Laboratory (LL) were different. The slight difference in the radiation element design caused a discrepancy between models in the differential gain, one of the most important polarimetric properties of the antenna. Once the TPD blueprints were examined, the topological model provided by LL was accepted as the correct model. The issue in the GTRI provided model was traced to the absence of the final "protective" (or radome) layer. Using the LL radiation element topology, a model of a single panel (consisting of 8x8 radiation elements) was developed using the WIresPLate-Dielectrics (VIPL-D) CEM tool. The panel was simulated in a single-excited-element mode for comparison with measurements on the panel delivered to NSSL by LL. Measurements of the panel with single-element excitation were carried out in the low-frequency anechoic chamber at the Advanced Radar Research Center (ARRC). The results showed remarkable agreement; this provided assurance in the validity of the CEM approach, which accounts for mutual coupling among elements, diffraction effects, as well as variable array impedances. Furthermore, in a set of data collected at vertical incidence using the TPD radar, a larger-than-expected variation of differential reflectivity (Z_{DR}) estimates was observed. A possible cause was traced to a 3-mm deep tub created by the TPD radome fixture, which fills with water (thus creating a "wet radome") and may change the radar behavior. To verify this assumption, a differential gain with and without the water layer on top of the radome was computed using CEM for a single panel. The results corroborated that the presence of a water layer can significantly increase the variation of differential gain. A development of a complete TPD model using CEM is underway.

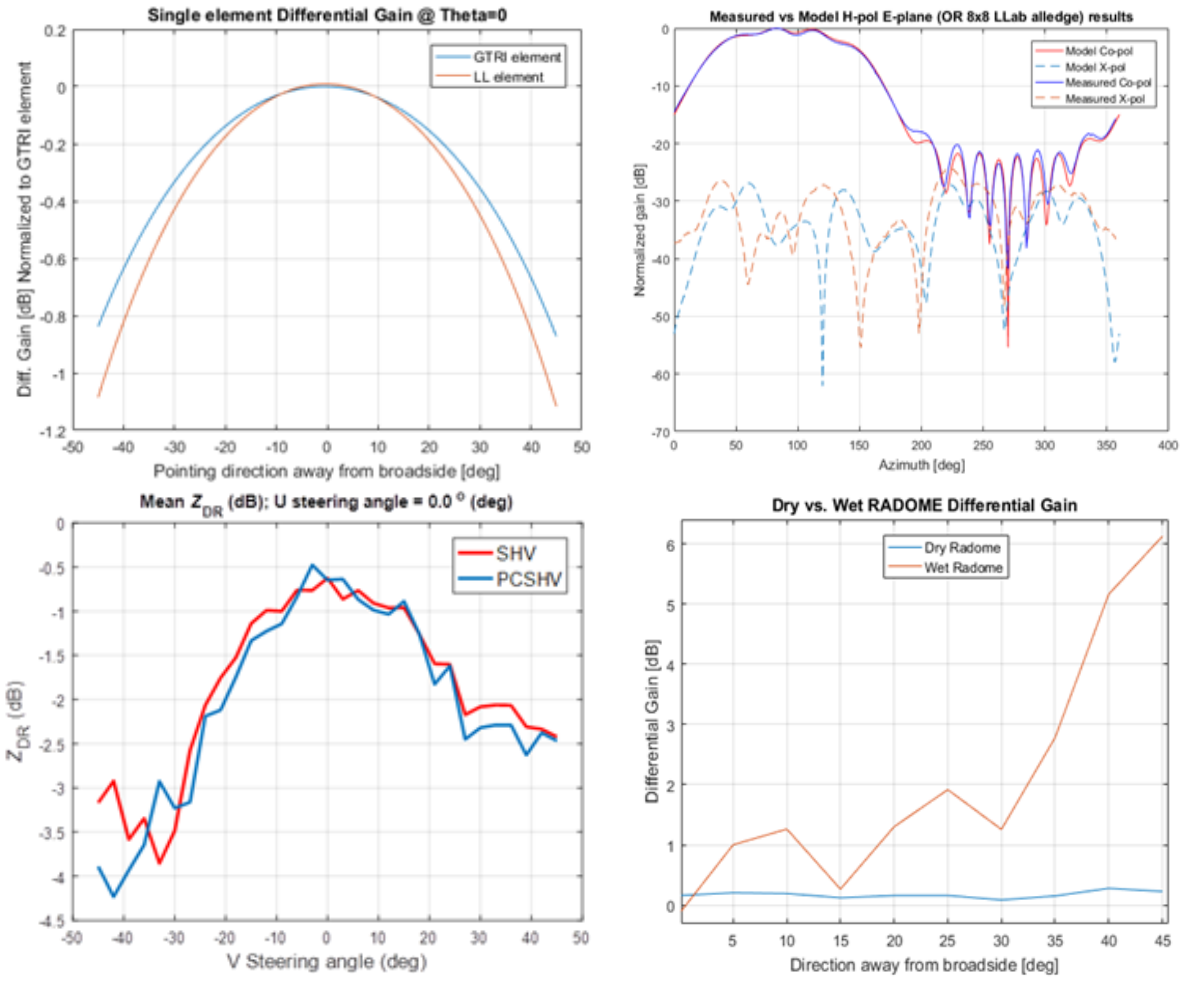

Comparison of the radiating element differential gain for the GTRI and LL elements (top left panel), and comparison of measured and simulated single-panel results when a single embedded element is excited (top right panel). Z_{DR} measured with the TPD antenna pointed upwards under the effects of a "wet radome" (bottom left panel), and a single-panel model with (wet) and without (dry) a water layer on top of the radome structure (bottom right panel).

f. PAR Pulse Compression

Sebastián Torres, Christopher Curtis, and David Schvartzman (CIMMS at NSSL)

With more weather radars relying on low-power solid-state transmitters, pulse compression has become a necessary tool for achieving the sensitivity and range resolution that are typically required for weather observations. While pulse compression is well understood in the context of point-target radar applications, the design of pulse-compression waveforms for weather radars is challenging because requirements for these types of systems traditionally assume the use of high-power transmitters and short conventional pulses.

During FY17, we proposed a requirement-driven approach for the design of pulse-compression waveforms for weather radars. Because explicit requirements on the range weighting function (RWF) are typically not provided, the criteria used for the antenna-sidelobe envelope on the WSR-88D were extended to derive an analogous range envelope for the RWF. Additionally, we proposed an optimization framework that produces minimum-bandwidth pulse-compression waveforms that meet high-level system requirements. This proposed framework considers the impact on the RWF of the transmitted waveform and also of any range-time signal-processing technique that may be needed to meet data-quality and/or update-time requirements. To demonstrate the generality of the proposed approach, fitness functions were tailored for three processing scenarios: pulse compression without additional range-time processing (PC), pulse compression with adaptive-pseudowhitening processing (PC + APTB), and pulse compression with incoherent-averaging processing (PC + IAB). The performance of these waveforms was illustrated using simulations based on real weather data fields, and results were compared to the performance of conventional, high-power transmitter.

g. PAR Signal Processing: ATD Digital Signal Processor

David Schvartzman, Christopher Curtis, and Sebastián Torres (CIMMS at NSSL)

As new technology becomes available, new and more sophisticated signal processing techniques can be applied and implemented on weather radars. Signal processing is a critical element of radar systems, and its constant enhancement is fundamental for continued improvements in data quality. The main goal of this work is to re-design and optimize the CIMMS/NSSL radar DSP software to produce a flexible platform that can be used to develop, test, and demonstrate advanced signal-processing techniques. The Advanced Radar Techniques (ART) team at CIMMS/NSSL has been developing and upgrading a research DSP that incorporates the latest signal processing techniques. Some of these are implemented in the WSR-88D radars, and others are currently under development and have not been transferred to operations yet. Our work during FY17 has resulted in a complete re-designing the DSP to make it more versatile in handling different radar modes (e.g., uniform PRTs, SZ-2 phase coding, Triple-PRF) and to incorporate new signal processing techniques in a modularized fashion.

The new DSP architecture is being used to develop and test algorithms that will be implemented on the Advanced Technology Demonstrator (ATD). For example, a new Triple-PRF mode was incorporated into the re-designed DSP to resolve range-and-velocity ambiguities, which are exacerbated with the use of long pulse-compression waveforms. This new mode also includes a pulse-merge capability that combines data obtained from two pulses that are transmitted back-to-back using two frequency sub-bands. One of these pulses uses an optimum-bandwidth pulse-compression waveform (a long pulse), the other pulse is referred to as a “fill pulse” and resembles the typical 250-m WSR-88D pulse (a short pulse) with less power. The fill pulse is used to provide data in the blind range of the longer pulse compression waveform.

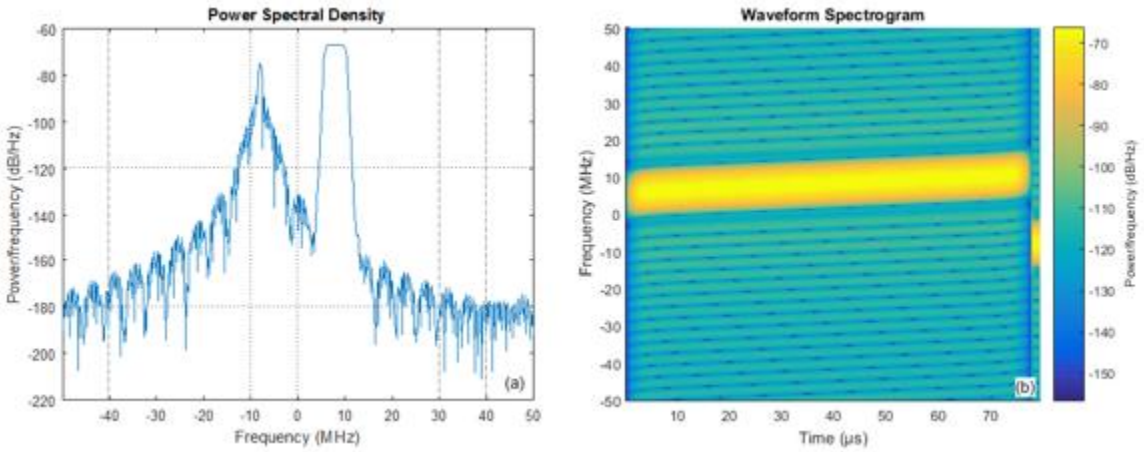

Power spectral density of waveform used in the ATD scan strategy (left panel). Spectrogram showing the bandwidth and time length of the long pulse-compression waveform and the short CW waveform (right panel).

Based on realistic simulations, we produced received IQ data and processed them using the re-designed DSP. Radar variables processed with the re-designed DSP are shown in the figure below. The same suite of processing functions was implemented in real-time for the ATD. With the latest signal processing techniques being tested and implemented in our DSP, we are improving data quality and ensuring that algorithms can perform as expected.

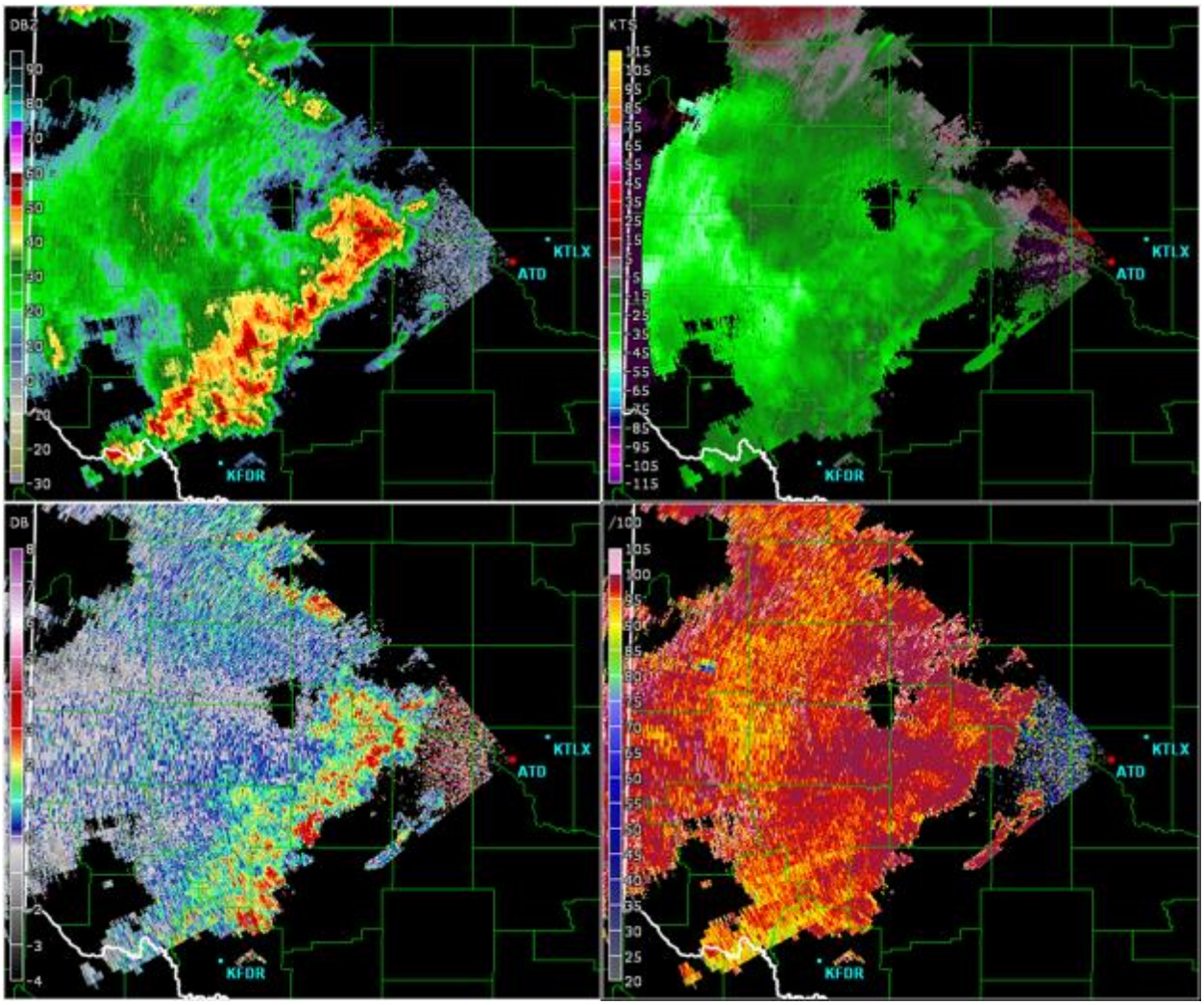

Example of radar variables (from left to right and top to bottom: reflectivity, Doppler velocity, differential reflectivity, and correlation coefficient) produced with the re-designed DSP using the ATD Triple-PRF mode.

h. PAR Signal Processing: Time-Series Simulator Using Archived NCEI Data

David Schvartzman and Christopher Curtis (CIMMS at NSSL)

The goal of this research is to design a realistic weather-radar time-series scenario simulator. The simulator is able to ingest archived dual-polarization level-II data and produce level-I data with the desired sampling and radar characteristics (e.g., pulse-repetition times, spatial resolution, antenna patterns, waveforms, etc.). This novel simulator is being used to model the ATD and to test signal processing techniques that will be implemented in the system, but it can also be used to simulate data from other types of radars. The simulator uses level-II weather radar data collected by WSR-88D radars, archived by the National Centers for Environmental Information (NCEI). The

data are first conditioned, and missing or censored data are filled in using a robust interpolation algorithm. Then, based on the six radar variables, scattering centers are generated in a grid that matches the desired spatial sampling. For each scattering center, a spectrum-shaping technique is used to create time-series data with the desired acquisition parameters. The effects of phase coding, pulse-compression, range-folding, waveform, and antenna pattern are incorporated in the data. The simulator can produce conventionally sampled data or range-oversampled data with the desired range correlation for range-time processing techniques. Furthermore, it adjusts the noise floor level to set the sensitivity based on the selected waveform power. The results of applying diverse signal processing techniques on the simulated data show that the simulator can be used to qualitatively analyze the impact of a variety of techniques and radar designs on radar observables for any archived weather scenario.

During FY17, we used the simulator to produce beamformed data with radar parameters and scanning strategies modeling the ATD. The data were used to run and validate the real-time digital signal processor, which is critical to achieve the goals of the ATD as a demonstrator system for improved weather-surveillance capabilities.

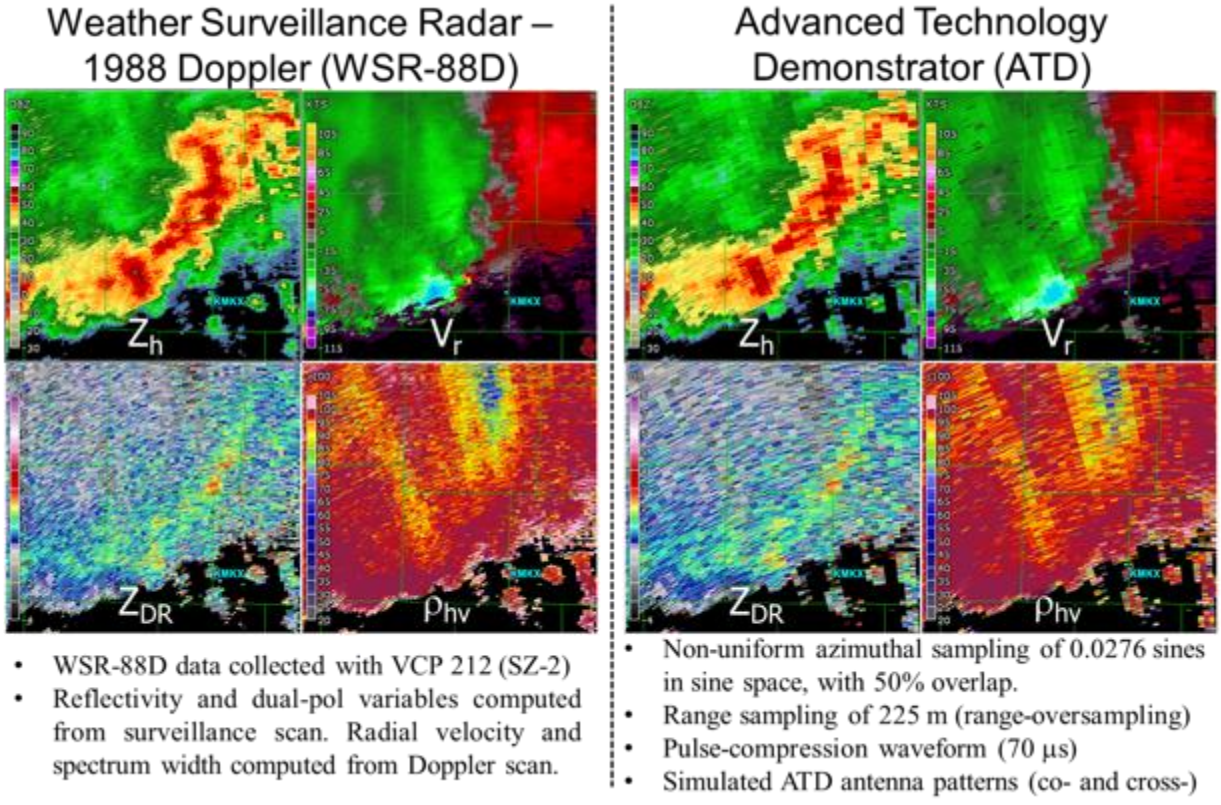

Comparison of WSR-88D data from KLOT on 13 July 2015 (left) and weather-radar data simulated using the ATD's radar system and sampling parameters (right). The azimuthal sampling of the simulated ATD data is, as expected, coarser, and range-time processing (adaptive pseudowhitening) is used to reduce the variance of estimates. Unlike the WSR-88D, the simulated ATD data assumes the use of pulse compression to meet sensitivity requirements.

i. PAR Data Quality: SENSR Simulations

Feng Nai, Jami Boettcher, and Christopher Curtis (CIMMS at NSSL)

The Spectrum Efficient National Surveillance Radar (SENSR) project aims to assess the feasibility of relocating the Air Route Surveillance Radar (ARSR) to S band. A critical component for achieving this overarching goal is to develop a set of well-defined technical requirements for SENSR's high-resolution weather surveillance mission to facilitate industry's design of potential solutions. Currently, the Preliminary Performance Requirements (PPR) are largely based on the capabilities of the existing WSR-88D. As a result, requirements specific to radars that use more advanced technologies (e.g. phased-array antenna, pulse compression techniques) are either missing or unclear in the PPR. Furthermore, some of the more stringent requirements in the PPR are likely to be significant cost drivers for SENSR. The team has identified several requirements in the PPR that could potentially be refined: antenna and range-sidelobe levels, spatial sampling (both azimuthal and range), sensitivity, and dwell time. A data-quality simulator was developed to demonstrate that any changes in requirements would not result in unacceptable loss in data quality or significant interpretation problems for forecasters.

During FY17, the existing weather-signal simulator (see previous project) was extended to simulate radar systems with user-defined antenna radiation patterns, range weighting functions, spatial sampling schemes, sensitivity levels, and dwell times. Typically, the requirements for antenna radiation patterns and range weighting functions are defined in terms of envelopes that must not be exceeded by the actual pattern or range weighting function. In our simulations, these envelopes defined by the requirements were used in place of antenna patterns and range weighting functions to illustrate the effects of worst-case scenarios and to allow the simulator to model a general system without having to define the exact configurations of a phased-array antenna. Different weather events were selected to quantitatively and qualitatively evaluate the impacts of changing requirements on data quality and on National Weather Service (NWS) forecast operations. Selection of the weather events for analysis was based on features that the WSR-88D system resolves well, and features that are mission critical to the NWS hazardous weather warning program.

The bow echo event shown in the first figure has characteristics particularly sensitive to antenna sidelobes with straight-line winds producing widespread tree damage (including large trees), some structural damage, and power outages. Qualitative impacts are explored using PPI images as in this figure, and quantitative impacts are shown using graphs as in the second figure.

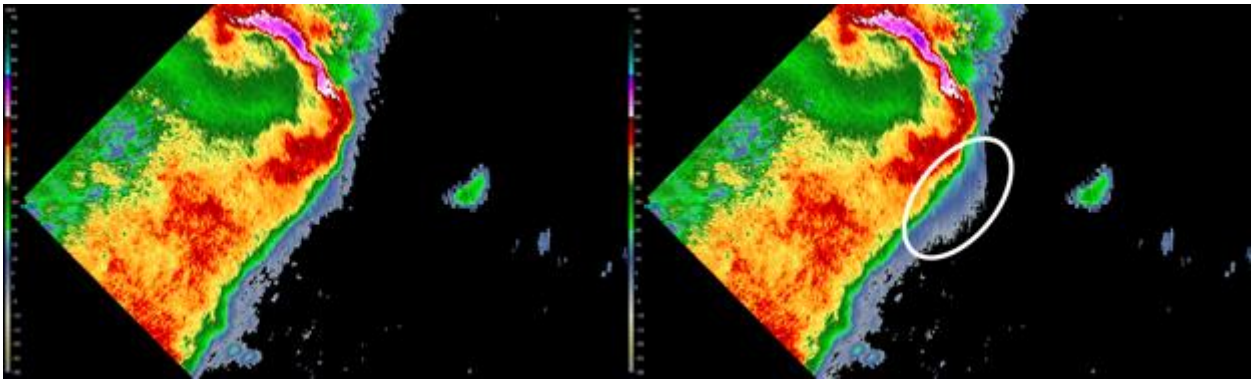

Simulated reflectivity fields for a radar with no antenna sidelobes (left) and for a radar with an antenna sidelobe envelope that has a -40 dB peak (right) corresponding to data collected with the KMPX on 11 June 2017 at ~14:23 UTC at an elevation of 0.5°. The most significant observed biases due to the -40 dB peak sidelobes are circled in the right panel.

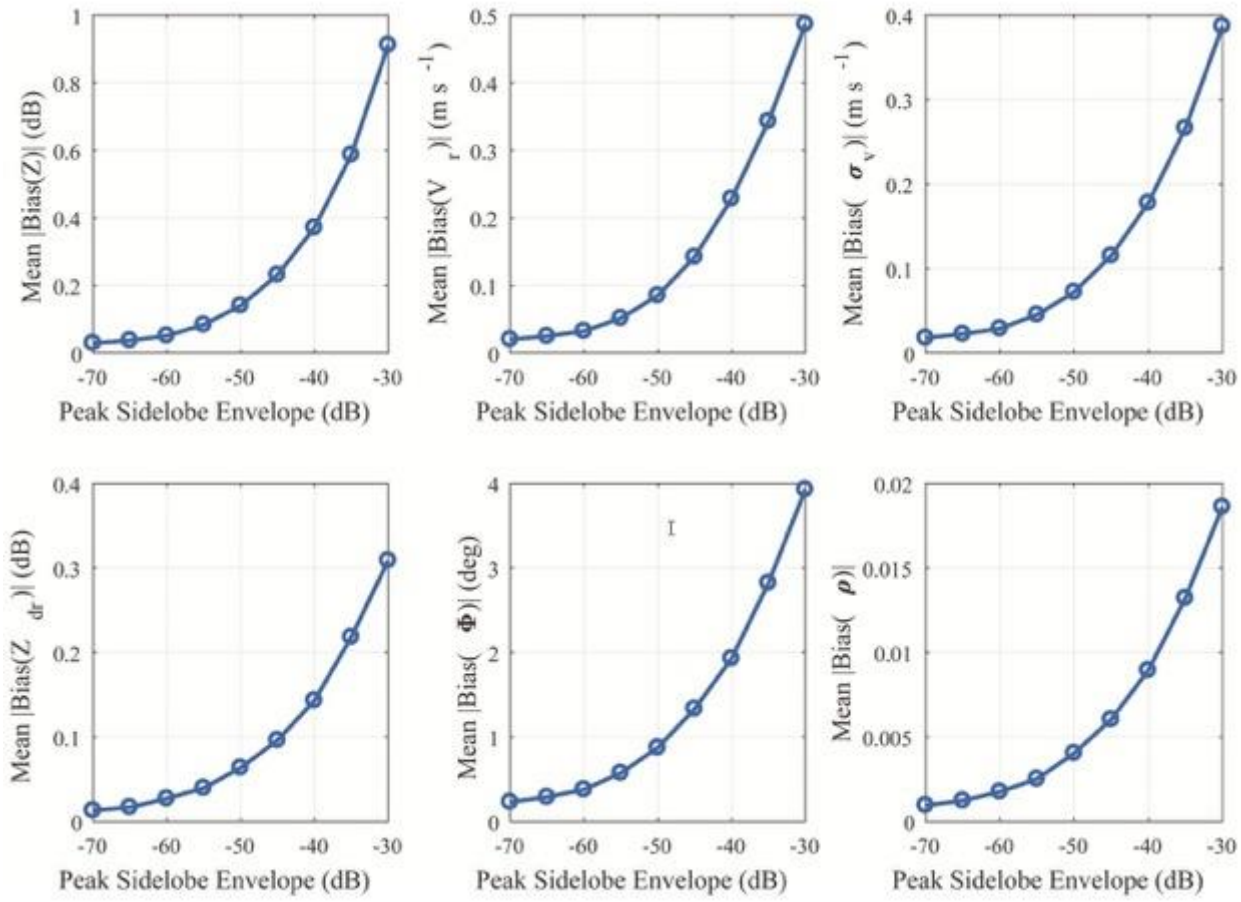

Average magnitude of the biases in the radar variables caused by antenna sidelobes for the weather scenario simulated in the first figure. As expected, the average magnitude of the biases for all the radar variables decreases as the peak of the antenna sidelobe envelope decreases. However, small biases alone are not sufficient to determine the requirements, and operational impacts of the artifacts must also be considered.

j. PAR Command and Control: SENSR Simulations

Sebastián Torres and David Schvartzman (CIMMS at NSSL)

One of the goals of the Spectrum Efficient National Surveillance Radar (SENSR) research program is to refine and justify, in terms of the National Weather Service (NWS) mission benefit, the radar technical requirements that will be provided in the planned Request for Proposals (RFP) to industry in 2018. Perhaps, the most promising candidate to meet the demanding SENSR requirements is a multifunction phased-array radar (MPAR). At the core of an MPAR design are the spatial and temporal sampling requirements for the different functions, which can be met with a combination of radar architecture and concept of operations. Unfortunately, a system that meets the most demanding requirements for all functions at all times would be prohibitively expensive. Thus, load-shedding algorithms have to be investigated to find optimum adaptive-scan tradeoffs that minimize the operational impact when not meeting one or more requirements. As such, a well-designed concept of operations exploits the PAR beam agility to surveil the atmosphere using focused and tailored scan strategies, a process commonly referred to as adaptive scanning. Defining rules for adaptive scanning is a complex process; it depends not only on the type and location of storms but also on their temporal evolution. Because data quality, spatial coverage, and temporal resolutions are coupled, improvements in one or more areas inevitably result in degradations in other areas. The goal of this project is to provide realistic command-and-control simulations in the context of weather surveillance under load-shedding conditions. That is, using archived data cases, we want to explore the tradeoffs associated with different adaptive-scanning algorithms and understand their impact in the design of a radar system for SENSR.

During this year, we began developing a closed-loop command-and-control framework as depicted in the figure below. Using (level-II) archive data from the National Centers of Environmental Information (NCEI), received (level-I) radar signals are simulated (DQ Simulator) for any combination of radar-system characteristics and concept of operations (scan). These simulated (level-I) signals can be processed using conventional and advanced signal processing techniques (DSP) to drive different adaptive-scanning algorithms, which dynamically define the scan to be used in the next iteration. The (level-II) data produced by the signal processor using adaptive scanning can be evaluated to refine and assess the operational benefits of different command-and-control schemes.

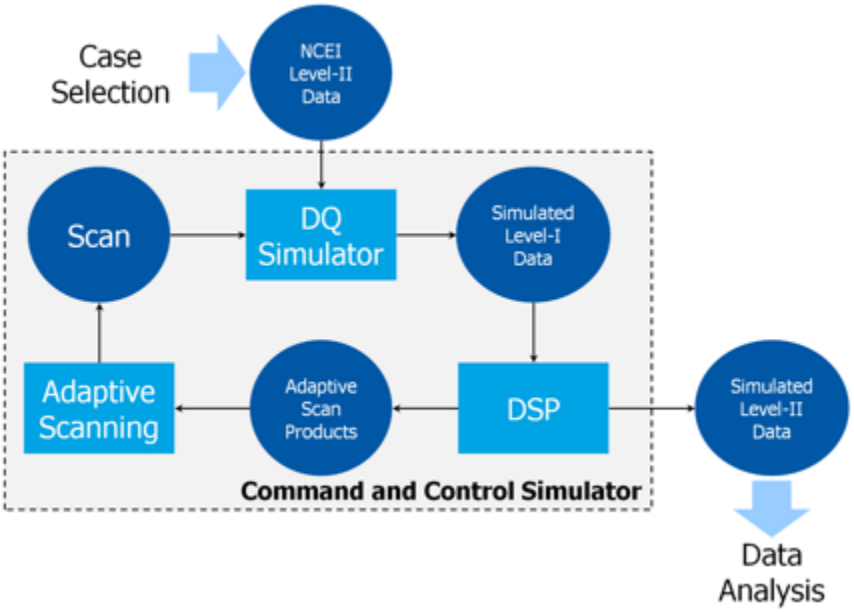

Block diagram of the command-and-control simulation framework designed to illustrate the tradeoffs of different adaptive-scanning algorithms for SENSR.

Publications

Ivić, I. R., 2017: Phase code to mitigate the copolar correlation coefficient bias in PPAR weather radar. *IEEE Transactions on Geoscience and Remote Sensing*, **55**, 2144–2166.

Ivić, I., and R. Doviak, 2016: Evaluation of phase coding to mitigate differential reflectivity bias in polarimetric PAR, *IEEE Transactions on Geoscience and Remote Sensing*, **54**, 431-451.

Schvartzman, D., S. Torres, and T. Yu, 2017: Weather Radar-Spatio Temporal Saliency: A first look at an information-theory-based human attention model adapted to reflectivity images. *Journal of Atmospheric and Oceanic Technology*, **34**, 137-152.

Torres, S., R. Adams, C. Curtis, E. Forren, D. Forsyth, I. Ivić, D. Priegnitz, J. Thompson, and D. Warde, 2016: Adaptive-weather-surveillance and multifunction capabilities of the National Weather Radar Testbed Phased-Array Radar. *IEEE Proceedings*, **104**, 660-672.

Torres, S., C. Curtis, and D. Schvartzman, 2017: Requirement-driven design of pulse compression waveforms for weather radars. *Journal of Atmospheric and Oceanic Technology*, **34**, 1351-1369.

CIMMS Task III Project – ARRC R&D Activities for the Multi-Mission Phased Array

NOAA Technical Lead: Kurt Hondl (NSSL)

NOAA Strategic Goal 2 – *Weather Ready Nation: Society is Prepared for and Responds to Weather-Related Events*

Funding Type: CIMMS Task III

Overall Objectives

Develop several complementary technologies that are essential to the forward progress of multi-mission phased array systems. The projects described below are ongoing.

1. Pulsed Interference Filters for MPAR

Mark Yeary and John Lake (ARRC), and Chris Curtis (CIMMS at NSSL)

Objectives

The goals of this project were to analyze the efficacy of various radio frequency interference (RFI) detection techniques, parameterize them for easier operational use, and to seek out potential improvements to the algorithms. Four algorithms were tested: the Interference Spike Detection Algorithm (ISDA) and the three RFI detection algorithms specified by Vaisala in the RVP8 User's Manual. Additionally, the performance of these algorithms was compared to the performance of several standard classification algorithms.

Accomplishments

a. Algorithm Parameterization

Each of the four RFI classification algorithms make their classification decision based on a parameter whose value is not based in any aspect of the weather or signal properties but is instead empirical. As a result, the choice of parameter value is difficult to relate to algorithm performance measures such as the probability of false alarm (PFA).

To address this shortcoming, a regression experiment was performed. First, a large amount of weather radar data was generated using the Zrnic simulation algorithm. Properties of the data, including the SNR, radial velocity, and spectrum width, were known recorded. The RFI classification algorithms were then executed on the data with a known parameter value and the subsequent performance (in terms of PFA) was recorded.

After many iterations, the generated data was split into training data and test data. A regression algorithm, elastic net regularization, was then applied to the training data. Elastic net regularization is a linear combination of two other regression tactics, Tikhonov regularization and the least-absolute-shrinkage-and-selection-operator. Because of this, elastic net regularization tends to prefer solutions that minimize coefficient values in the final solution and to eliminate variables that have no impact on regression performance. Figure 1 shows the regression performance on the test data using elastic net regularization.

The regression was a linear combination relating signal statistics and algorithm parameter to PFA. The resulting formula was inverted to get a formula that yielded the best algorithm parameter as a function of signal statistics and desired algorithm performance (in terms of PFA). In an operational context, a user could define their desired performance (in terms of PFA) and let this formula determine the appropriate algorithm parameter value.

b. Algorithm Performance Assessment

Once the formula for the algorithm parameter was found, the classification algorithms were assessed against each other and against decision tree and random forest machine learning classification algorithms. These specific machine learning algorithms were chosen because of their potential to be simplified into operational algorithms, and also as a measure of what kind of performance could be expected under a more complex algorithm.

First, the simulated data from before was corrupted with RFI of known power at known locations, and the data was again split into test and training data. For the RFI detection algorithms, the “best” parameter (according to the regression) was known because signal statistics were known, so these algorithms were executed on the test data using this parameter and their performances, in terms of PFA and probability of detection, were recorded. The machine learning algorithms were allowed to train on the training data and then were executed on the test data; performance metrics, in terms of PFA and probability of detection, were recorded.

In order to compare algorithm performance, a metric known as the area under the curve (AUC) was used. The AUC is measured by integrating the area under the receiver-operator curve, a line that traces the probability of detection as a function of probability of false alarm. An ideal AUC, indicating perfect classification, has a value of 1; the AUC of an algorithm that randomly classifies has an AUC of 0.5. In terms of assessing algorithm performance, better classifications algorithms have an AUC that approaches 1, while algorithms with an AUC perform worse at classifying than simply flipping a coin. Figure 2 shows the performance of the RFI detection algorithms and the machine learning algorithms for a set of data where the SNR was 20 dB and the INR was 40 dB.

Finally, the algorithm performance of each of the algorithms was compared for a range of SNRs and INRs. Figure 3 shows plots of the AUCs as a function of SNR and INR. In general, ISDA AUCs were higher than Vaisala AUCs for the same SNR and INR, but less than the machine learning algorithms’ AUCs. However, the decision trees generated by the machine learning algorithms were complex and while effective in an offline environment, could potentially suffer from latency issues in an online environment.

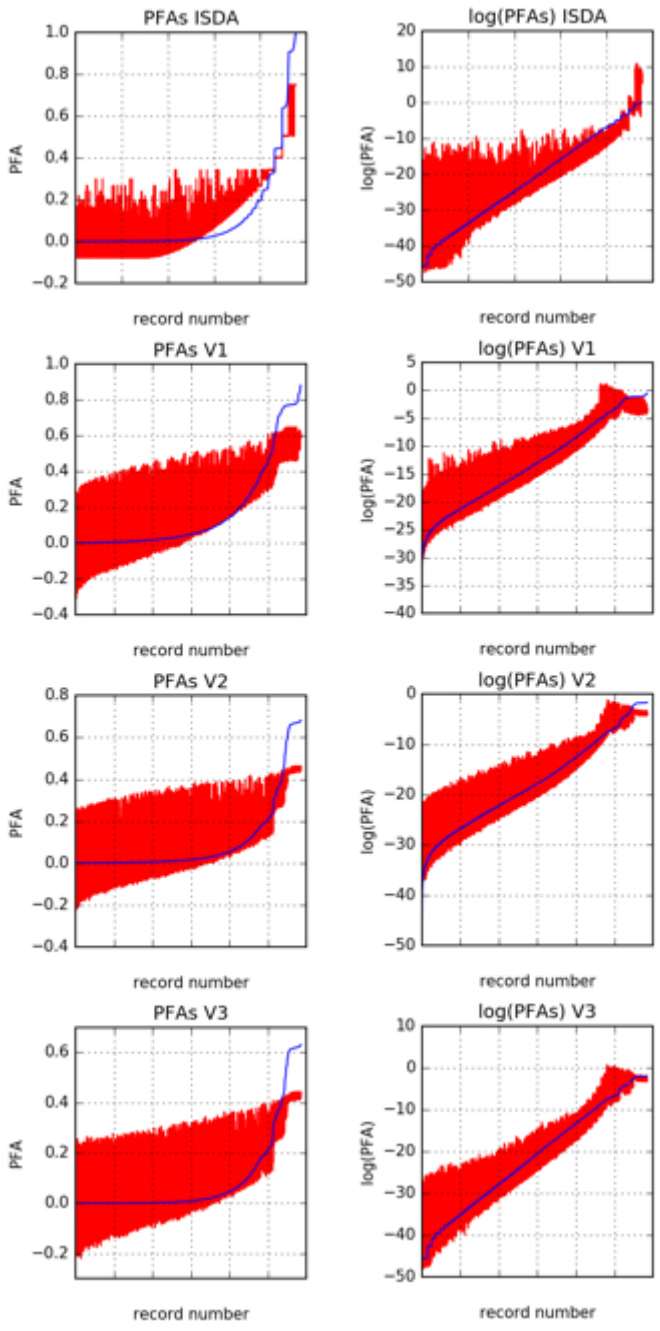

Figure 1: *The PFA predicted by the regression algorithm (blue) and the actual PFAs of the test set (red dots). In the first column, performance for the regression performed with PFA; in the second column, performance for the regression performed with the logarithm of the PFA. Predictions were much better for the regression with the logarithm of the PFA instead of just the PFA, though still not as good as hoped. Other regression methods yielded better performance but were not easily represented as a linear formula, meaning that extracting algorithm parameter as a function of desired PFA was not readily possible.*

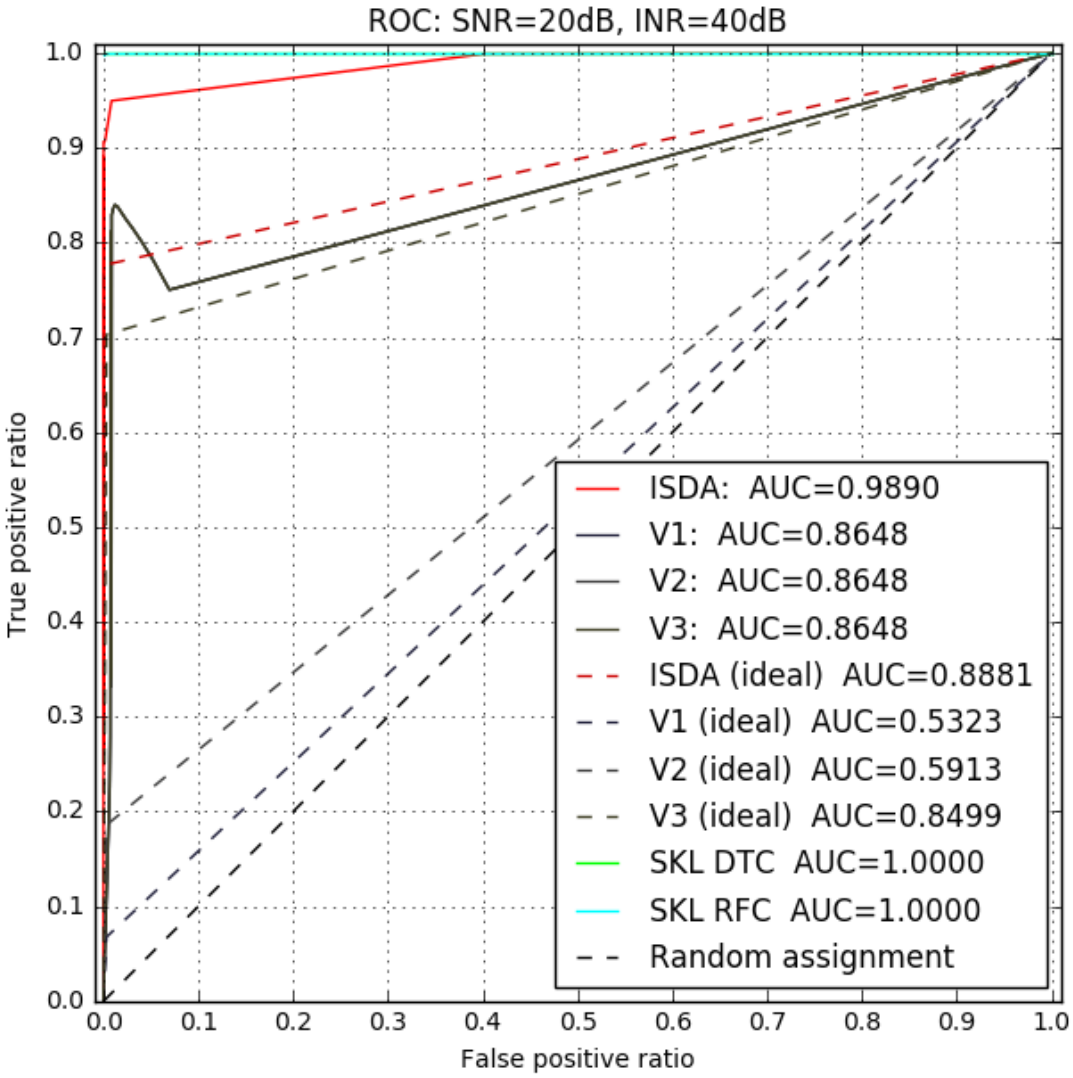

Figure 2: *The receiver-operator curve for simulated data in which the SNR is 20 dB and the INR is 40 dB. The cyan and green lines represent the machine learning algorithms, which perfectly classified all the data in this instance; thus, their area under the curve (AUC) is 1. Solid red line is the best possible performance of ISDA in this situation (but is not feasible operationally), while the dotted line is the performance of ISDA using a single "ideal" algorithm parameter (yielded using the formula from the regression experiment) for a PFA = 0.1. The solid grey lines represent the best possible performance of the Vaisala algorithms, while the dashed lines represent their performance using the single "ideal" algorithm parameter for a PFA = 0.1.*

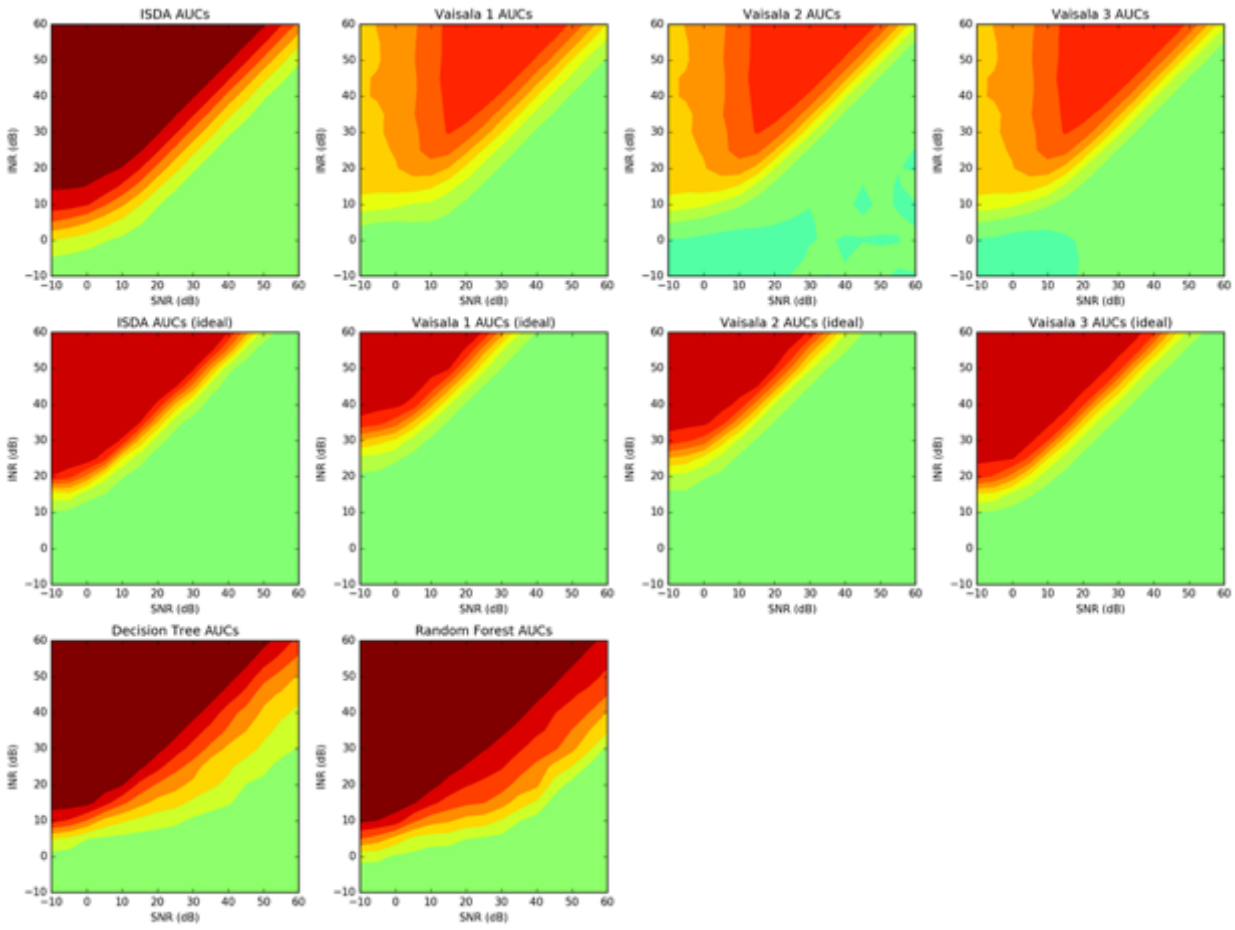

Figure 3: *The AUCs as a function of SNR and INR of the simulated signal. Values closer to 1 (darker red) indicate better algorithm performance. The first row is the best possible performance of the RFI detection algorithms (not feasible operationally); the second row is the performance using the parameter values indicated by the regression; the third row is the performance of the machine learning algorithms, which would be difficult to implement operationally but perform notably better than the algorithms currently in use.*

2. Polarimetric Phased Array Radar Research in Support for MPAR Strategy

Guifu Zhang, Hjalti Sigmarsson, Lesya Borowska, Hadi Saeidi-Manesh, Mirhamed Mirmozafari, Zhe Li, and Mohammad-Hossein Golbon-Haghighi (ARRC), and Richard Doviak, Allen Zahari, and Dusan Zrnic (NSSL)

Objectives

Conduct research on practical issues for designing and developing the Polarimetric Phased Array Radar (PPAR), including the Cylindrical Polarimetric Phased Array Radar (CPPAR), to better understand the scientific advantages, technical challenges & limitations and cost-performance tradeoffs, as well as to support MPAR strategy in

decision-making to sustain Norman's leadership in weather radar and to expand its radar expertise for broad research and multi-mission applications.

Accomplishments

This project team continues to work on i) radiating element design and testing, applicable to both the PPPAR and the CPPAR, ii) array configuration study to achieve high performance for a PPAR, iii) design of the frequency-scan beam matched column antennas and iv) advanced signal processing. A highly isolated dual-polarization dipole antenna has been designed and tested with polarization purity with cross-pol level below -40dB from the co-pol peak (Mirmozafari et al. 2017) as shown in Figure 4. Figure 5 shows the concept and calculation of image arrangement of an array antenna (Saeidi-Manesh and Zhang 2017). The designed CPPAR antenna and test results are shown in Figure 6, indicating well-matched dual-pol antenna patterns can be achieved (Saeidi-Manesh et al. 2017).

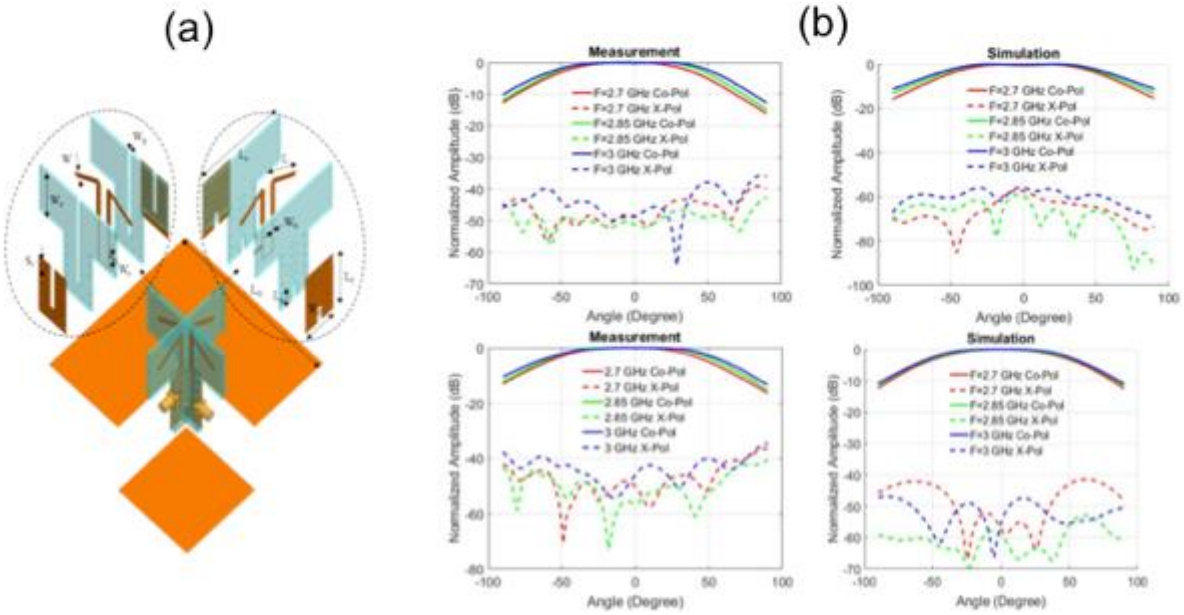

Figure 4: *Design of a dual-polarization crossed dipole antenna: (a) geometry and (b) radiation patterns of designed. Cross-pol level is below -40dB from the co-pol peak, satisfying the MPAR requirements.*

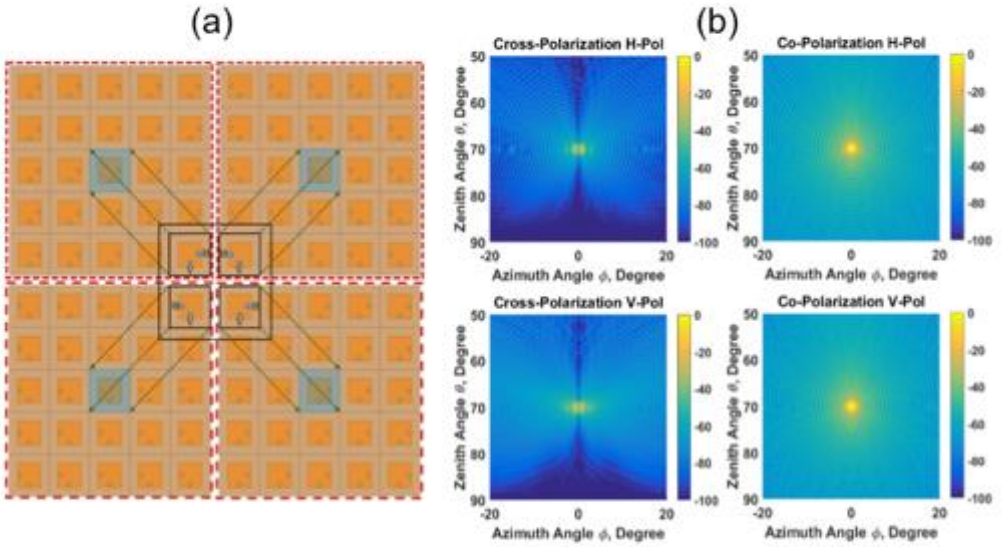

Figure 5: *Image arrangement to improve polarization purity: (a) configuration sketch, and (b) 3D radiation patterns for co- and cross-polarizations.*

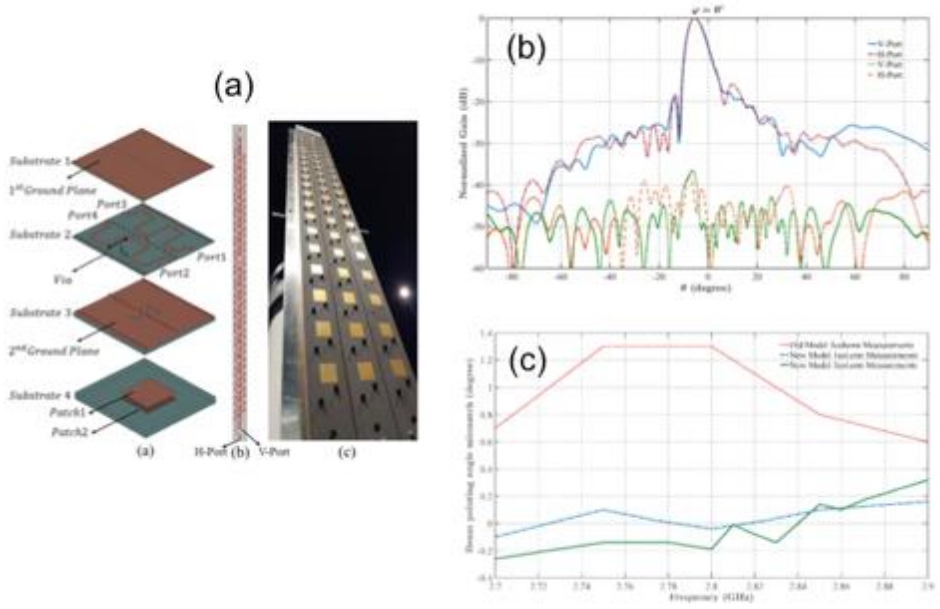

Figure 6: *CPPAR antenna design and test results: (a) geometry of 19-element array antenna, (b) measured H-Pol and V-Pol co- and cross-polarization radiation patterns of the embedded column, and (c) beam pointing angle mismatch versus frequency.*

3. RF Filters for Improved MPAR Interference Protection

Hjalti Sigmarsson, Shahrokh Saeedi, and Caleb Fulton (ARRC)

Objectives

In this task, the possibility of embedding RF filters into a phased array radar front-end module is being investigated. Substrate-integrated cavity filters are being embedded into the bottom two layers of the antenna stack-up without affecting the antenna performance but still providing significant improvement in the out-of-band interference rejection. The goal is to design filters that operate at 2.85 GHz, cover the entire band of interest from 2.7 to 3 GHz, and add more than 30 dB of additional rejection while maintaining low loss. The full specifications of the filters are shown in Table 1.

Table 1: Filter specifications

Parameter	Target Value
Center Frequency	2.85 GHz
Bandwidth	350 MHz
Fractional BW	12%
Insertion Loss	< 1 dB
Rejection @ (1 ± 0.3) f_0	> 30 dB

Accomplishments

a. Resonator Design and Challenge

In the current design for integrated bandpass filter (BPF), substrate integrated waveguide (SIW) coaxial evanescent-mode cavity resonator is used as the building block. The post in the resonator is capacitively loaded to provide the resonance condition, at a smaller frequency than the natural resonant frequency of a half wave-length coaxial resonator. Therefore, the resonator size is shrunk. The current design utilizes coaxial cavity with only 10 mm in diameter and almost 1.8 mm in thickness. Lumped components are used to load the resonator, while the measured quality factor is still greater than 150. The structure of the SIW coaxial evanescent-mode cavity resonator loaded by lumped capacitor is shown in Figure 7.

Evanescent-mode cavity resonators can be miniaturized by highly loading the capacitive posts. However, heavily loading the resonator not only lowers the resonant frequency of the first mode, but also it lowers the resonant frequency of the higher-order modes. This frequency shift is even faster for higher-order modes, as their dependency to dimension is stronger. Consequently, the separation between the main passband and spurious response in a heavily loaded filter is degraded. Figure 8 shows such a case for a second order heavily loaded evanescent-mode cavity BPF centered at 2.85 GHz, where the second and third passbands at 5.0 GHz and 7.5 GHz limit the filter rejection in the high frequency side of the main passband. Since this issue is inherited from the loaded resonator, increasing the filter order cannot resolve the problem.

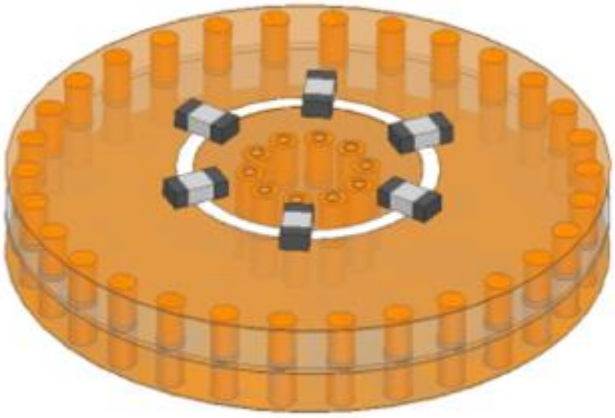

Figure 7: *Structure of the capacitor-loaded evanescent-mode cavity resonator implemented using SIW technology.*

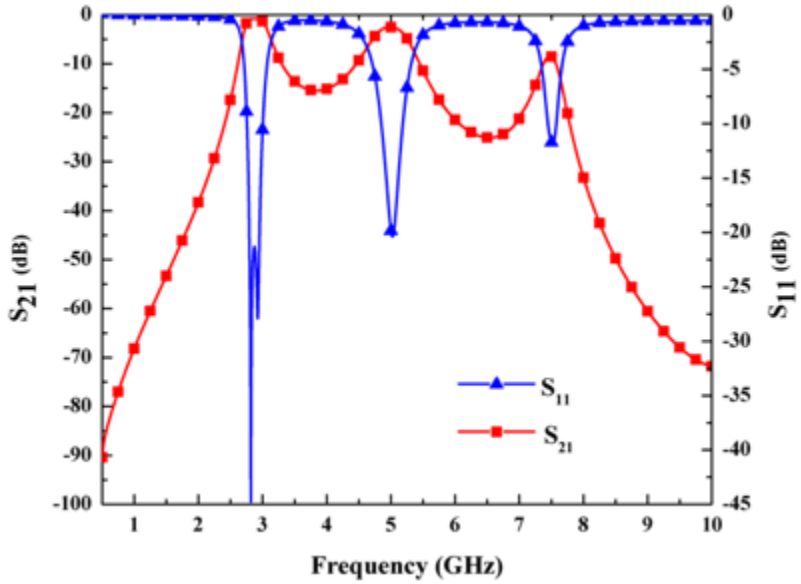

Figure 8: *Frequency response of a second-order highly loaded evanescent-mode cavity BPF.*

b. Bandpass Filter with Extended Stopband

In order to mitigate the effect of higher resonances within the cavity, several methods have been investigated. In general, these methods can be categorized in three main groups.

1. Adding Transmission Zeros (TZs) at or around the spurious passbands can improve the filter rejection. However, this technique requires a higher order filter, which results in a higher insertion loss in the passband. Additionally, the added transmission zeros usually provide narrowband notches; unless multiple of them

are implemented. For having multiple TZs again the order of the BPF needs to be increased, which results in a larger filter. Figure 9 shows the frequency response of a fourth-order BPF with two TZs, one at each side of the passband. It is seen that although a single TZ at the higher side of the passband improves the rejection of the filter, it cannot completely mitigate the effect of the second passband.

2. Another method to achieve a wide stopband in the coaxial evanescent-mode cavity resonator is to change the impedance of the coaxial structure by manipulating the ratio of the outer to inner conductor diameters. Such a manipulation can change the resonant frequency of the resonating modes as well as their quality factors. By increasing the ratio of the outer to the inner conductor diameter, the frequency of the second resonating mode can be pushed to a higher value. This, of course, is achieved at the cost of lowering the first mode quality factor, which results in a higher insertion loss.
3. By changing of the geometry of the capacitive loading from the lateral direction into axial (along the post), the field distribution for higher resonating mode can be changed. Consequently, their resonant frequencies also change. Similar to the previous method, the second passband frequency can be pushed to higher values at the cost of higher insertion loss for the first passband. Figure 10 shows a comparison between the frequency responses of the second-order evanescent-mode cavity BPFs loaded laterally and axially.

A common way for expanding the stopband in a BPF is cascading the BPF with another filter with a broad stopband and steeper slope. Usually, an elliptic lowpass filter (LPF) is a good candidate. Because it exhibits very low insertion loss in its passband, while providing a sharp roll-off and a constant attenuation level in its stopband. One concern about using this technique is the total size of the cascade. However, such a cascade can result in a low profile BPF with a wide stopband, provided that each individual filter being designed properly. The structure of a second order evanescent-mode cavity BPF cascaded with an elliptic LPF is shown in Figure 11. The LPF is implemented using non-symmetric stripline technology, which is used in the antenna stack-up. The frequency response of the BP-LP cascade filter is shown in Figure 12. The elliptic LPF has been designed and its fabrication will be completed soon. The next step will be measuring and finalizing the design of the LPF. Following that, the filters will be cascaded.

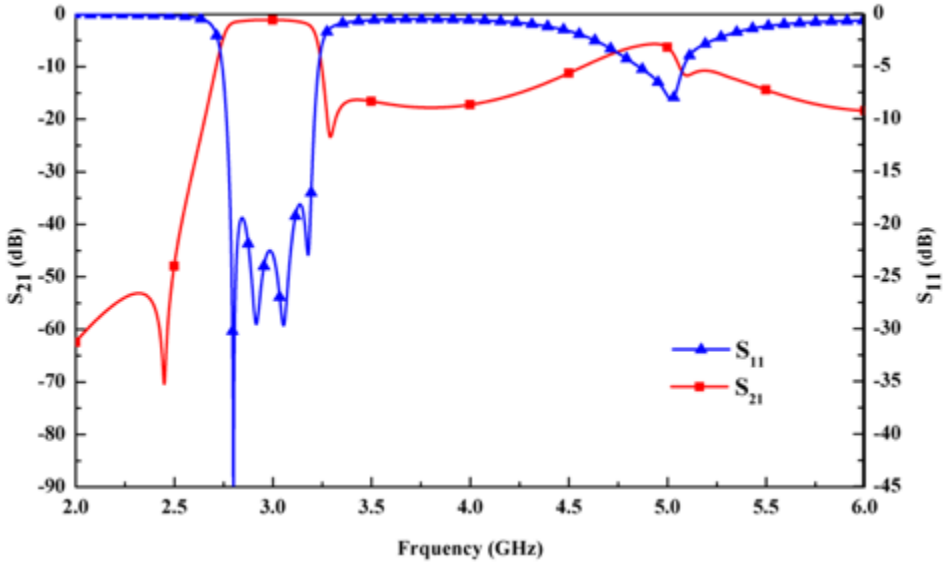

Figure 9: *Frequency response of a fourth-order highly loaded evanescent-mode cavity BPF with two transmission zeros.*

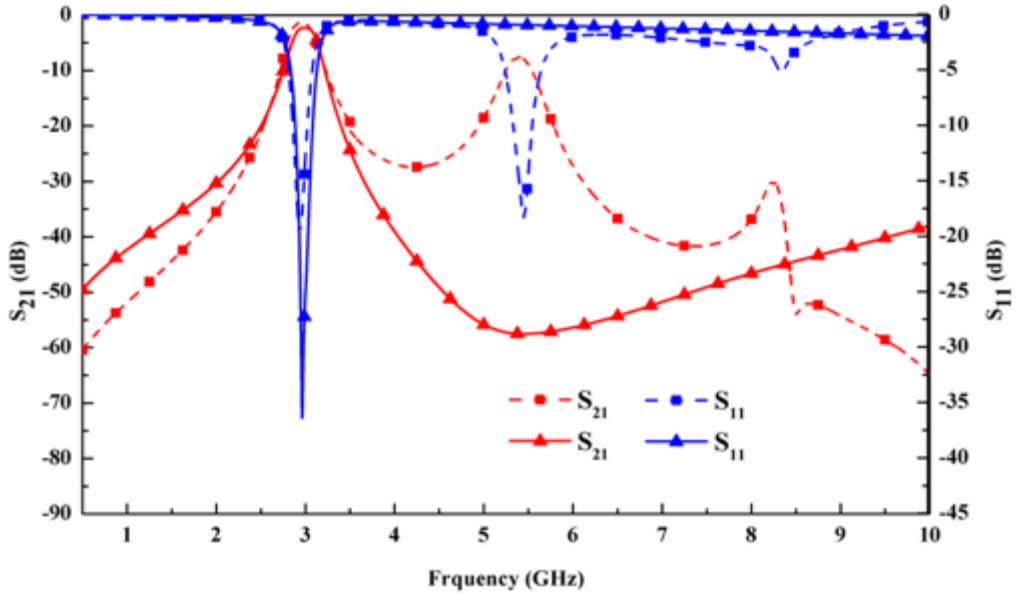

Figure 10: *Frequency responses of two second-order evanescent-mode cavity BPF with different loading geometries.*

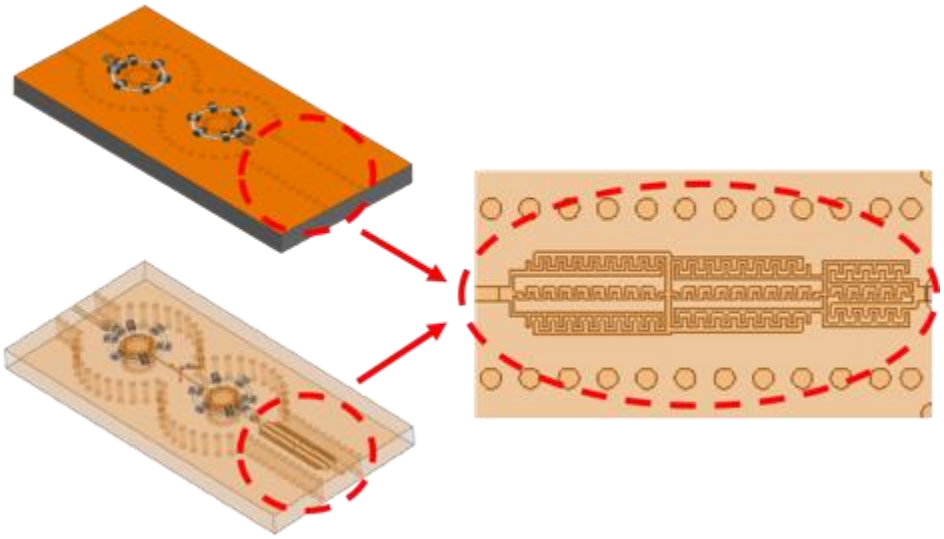

Figure 11: *Structure of the integrated filter showing an elliptic LPF cascaded with a SIW evanescent-mode cavity second-order BPF.*

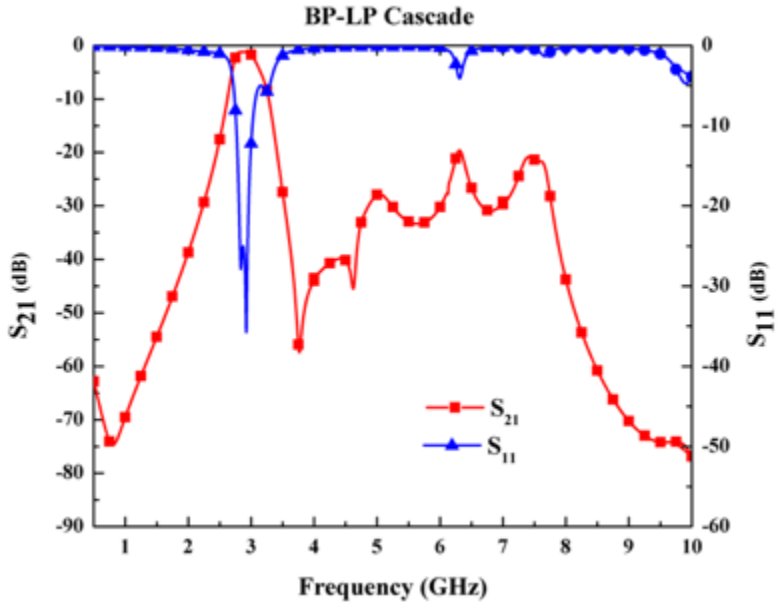

Figure 12: *Frequency response of the BP-LP cascade filter.*

4. Design and Characterization of a High-Performance S-Band Dual-Polarized Radiating Antenna

Jorge Salazar, Caleb Fulton, Nafati Aboserwal, Jose Diaz, and Javier Ortiz (ARRC), and Dusan Zrnic (NSSL)

Objectives

The overall effort for this task involves the design and prototype of a high-performance radiating antenna element for weather phased array antennas. The main objective in this research is to develop a radiating element that provides a cross-polar isolation below -40 dB in an array environment. To achieve this goal, several mechanisms to minimize spurious radiation, higher modes, and diffracted fields were proposed.

Accomplishments

The radiating element under consideration is composed of a multilayer aperture-coupled cross-patch antenna. Electromagnetic coupling between the fed and patch enable trough a cross-slot aperture in the ground plane was used to improve the port isolation of -50 dB. Independent fed layers for each polarization (H and V) was proposed. High symmetry in the fields of the radiating elements is a key feature to enable cross-polarization cancellation in the non-radiation edges. Characterization of the diffracted fields produced at the external and internal edges in the antenna and array is also contemplated. Figure 13 illustrates the effect of the external and internal diffracted field using simulated and measured co- and cross-polarization antenna patterns. From measured results, it is observed that small internal gaps (~$0.1\lambda_o$) significantly impact the cross-polarization. About 10 dB is observed in an isolated rectangular aperture in a ground plane of $4\lambda_o$ x $4\lambda_o$.

Results of an isolated radiating element are illustrated in Figure 15. The antenna element patterns for H- (top part) and V-polarization (lower part) show a co-polar mismatch below 0.1 dB for 120^o and cross-polarization isolation below -37 dB.

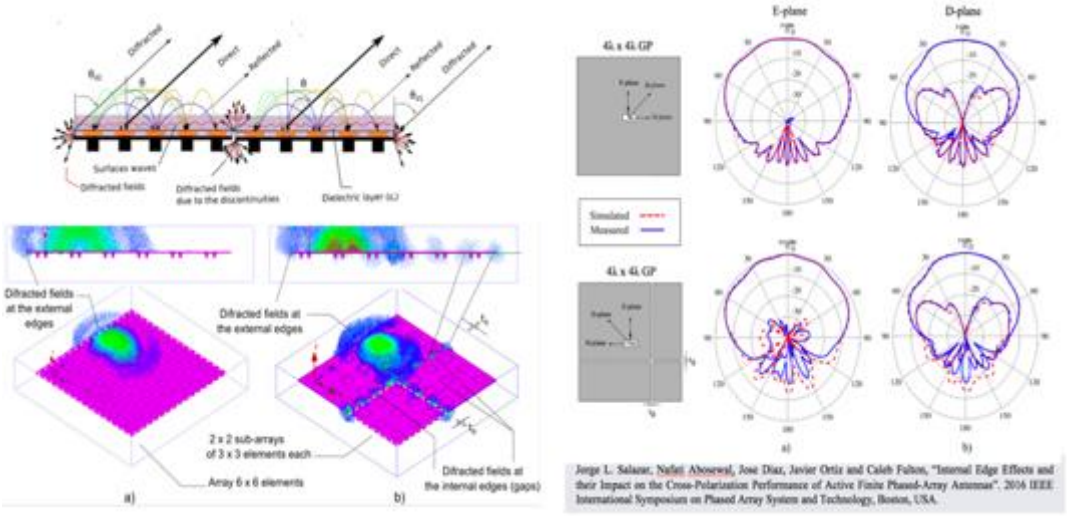

Figure 13: *On the left, a representation of the external and internal field in a MS cross-patch antenna array of 6x6 elements is shown. On the right, a comparison of simulated and measured results of single rectangular aperture in a finite ground plane of $4\lambda_o$ x $4\lambda_o$ size and single element in a ground plane of $4\lambda_o$ x $4\lambda_o$ size with $0.1\lambda_o$ gaps is shown.*

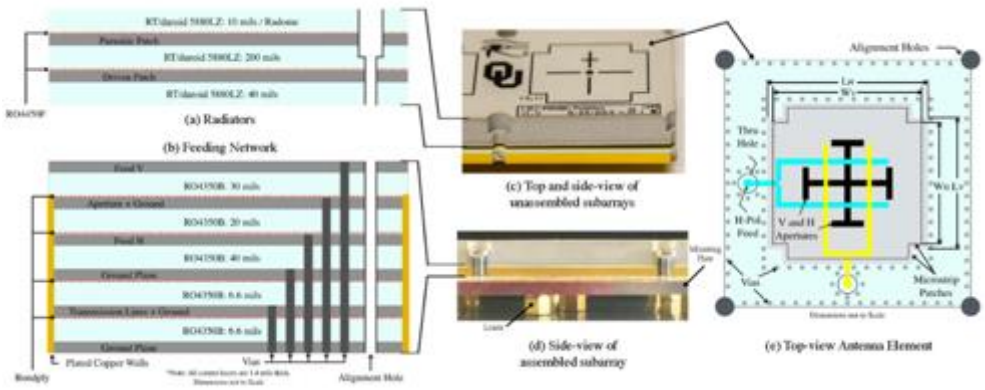

Figure 14: *Antenna element stack-up and side and top view of fabricated prototype. The driven patch dimensions are LH = 2.7 mm and LV = 2 2.7 mm. For the parasitic patch, LH = 33.9 mm and WH = 23.9 mm.*

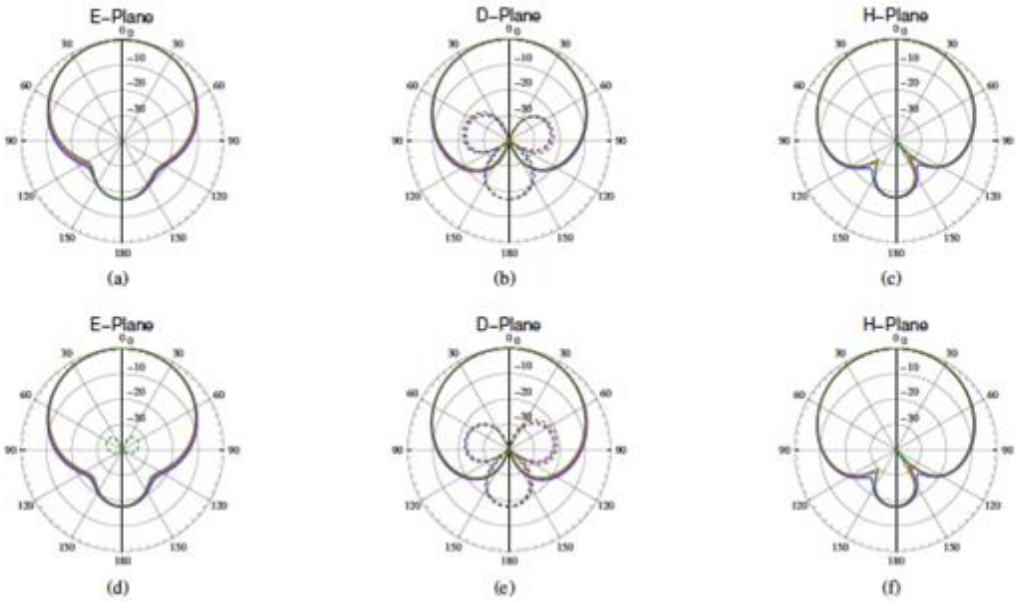

Figure 15: *Antenna element patterns for H- (top part) and V-polarization (lower part) for the isolated antenna element. The solid (-) and dashed (--) lines refer to co- and cross-polarization.*

5. Electromagnetic Dipole-Based Dual-Polarized Radiating Elements – Improvements on the LMCO Design

Yan (Rockee) Zhang, Jorge Salazar, and Ridhwan Khalid Mirza (ARRC), and Dusan Zrnic and Richard Doviak (NSSL)

Objectives
The goal is to investigate electromagnetic dipole and array designs for low-cross-pol level array designs.

Accomplishments
The team has investigated various designs for electromagnetic dipole array antennas. A prototype design was developed and fabricated. The individual element performance was measured and was proven improvements to original designs from Lockheed Martin and commercial dipole products.

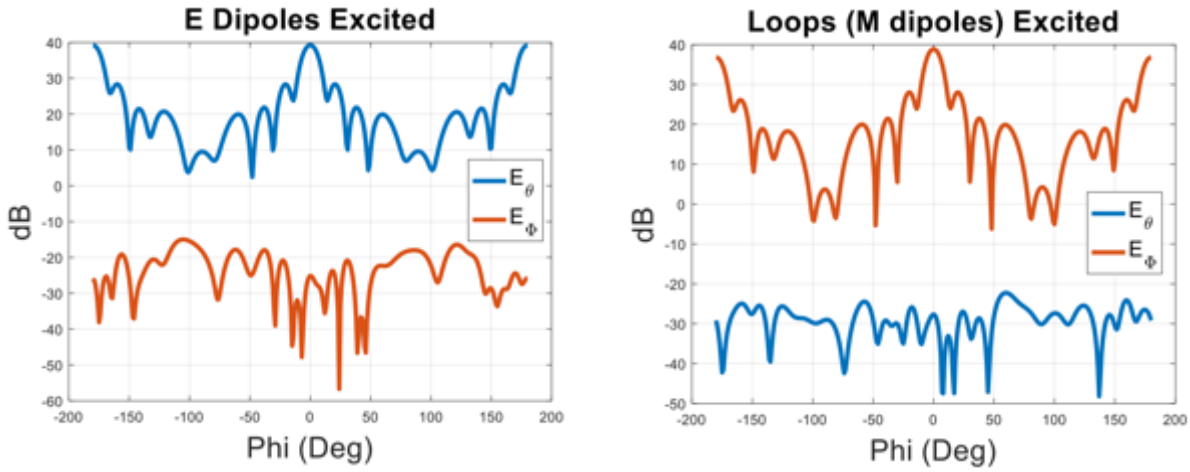

Figure 16: *HFSS simulation of radiation pattern of an 8 by 1 linear array using EM dipole elements.*

6. Parallelization in MPAR Backend Functions and Architectures – Implementation and RapidIO Testbed

Yan (Rockee) Zhang, Hernan Suarez, Xining Yu, and Ankit Patel (ARRC), Mark Weber (CIMMS Senior Research Scientist affiliated with NSSL), and Allen Zahari (NSSL)

Objectives
The goal is to investigate massive parallelism processing and SRIO data transportation and their impact on the performance of MPAR back ends.

Accomplishments
The team developed a real-time, scalable processing framework for basic radar functions based on FPGA (for data transportation) and DSP (for parallel processing). Based on engineering analysis and emulations, the system achieves reasonable end-to-end latencies for a basic PAR processing chain, to potentially achieve the real-time requirements of a full-size MPAR. The current designs assume using the similar system parameters as the ATD. Small scale testing experiments verified the real-time processing performance.

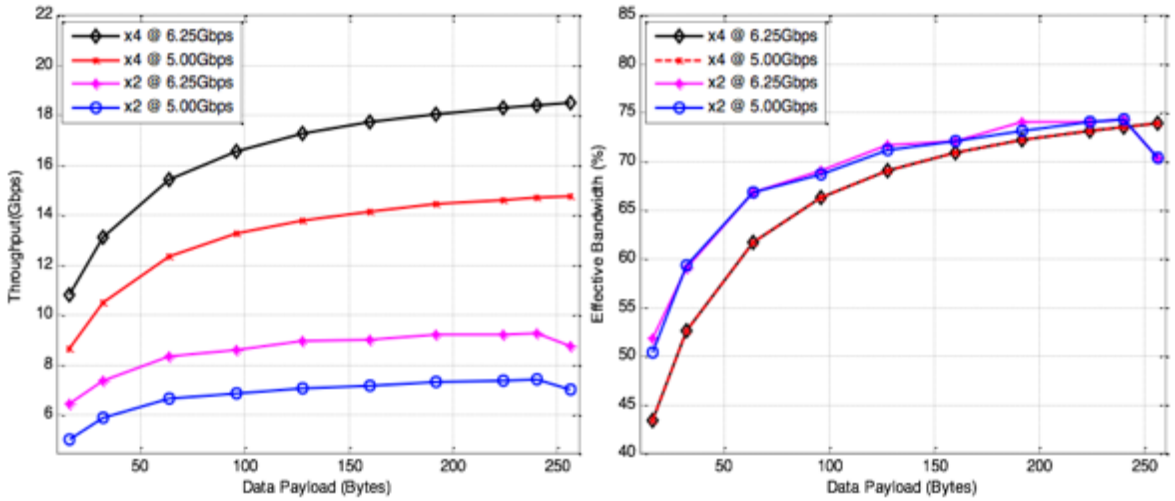

Figure 17: *SRIO throughput measured from implementation based on Arria 10 FPGA.*

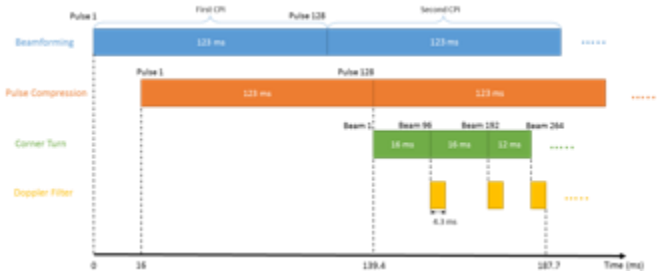

Figure 18: *Real-time System Timeline for the Example Backend System based on ATD system parameters.*

7. Impacts of Array Manifold on Polarimetric Steering Array Patterns – Comparative Measurements and Numeric Simulations

Yan (Rockee) Zhang, Guifu Zhang, Sudantha Perera, and Li Zhe (ARRC), and Dusan Zrnic and Richard Doviak (NSSL)

Objectives

The goal is further development scalable time-domain CEM-based simulations and measurement validations for polarimetric array antennas, especially for the cylindrical array manifolds.

Accomplishments

The team performed a series of array antenna pattern measurements (Figure 19) in chamber as a basis for validating computational electromagnetic (CEM) simulations, and achieved matching results as in simulations. The standard FDTD method based on a rectangular coordinate system was extended to cylindrical and non-orthogonal coordinate systems (Figure 20). These non-rectangular grids can have large manipulation over accurate simulation of cylindrical array and faceted cylindrical array.

The active elements of an infinitely large planar, cylindrical, or faceted-cylindrical array could be simulated based on a proper coordinate system for synthesizing the radiation pattern of large sub-array embedded in an infinitely large array.

Two schemes were developed to generate the simulation data of finite large arrays. The first scheme was simulating a few small subarrays to extract the electric and magnetic current distribution of elements at different locations. The second one using new kind of boundary condition called “X-boundary” and extract the current distributions. The second innovative solution based on periodic boundary condition (PBC) and so-called X-boundaries (Figure 21) could perform full-wave simulation of arbitrarily large arrays with tremendously reduced computational loads. The simulation of 32x32 array was published as a demonstration of the computational resource usage for analyzing large arrays. The comparisons between measurements and simulation of 8x8 array were presented as an illustration of the accuracy (Figure 22). This novel approach can be used as a full-wave simulation method which is alternative to the element-by-element approach and the infinite periodic structure approach for analyzing very large arrays. The X-boundaries method is being used in the new simulation tool (called PASIM) being developed for the new SENSR project.

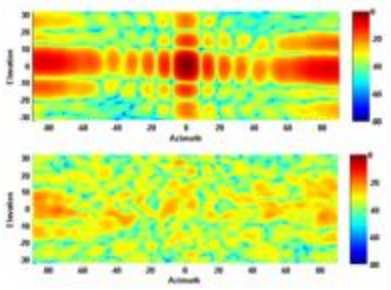

Figure 19: *Measured patterns of an 8 by 8 cylindrical phased array antenna (based on AEPs and software-calibration).*

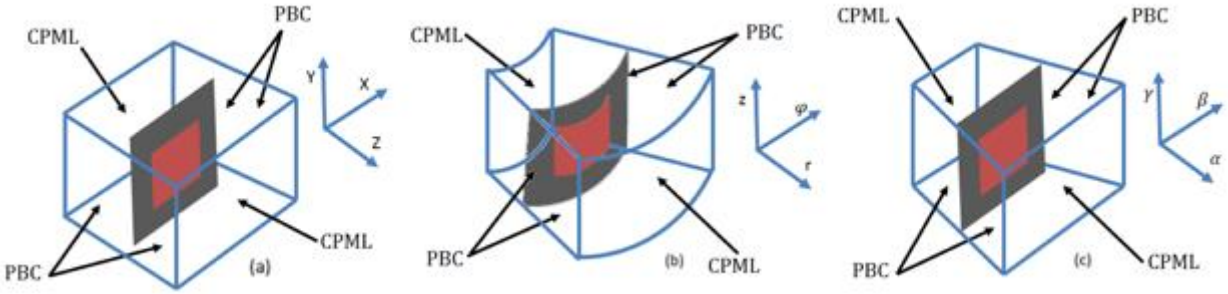

Figure 20: *Unit cell for FDTD simulation for (a) planar array, (b) cylindrical array, and (c) faceted cylindrical array.*

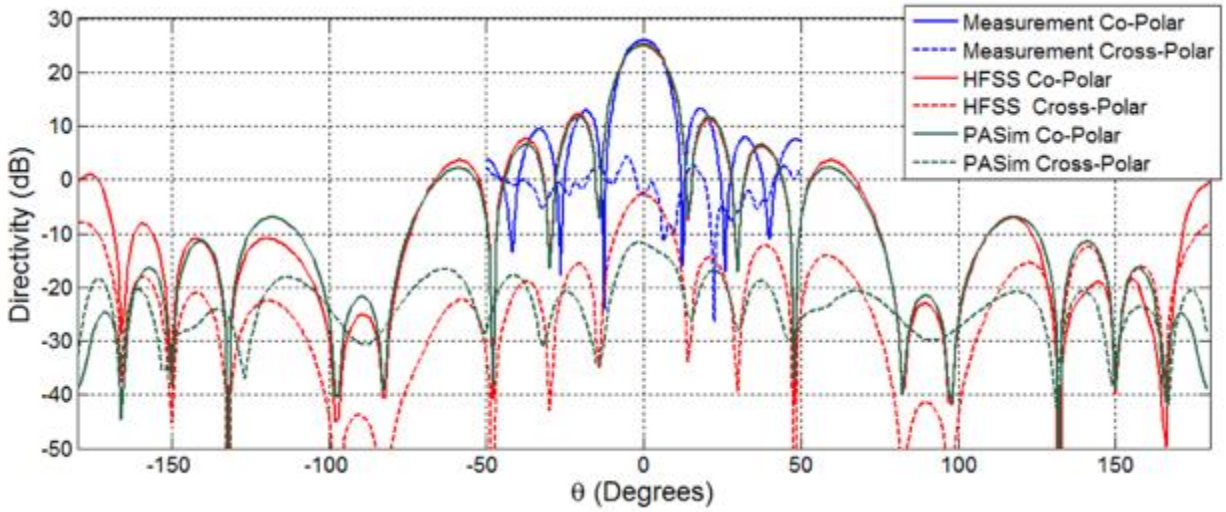

Figure 21: *Large finite phased array antenna Simulation using X-Boundary and Periodic Boundary Condition.*

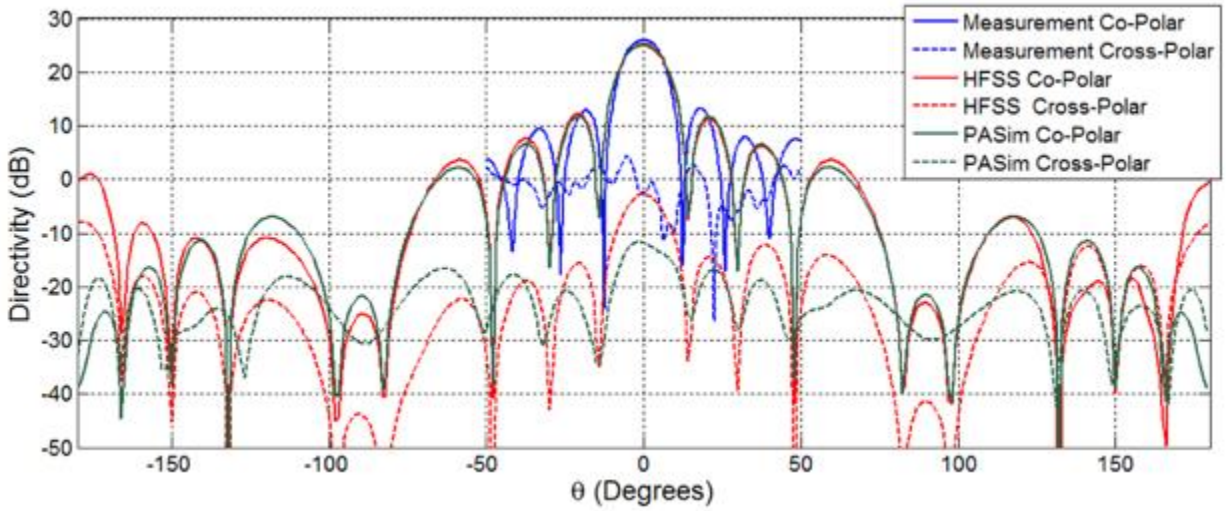

Figure 22: *Principal plane cuts of 8x8 array simulations and measurements.*

8. Cylindrical Surface Wave Analysis of CPPAR and General Antennas

Caleb Fulton and Kristin Sperzel (ARRC)

Objectives

Better understand the fundamental mechanisms for the generation of surface and creeping waves on cylindrical arrays, leading towards engineered solutions that can mitigate their associated deleterious effects. And, determine the root causes of the CPPAR front-to-back isolation, as they are related to mutual coupling, surface waves, and creeping waves.

Accomplishments

Most of the work accomplished thus far has been primarily simulation based, as the remaining 48 columns, or half-cylinder, of the CPPAR Demonstrator is waiting to be populated. Thus, the current focus has been on creeping wave mechanisms. It was found that eliminating certain creeping wave modes causes the back radiation to drop significantly. More specifically, due to the CPPAR Demonstrator having un-populated back half of the cylinder the creeping wave modes near the speed of light are enhanced. Figure 23 shows measured data for CPPAR demonstrator that was then run through MATLAB to find what would occur when certain creeping wave modes were eliminated. It can be seen that the back radiation level, before the creeping wave modes near the speed of light are eliminated, is equal to about -50dB. The first set of significant modes to be eliminated are the creeping wave modes near the speed of light, which are depicted by the yellow regions in the phase mode index column. Finally, once all of the creeping wave modes are eliminated, the back radiation levels drop to roughly -60dB. This indicates that creeping wave modes directly affect back radiation levels.

In order to better understand the creeping wave modes at a fundamental level, a cylindrical array of simple slot antennas has been analyzed using the ANSYS HFSS finite element method solver. This simulation can capture creeping wave and surface wave effects, and presents an early investigation into the mechanisms for generation (and potential suppression) of these waves. The simulation used a unit-cell simulation technique, which means this HFSS simulation only calculates the electromagnetic fields of one element only to save computation time. As arrays become large, the computation time and resources used for other simulation methods increases by N^3, where N is the total number of array elements. Using the unit-cell simulation technique, computation time and resources are reduced to increasing linearly with N. The fully populated array pattern is then analyzed by exporting the unit-cell data obtained from HFSS and importing it into MATLAB for mathematical computations. A specific MATLAB function was created to take the 0^{th} element pattern, phase shift the array by $2\pi/N$, and then add the phase-shifted calculation to the total pattern for each phase mode number. The initial physical design parameters for this set of simulations matched those of Sureau and Hessel (1971) in order to ensure the simulation technique is in agreement with pre-existing results. After making a few adjustments and corrections it was found that the simulation results and the paper's computation results were similar in shape, but the simulation results have about a 5dB gain over the paper results for angles greater than 40° off broadside and angles less than -40° off broadside, as seen in Figure 24. We will continue to try and correlate new simulations with established publications to better understand the surface and creeping wave effects on simple structures.

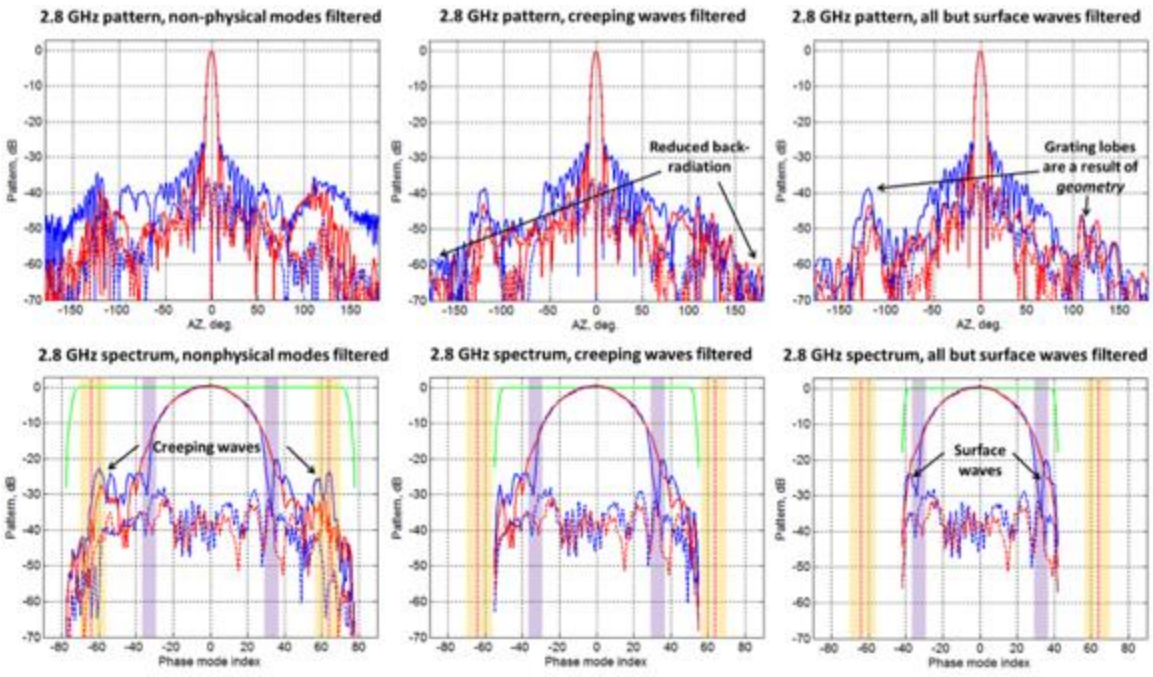

Figure 23: *The radiation pattern is shown in the top row, where the H-polarization is depicted in blue and the V-polarization is depicted in red, and the three plots show before, just after, and well after creeping waves near the speed of light (yellow section) are removed. The bottom row shows the phase mode spectrum before, just after, and well after the creeping wave modes near the speed of light have been removed.*

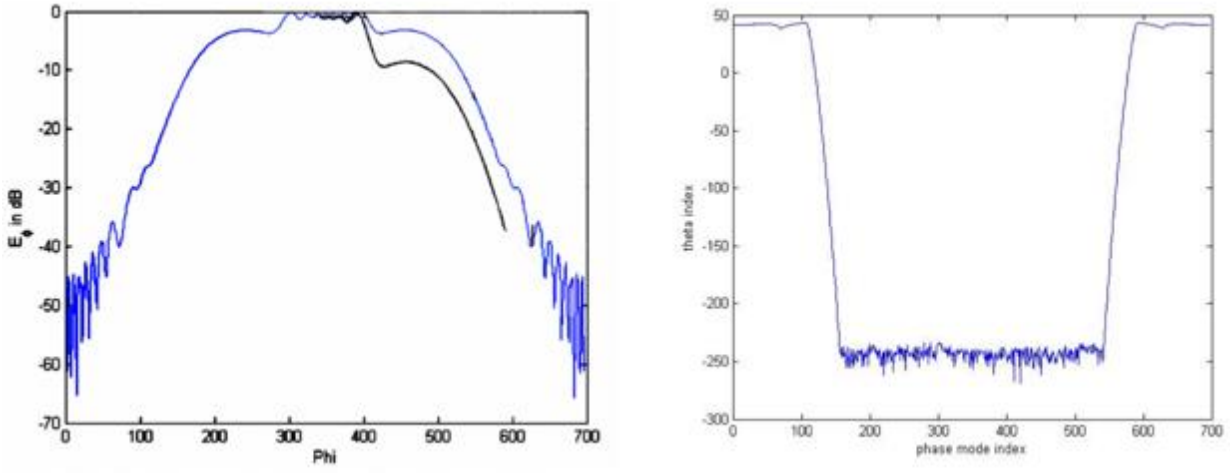

Figure 24: *The radiation pattern (left) of the HFSS slot antenna unit-cell simulation in blue compared with the radiation pattern from Sureau and Hessel (1971). The phase mode spectrum of the HFSS slot antenna unit-cell simulations is shown on the right.*

Publications

Aboserwal, N., J. L. Salazar, J. Diaz, J. Ortiz, C. Fulton, and R. D. Palmer, 2017: Polarization current impact on the cross polarization definition of practical antenna elements and arrays: Part I: Theory. *IEEE Transactions on Antennas and Propagation*, Accepted.

Aboserwal, N., J. L. Salazar, J. Diaz, J. Ortiz, C. Fulton, and R. D. Palmer, 2017: Polarization current impact on the cross polarization definition of practical antenna elements and arrays: Part II: Applications. *IEEE Transactions on Antennas and Propagation*, Accepted.

Borowska, L., G. Zhang, and D. S. Zrnic, 2016: Spectral processing for step scanning Phased Array Radars. *IEEE Trans. On Geoscience and Remote Sensing*, **54**, 4534-4543.

Curtis, C., M. Yeary, and J. Lake, 2016: Adaptive beamforming to mitigate ground clutter on the National Weather Radar Testbed phased array radar, *IEEE Transactions on Geoscience and Remote Sensing*, **54**, 1282-1291.

Diaz, J., J. L. Salazar, J. Ortiz, N. Aboserwal, C. Fulton, and R. D. Palmer, 2017: A cross stacked patch antenna with enhanced scanning for digital beam-forming phased array radars. *IEEE Transactions on Antennas and Propagation*, Accepted.

Fulton, C., M. Yeary, D. Thompson, J. Lake, and A. Mitchel, 2016: Digital phased array systems: Challenges and opportunities. *Proceedings of the IEEE*, Special Issue on Phased Arrays, **104**, Feb. 2016.

Fulton, C., M. Yeary, D. Thompson, J. Lake, and A. Mitchell, 2016: Digital phased arrays: Challenges and opportunities. *Proceedings IEEE, Special Issue on Phased Arrays*, **104**, 487-503.

Mirmozafari, M., G. Zhang, S. Saeedi, and R. J. Doviak, 2017: A dual-linear polarized highly isolated crossed dipole antenna for MPAR application. *IEEE Antennas and Wireless Propagation Letters*, **16**, 1879-1882.

Mirza, R., Y. Zhang, D. S. Zrnic, and R. J. Doviak, 2016: "EM dipole array antenna for polarimetric phased array radar". In *Modern Antenna Systems*, Mohammad A. Matin, ed. InTech.

Nai, F., S. M. Torres, and R. D. Palmer, 2016: Adaptive beamspace processing for phased-array weather radars. *IEEE Transactions on Geoscience and Remote Sensing*, **54**, 5688-5698.

Perera, S., Y. Zhang, D. S. Zrnic and R. J. Doviak, 2017: Electromagnetic (EM) simulation and alignment of dual-polarized array antennas in multi-mission phased array radars. *Aerospace*, **4**, 7.

Saeidi-Manesh, H., M. Mirmozafari, G. Zhang, 2017: Low cross-polarisation high-isolation frequency scanning aperture coupled microstrip patch antenna array with matched dual-polarisation radiation patterns. *Electronics Letters*, **53**, 901-902.

Saeidi-Manesh, H., and G. Zhang, 2017: Cross-polarization suppression in cylindrical array antenna. *IET Electronics Letters*, **53**, 577-578.

Saeidi-Manesh, H., and G. Zhang, 2017: Characterization and optimization of cylindrical polarimetric array antenna patterns for multi-mission applications. *Progress In Electromagnetic Research B*, **158**, 49-61.

Yu, X., Y. Zhang, A. Zahari and M. Weber, 2016: An implementation of real-time phased array radar fundamental functions on a DSP-focused, high-performance, embedded computing platform. *Aerospace*, **3**, 28.

Zhang, G. 2016: *Weather Radar Polarimetry*, CRC Press, 322 p.

Patents and Invention Disclosures

Salazar, J. L., et. al, "Radio Frequency (F) Scanner Multi Degree of Freedom Antenna Calibration and Characterization Robot" U.S. Provisional Patent 16N0R006, submitted September 15, 2016.

Salazar-Cerreno, J. L., et. al., "An Instrument for In-situ Antenna Characterization, Radome Inspection and Radar Calibration.", Invention disclosure submitted to the University of Oklahoma on March 12, 2017.

CIMMS Task III Project – Polarimetric Phased Array Radar Research in Support of MPAR Strategy

Guifu Zhang and Hjalti Sigmarsson (ARRC, OU School of Meteorology and ECE), Richard Doviak, Allen Zahrai, and Dusan Zrnic (NSSL), Lesya Borowska (ARRC Post Doc), and Hadi Saeedimanesh, Mirhamed Mirmozafari, Zhe Li, and Mohammadhossein Golbonhaghighi (ARRC/ECE/SoM Students)

NOAA Technical Lead: Kurt Hondl (NSSL)

NOAA Strategic Goal 2 – *Weather Ready Nation: Society is Prepared for and Responds to Weather-Related Events*

Funding Type: CIMMS Task III

Objectives

Conduct research on practical issues for designing and developing the Polarimetric Phased Array Radar (PPAR), including the Cylindrical Polarimetric Phased Array Radar (CPPAR), to better understand the scientific advantages, technical challenges & limitations and cost-performance tradeoffs, as well as to support MPAR strategy in decision making to sustain Norman's leadership in weather radar and to expand its radar expertise for broad research and multi-mission applications.

Accomplishments

This project team continues to work on i) radiating element design and testing, applicable to both the PPPAR and the CPPAR, ii) array configuration study to achieve high performance for a PPAR, iii) design of the frequency-scan beam matched column antennas, and iv) advance signal processing. A highly isolated dual-polarization dipole antenna has been designed and tested with polarization purity with cross-pol level is below -40dB from the co-pol peak (Mirmozafari et al. 2017) as shown in the first figure below. The second figure below shows the concept and calculation of image arrangement of an array antenna (Manesh and Zhang 2017). The resigned CPPAR antenna and test results are shown in the third figure below, indicating well-match dual-pol antenna patterns can be achieved (Manesh et al. 2017).

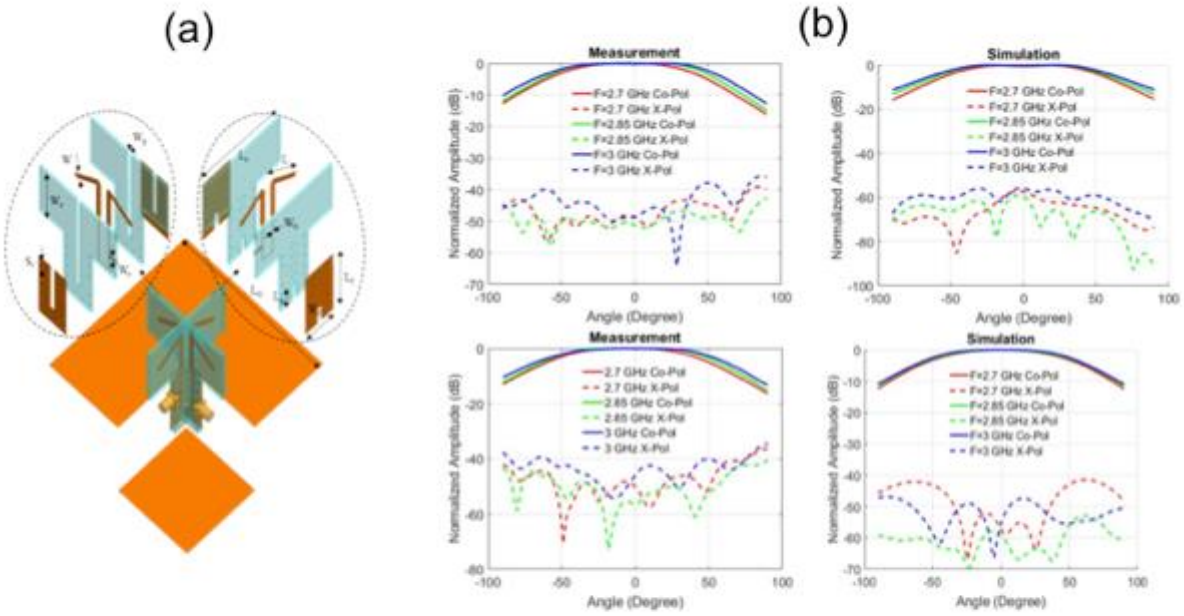

Design of a dual-polarization crossed dipole antenna: (a) geometry and (b) radiation patterns of designed. Cross-pol level is below -40dB from the co-pol peak, satisfying the MPAR requirements

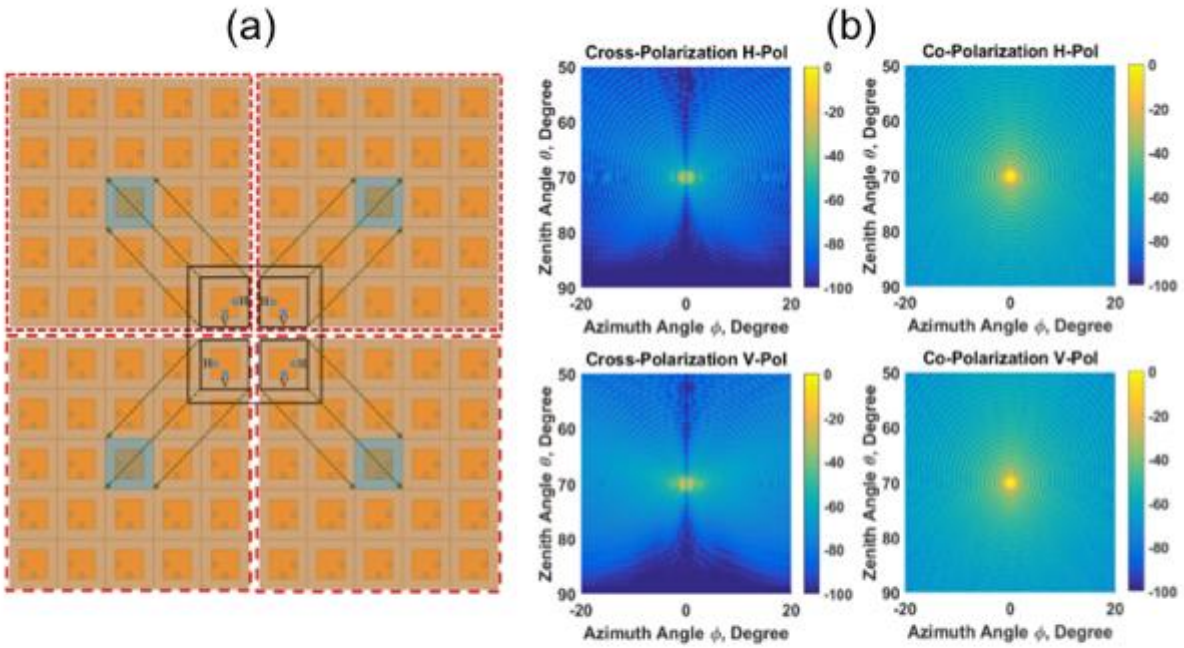

Image arrangement to improve polarization purity: (a) configuration sketch, and (b) 3D radiation patterns for co- and cross-polarizations.

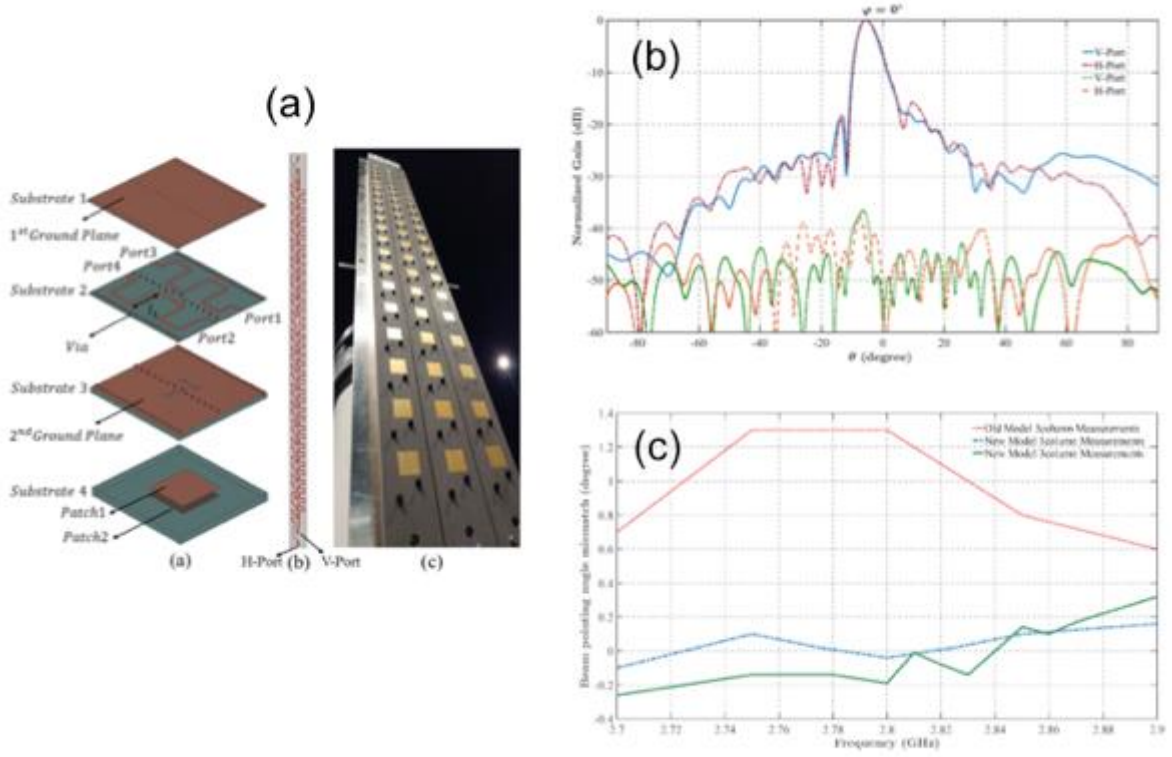

CPPAR antenna design and test results: (a) geometry of 19-element array antenna, (b) measured H-Pol and V-Pol co- and cross-polarization radiation patterns of the embedded column, and (c) beam pointing angle mismatch versus frequency.

Publications

Borowska, L., G. Zhang, and D. S. Zrnic, 2016: Spectral processing for step scanning phased array radars, *IEEE Trans. On Geoscience and Remote Sensing,* **54**, 4534-4543.

Mirmozafari, M., G. Zhang, S. Saeedi, and R. J. Doviak, 2017: A dual-linear polarized highly isolated crossed dipole antenna for MPAR application, *IEEE Antennas And Wireless Propagation Letters*, **16**, 1879-1882.

Saeidi-Manesh, H., and G. Zhang, 2017: Cross-polarization suppression in cylindrical array antenna. *IET Electronics Letters*, **53**, 577-578.

Saeidi-Manesh, H., and G. Zhang, 2017: Characterization and optimization of cylindrical polarimetric array antenna patterns for multi-mission applications. *Progress in Electromagnetic Research B,* **158**, 49-61.

Saeidi-Manesh, H., M. Mirmozafari, G. Zhang, 2017: Low cross-polarisation high-isolation frequency scanning aperture coupled microstrip patch antenna array with matched dual-polarisation radiation patterns. *Electronics Letters*, **53**, 901-902.

Zhang, G. 2016: *Weather Radar Polarimetry*. CRC Press, 322 p.

Theme 2 – Stormscale and Mesoscale Modeling Research and Development

NSSL Project 7 – Synoptic, Mesoscale and Stormscale Processes Associated with Hazardous Weather

NOAA Technical Lead: Lans Rothfusz (NSSL)

NOAA Strategic Goal 2 – *Weather-Ready Nation – Society is Prepared for and Responds to Weather-Related Events*

Funding Type: CIMMS Task II

1. VORTEX-SE Planning and Spring 2016 Campaign

Erik Rasmussen (CIMMS at NSSL)

Objectives
VORTEX-SE, a Congressionally-mandated research program to investigate the aspects of tornadoes in the southeastern U.S. that are associated with unusually high mortality. Project Manager Rasmussen leads the work of a 22-member Scientific Steering Committee, monitors and facilitates research through approximately fifty research grants, and incorporates the guidance of a four-agency (NOAA, NSF, NASA, NIST) Executive Committee.

Accomplishments
A third consecutive grant competition was conducted via a Federal Funding Opportunity. This competition will result in awards of slightly more than $3M for deserving projects. In addition, a collaborative research proposal was solicited from several OAR laboratories, with funding beginning in the summer of 2017. The overarching objective of the supported physical science research is to advance numerical forecast models sufficiently that they can highlight future observing needs, both to validate the models and to explore heretofore unidentified atmospheric features that contribute to the difficulties in forecasting southeastern tornadoes.

A major effort with the Scientific Steering Committee, and a community workshop, resulted in the overhaul of the Science Plan, informing the 2017 grant competitions, and outlining a multi-year research program that will be supported by VORTEX-SE NOAA funding as well as perhaps the NSF.

A successful field observing campaign was conducted in northern Alabama in March-April 2016.

VORTEX-SE investigators planning the daily operations during one of the 2016 Field Campaign Intensive Observing Periods.

2. Evaluation of Near Real-Time Preliminary Tornado Damage Paths

Chris Karstens (CIMMS at NSSL)

The ability to preliminarily diagnose areas damaged by a tornado was examined using both a manual and an automated approach. The manual method consists of using WSR-88D base data to track radar-indicated centroids of low-level rotation over the entirety of a tornado event. This method was developed at the National Weather Service (NWS) Weather Forecast Office (WFO) Norman, Oklahoma. According to the May 2013 Oklahoma Tornadoes and Flash Flooding Service Assessment, these preliminary damage paths were found to be beneficial to local first responders in the affected areas, to FEMA, and eventually to the public in graphical form via social media (first figure below). The purpose of this study was to analyze the performance of manually-derived preliminary tornado damage paths for an expanded, though limited, set of tornado events, and to compare the quality of these paths to those using an automated method using a geospatial verification technique. The automated method utilizes 0–2 km and 3–6 km AGL azimuthal shear from the Multi-Radar Multi-Sensor

(MRMS) system to link together a series of strong azimuthal shear clusters and create a proposed damage path polygon.

The verification results indicate, in general, that the damage paths of the manual method do a better job of detecting areas with tornado damage, along with indicating marginally less false area, compared to the damage paths of the automated methods (second and third figures below). All methods have a high bias, indicating that the preliminary damage paths denote an area much larger than the observed damage path. The high biases are attributable to uncertainty of the exact areas with tornado damage, as the methods utilize remotely sensed data to derive a preliminary damage path. Because the exact tornado damage path cannot be known with a higher level of certainty until a damage survey is conducted, denoting large areas in the vicinity of the observed damage path seems reasonable until refinements can be made. This tradeoff is relevant when comparing the performance of the manual (available within approximately one hour after the event) and automated methods (available within a few minutes after the event). With these results it is important to be mindful of the small sample of events used in this study.

When evaluating the performance for the preliminary damage paths individually, the damage paths of the manual method had the best overall performance, followed by the automated methods using 0–2 km and 3–6 km azimuthal shear, respectively. Additionally, the metrics from damage paths using the manual method show greater variability compared to the automated method using 3–6 km AGL azimuthal shear, but similar to those using azimuthal shear from the 0–2 km layer. The larger variance of the manually-derived damage paths is likely attributable to the narrowness of these paths, given that this method is intended to denote uncertainty about the central axis of the tornado track (line) as opposed to a damage path (area). Many of the automated damage paths using the 0–2 km azimuthal shear appear to align well with the axis of observed damage paths, but the object identification appears out of sync with the observed damage path length. The degraded performance of the 3–6 km automatically-derived damage paths appears to be, in some cases, attributable to an offset in the axis of the damage path polygon, as compared to the observed damage path. This spatial offset is likely attributable to using mid-level rotation for identifying surface damage, as the two are not always correlated, especially during the later stages of a tornado.

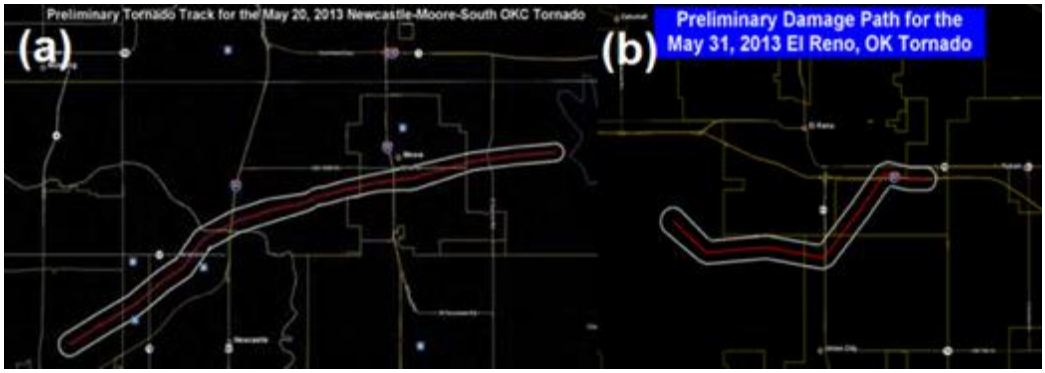

Preliminary tornado damage paths from 20 (left) and 31 (right) May 2013 produced by WFO Norman in a GIS-compatible format.

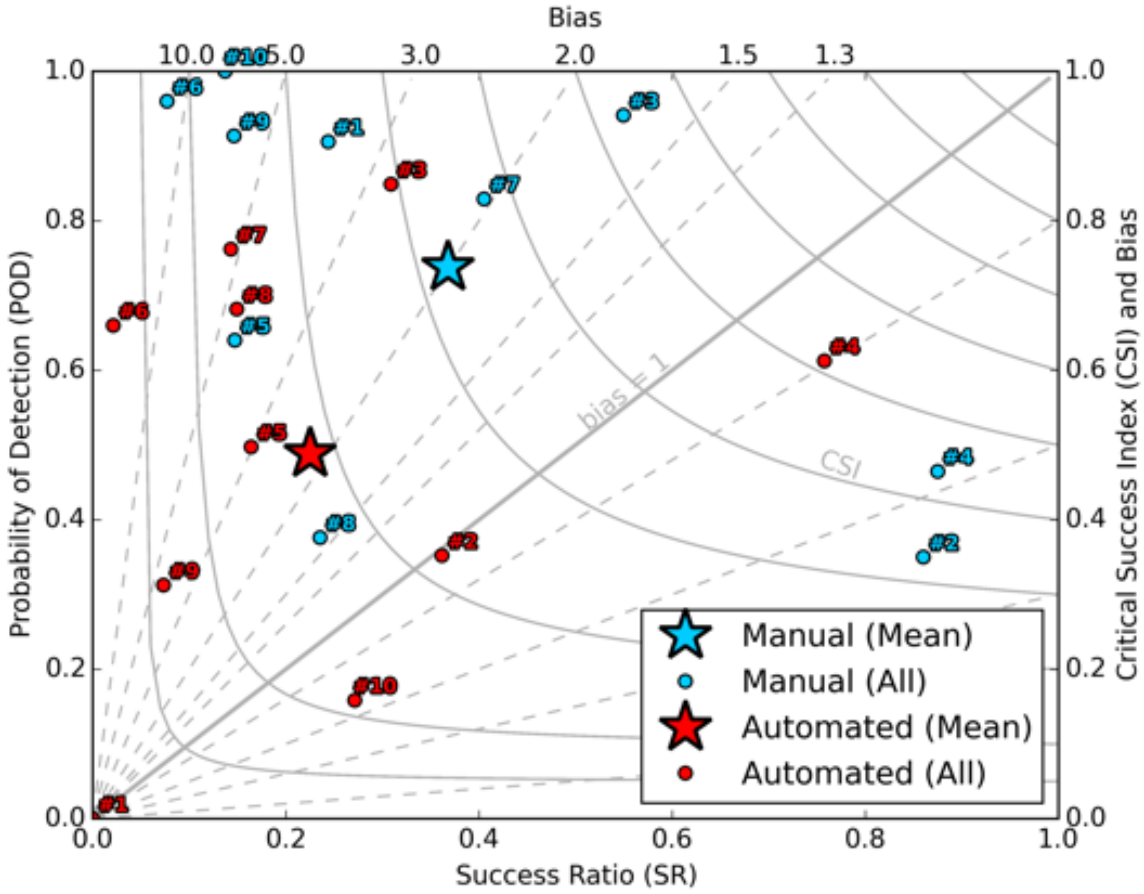

Performance diagram for evaluating the quality of the preliminary damage paths from the manual and automated (using 0–2 km AGL azimuthal shear) methods.

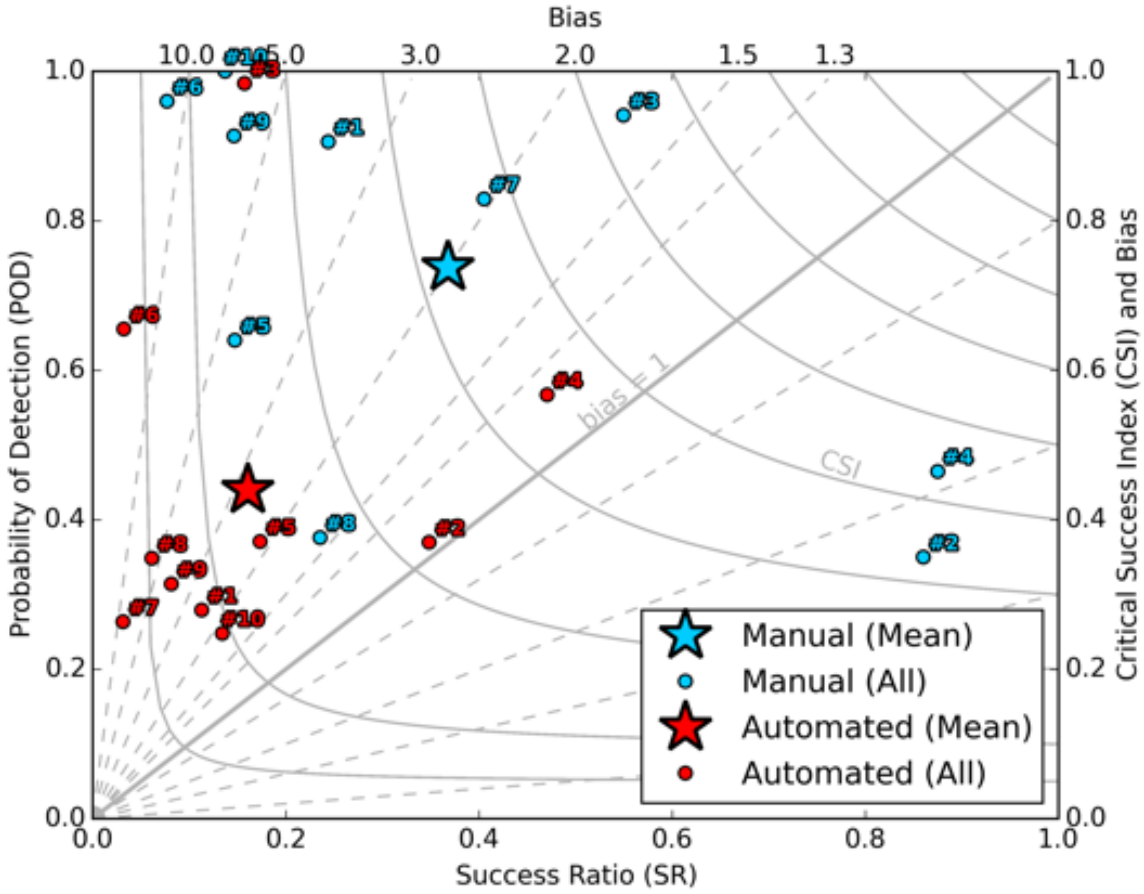

As above, except using 3–6 km AGL azimuthal shear with the automated method.

Publications

Karstens, C. D., K. Shourd, D. Speheger, A. Anderson, R. Smith, D. Andra, T. M. Smith, and V. Lakshmanan, 2016: Evaluation of near real-time preliminary tornado damage paths, *Journal of Operational Meteorology,* **4,** 132-141.

3. Numerical Simulations of Electrification Processes within Tropical Cyclones

Alexander Fierro (CIMMS at NSSL), and Don MacGorman, Ted Mansell, and Conrad Ziegler (NSSL)

Our main goal was to conduct and subsequently use the output from very high–resolution real or idealized numerical simulations (250-m to 2-km) of the small-scale electrification processes within tropical cyclones (TCs) to augment our understanding on these processes and, potentially, to derive functional relationships between various lightning metrics and the microphysics/kinematics of TCs. Total lightning is emphasized because it is much better correlated to convective strength than cloud-to-ground lightning is. Lightning information is particularly critical in regions where radar data are scarce, such as over oceans where all TCs develop and eventually intensify.

With the assistance of Dr. Mansell, we continued to implement new physics and initialization procedures into the NSSL COMMAS model to simulated idealized hurricanes. We successfully addressed all the required reviews for the idealized TC submitted last year to the *Journal of Atmospheric Science*, leading to its formal acceptance.

We conducted additional cloud-scale idealized electrified TCs simulations focusing on the intensifying case scenario. We also performed in depth analyses of the model output from the simulations described above and submitted a new manuscript describing these results to an AMS journal.

We organized a conference call with Co-PIs at NHC during spring 2017 to synthesize the results described in the work in (iv) and discuss future collaboration routes with regard to the analysis of GOES-R GLM data during forthcoming hurricane seasons.

We also assisted (including troubleshooting) NSSL to archive, process and transfer real time LMA data onto its local machines. We collaborated with lightning research group in Greece to explicitly forecast lightning over the Mediterranean using the official release of the lightning forecast model implemented into WRF in 2013 (E-WRF, Fierro et al. 2013). And, we continue to update and maintain E-WRF and provide support to interested research groups/teams when time/resources allow(s).

Publications

Fierro A. O., 2016: "Present State of Knowledge of Electrification and Lightning within Tropical Cyclones and Their Relationships to Microphysics and Storm Intensity." Chapter 7 in *Advanced Numerical Modeling and Data Assimilation Techniques for Tropical Cyclone Predictions*, U. C. Mohanty and S. Gopalakrishnan, eds. Co-published by Springer International Publishing, Cham, Switzerland, with Capital Publishing Company, New Delhi, India, pp. 197-220.

Fierro, A. O., J. Gao, C. Ziegler, K. Calhoun, E. R. Mansell and D. R. MacGorman, 2016: Assimilation of flash extent data in the variational framework at convection-allowing scales: Proof-of-concept and evaluation for the short term forecast of the 24 May 2011 tornado outbreak. *Monthly Weather Review,* **144**, 4373-4393.

Fierro, A. O. and E. R. Mansell, 2017b: Relationships between electrification and storm-scale properties based on idealized simulations of an intensifying hurricane-like vortex**.** *Submitted to the Journal of the Atmospheric Sciences.*

Fierro, A. O. and E. R. Mansell, 2017a: Electrification and lightning in idealized simulations of a hurricane-like vortex subject to wind shear and sea surface temperature cooling. *Journal of the Atmospheric Sciences,* **74**, 2023-2041.

Li Y., K. E. Pickering, D. Allen, M. C. Barth, M. M. Bela, K. A. Cummings, L. Carey, R. Mecikalski, A. O. Fierro, T. Campos, A. Weinheimer, T. Ryerson and G. S. Diskin, 2017: Evaluation of deep convective transport in storms of different scales during the DC3 field campaign using WRF-Chem with lightning data assimilation*. Journal of Geophysical Research-Atmospheres*, **122**, doi:10.1002/2017JD026461.

4. Thunderstorm Modification by Urban Environments

Darrel Kingfield and Kristin Calhoun (CIMMS at NSSL), Kirsten de Beurs (OU Department of Geography and Environmental Sustainability), and Geoffrey Henebry (South Dakota State University)

Urban areas are the most extreme form of land cover change as they reduce local biodiversity, modify atmospheric contributions of aerosols, and alter surface radiative energy budgets. How the size of an urban area influences precipitation patterns is an underexplored topic to date. Radar data provides an event-based view of precipitation echoes that can be used to examine the horizontal and vertical extent of thunderstorms, particularly when data from multiple radars are composited together. Yet, not many multi-radar studies exist in the research literature that perform such an analysis.

In this study, five years of 0.01° latitude x 0.01° longitude multi-radar multi-sensor grids of composite reflectivity, maximum expected size of hail (MESH), and vertically integrated liquid (VIL) were created to examine the role of city size on thunderstorm occurrence and strength around four cities: Dallas/Ft. Worth, TX; Minneapolis/St. Paul, MN; Oklahoma City, OK; and Omaha, NE. A storm tracking algorithm identified thunderstorm areas every minute and connected these areas together to form tracks. These thunderstorm tracks defined the upwind and downwind regions around each city on a storm-by-storm basis and were analyzed in two ways: (1) by sampling the maximum composite reflectivity, MESH, and VIL every 10 min. and (2) accumulating the thunderstorm spatial footprint over its lifetime. In addition to examining all thunderstorm events (i.e., the full climatology), a subset of events corresponding to favorable conditions for thunderstorm modification were explored. This urban favorable (UF) subset consisted of non-supercells occurring in the late afternoon/evening in the meteorological summer on weak synoptically forced days.

When examining all thunderstorm events, regions at variable ranges upwind of all four cities generally had higher areal mean values of reflectivity, MESH, and VIL compared to areas downwind of each city. In the UF subset, the larger two cities (Dallas/Ft. Worth and Minneapolis/St. Paul) had a 24-50% increase in the number of downwind thunderstorms, resulting in an increase in the frequency of stronger radar-based values and a higher overall downwind areal mean reflectivity, MESH, and VIL. The two smaller cities – Oklahoma City and Omaha – did not show such a downwind enhancement in thunderstorm occurrence and strength for all three radar variables examined. This pattern suggests that larger cities could increase thunderstorm occurrence and intensity downwind of the prevailing flow under appropriate environmental conditions.

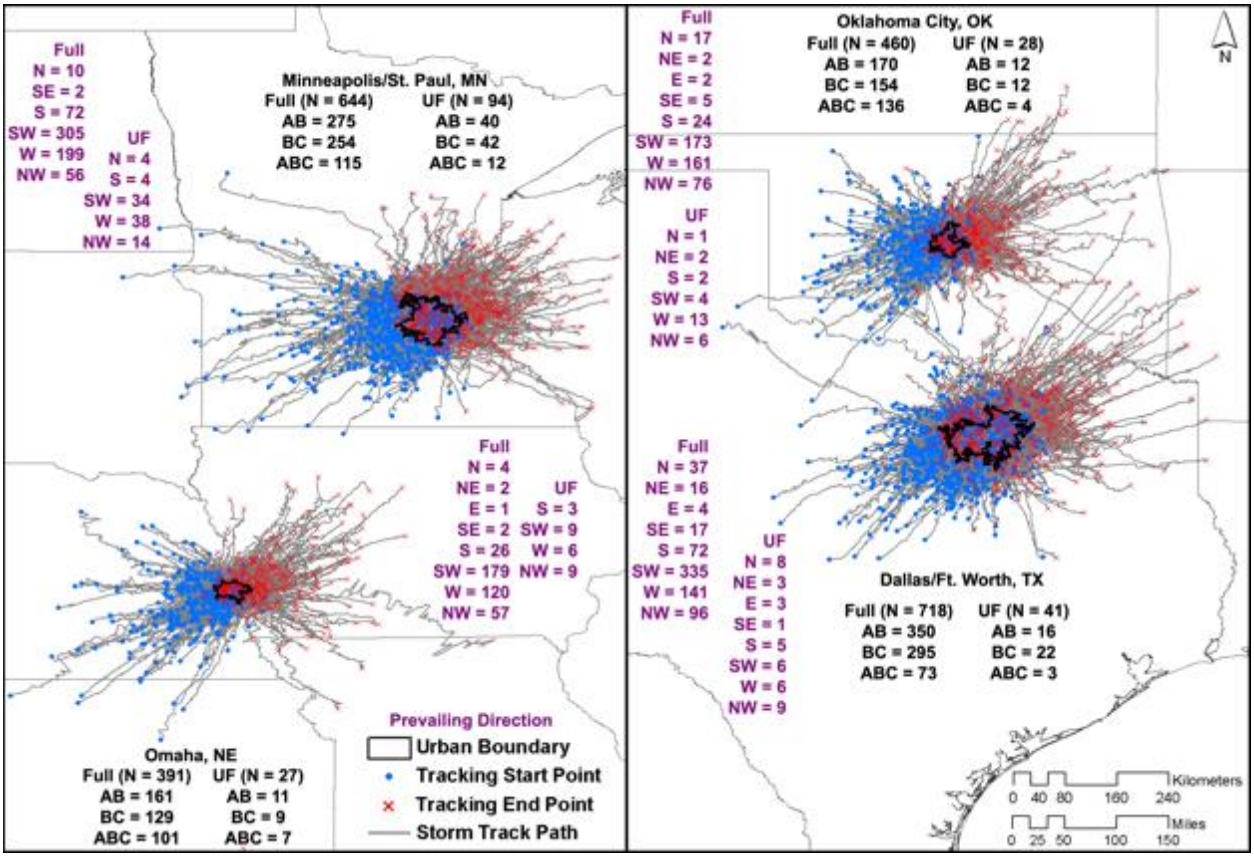

Thunderstorm trajectories (gray lines) with their initiation (blue points) and decay (red points) location around four cities in the United States Central Plains. The number of storms that formed upwind of the city and decayed over the city (AB), formed over the city and decayed downwind (BC), and formed upwind and decayed downwind (ABC) of each city are annotated in black for both the full climatology and UF subset of events. The frequency of thunderstorms by prevailing direction for each of these event datasets is annotated in purple.

Publications

Kingfield, D. M., K. M. Calhoun, K. M. de Beurs, and G. M. Henebry, 2017: Effects of city size on thunderstorm evolution revealed through a multi-radar climatology of the central United States. *Journal of Applied Meteorology and Climatology*. Accepted.

5. A High-Resolution Retrospective of Multi-Radar/Multi-Sensor Radar Reflectivity Products from the Multi-Year Reanalysis of Remotely Sensed Storms (MYRORSS)

Kiel Ortega, Anthony Reinhart, Brandon Smith, and Darrel Kingfield (CIMMS at NSSL)

In 2012 a partnered effort called the Multi-Year Reanalysis of Remotely Sensed Storms (MYRORSS) between the Cooperative Institute of Mesoscale Meteorological Studies, the National Severe Storms Laboratory, the Cooperative Institute for Climate and Satellites—North Carolina, and the National Center for Environmental Information, began to process the WSR-88D archive through the Warning Decision Support

System—Integrated Information software suite in order produce three-dimensional mosaics and derived severe weather products. This framework operationally is known as the Multi-Radar, Multi-Sensor (MRMS) system and is generated on a 0.01x0.01-degree horizontal grid that covers the CONUS with 35 vertical levels stretched from 250 m MSL to 20 km MSL at a 5-minute frequency. Currently, the MYRORSS project has completed reflectivity and reflectivity-derived products from 2000-2011, with the processing of Doppler velocity-derived products currently ongoing. Yet, with 12 years of MRMS reflectivity products available, initial analyses regarding the geographic occurrence and frequency of such radar signatures can be examined.

An overview of the potential studies that can be accomplished using reflectivity products was performed. Seasonal and monthly climatologies of the CONUS using the -10°C isothermal reflectivity product were conducted, examining the exceedance of a 50 dBZ reflectivity threshold at the -10° C level for each of the four seasons, in addition to calculating the maximum dBZ value of each month (January – December). Both studies display noticeable geographical variation with time that coincide with other climatologies that used non-reflectivity MYRORSS products. In addition to these analyses, other potential uses of the MYRORSS reflectivity products that were undertaken include diurnal comparisons of reflectivity (e.g., temporal variations of Southwestern U.S. monsoon), geographical variability of reflectivity (e.g., convective difference over land versus water), ground clutter mapping (e.g., wind farms), and non-meteorological scatters (e.g., migratory bird movements).

Maximum estimated size of hail (MESH) accumulations greater than 12.7 mm spanning the CONUS for each meteorological season were performed. The accumulations of MESH show a minimum of MESH occurring over the winter months (December – February) across the CONUS. During spring (March – May), there is a maximum of days where MESH values greater than 12.7 mm occur located in the Southern Great Plains centered over Southern Oklahoma and North Texas. In summer (June – August) the number of days that are above the 12.7 mm MESH threshold over the 12 year climatology increase in number to over 30 days in the last 12 years and shift poleward to the Northern Great Plains with a maximum centered over Nebraska. Through the fall months (September – November) a decrease in number of days exceeding the 12.7 mm threshold decrease and shift southeastward towards the Central Great Plains. The frequency of MESH exceeding the threshold also decreases as the shift to fall occurs.

A geographical retrospective of the 50 dBZ echo top height (i.e., height of the highest 50 dBZ reflectivity echo above ground level) was also performed. Over the 12-year period, the maximum 50 dBZ echo top height reached its highest values ($\geq$ 40 kft) in a corridor extending east from the Rocky Mountains through the Great Plains states. Examining the number of convective days with a 50 dBZ echo top height $\geq$ 25 kft by season reveals a minimum in the winter months (December – February) restricted to the southeast Gulf Coast states with a northward expansion in echo top coverage and frequency into the central United States in the spring (March – May) and summer months (June – August). In the central United States, any given grid cell in this region experienced a 50 dBZ echo top taller than 25 kft across 20-30 convective days. In the fall (September –

November), the areal coverage of echo tops is similar to the summer months but at a lower frequency (1-5 convective days). Breaking down echo top coverage reveals that the greatest spatial coverage occurs between 18 UTC and 02 UTC with a minimum around 14 UTC.

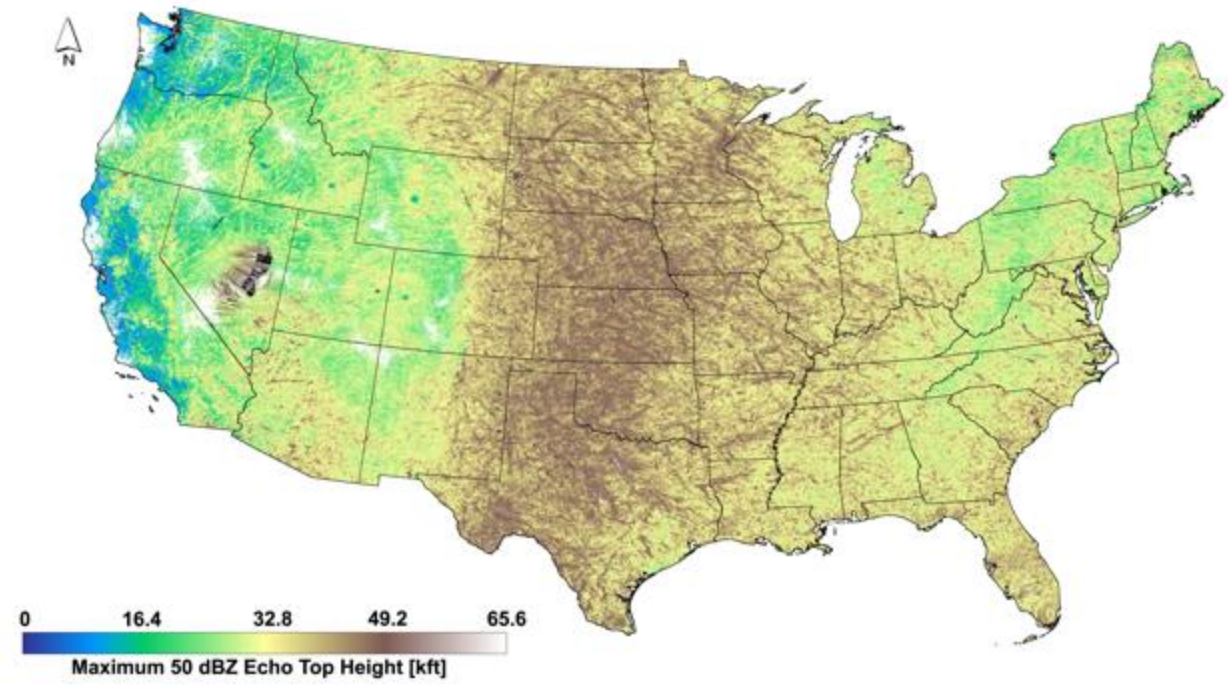

Geographic location of the maximum 50 dBZ echo top height measured between 2000-2011. A corridor of 40+ kft echo tops extends east of the Rocky Mountains through the Great Plains states and slightly eastward. Echo top heights gradually decline towards the southeastern United States and decline more rapidly towards the west and northeastern states.

6. A High-Resolution Retrospective of Cloud-to-Ground Lightning in the United States: 1995-2015

Darrel Kingfield and Kristin Calhoun (CIMMS at NSSL)

Cloud-to-ground (CG) lightning data are valuable in estimating thunderstorm location in data spare or void regions. In preparation for incorporation into the Multi-Year Reanalysis of Remotely Sensed Storms (MYRORSS) initiative, 20 years of quality-controlled CG lightning data from the National Lightning Detection Network (NLDN) were processed and gridded over the conterminous United States (CONUS) in both the MYRORSS spatial resolution (0.01° latitude x 0.01° longitude) and at 500 m spatial resolution (i.e., the median location error for the sensor network).

A geographical analysis of the 500 m lightning data revealed that around 10% of the CONUS area had no detected CGs while 1% had $\geq$ 40 CGs corresponding to 4.25% of

all lightning detected over the 20 year period. A manual analysis of these locations reveals the presence of tall human-made structures, mainly antenna towers, within 1 km of the high frequency grid cell. Spatially comparing these high lightning regions to records from the Federal Communications Commission (FCC) Antenna Structure Registration database reveals that 98.2% (24.8%) of grid cells with $\geq$ 100 CGs had an antenna structure taller than 200 m (500 m) above ground level (AGL). Tower height is correlated with lightning occurrence with a median lightning frequency of 173 CGs near towers $\geq$ 500 m AGL compared to 138 CGs near towers $\leq$ 200 m AGL.

Examining lightning density and peak current by tower height around 435 antenna structures isolated by 10 km from any other structure reveals that 96% of towers $\geq$ 200 m AGL had a higher lightning density within 1 km of the structure compared to 2-5 km away. Tower locations also registered more negative CGs (-CGs) than positive CGs (+CGs) at higher peak compared to locations 2-5 km away.

Exploring the seasonal influence of tower-lightning initiation reveals that shorter towers in the Northern Great Plains states experience a greater positive increase in CG lightning density in the cold season months (September-February) compared to the warm season months (March-August). Eight towers ranging from 343-609 m AGL had at least a 400% higher CG lightning density in the cold season compared to three towers ranging from 457-609 m AGL in the warm season. This is likely due to winter convective events having lower lightning charge centers compared to summertime convection.

Examining increases in CG lightning due to new tower construction during the 20-year period reveals that 74% of new construction projects had a higher CG lightning density within 1 km of the site compared to 2-5 km away the following year after construction. This was also correlated with tower height with 90% of new towers $\geq$ 500 m AGL having a higher CG density the following year.

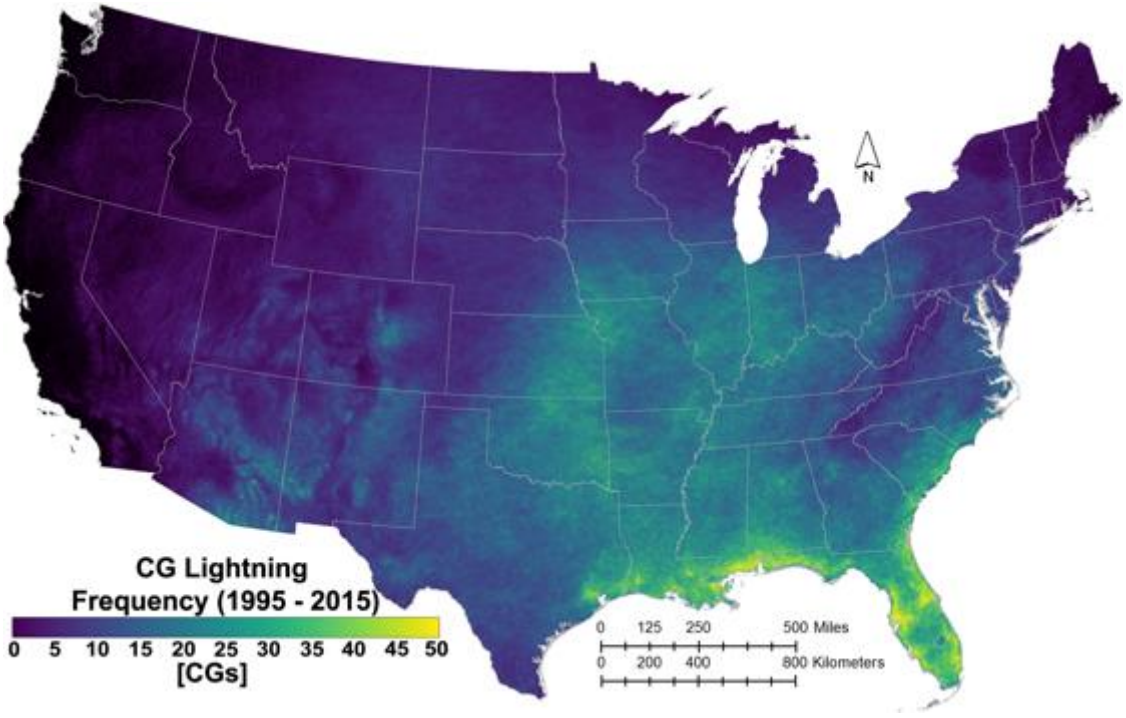

A 20 year, 500 m spatial resolution map of CG lightning frequency across the CONUS. Around 10% of the CONUS area had no detected CGs between 1995-2015 while 1% had ≥ 40 CGs.

Publications

Kingfield, D. M., K. M. Calhoun, and K. M. de Beurs, 2017: Antenna structures and cloud-to-ground lightning location: 1995–2015. *Geophys. Res. Lett.*, **44**, 5203-5212.

Awards

American Geophysical Union Research Spotlight Article written for the paper listed above, published in *EOS*.org on 26 May 2017:

Kingfield, D. M., K. M. Calhoun, and K. M. de Beurs, 2017: Antenna structures and cloud-to-ground lightning location: 1995–2015. *Geophys. Res. Lett.*, **44**, 5203-5212.

CIMMS Task III Project – Operation of VHF Lightning Mapping Systems to Provide Data for GOES-R GLM Verification and Algorithm Development and Testing

Don MacGorman (NSSL), Dennis Nealson (CIMMS at NSSL), Dustin Jarreau, Crystal Nassir, Justin Kleiber, and Jessica Wiedemeier (OU School of Meteorology), and collaborators Alexandre Fierro (CIMMS at NSSL) and Douglas Kennedy (NSSL)

NOAA Technical Lead: Steve Goodman (NOAA NESDIS)

NOAA Strategic Goal 2 – *Weather Ready Nation: Society is Prepared for and Responds to Weather-Related Events*

Funding Type: CIMMS Task III

Objectives
The primary objective of this grant is to maintain and operate the Oklahoma Lightning Mapping Array(OKLMA), which provides data for continuing basic storm research, for testing possible applications of total lightning mapping data in National Weather Service operations, and for providing ground truth data to validate performance of the new GOES-16 Geosynchronous Lightning Mapper (GLM).

Accomplishments
We found and addressed a problem discovered toward the end of 2016 with the data from several stations that interfered with data quality enough at times to make the data unusable. We have been working on a technique that hopefully will enable us to reconstruct those data, but the greater priority was to fix the malfunction before the beginning of the GOES-16 GLM validation field campaign. What we discovered, with help from Lightning Mapping Technologies, the original vendor for the equipment, was that the timing data stream from GPS receivers we had bought to replace failing units in some stations produced sporadic errors in the times recorded by the station. When this occurred, the system could not determine lightning locations. We successfully replaced these GPS units with units by the same manufacturer used in the stations originally. Data quality from the system since then has been excellent.

As part of our planned preparation for the GOES-16 field program, we identified a new site for a station near Goldsby, Oklahoma, to replace a site no longer available to us. Because the new solar powered stations do not require power to be run to the station, thereby allowing much greater freedom in choosing a good site and costing less to operate, we purchased one of the new stations and installed it last winter. It contributed reliably to the operation of the OKLMA during the field program and continues to run well. In addition, because the Lightning Mapping Array mother boards in the older stations were becoming unreliable, this year we replaced the boards purchased last year in all the stations in central Oklahoma to make them reliable once again before the field program began.

The OKLMA provided data sets for several storms during the field campaign, as well as providing data for additional evaluations of the GLM after the field program. We have been comparing OKLMA detections with GLM detections in the Hazardous Weather Testbed at the National Severe Storms Laboratory and have begun analyzing lightning data from both the OKLMA and GLM in storm studies. OKLMA data also have been provided to other scientists investigating topics of interest to the GLM program.

We have prepared a draft of a paper for journal publication describing the methodology we developed in previous years of this project to construct a decade-long climatology of the total lightning detected by the OKLMA. This initially required that we determine how to correct the lightning detections for the rapid decrease in the number detected with range. We tried two techniques: (1) determining the weakest signals from lightning detected reliably at the farthest range of our analysis and then using that as a threshold

to eliminate weaker signals from the detections at all ranges; (2) evaluating whether the range effect could be obviated by using flash detections, instead of using every detected signal. Our conclusion was that using flashes eliminated the range dependence as well as the thresholding of signals did, because the signals radiated by a flash have a range of amplitudes and typically included enough signals with stronger amplitudes to be detected by the OKLMA. Because we were computing flashes for some aspects of our climatology, we decided simply to use flashes for all aspects of our climatology to avoid range effects. After we complete the paper detailing our evaluation of the two techniques for correcting range effects, we will prepare a paper describing the climatology derived from the OKLMA. A draft of another paper based on OKLMA data is expected to be submitted to a journal this fall, this one describing the kinematic and microphysical characteristics leading to the formation of secondary thunderstorms within the anvil of a supercell.

Publications

DiGangi, E. A., D. R. MacGorman, C. L. Ziegler, D. Betten, M. Biggerstaff, M. Bowlan, and C. Potvin, 2016: An overview of the 29 May 2012 Kingfisher supercell during DC3. *Journal of Geophysical Research – Atmospheres*, **121**, 14316-14343.

Lang, T. J., S. Pédeboy, W. Rison, R. S. Cerveny, J. Montanyà, S. Chauzy, D. R. MacGorman, R. L. Holle, E. E. Ávila, Y. Zhang, G. Carbin, E. R. Mansell, Y. Kuleshov, T. C. Peterson, M. Brunet, F. Driouech, and D. Krahen, 2017: WMO world record lightning extremes: Longest detected flash distance and longest detected flash duration. *Bulletin of the American Meteorological Society*, **98**, 1153-1168.

MacGorman, D. R., M. S. Elliott, and E. DiGangi, 2017: Electrical discharges in the overshooting tops of thunderstorms. *Journal of Geophysical Ressearch – Atmospheres*, **122**, 2929-2957.

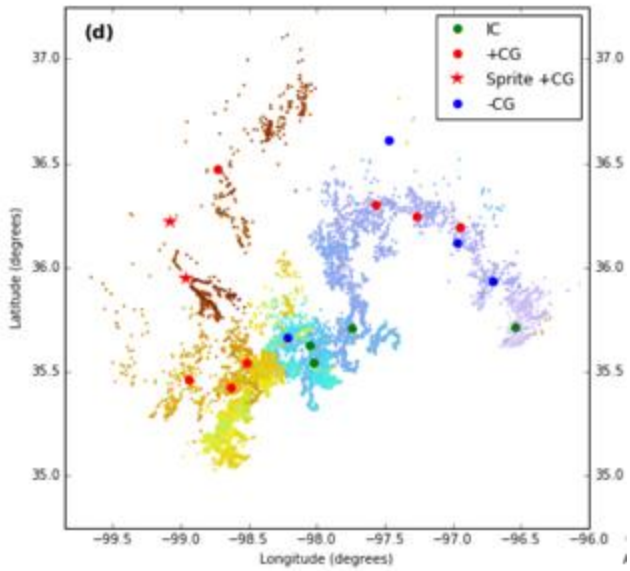

Characteristics of the Oklahoma flash at 0607:22 UTC on 20 Jun 2007, the longest spatial extent of a flash on record anywhere, spanning a great-circle distance of 321 km over a period of almost 6 seconds. Each dot is a VHF source location from a lightning channel mapped by the OKLMA, with color indicating the sequence of occurrence, from blue, through cyan, green, gold, and brown. Also shown are locations of intracloud flashes, positive cloud-to-ground flashes, and negative cloud-to-ground flashes located by the National Lightning Detection Network during the flash. The location of sprites triggered by the flash also are shown (adapted from Lang et al. 2017).

Theme 3 – Forecast and Warning Improvements Research and Development

NSSL Project 5 – Hazardous Weather Testbed

NOAA Technical Leads: Alan Gerard, Jack Kain, Pamela Heinselman, and Adam Clark (NSSL)

NOAA Strategic Goal 2 – *Weather-Ready Nation – Society is Prepared for and Responds to Weather-Related Events*

Funding Type: CIMMS Task II

Objectives

Experimental Forecast Program (EFP) objectives include:

- Evaluate the utility of high-resolution ensemble forecast systems for severe storm guidance at both 24 and 3 hourly time scales;
- Continue improving information extraction from the ensembles and verify high-resolution forecasts.

Experimental Warning Program (EWP) objectives include:

- Evaluate the accuracy and the operational utility of new science, technology, and products in a testbed setting to gain feedback for improvements prior to their potential transition into NWS severe convective weather warning operations;
- Foster collaboration between NSSL and GOES-R scientists and operational meteorologists.

Accomplishments

1. Forecast Verification and CLUE Evaluation During Spring Forecast Experiment 2017

Kent Knopfmeier**,** Chris Karstens, Scott Dembek, and Gerry Creager (CIMMS at NSSL), Robert Hepper and James Correia Jr. (CIMMS at SPC), and Burkely Gallo (OU School of Meteorology)

Two periods of formal evaluation were completed during SFE2017 where both subjective and objective assessments were made. In the first period, SFE2017 participants provided their subjective evaluations of the strengths and weaknesses of the outlooks generated by themselves, calibrated guidance, and a temporal disaggregation first-guess method through comparison to observed radar reflectivity, severe reports, NWS warnings, and MRMS radar-estimated hail size over the same time periods. Objective verification metrics such as the Critical Success Index (CSI) and Fractions Skill Score (FSS) were also computed to evaluate the experimental probabilistic forecasts of individual severe weather hazards such as tornadoes, hail, and damaging winds. In addition to using local storm reports as verification for the objective

metrics, supplemental observations from the MRMS-based Maximum Estimated Size of Hail (MESH) were used in near real-time to calculate these scores to examine the usefulness of alternative verification sources. These evaluations allowed for the determination of the relative skill of the computer- and human-generated forecasts over all time periods, assessing the feasibility of issuing operational high-temporal resolution severe weather outlooks.

The second period involved comparisons of different ensemble diagnostics and CLUE subsets. Similar to previous years, hail and tornado guidance, along with CLUE member microphysics guidance was examined. CLUE model physics member groups utilizing a single, a mixed, and a stochastic physics package was surveyed. Also compared were new experimental models to current operational ones, such as the HREFv2 to the SPC-produced Storm Scale Ensemble of Opportunity (SSEO) and the HRRRv3 versus the HRRRv2.

Of particular interest during SFE2017 was the performance of the two convection-allowing versions of the Finite Volume Cubed-Sphere (FV3) model provided by the NOAA Geophysical Fluid Dynamics Laboratory (GFDL) and the Center for the Analysis and Prediction of Storms (CAPS). Both use the same basic configuration except for the microphysics scheme, as the GFDL version employs the GFDL microphysics package while the CAPS version uses the Thompson microphysics package. The FV3 model was selected to replace the GFS as part of the Next Generation Global Prediction System program. The NOAA plans for the FV3 model to be the foundation of a unified modeling suite encompassing all prediction time scales. However, the FV3 model has not yet been tested in real-time for convective-scale forecasting applications. The auspices of the HWT and the SFE permit this testing, which is an important first step in its pathway toward operations. The GFDL and CAPS versions of the FV3 model were compared to other CAMs with well-known characteristics in terms of simulated storm structure, evolution, and placement. This should provide useful information to both the GFDL and CAPS FV3 model developers to make improvements to its dynamical core and physics packages.

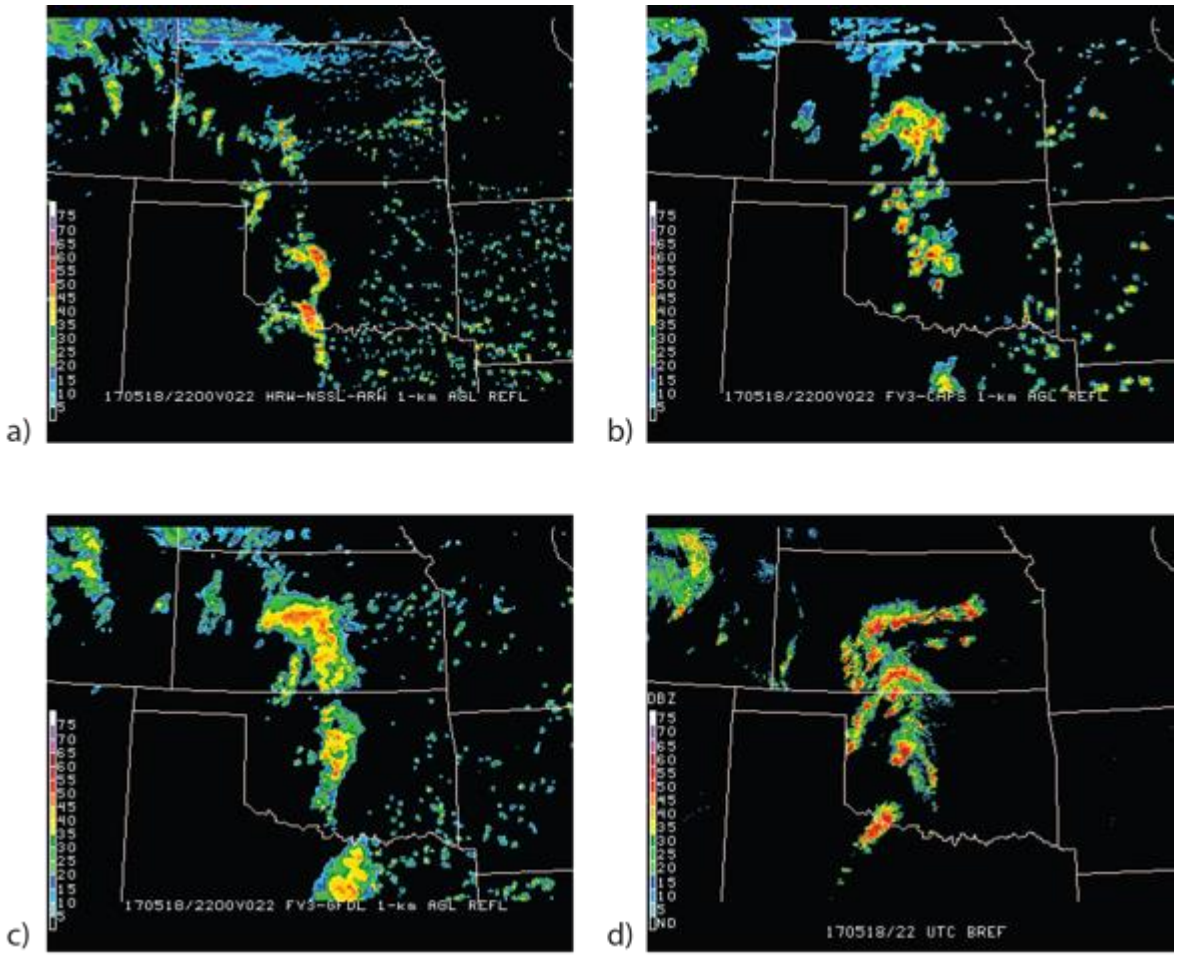

22-hr forecast of 1-km AGL simulated reflectivity valid at 2200 UTC 18 May 2017 from the a) Hi-Res Window NSSL WRF model, b) GFDL version of the FV3 model, and c) CAPS version of the FV3 model. d) NEXRAD base reflectivity valid at 2200 UTC 18 May 2017.

2. GOES-R and JPSS Development and Evaluation

Kristin Calhoun, Tiffany Meyer, and Darrel Kingfield (CIMMS at NSSL)

The goal of the Satellite proving ground evaluation is to introduce and familiarize users with newly developed products associated with the next generation of satellites including both the recently launched GOES-16 (previously GOES-R) and additional demonstration of JPSS products. The 2017 HWT evaluation provided one of the first opportunities to receive feedback and continue development from the GOES-R satellite, instruments and relevant algorithms.

This HWT evaluation focused on gauging the effectiveness of the GOES-R training, testing forecaster understanding of GOES=R data, understanding the usability and effectiveness of the visualizations in AWIPS, and identifying best practices for integrating the new data. Experimental and operational satellite products evaluated in

the HWT included the multiple products from the GOES-16 Advanced Baseline Imager, the Geostationary Lightning Mapper, Atmospheric Motion Vectors, the ProbSevere Hazard Model, Lightning Jump Algorithm, and NUCAPS temperature and moisture profiles. Feedback received during GOES-R and JPSS product demonstrations will be integrated into training initiatives and into research regarding future product development and visualizations.

In particular, since this was the first operational use of the Geostationary Lightning Mapper (GLM) data, quick-response development was required within the HWT to make the data usable for forecasters in an operational setting. This included baseline modifications to the AWIPS ingest and display of the GLM data that included “groups”, “events”, and “flashes” as this was improperly brought through the ground-based lightning systems and displayed as negative cloud-to-ground lightning (figure below). Additionally, new color tables and training materials were developed across the period of evaluation with iterative feedback from NWS forecasters.

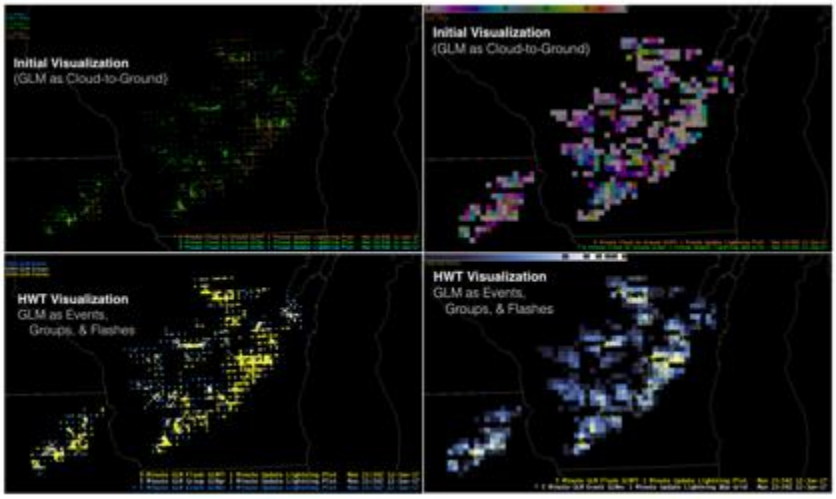

Initial visualizations of GLM data as received at the HWT (top) and updates made within the HWT for the data ingest and display made prior to displaying data to forecasters as part of the Proving Ground experiment (bottom).

3. Operations Coordination for the Experimental Warning Program

Gabe Garfield (CIMMS at OUN)

During the period, the Experimental Warning Program (EWP) conducted three projects intended to improve severe weather warnings. These included the following: (1) Hazard Services--Probabilistic Hazard Information; (2) Prototype--Probabilistic Hazard Information; and (3) GOES-16/JPSS. Over 50 forecasters and visitors participated, spanning 12 weeks during the summer of 2016 and spring of 2017.

In order for these projects to run smoothly, coordination was required. This included

experiment planning, facility management, forecaster recruitment, logistics planning, and the sharing of results. The following was accomplished:

- Monthly planning meetings with EWP scientists
- Management of experiment schedules
- Production of single recruitment letter with the EFP
- Collaboration with NOAA managers to recruit experiment participants
- Creation of selection committees to select EWP participants
- Modernization of program application using Google forms
- Arrangement of travel logistics for experiment participants
- Experiment status updates through email lists
- Development of webpage identifying EWP project leads, funding sources, and duration
- Sharing of EWP results and plans through teleconferences, workshops, and a summary paper

4. Merging of Experimental Warning Program Studies under Institutional Review Board Umbrella

Gabe Garfield (CIMMS at OUN)

In order to comply with government regulations concerning human research, the EWP worked with the University of Oklahoma to renew Institutional Review Board (IRB) approval for Experimental Warning Program activities. This year, in order to reduce IRB paperwork, three separate EWP studies were merged into one Hazardous Weather Testbed study. This entailed gathering the requisite information from each of the study leads, re-submitting the application, and ensuring that each scientist completed the requisite IRB training. The application was submitted, which the OU IRB approved.

5. Facilitation of the Prototype-Probabilistic Hazards Information (PHI) and GOES-16/JPSS Experiments

Gabe Garfield (CIMMS at OUN)

Before the Prototype PHI Experiment began, weather briefings were narrated for each displaced real-time case were produced (4 cases in total). Forecasters used these briefings to acquaint themselves with each case before beginning. Additionally, real-time weather briefings for the GOES-16 / JPSS experiment were provided.

SPC Project 11 – Advancing Science to Improve Knowledge of Mesoscale Hazardous Weather

NOAA Technical Leads: Russell Schneider and Steven Weiss (SPC)

NOAA Strategic Goal 2 – *Weather-Ready Nation – Society is Prepared for and Responds to Weather-Related Events*

Funding Type: CIMMS Task II

Overall Objectives

Conduct activities to maximize the diagnostic and forecast value of geostationary satellite data and products, within the SPC, HWT, and the GOES-R Proving Ground. A key component is to test and validate new satellite products associated with GOES-R, and to interact with NWS operational forecasters to prepare them for new satellite products. Emphasis will be on assessing the value of advanced satellite products for detection and short-term prediction of convective storms and associated hazards.

Support the HWT Experimental Forecast Program (EFP) and collaboration and sharing of information with the Experimental Warning Program (EWP). This involves performing research into application of new tools and applying verification techniques to convection allowing models/ensembles and experimental forecasts in near real-time within the HWT; and transferring of those activities found to be promising and of value from the HWT into daily operations at SPC. In addition, basic research is conducted to improve understanding of severe, fire, and winter weather topics that are of interest to SPC but are not related to any formal activities within the HWT. Finally, SPC partners are engaged to improve communication with the public to better mitigate the impacts of severe weather.

Develop probabilistic calibrated forecasts of cloud-to-ground (CG) lightning density through Day 8 based on input from operational numerical weather prediction models including convective allowing and ensemble models. Collaborating with NWS partners and the wildfire community is imperative to develop a broader unified probabilistic guidance suite that includes lightning occurrence and dry lightning. The probabilistic CG lightning density guidance will be distributed to NWS offices and external customers in a gridded format. The guidance will enhance the ability of fire agencies to prepare for lightning ignited wildfires by prepositioning and allocating appropriate wildfire suppression resources.

Project IMPACTS (Integrated Machine-based Predictive Analytics for Convective Threats to Society) involves the development of a statistical model that estimates the plausible impacts to life and property due to tornadoes and other convective hazards.

Accomplishments

1. Project IMPACTS – SPC Tornado Predictive Analytics System

Robert Clark (CIMMS at SPC), Patrick Marsh and Russell Schneider (SPC), and Somer Erickson (DHS FEMA)

During the period, we reached the initial operating capability for this system. The system consists of two components: a weather generator, which produces hypothetical tornadoes drawn from a series of statistical relationships, and an impact model, which

uses multilinear regression to estimate the societal impacts of individual tornadoes based upon certain tornado characteristics. Version 1 of this model was deployed in April 2017 and Version 2 of the model was under active development at the end of the reporting period.

Version 1 of the predictive analytics system (PAS) yields estimates of the population exposed to tornadoes and of fatalities due to tornadoes based upon SPC Day 1 Probabilistic Tornado Outlooks. To test the efficacy of the PAS methodology, we retrospectively re-ran PAS simulations for all tornado-driven SPC Day 1 Moderate and High-risk days over the last decade. We then compared the predicted (modeled) tornado fatalities to the observed fatalities for each day, as shown in the first figure below. One of our primary goals was to demonstrate that major, high-end tornado outbreaks can be identified *a priori* via the PAS method. The major tornado outbreaks of the last decade are distinguished from more typical tornado days based on PAS outputs. We also generated "practically perfect" (a technique for producing historical forecasts that would have been drawn by a forecaster possessing "perfect" knowledge of the location of the actual severe storm phenomena being forecast) SPC Tornado Outlooks for each tornado day going back to 1950, so that the analysis begun in the first figure can be extended to cover many more significant tornado events of the last 65+ years.

Version 2 of the PAS primarily concerns upgrades to the weather generator component of the system. Many assumptions underlying Version 1 were based on estimates and experience, rather than the statistical characteristics of observed tornadoes throughout the documented record since 1950. Much of the reporting period was spent conducting the research to implement improvements for Version 2. As shown in the second figure, we delineated two separate probability density functions (PDFs) for the relative frequencies of tornadoes of various damage ratings, which are used as a proxy for tornado intensity. These PDFs are based upon historical SPC tornado forecasts, and can be used to better-distinguish between higher-end and lower-end tornado days. This is critical, because tornado intensity is the single most important factor from an impact perspective. We have also substantially improved the number and location of hypothetical tornadoes produced by the weather generator, by accounting for the size of the area under tornado threat on any given day. In other words, larger threat areas tend to experience more tornadoes, and we now account for this fact.

We have also implemented new, related products for the FEMA Portal housed on SPC web resources. In consultation with FEMA's liaison to the SPC, Somer Erickson, we have developed an 8-day SPC Convective Outlook summary graphic for her daily briefings to FEMA leadership (see the third figure). We have also created "tornado analog" plots, which show examples of past SPC Tornado Outlooks (and their corresponding verification), which can be used by Somer to place current SPC forecasts into a historical context for the primarily non-meteorological audience that participates in her briefings.

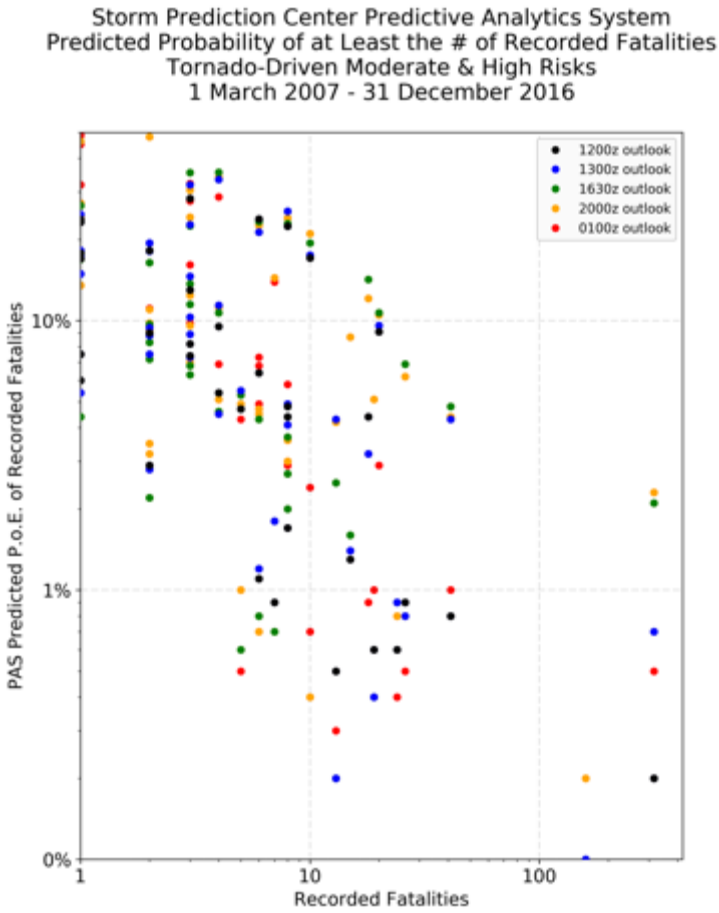

PAS predicted probability (vertical axis, log scale) of exceeding the observed number of fatalities compared to the actual observed fatalities (horizontal axis, log scale) for each SPC outlook on all tornado-driven Moderate and High-risk days.

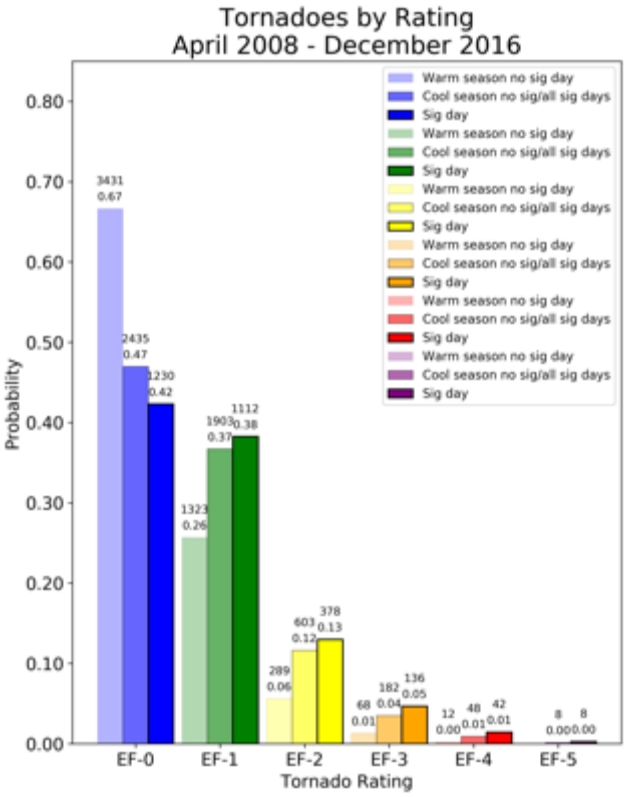

Observed tornado damage ratings broken down by the characteristics of the SPC Tornado Outlooks in effect on the days in which each tornado occurred. In the lightest color are the relative frequencies of tornadoes occurring May - October when no SPC significant tornado area was in effect, in the medium colors are all tornadoes occurring November – April, and in the darkest colors are all tornadoes throughout the year occurring on days with an SPC significant tornado area in effect. The topmost number above each bar is the total number of tornadoes contributing to that bar, and the lower number above each bar is the relative frequency of that tornado rating within that criterion.

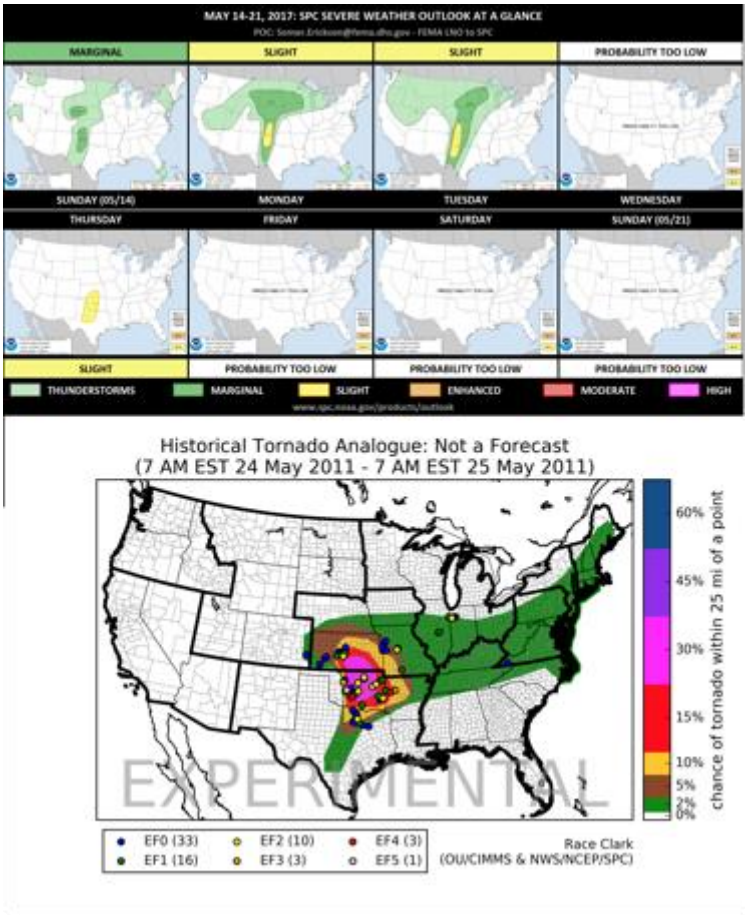

Example 8-day SPC Convective Outlook summary graphic for FEMA leadership briefings (top) and example SPC tornado analog graphic for FEMA use (bottom).

2. SSEO/SREF Calibrated Guidance

Caleb Grunzke (CIMMS at OU) and Israel Jirak (SPC)

This subproject builds from earlier work completed by Israel Jirak and colleagues at SPC (Jirak et al. 2014). Jirak had already developed once-daily Storm Scale Ensemble of Opportunity (SSEO) / Short Range Ensemble Forecast (SREF) Calibrated Guidance for tornadoes, large hail, and severe wind. This was running in real-time and made available to the SPC forecasters and external users, using mesoscale environment information [most-unstable convective available potential energy, vertical wind shear, and significant tornado parameter (STP) parameters] from the 2100 UTC SREF and explicit storm attribute information (updraft helicity) from the 0000 UTC SSEO. The probabilistic severe hazard output was valid for each 3-h period within the 24-h Day 1 Convective Outlook period starting at 1200 UTC. The first two objectives of this subproject were to create multiple runs of this calibrated guidance per day and to modify the individual valid period from 3-h to 4-h. The reasoning for producing the multiple runs per day was, as the severe weather event drew closer, the updated numerical guidance would likely produce improved environment (SREF) and storm attribute (SSEO)

forecasts and thus produce more accurate probabilistic hazard guidance. The 4-h forecasts were designed to align directly with the valid period of SPC experimental short-range outlook products. The methodology is as follows: For the 4-h forecasts, at every valid forecast hour the maximum of each environment and storm attribute exceedance probability variable over the previous 4 hours are paired at each grid point. Using data from a multi-year archive, the historical frequency of occurrence of a hazard (i.e., tornado, hail, or wind) report within 25 miles of that grid point and within the 4-h period for that forecast pair of probabilities is determined, and this observed frequency is used to provide a 4-h calibrated hazard probability.

A final objective was to create 24-h forecast guidance for tornadoes, large hail, and severe wind (similar to a SPC Day 1 Convective Outlook). For the 24-h forecasts, the output probabilities of the 4-h forecasts are utilized. Every other valid hour of the 4-h forecasts are employed. At every grid point, the cumulative sum of the 4-h probabilities and the maximum 4-h probability are paired. Using the same multi-year data base, the historical frequency of a report occurring within 25 miles of that grid point and within the 24-h period for those 4-h calibrated hazard probabilities is determined, and this observed frequency is used to provide the 24-h calibrated hazard probability.

We were able to successfully implement these changes and the SSEO/SREF Calibrated Guidance now runs at 0300 UTC (based 0300 UTC SREF and 0000 UTC SSEO), at 0900 UTC (based on 0900 UTC SREF and 0000 UTC SSEO), and at 1500 UTC (based on 1500 UTC SREF and 1200 UTC SSEO) each day. The forecasts are valid every 2 hours over the previous 4-h periods and end at 1200 UTC the next day. The guidance has been available in SPC operations since late February 2017 and is available to the external users on the SSEO web page under the “SPC Guidance” tab on the SPC website (www.spc.noaa.gov/exper/sseo).

The SSEO/SREF Calibrated Guidance was tested and evaluated within the 2017 Hazardous Weather Testbed (HWT) Spring Forecasting Experiment (SFE). Each day, participants in the experiment considered the guidance during the daily real-time forecasting activities. The next day, as part of the assessment of experimental forecasts and guidance for the previous day, participants evaluated the utility of the guidance and gave a subjective rating for the placement and magnitude of the forecast probabilities for each severe hazard. Daily and cumulative Fractions Skill Scores (FSS) were also computed for the 2017 HWT SFE 5-week period.

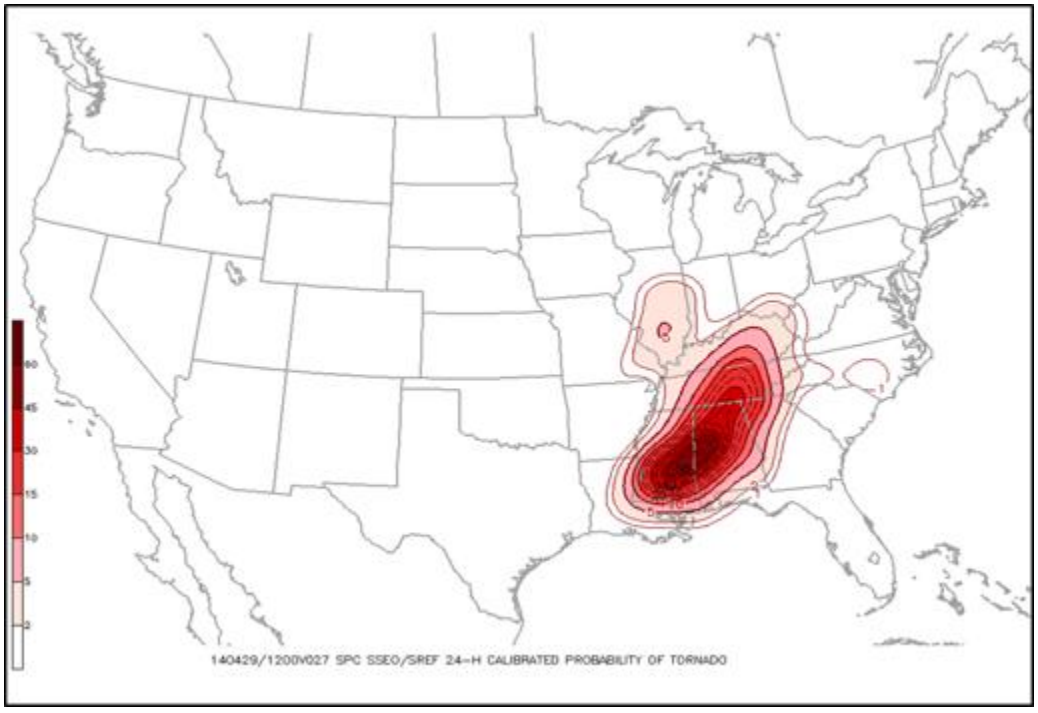

0900 UTC SSEO/SREF Calibrated Guidance for tornadoes valid on April 29, 2014 at 1200 UTC over the previous 24 hours for the CONUS.

3. Calibrated STP Tornado Intensity Guidance

Caleb Grunzke (CIMMS at OU), and Israel Jirak, Bryan Smith, and Richard Thompson (SPC)

The objective of this sub-project was to develop short-range calibrated probabilistic guidance for tornado intensity, especially for significant tornadoes defined as EF2 or greater on the Enhanced Fujita scale. The forecast guidance runs hourly out to 15 hours and is valid at 2-h intervals over the prior 4-h. This forecast guidance utilizes the research results led by SPC forecasters Bryan Smith and Rich Thompson (Thompson et al. 2017). They manually examined a multi-year archive of radar-observed tornadic supercells to determine the statistical relationship between the STP in the near-supercell environment and the tornado EF-scale rating. Calibration tables were then created for EF0+, EF2+, and EF4+ tornadoes based on value ranges of STP.

The calibrated probability of tornado intensity guidance uses information from the last four hourly runs of the High-Resolution Rapid Refresh (HRRR) numerical model to create a time-lagged ensemble. The guidance also uses the last hourly run of the Rapid Refresh (RAP) numerical model. These are used to provide environment (RAP) and storm attribute (HRRR) forecast information. The maximum value of STP from the RAP over the 4-h period is taken at each grid point and the statistical relationship between STP and observed tornado EF-scale distribution is used to determine conditional exceedance probabilities for various EF-scale ratings. This probability is

then multiplied by the probability of 4-h maximum updraft helicity ≥ 100 m^2/s^2 (representing the probability of a supercell) to create an “unconditional” probability of tornado intensity. For SPC forecasting purposes, the probability of a significant tornado (EF2+) is part of the operational probabilistic tornado outlooks, and one version of calibrated guidance has been specifically created to address this need (see accompanying figure).

The calibrated tornado intensity guidance was tested and evaluated within the 2017 HWT SFE. Each day, participants in the experiment considered the guidance during the daily real-time forecasting activities. The next day, as part of the assessment of experimental forecasts and guidance for the previous day, participants evaluated the utility of the tornado intensity guidance and gave a subjective rating for the placement and magnitude of the forecast probabilities for the tornado intensity. Daily and cumulative FSSs were also computed for the 2017 HWT SFE 5-week period.

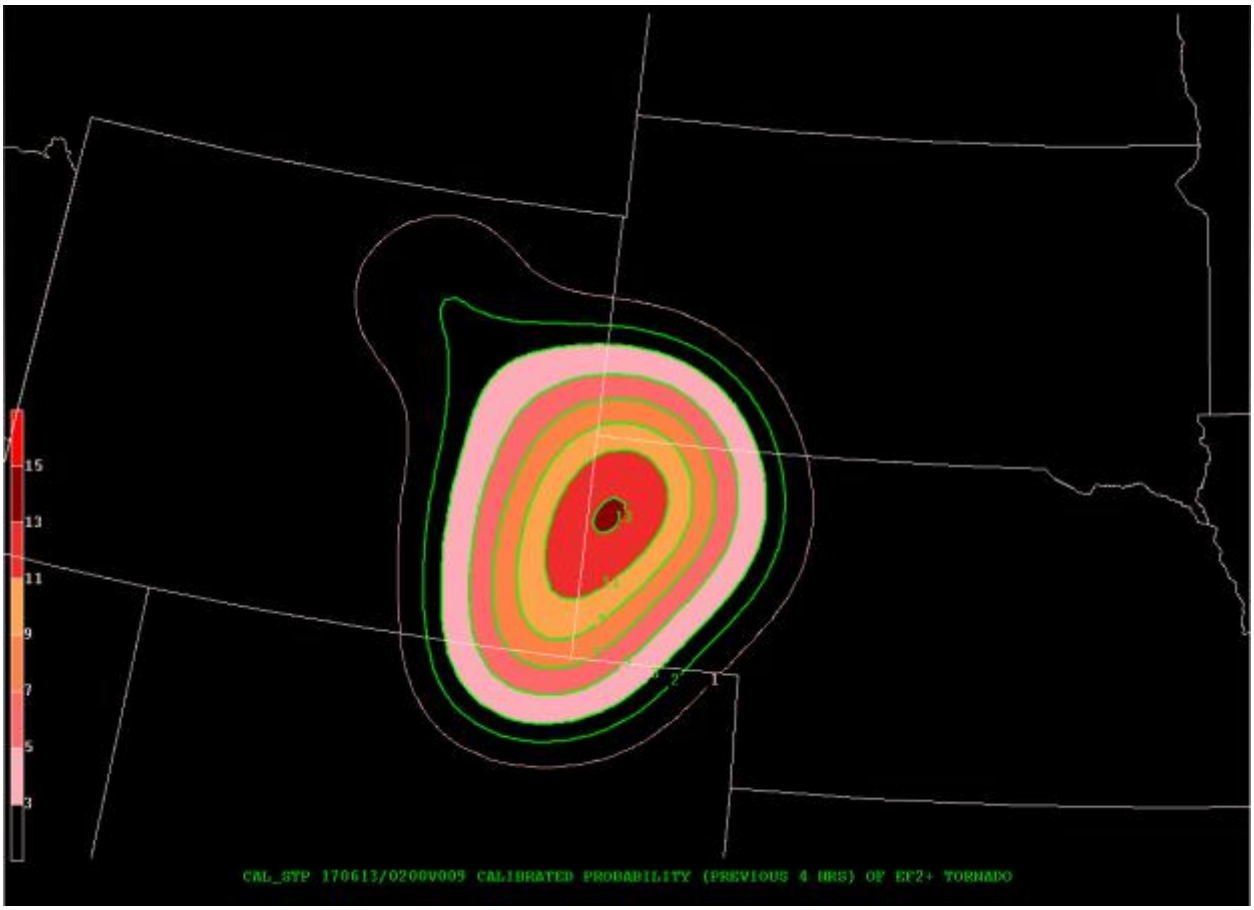

1700 UTC Calibrated Guidance for EF2+ tornadoes valid on June 13, 2017 at 0200 UTC over the previous 4 hours. Region is zoomed over the High Plains region of the United States.

4. Calibrated SSCRAM-HRRR Guidance

Caleb Grunzke (OU CIMMS), and Israel Jirak, John Hart, and Ariel Cohen (SPC)

The objective of this sub-project was to develop additional short-range calibrated probabilistic guidance for tornadoes, large hail, and severe wind utilizing the Statistical Severe Convective Risk Assessment Model (SSCRAM) created by SPC forecasters John Hart and Ariel Cohen (Hart and Cohen 2016). The forecast guidance runs hourly out to 15 hours and is valid at 2-h intervals over the prior 4-h. SSCRAM generates real-time probabilistic hazard guidance from a small number of atmospheric variables thought to be most closely related to each particular hazard.

The calibrated SSCRAM-HRRR guidance combines time-lagged HRRR numerical model output, using the last four hourly runs of the HRRR, and the SSCRAM probabilistic guidance based on the RAP, which is conditional on the occurrence of a thunderstorm. The SSCRAM guidance for each hazard is taken at each grid point and then multiplied by the 4 hourly maximum probability of simulated reflectivity being greater than 40 dBZ from the time-lagged HRRR, which is to represent the probability of a thunderstorm. This creates an “unconditional” probability of each severe hazard valid at each forecast hour covering the previous 4 hours.

The calibrated SSCRAM-HRRR guidance was tested and evaluated within the 2017 HWT SFE. Each day, participants in the experiment considered the guidance during the daily real-time forecasting activities. The next day, as part of the assessment of experimental forecasts and guidance for the previous day, participants evaluated the utility of the hazard guidance and gave a subjective rating for the placement and magnitude of the forecast probabilities for tornadoes, large hail, and severe wind. Daily and cumulative FSSs were also computed for the 2017 HWT SFE 5-week period.

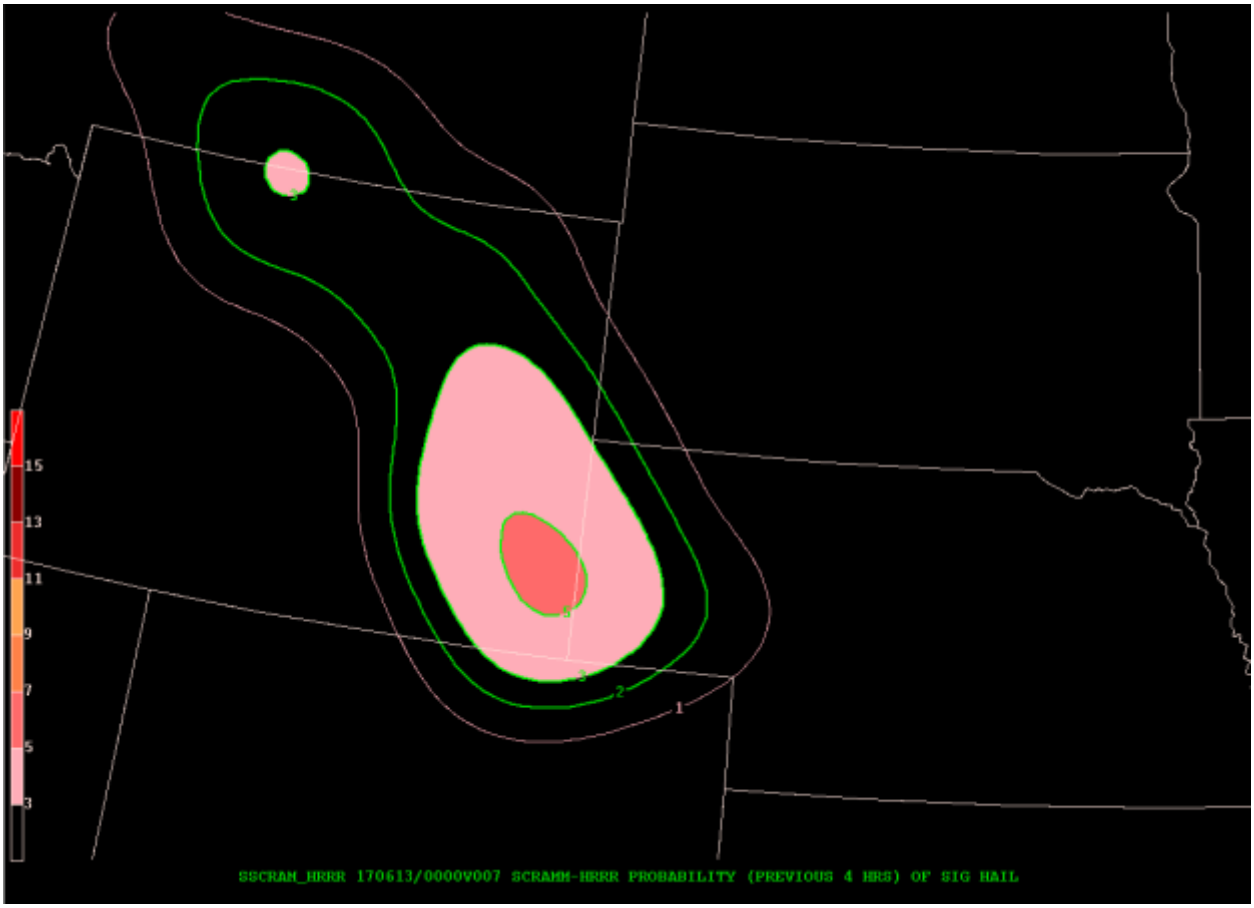

1700 UTC Calibrated SSCRAM-HRRR Guidance for significant hail valid on June 13, 2017 at 0000 UTC over the previous 4 hours. Region is zoomed over the High Plains region of the United States.

5. Lightning Density Prediction

Nicholas Nauslar (CIMMS at SPC), and Steven Weiss, Israel Jirak, Patrick Marsh, and Andy Dean (SPC)

The main objective for this project is to develop probabilistic calibrated forecasts of cloud-to-ground (CG) lightning density through Day 8 based on input from operational numerical weather prediction (NWP) models including convection allowing models (CAMs) and ensemble prediction systems. Collaborating with National Weather Service (NWS) partners and the wildfire community is imperative to develop a broader unified probabilistic guidance suite that includes lightning occurrence and dry lightning. The probabilistic CG lightning density guidance will be distributed to NWS offices and external customers in a gridded format. The guidance will enhance the ability of fire agencies to prepare for lightning ignited wildfires by prepositioning and allocating appropriate wildfire suppression resources.

Lightning-ignited wildfires are responsible for the majority of acreage burned across the United States. Thunderstorm and lightning guidance are imperative to fire weather forecasts, which are used by wildland fire managers when making decisions about resource allocation and suppression tactics. The Storm Prediction Center (SPC) Short Range Ensemble Forecast (SREF) calibrated thunder forecast guidance (SPC SREF CalThunder) currently provides probabilistic forecasts on different temporal scales detailing the probability of ≥ 1 and ≥ 100 CG lightning flashes in a 40-km grid box across the CONUS and adjacent oceanic areas. The SPC SREF CalThunder utilizes the probability of the non-dimensional cloud physics thunder parameter (CPTP) exceeding a value of one and the probability of precipitation equaling or exceeding 0.01" (Pr01). Then archived CG lightning flashes are used to create calibrated probabilities based on the probability pair of CPTP exceeding one and Pr01. The CPTP and Pr01 probabilities are grouped at 10% intervals and paired together into 121 different paired probability bins.

The SPC SREF CalThunder was refined to improve lightning density guidance. The lightning density threshold was lowered to 25 CG lightning flashes, since analysis of multi-year lightning flash climatology indicated more than 80% of all 3-hour CG lightning flash totals occur below this threshold. This threshold, therefore, is used to represent more significant occurrences of high lightning density. Utilizing the calibration method from the current SPC SREF CalThunder, a variety of analysis techniques including multiple grid point distance and CG lightning flash frequency weighting, statistical calibration, and smoothing methods, were tested on the new 25 CG lightning density flash threshold. One year of National Lightning Detection Network CG lightning and SREF model data were utilized to calibrate the forecasts, with the probabilities calculated by dividing 'hits' by 'totals' at every grid point, forecast cycle and hour, and each binned probability pair. Once the probabilities are generated, they are smoothed using the surrounding 24 grid points within +/- 2 grid points in x-y directions.

Based on preliminary results, the best method to create a new lightning density probabilistic forecast for ≥ 25 CG lightning flashes utilizes the calibration method from SPC SREF CalThunder with inverse-distance weighting (IDW) ((1/ $\sqrt{}$(i2 + j2)); where i is the number of grid points away from the grid point being calibrated in the x-direction and j is the number of grid points away from the grid point being calibrated in the y-direction) up to five grid points away in the x-y directions (i.e., a spatial neighborhood is considered). When CG lightning flashes exceed 25, the IDW is utilized and that value is added to 'hits' and 'totals' for the grid point being evaluated at that forecast cycle and hour. However, when lightning occurs but is less than 25 flashes, that IDW value is multiplied by the inverse difference between 25 and the number of CG lightning flashes for the grid point being evaluated at that forecast cycle and hour and added to both 'hits' and 'totals'. When there are no CG lightning flashes, the IDW is added to 'totals'. In addition to the specified period (i.e., 3-hour) of lightning data used to calibrate against, one hour before and one hour after each period are included (i.e., a temporal neighborhood) with those amounts reduced by one-half. This process was applied to all time periods (1, 3, 4, 8, 12, 24-hour), and verification statistics were generated including receiving operating characteristic (ROC) and reliability plots (see two figures below). All

the SPC SREF CalThunder guidance for ≥ 25 CG lightning flashes demonstrated good reliability and excellent AUC values (≥ 0.89).

Output from CAMs will be incorporated with current SREF output to generate refined probabilistic lightning density forecasts as the project moves forward. Thresholds of CAMs output that is conducive for lightning or indicative of convection (i.e., reflectivity at -10 °C) are being examined from the National Severe Storms Laboratory Weather Research and Forecasting model. We have been archiving EMC High-Resolution Ensemble Forecast (HREFv2) model data since 1 April 2017 and will continue through 30 September 2017 that will be used as a development dataset. This will allow us to investigate ensemble probabilistic CAMs output that would supplement the SPC SREF CalThunder by utilizing SREF environment information and explicit convective storm fields from a CAM ensemble.

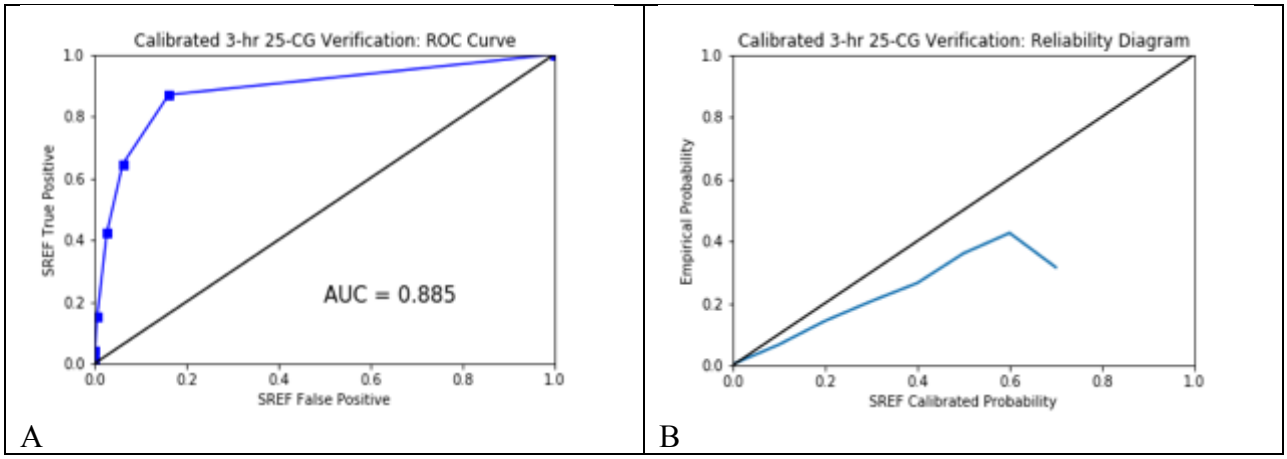

A) Receiver operating characteristic curve for the 3-hour SPC SREF based calibrated ≥ 25 CG lightning flashes guidance. B) Reliability diagram the 3-hour SPC SREF based calibrated ≥ 25 CG lightning flashes guidance

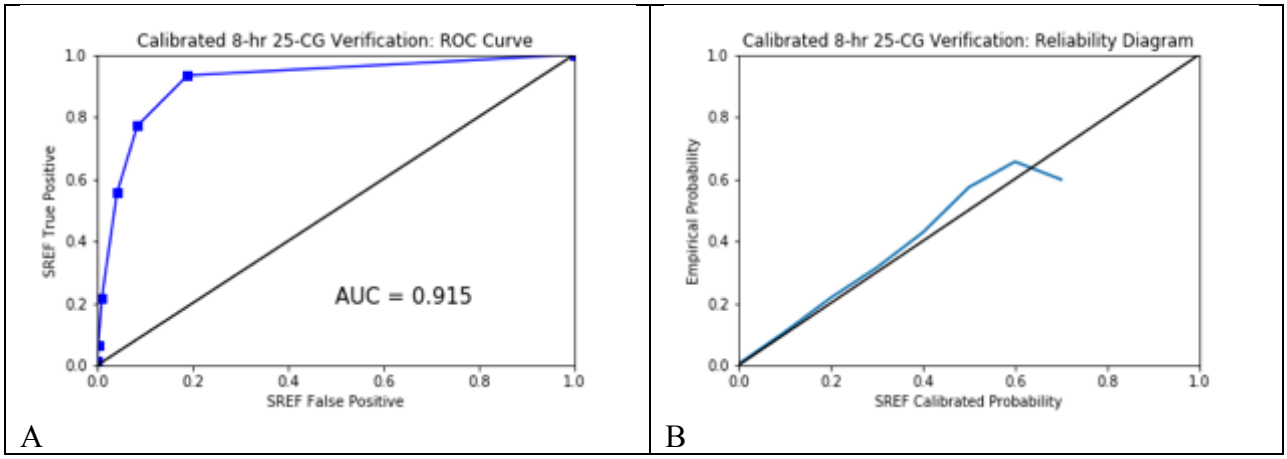

A) Receiver operating characteristic curve for the 8-hour SPC SREF based calibrated ≥ 25 CG lightning flashes guidance. B) Reliability diagram the 8-hour SPC SREF based calibrated ≥ 25 CG lightning flashes guidance.

6. GOES-R and JPSS Proving Ground Activities

Michael Bowlan and William Line (CIMMS at SPC)

The Storm Prediction Center (SPC) and Hazardous Weather Testbed (HWT) provide the GOES-R and JPSS Proving Ground with an opportunity to conduct demonstrations of Baseline, Future Capabilities and experimental products associated with the next generation GOES-R geostationary and JPSS polar satellite systems. Many of these products have the potential to improve hazardous weather nowcasting and short-range forecasting. Feedback from forecasters in the SPC and HWT has led to the continued modification and development of GOES-R and JPSS algorithms.

During the HWT 2017 GOES-R/JPSS Summer Experiment, GOES-R and JPSS products were demonstrated within the real-time, simulated warning operations environment of the Experimental Warning Program (EWP) using AWIPS-II (see figure below). This experiment was conducted Monday-Friday during the weeks of June 19, June 26, July 10, and July 17, and participants included a new group of three visiting NWS forecasters and one broadcast meteorologist each week. Product developers from various collaborating institutions were also in attendance to observe the activities and interact with the forecasters. Monday-Thursday included eight hour forecast/warning shifts, while Friday was a half-day dedicated to final feedback collection. During the simulated forecast shifts, the four forecasters utilized the baseline GOES-16 data along with other experimental satellite products, in conjunction with operationally available meteorological data, to issue non-operational short-term mesoscale forecast updates and severe thunderstorm and tornado warnings. Forecaster feedback was collected through the completion of daily and weekly surveys, daily and weekly debriefs, and blog posts.

GOES-R algorithms demonstrated during the HWT 2017 GOES-R/JPSS Summer Experiment included: GOES-16 baseline ABI cloud and moisture imagery, GOES-16 baseline derived products such as GOES derived stability indices, TPW, and derived motion winds, GOES-16 multi-spectral RGB composites, GOES-16 channel differences, UW/CIMSS ProbSevere Model and ProbTor Model, the Geostationary Lightning Mapper (GLM). From the JPSS program, the NOAA Unique Combined Atmospheric Processing System (NUCAPS) temperature and moisture profiles were demonstrated in the AWIPS-II NSHARP sounding analysis program. An experimental version of the NUCAPS profiles, which applies a boundary layer correction, was also demonstrated. The NUCAPS profiles derived parameters were also able to be looked at in a gridded plan view and cross section format.

The SPC has been involved in additional activities related to the launch and data flow of GOES-R. SPC has been receiving GOES-16 data since mid-February via a terrestrial GOES ReBroadcast (GRB) and since late March via the local GRB satellite antennas. GOES-16 has been used extensively in operations this severe weather season by SPC forecasters and the satellite liaison has been training staff on the new technologies of the satellite. SPC is also preparing for the receipt of GLM data once it is released and

preparing ways to best view the data in the forecasters' operational environment. Results from the 2016 GOES-R and JPSS product demonstrations in the SPC and HWT were documented by the satellite liaison in final reports and presented at various science meetings. Finally, the satellite liaison continues to contribute to the GOES-R training plan and development.

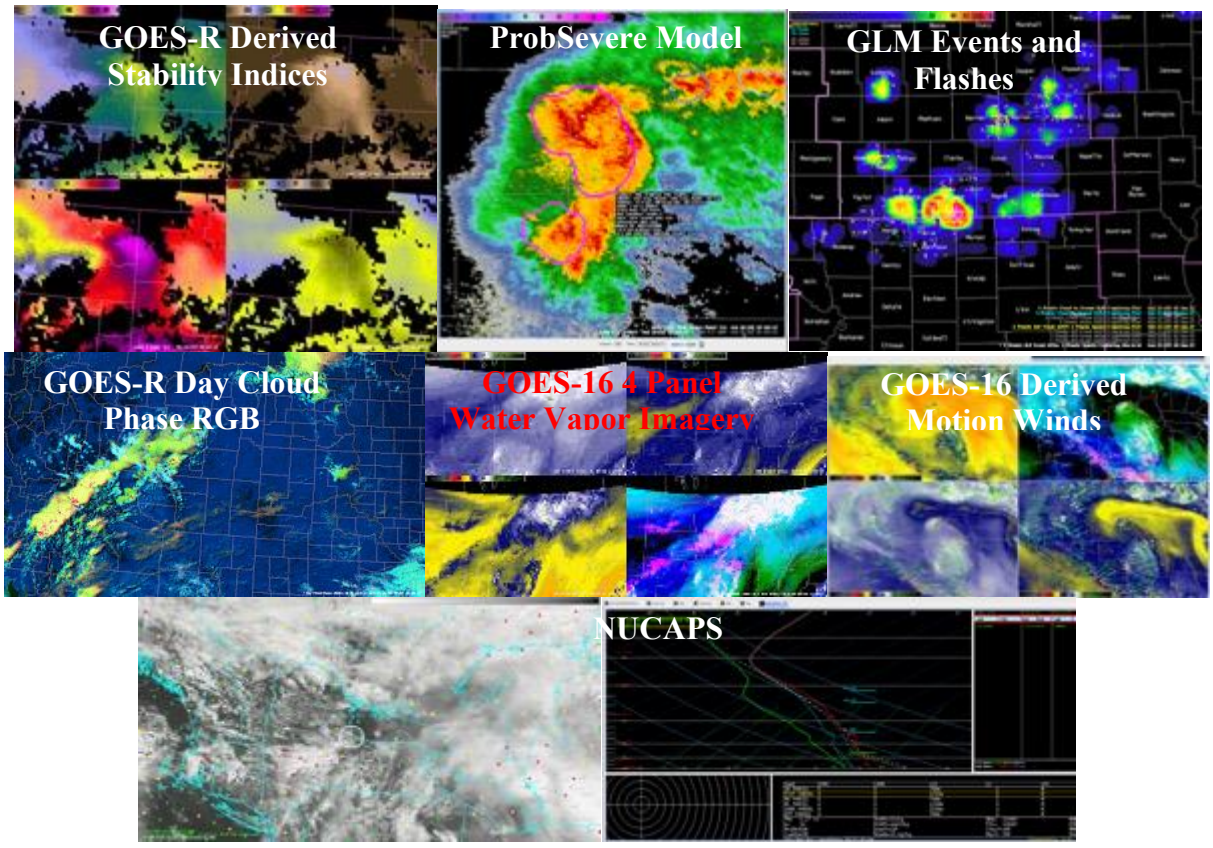

GOES-R and JPSS products and capabilities demonstrated during the HWT 2017.

7. Hazardous Weather Testbed

James Correia Jr. (CIMMS at SPC)

Performed the liaison duties between the Social Science community, Hazardous Weather Testbed (HWT), and Warn-on-Forecast programs on behalf of the Storm Prediction Center. This includes studying the capability of Convection-Allowing Models (CAMs) and ensembles, relating the output to forecasters through social science methods, and bringing this knowledge to, and testing it in, the HWT.

Supported various activities within the Experimental Forecast Program activities of 2017 including:

A. Ensemble forecasts of severe weather using updraft helicity objects for 3 systems (NCAR, SSEO, NSSL),

B. Exploratory visualization of CAPE-shear phase space for rotating storms using 3 ensemble systems,
C. Planning and support of the EWP-Probabilistic Hazard Information (PHI), and PHI-Emergency Manager projects to explore the use of PHI and its communication with emergency managers. Tailored briefings were provided for real-time cases while some graphics were provided for case study briefings.
D. Grant project (*Test and Evaluation of Rapid Post-processing and Information Extraction from large Convection-Allowing Ensembles applied to 0-3hr Tornado Outlooks.*) implementation of object based, rapid post-processing techniques in warning operations for probabilistic hazard information.
E. Continued to assist Harold Brooks and Kenzie Krocak on developing techniques for the extraction of time based severe weather probabilities. Concepts from these discussions resulted in the production of timing graphics of severe weather for the NCAR ensemble, using object-based techniques. Verification of observed timing is being investigated.

8. Tornado Warning Verification

James Correia Jr. (CIMMS at SPC)

While investigating convection allowing model uptake in the NWS, Harold Brooks and I noticed through quick verification of warnings that performance had suddenly changed. We have been updating tornado warning verification and its implications for performance as it relates to philosophy and informal policy of perceived problem areas. This work has cross collaboration with previous PHI work and is relevant to SPC's mission given the recent work on tornado report environments in an effort to improve performance resulting from continued improvements in discrimination between environments that produce tornadoes and those that do not. This work further has implications on formal product changes and informal policy changes that may be detectable as the SPC product suite evolves.

9. Mentoring

James Correia Jr. (CIMMS at SPC)

Emily Tinney was mentored as part of the Research Experience for Undergraduates program run by Dr. Daphne LaDue. She investigated low level jets from the NSSL Experimental Warn on forecast System for ensembles (NEWS-e).

10. Rain Outlooks

James Correia Jr. (CIMMS at SPC)

Explored the use of combined graphical representations of both SPC and WPC graphics when both severe weather and excessive rain outlooks overlap posing a double threat to areas of the United States.

11. Local Storm Reports Processing Display at SPC

Chris Melick (CIMMS at SPC)

Conduct activities to maximize the diagnostic and forecast value of geostationary satellite data and products, within the SPC, Hazardous Weather Testbed (HWT), and the GOES-R Proving Ground. A key component is to test and validate new satellite products associated with GOES-R, and to interact with NWS operational forecasters to prepare them for new satellite products. Emphasis will be on assessing the value of advanced satellite products for detection and short-term prediction of convective storms and associated hazards.

Support the Hazardous Weather Testbed (HWT) Experimental Forecast Program (EFP); Collaboration and sharing of information with the Experimental Warning Program (EWP); Perform research into application of new tools and applying verification techniques to convection allowing models/ensembles and experimental forecasts in near real-time within the HWT; Transfer of those activities found to be promising and of value from the HWT into daily operations at SPC. In addition, basic research was conducted to improve understanding of severe, fire, and winter weather topics that are of interest to SPC but are not related to any formal activities within the HWT. Finally, engage SPC partners to improve communication with the public to better mitigate the impacts of severe weather.

The spectrum of Local Storm Report (LSR) event types processed by the LSR Decoder software was expanded in fall 2016 to include additional high impact weather event types of interest to SPC and the NWS, specifically heavy rain, flood, flash flood and lightning. The LSR Decoder now processes event types pertinent to severe convection, fire weather, winter weather, and heavy rain. All LSR event categories are being processed and displayed in the prototype interactive SPC Storm Report display web page (see figure below).

This LSR Decoder system upgrade also merged the existing operational system to include attributes of the more advanced development system. The merging of both data formats eliminates the maintenance of redundant software and datasets, but continues required legacy rough log summaries which minimize downstream impacts on existing NWS data listings and displays.

The LSR code update also prepares the decoder to adapt to mixed-case text LSRs that will be implemented by the NWS in the fall of 2017.

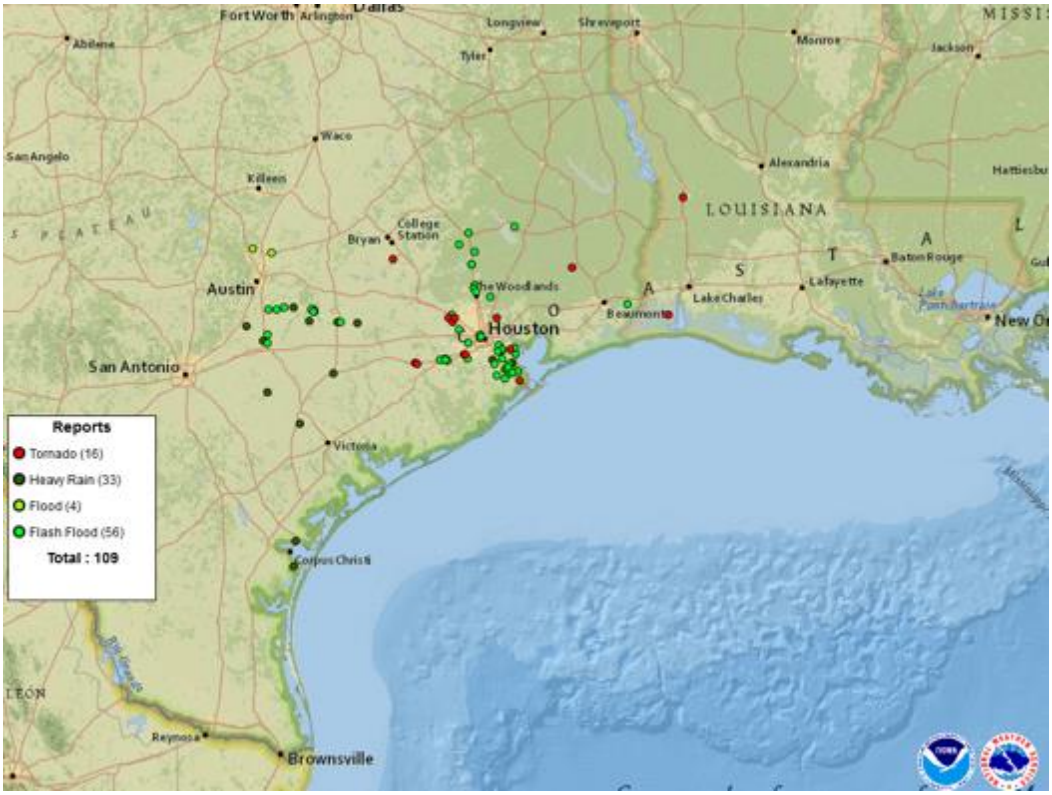

Prototype severe reports display showing heavy rain (dark green circles), flood/flash flood (light green circles) and tornado (red circles) LSR events for 26 August 2017 during Hurricane Harvey over Texas.

12. Cloud Flash Lightning Characteristics for Tornadoes without Cloud-to-Ground Lightning

Chris Melick (CIMMS at SPC)

This research (Melick et al. 2016) extended prior work at SPC by examining United States tornado events that were not associated with Cloud-to-Ground (CG) lightning for a subset of their time period for which Cloud Flash (CF) lightning data was available from Earth Networks (2013-2015). Characteristics of CF data are examined to provide a more comprehensive viewpoint of total lightning activity for these unique situations. In addition, the environmental conditions during these tornadoes are explored regarding the relationship to CF activity. Results indicated that CG lightning was absent in about 2% (66) of all tornadoes during a three year period (2013-2015) with a significant portion of these rated as EF0. Unexpectedly, though, only 17% (11) of no-CG tornado reports occurred with CF, thus implying that total lightning was often lacking in these tornadic storms as well. Findings were presented at the NWA Annual Meeting in Norfolk, VA (September 10-15, 2016).

13. Convection-Allowing Model Data Processing to Objectively Identify Convective Mode

Chris Melick (CIMMS at SPC)

This work summarizes research to objectively extract beneficial information about convective mode information from simulated storms in convection-allowing models (CAMs). Convective mode encompasses the geometric orientation and structure of convective storms and is closely related to mesoscale and storm-scale dynamic processes influencing thunderstorm development, evolution and associated severe weather hazards. For example, tornadoes occur most frequently with discrete supercells, whereas damaging wind gusts are more prevalent from quasi-linear convective systems (QLCS) and bow echoes.

The exploratory research utilizes "neighborhood" fractional probabilities from a single deterministic model or ensemble member. By computing a neighborhood coverage from CAM data at each grid point, the number of grid boxes with 1-km AGL simulated reflectivity ≥ 40 dBZ within a 40-km radius of influence (ROI) can provide an estimate of convective storm coverage within that "neighborhood". The resultant field is hypothesized to provide some information on convective mode (e.g., given the presence of updraft helicity, low fractional reflectivity coverage may correspond better with isolated supercells than mesoscale convective systems). For the current work, a few severe weather days were subjectively evaluated to determine whether neighborhood fractional coverage of simulated reflectivity can serve as a reliable proxy for identifying convective mode. Algorithms developed will subsequently be tested in the Hazardous Weather Testbed. Results were presented at a poster session at the AMS Annual Meeting Seventh Conference on Transition of Research to Operations in Seattle on January 25, 2017. This project is ongoing.

14. Evaluation of Precipitation Type from Observational Datasets to Improve Monitoring of Hazardous Winter Weather

Chris Melick (CIMMS at SPC)

This collaborative research project (Wawrzyniak et al. 2017) during the fall semester of 2016 involved mentoring a student at the OU School of Meteorology to examine a multiple datasets (METAR surface observations, NWS Local Storm Reports, and mPING reports) and compare precipitation type from these sources (figure below). The work examined spatial and temporal continuity and consistency to identify potential biases and overall accuracy. The results here suggested that the distance between different report types has a much more significant impact on the similarity of precipitation type compared to surface METAR observations than the time between reports. The median distance for ‘’matched’ pairings for each comparison was less for LSRs and mPING reports than the median distance for "mismatched" pairings. In contrast, the median time of both pairings is approximately 30 minutes for each comparison against the METARs. This implies that the time difference between reports

did not have a significant impact, since this is also the median on the 60-minute time frame chosen for this study. Results were presented at the AMS Annual Meeting Seventh Conference on Transition of Research to Operations in Seattle, WA on January 25, 2017.

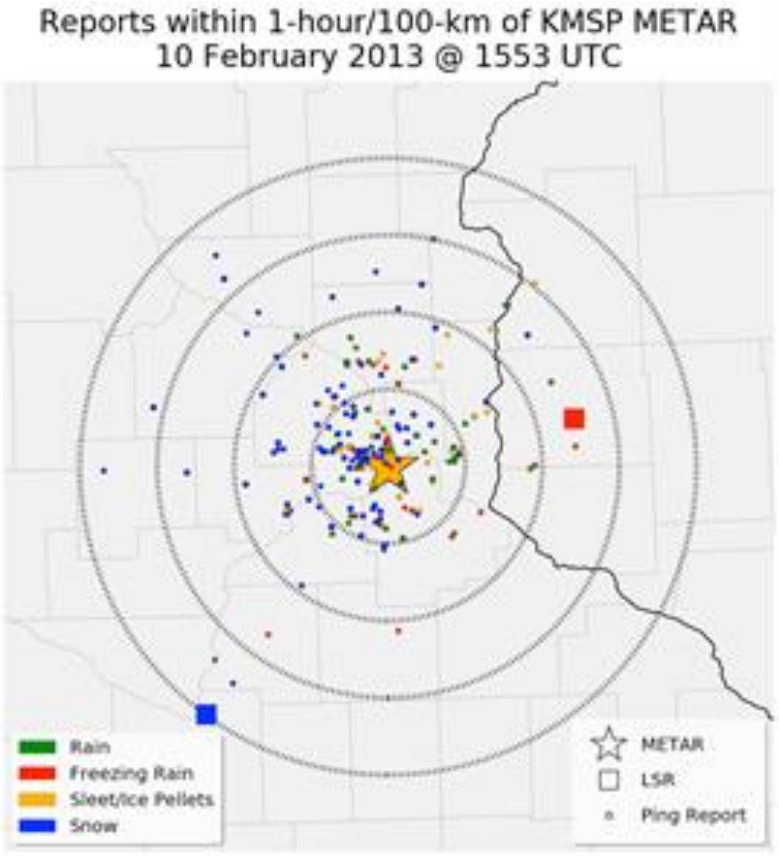

Case study of all LSRs and mPINGs within 1 hour and 100 km of a METAR at KMSP. Each ring represents 25 km from the surface station. Report and precipitation type are represented by symbols and colors respectively.

15. GEMPAK Software Routines: Neighborhood Functions

Chris Melick (CIMMS at SPC)

During the fall of 2016, new diagnostic functions for GEMPAK code were developed and tested to incorporate spatial neighborhood computations into the NWS baseline GEMPAK software library for NWS/NCEP. Several new subroutines were added to the baseline code to determine a type of neighborhood statistical value for a given radius surrounding a grid point for any scalar field. A more flexible and efficient version of a 2-D Gaussian filter was also included. The software development was first developed and tested for Hazardous Weather Testbed applications.

NWSTC Project 14 – Forecast Systems Optimization and Decision Support Services Research Simulation and Training

NOAA Technical Leads: Jeff Zeltwanger (NOAA OCLO) and Kim Runk (NOAA OPG)

NOAA Strategic Goal 2 – *Weather-Ready Nation – Society is Prepared for and Responds to Weather-Related Events*

Funding Type: CIMMS Task II

Objectives

1. Forecast Systems Optimization

Sub-Objective 1: Provide end-user training for meteorologists and hydrologists using Advanced Weather Interactive Processing System (AWIPS) in the NWS. This includes updating previously created training to more useful and functional products.

2. NWS Operations Proving Ground Operational Service Delivery Simulations

Sub-Objective 1: Collaborate with the Aviation Weather Testbed (AWT) on a project to assess Digital Aviation Services.

Sub-Objective 2: Prepare and train all SOOs and DOHs for GOES-16 satellite imagery.

Sub-Objective 3: Study the impact of color vision deficiencies on the utility of GOES-16 satellite imagery.

Sub-Objective 4: Evaluate the usefulness of the Near-Storm Environmental Awareness Cursor Readout Bundles and Application for NWS forecasters.

3. Impact Based Decision Support Services Research and Development

Sub-Objective 1: Prepare all operational NWS employees for providing decision support services from their offices. To accomplish this goal, operational employees need online training. This is the main goal behind the Impact-Based Decision Support Services Professional Development Series.

Sub-Objective 2: Prepare NWS employees for deployment in the field, and train them to communicate weather information to the public and partners effectively. Accomplishing this is the main goal of the Impact-Based Decision Support (IDSS) Deployment Boot Camp residence course.

Sub-Objective 3: Conduct or assist with training sessions outside of IDSS Deployment Boot Camp that continues learning in communication best practices. This may include

guest speaking in other residence courses in Kansas City, or consulting with offices or individuals as requested.

Sub-Objective 4: Support Weather-Ready Nation goals, conduct training on impact-based decision support services as applicable specifically to hurricane messaging. This is the primary function of the Effective Hurricane Messaging Course hosted in Miami, Florida.

4. Advanced Training Development

Sub-Objective 1: Develop expertise in useful technology, best practices, and methodologies in effort to produce better training and share information. This might include attending professional development training and conferences, and pushing the boundaries of instructional design, training, and technology.

Sub-Objective 2: Help OCLO and OPG employees grow and learn new tools for training and collaboration.

Sub-Objective 3: Reach out to others in the agency through various methods, and spread information about available training, professional development, and the roles NWS “staff play” in a Weather Ready Nation.

Sub-Objective 4: Use expertise to join and help OCLO and OPG focal point teams.

Sub-Objective 5: Prepare new NWS employees for work in the federal government. Accomplishing this is the main goal of the New-Hire Orientation Training course

Accomplishments

1. Forecast Systems Optimization

a. Sub-Project 1: Advanced Weather Interactive Processing System (AWIPS II) and Graphical Forecast Editor (GFE) Distance Learning

Megan Taylor and Brent Pesel (CIMMS at NWSTC), and Jeffrey Zeltwanger (OCLO)

Work on AWIPS distance learning courses were limited during this reporting period to maintenance on existing courses. This included ensuring the courses still worked and that any aged information was address.

2. NWS Proving Ground Operational Service Delivery Simulations

a. Sub-Project 1: Collaborate with the Aviation Weather Testbed (AWT) on Digital Aviation Services Evaluation

Katie Vigil and Derrick Snyder (CIMMS at NWSTC), Chad Gravelle (CIMSS-Wisconsin), Kim Runk (OPG), Jack Richardson (NWSTC and OPG Contractor), Matthew Foster (OPG), Steve Lack, Austin Cross, and Joshua Scheck (AWC), Benjamin Schwedler, Adam Kankiewicz, and Stephanie Avery (CIRA-Colorado State University), Cammye Sims (NWS ASB), and Aviation Weather Testbed and ESRL GSD staff

The OPG collaborated with the Aviation Weather Testbed (AWT) using Digital Aviation Services to assess whether there is an optimal methodology for generating grids that can serve as a foundation for the creation of WFO products for aviation partners. Multiple methodologies are used today and anecdotal evidence suggests a broad range of opinions about the workload required to achieve the quality needed for terminal aerodrome forecast (TAF) production. The first set of evaluations focused on comparing and contrasting the existing methodologies for both meteorological quality and forecaster workload impact, across a variety of weather hazards and geographical locations. Some cases were archived simulations from a two-week period that coincided with the AWT Winter Experiment in February 2016. This allowed OPG to compare two different starting points for the scenarios: CONSShort and a national CIG/VIS grid generated by AWC. Live data was also used during the evaluation.

Along with planning and executing the evaluation Katie Crandall and Derrick Snyder performed specific job tasks: Crandall – (1) developed surveys to collect feedback from forecasters; (2) created detailed maps with aviation TAF locations and airport information; (3) recorded and transcribed audio recordings of group discussions; (4) analyzed evaluation data and made that data accessible to other OPG members; and (5) helped create evaluation reports and findings to NWS management. Snyder – (1) assisted in configuring AWIPS-II to test various methods of TAF production, using archived “displaced real-time” cases and using live data; (2) obtained GFE and AvnFPS configuration files from Weather Forecast Offices to allow for TAF production; and (3) obtained archived meteorological data sets (radar, model, surface observations, etc.) to run archived simulations using AWIPS-II.

Operations Proving Ground and Aviation Weather Testbed visiting forecasters collaborating on Digital Aviation Services grids.

b. Sub-Project 2: Prepare and Train all SOOs and DOHs for GOES-16 Satellite Imagery.

Katie Vigil and Derrick Snyder (CIMMS at NWSTC), Chad Gravelle (CIMSS-Wisconsin), Kim Runk and Matthew Foster (OPG), Jack Richardson (NWSTC and OPG Contractor)

OPG led a training session for NWS SOOs and DOHs on GOES-R satellite imagery. The training session was performed on AWIPS and demonstrated how to use and interpret multiple spectral bands and RGB imagery from GOES-R. Specifically, we ran the AWIPS workstation while the instructor demonstrated how to analyze and interpret GOES-R satellite imagery. Collected and prepared satellite data sets for use in AWIPS-II. Configured AWIPS-II to optimize performance for NWS forecasters. Obtained archived meteorological data sets to run archived exercises using AWIPS-II.

Operations Proving Ground Director Kim Runk presenting at the GOES-R SOO/DOH Prep Course.

c. Sub-Project 3: Study the Impact of Color Vision Deficiencies on the Utility of GOES-16 Satellite Imagery

Katie Vigil and Derrick Snyder (CIMMS at NWSTC), Chad Gravelle (CIMSS-Wisconsin), Kim Runk and Matthew Foster (OPG), and Jack Richardson (NWSTC and OPG Contractor)

OPG conducted experiments with three forecasters who tested as having moderate to severe color vision deficiency. Using archived cases of various meteorological phenomena, participating forecasters provided feedback on their capability to identify particular features in both single band imagery and RGB composites. Phenomena assessed included the formation and decay of fog and stratus, both daytime and nighttime; capability to differentiate between snow/ice fields and cloud cover; initiation and evolution of wildfires; development of a synoptic scale dust storm; initiation and evolution of two types of convective environments; and analysis of three different layers of water vapor.

We created grant proposal for funding through CIMMS, acted as Principal Investigator for the project, planned and executed operational evaluation, analyzed data from evaluation, and wrote reports and created presentations. We also configured AWIPS-II to optimize performance for NWS forecasters, and collected feedback from NWS forecasters with color vision deficiencies on the utility of color vision deficiency

correction technology. This work was funded by the CIMMS Director's Discretionary Research Fund.

CIMMS Research Scientist Katie Vigil introducing an iPad application designed to mitigate color vision deficiency.

d. Sub-Project 4: Evaluate the Usefulness of the Near-Storm Environmental Awareness Cursor Readout Bundles and Application for NWS Forecasters

Katie Vigil and Derrick Snyder (CIMMS at NWSTC), Chad Gravelle (CIMSS-Wisconsin), Kim Runk and Matthew Foster (OPG), and Jack Richardson (NWSTC and OPG Contractor)

The OPG hosted Operational Readiness Evaluations for a collection of AWIPS-based tools designed to enhance a forecaster's Near Storm Environmental Awareness (NSEA) during convective warning events. The NSEA toolset, comprised of a GUI application and a Cursor Readout, was developed as a collaborative National SOO Project to provide NWS meso-analysts and warning forecasters with a flexible, locally configurable, and user-friendly way to monitor a variety of relevant parameters in rapidly evolving convective storm environments.

We developed surveys to collect feedback from forecasters, recorded and transcribed audio recording of group discussions, analyzed evaluation data and made that data accessible to other OPG members, and helped with creating evaluation reports and findings for NWS management. We also obtained archived meteorological data sets

(radar, model, surface observations, etc.) to run archived exercises using AWIPS-II, configured AWIPS-II to optimize performance for NWS forecasters, recorded pre-simulation weather briefings for NWS forecasters, and created situational awareness displays for NWS forecasters to use during archive exercises.

Operations Proving Ground visiting forecasters analyzing atmospheric variables using Near Storm Environmental Awareness tools.

3. Impact-Based Decision Support Services Research and Development

As part of the Weather-Ready Nation initiative, the NWS is undergoing a change in culture. Part of this change includes providing more impact-based decision support services to NWS core partners and improving communication to partners and the public. During this reporting period, numerous training initiatives occurred in effort to support this need. These include:

a. Sub-Project 1: Impact-Based Decision Support Services (IDSS) Professional Development Series

Megan Taylor, Denise Balukas and Brent Pesel (CIMMS at NWSTC), Jeffrey Zeltwanger, Marco Bohorquez, Doug Streu, Jerry Griffin, Hattie Wiley, and Cathy Burgdorf (OCLO), Kim Runk (OPG), Derek Deroche (NWS Central Region HQ), and Numerous NWS HQ and Region PDS Team Members, and subject-matter experts

While the previous reporting period was focused on planning for the IDSS PDS, this reporting period signifies the beginning of training development. This is one of the largest training initiatives in some time and it is highly visible across the agency. The overall plan for the curriculum is:

Professional Competency Unit 1 - Intro to IDSS Basics and Incident Command Structure (FEMA)
Professional Competency Unit 2 - Customer-Focused Support
Professional Competency Unit 3 - Effective Communication
Professional Competency Unit 4 - Operating within ICS & NIMS
Professional Competency Unit 5 - Partnership Building
Professional Competency Unit 6 - Threat Assessment & Risk Communication
Professional Competency Unit 7 - Deployment-Ready Task Book
Professional Competency Unit 8 - Advanced ERS for Complex Incidents
Professional Competency Unit 9 - ERS Endorsements

PCUs 1-3 are required for all operational NWS employees regardless of location or office type. PCUs 4-7 are for those operational employees wishing to be "deployment-ready." PCUs 8-9 involve advanced studies into specific types of incidents.

Planning for courses within the first three PCUs began in late August 2015. During the fall, Megan Taylor, with assistance from Jeff Zeltwanger & Hattie Wiley, researched and performed analysis regarding existing NWS courses related to IDSS concepts, analyzed audience type, need, gaps, etc. for the new training series. During that time, Megan took numerous courses to evaluate for potential use. During the winter of 2015-2016, Megan Taylor and Denise Balukas, continued to refine the course list, goals, and objectives. At the end of this period, a proposal was sent to the PDS Team and NWS Mission Delivery Council for approval. Course development began in spring 2016 and has continued through summer 2017. Megan Taylor, Denise Balukas, and Brent Pesel developed numerous courses for the IDSS PDS

Screenshot of the Body Language Course (Top-Left) and screenshot of the IDSS Presentations Course (Bottom-Left) for the IDSS PDS.

b. Sub-Project 2: Conduct IDSS Deployment Boot Camp

Megan Taylor, Denise Balukas, Brent Pesel, Katie Vigil, and Derrick Snyder (CIMMS at NWSTC), Jeff Zeltwanger, Marco Bohorquez, and Doug Streu (OCLO), Kim Runk (OPG), and Derek Deroche and Chris Foltz (NWS Central Region HQ), plus numerous guest facilitators and guest instructors

The popular Impact-Based Decision Support Services Deployment Boot Camp was held three times during the reporting period. The goal behind these courses is to prepare NWS employees for deployment in the field and train them to communicate weather information to partners and the public. Beginning the next reporting period, this course will be built into the IDSS Professional Development Series (Sub-Project 1).

Megan Taylor has been involved in the training since 2012, and continues to help plan and organize the course. She continues to teach media training and act as a reporter during the full-day simulation. Denise Balukas became heavily involved in planning and organizing the course. Additionally, she helped with the simulation both by acting as a unit advisor in all offerings, and by helping the simulation lead (Doug Streu) create and refine documentation for the event. Brent Pesel has taken on a larger role with the course as he has completed training. In the July 2017 session, he helped prepare materials for the course and participated in simulations with the students.

CIMMS Katie Vigil and Derrick Snyder play newspaper reporters in the full-day simulation and participate in the mock-press conference.

Denise Balukas (Left) listens as instructions for the simulation are given. Megan Taylor (Right) polls the participants with a paper clicker tool.

c. Sub-Project 3: Conduct Additional IDSS-Related Training Sessions

Because IDSS training is needed in many avenues of operational life in the NWS, additional training opportunities were pursued and continued during this reporting period. These additional sessions included:

IDSS Virtual Conference Webinars

Megan Taylor Denise Balukas, and Brent Pesel (CIMMS at NWSTC), Jeff Zeltwanger and Marco Bohorquez (OCLO), Charlie Woodrum (NWS Pacific Region HQ), and numerous guest speakers

NWS Headquarters and OCLO hosted numerous IDSS Virtual Conference webinars over the reporting period. These webinars focused on a different topic each time, and gave numerous guest speakers a chance to share some IDSS best practices with the agency. Denise Balukas, Brent Pesel, and Megan Taylor attended offerings, and processed some resulting videos for publishing on YouTube. Megan Taylor also helped the Operations Proving Ground create a video published on YouTube about using GOES-16 to enhance wildfire IDSS.

Denise Balukas (Top-Left) provides assistance during an activity. Megan Taylor (Top-Right) conducts an interview practice session. Sarah Grana (Bottom) teaches communication to the class.

Warning Coordination Meteorologist (WCM) Development Course

Megan Taylor (CIMMS at NWSTC), Doug Streu, Dave Cokely, Jerry Griffin, and Jeff Zeltwanger (OCLO), and numerous guest speakers

IDSS concepts such as communication and customer service are essential to the role of Warning Coordination Meteorologist (WCM). For the 2016 course, Megan participated in some planning discussions and taught two subjects in December.

NWS Public Speaking Video Series and Coaching

Megan Taylor (CIMMS at NWSTC), Cathy Burgdorf and Jeff Zeltwanger (OCLO), Brooke Bingaman (NWSFO Sacramento), Renee Wise (NWSFO Aberdeen), and Dave Snider (NOAA Alaska TV)

The OCLO was approached with a project in late summer 2015. Three WFO public speaking SMEs (Brooke Bingaman, Renee Wise, and Dave Snider) wanted to create a set of public speaking "how-to" videos in conjunction with a new coaching program. The OCLO decided to move forward. Megan Taylor and Cathy Burgdorf filmed the proposed videos in January 2016. To do so, they also had to install a new cove green screen for maximum filming area. Megan directed the video shoot, and conducted discussions on planning the new coaching program. She began building the coaching website and reviewed videos as they were edited by Cathy Burgdorf. The project was completed in 2017.

Graphics Consultation

Megan Taylor and Katie Vigil (CIMMS at NWSTC) and Derek Deroche and Brian Walawender (NWS Central Region HQ)

Keeping IDSS principles and basic graphic design concepts in mind, Megan Taylor and Katie Vigil have consulted in various instances on Central Region Headquarters social media and website projects. One example of such is the Impacts Warnings automatically disseminated on Twitter.


Screenshot (Top-Left) from WFO communications presentation and screenshot (Top-Right) of the new Twitter impacts warnings. Still image of Brooke Bingaman (Bottom-Left) preparing to film a segment on body language and still of Megan Taylor (Bottom-Right) teaching in WCM Class.

Cooperative Network Operations Course

Megan Taylor (CIMMS at NWSTC) and Marco Bohorquez (OCLO)

Because IDSS concepts such as communication are vital to the success of the Cooperative Observer Program, Megan Taylor continues to prepare materials and teach communications in the Cooperative Network Operations residence course. Megan taught in the spring of 2016.

e. Sub-Project 5: Conduct Effective Hurricane Messaging Course

Denise Balukas (CIMMS at NWSTC), Marco Bohorquez and Shannon White (OCLO), Dan Brown (National Hurricane Center), Jen McNatt (NWS Southern Region HQ), Matt Moreland and Andy Devanas (NWSFO Key West), John Koch (NWS Eastern Region HQ), David Sharp (NWSFO Melbourne), and Lance Wood (NWSFO Houston)

The EHM course supports the goal of Weather Ready Nation. Like the Deployment Boot Camp, one of the primary objectives of the EHM is that students gain the ability to

effectively communicate weather and water threats, impacts, forecasts, and other technical information to both the public (primarily through media interviews and social media) and to core NWS partners such as emergency management and Coast Guard (through various means including remote and on-site briefings). Another primary goal of both Boot Camp and EHM is to instill the importance of developing the trust of core partners and of fostering deep and lasting relationships with these partners. Because of the unique nature of the hurricane threat, the EHM has hazard-specific components related to the appropriate use and messaging of the National Hurricane Center's tropical cyclone products which are addressed during the course.

Denise Balukas has been involved with the planning and development of future EHM course offerings as the OCLO has taken over the course. She met with facilitators and assisted with developing objectives, facilitating discussion between experts, facilitators, and instructors, and aided in refining the feedback strategy for the 2017 course. Denise observed the course in April 2017 at the National Hurricane Center in Miami, Florida.

Week-long Effective Hurricane Messaging planning meeting at the National Hurricane Center.

4. Advanced Training Development

All CIMMS staff at OCLO and OPG must maintain a level of expertise in many areas in order to fully support the local NWS staff. This may mean developing new or more advanced skills, training others in the office, participating in outreach, or joining one of the building teams.

a. Sub-Project 1: Develop Expertise in Technology, Best Practices, and Methodologies to Better Fulfill Roles and Help Others.

The activities relevant to this objective included attending and participating in conferences, meetings, workshops, and training courses, and making NWS Forecast Office visits, a visit to the National Hurricane Center.


Photos taken at the 2017 American Meteorological Society Annual Meeting.

b. Sub-Project 2: Help NWSTC Employees Learn New Tools and Methodologies for Training and Collaboration

Internal training is conducted, and job sheets created or reviews completed by CIMMS staff in Kansas City in effort to train or assist OCLO/OPG employees.

c. Sub-Project 3: Assist with New Hire Orientation Training Course

The course is designed to prepare newly hired NWS employees for federal employment. During the course, they receive information on the organization, federal benefits, the employee union, travel, and time reporting. They also receive training on effective team work, leadership, communication, and learning

Publications

Crandall, K. L., P. S. Market, A. R. Lupo, L. P. McCoy, R.J. Tillott, and J. J. Abraham, 2016: The application of diabatic heating in Q-vectors for the study of a North American cyclone event. *Advances in Meteorology*, Article ID 2908423, 11 pages.

Gravelle, C. M., K. J. Runk, K. L. Crandall, and D. W. Snyder, 2016: Forecaster evaluations of high temporal satellite imagery for the GOES-R era at the NWS Operations Proving Ground. *Weather and Forecasting*, **31**, 1157-1177.

CIMMS Task III Project – The GOES-R GLM Lightning Jump Algorithm: A National Field Test for Operational Readiness

Kristin Calhoun and Darrel Kingfield (CIMMS at NSSL)

NOAA Technical Leads: Steve Goodman, Dan Lindsey, and Andy Heidinger (NOAA NESDIS)

NOAA Strategic Goal 2 – *Weather Ready Nation: Society is Prepared for and Responds to Weather-Related Events*

Funding Type: CIMMS Task III

Objectives

A fully automated, real-time Lightning Jump Algorithm (LJA) is being developed and tested for National Weather Service implementation in collaboration with the University of Alabama-Huntsville. The LJA is designed to highlight rapid intensification in thunderstorms preceding severe weather such as tornadoes, hail and straight-line winds at the surface by tens of minutes. While the GOES-R Geostationary Lightning Mapper (GLM) provides a general path to operations for the use of continuous total lightning observations and the lightning jump concept over a hemispheric domain, the operational implementation for the Hazardous Weather Testbed (HWT) of the LJA pre-GLM is being produced using data from the Earth Networks Total Lightning Network (ENTLN) and Lightning Mapping Array data on localized domains.

Accomplishments

Following the final evaluation of the algorithm in the Hazardous Weather Testbed as part of the GOES-R proving ground in 2016, work has continued to make the algorithm operational. The primary gap at this time is the limitation posed by the operational framework at NCEP as it is unable to handle the system demand. Due to inherent system memory footprint of the algorithm, experimental modifications are being made to improve the tracking algorithm and reduce the system memory demands of tracking and integrating multiple fields simultaneously while not increasing data latency over that which was examined in the HWT.

Additionally, development coordinated with NASA-Marshall Space Flight Center and the University of Alabama-Huntsville has begun to move the algorithm to incorporate actual GLM data following the instrument launch during the calibration/validation period in 2017 (figure below). Future HWT demonstrations (2018 and beyond) are expected to evaluate a GLM-based lightning jump based on recently awarded GOES-R Risk Reduction Research (GOESR3 – 2017-2020).

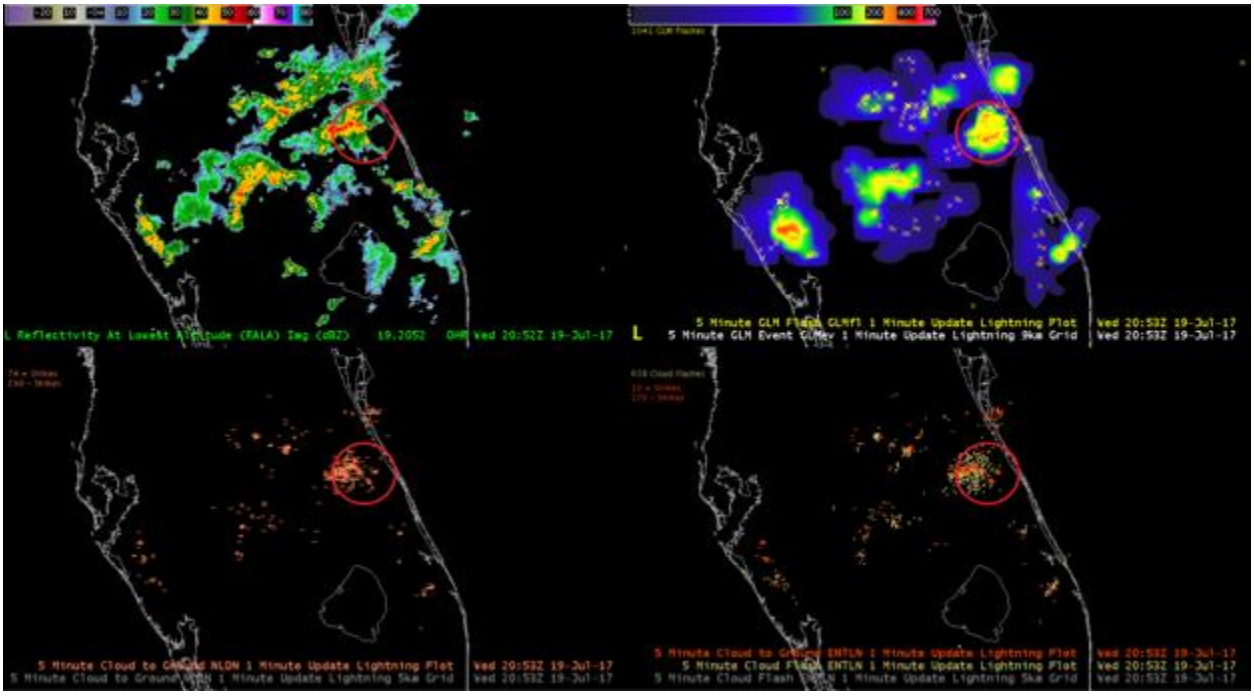

Initial comparison of storm-based lightning jump from multiple lightning detection platforms, red circle denotes storm with forecaster-indicated lightning jump during the 2017 HWT evaluation integrating GLM data. Top left: Multi-Radar/Multi-Sensor reflectivity at lowest altitude. Top right: 5-min GLM event density (gridded) and GLM flash points (yellow x). Bottom left: 5 min cloud-to-ground flash (coral) points. Bottom right: 5-min cloud (tan) and cloud-to-ground (red) flash points.

CIMMS Task III Project – National Sea Grant Weather & Climate Extension Specialist Activities

Kodi Monroe and Holly Obermeier (CIMMS at NSSL), and Alan Gerard (NSSL)

NOAA Technical Lead: Elizabeth Rohring (NOAA Sea Grant)

NOAA Strategic Goal 2 – *Weather-Ready Nation – Society is Prepared for and Responds to Weather-Related Events;* ***and***

NOAA Strategic Goal 1 – *Climate Adaptation and Mitigation: An Informed Society Anticipating and Responding to Climate and its Impacts, and Weather-Ready Nation – Society is Prepared for and Responds to Weather-Related Events*

Funding Type: CIMMS Task III

Objectives
Connect NSSL research with the Sea Grant Extension Network; develop a capacity to forecast high-impact threats for coastal communities using the FACETs framework and

methodologies; maintain the Coastal and Inland Flooding Observation and Warning (CI-FLOW) project to predict total water level for coastal watersheds.

Accomplishments

The Sea Grant Weather & Climate Extension Specialist at CIMMS/NSSL and Holly Obermeier conducted a preliminary analysis of results from the broadcast meteorologist sub-project of the 2016 Hazardous Weather Testbed (HWT) Probabilistic Hazard Information (PHI) experiment. Broadcast participants performed typical job functions under a simulated television studio environment as they received experimental probabilistic advisories and warnings from NWS forecasters during three real-time and three displaced real-time events. Research protocols were used to investigate how broadcast meteorologists interpreted, used, and communicated both probabilistic information and experimental warning messaging. Results from the 2016 project indicated that probability information added complexity into the participants' typical decision-making and communication routines. The participants were overwhelmed managing studio resources alone when multiple warnings were in effect and updating swiftly. Further, the hazard-following, probabilistic warnings presented unique challenges regarding the incorporation of PHI into the on-air crawl and graphics system, which are currently optimized for binary polygons. A breakdown of decision-making for each hazard revealed that tornado warnings received the most coverage decisions, followed by wind/hail, and lightning. Probabilistic tornado and wind/hail information received the most on-air television coverage in the form of cut-ins and continuous coverage. Social media and crawl systems were predominantly used to cover lightning hazards. Building off these findings, the Sea Grant Weather & Climate Extension Specialist and Holly Obermeier planned and conducted the 2017 broadcaster sub-project to vary warning update frequencies daily to better understand optimal flow of information for the specific needs of broadcast meteorologists and their television stations.

The Sea Grant Weather & Climate Extension Specialist leads NOAA's CI-FLOW project. During the 2016 and 2017 Atlantic hurricane seasons, the CI-FLOW collaborators maintained the real-time coupled modeling system. Quantitative precipitation estimates produced by the NSSL MRMS system provided input data to the 128-member ensemble of the National Weather Service (NWS) Hydrologic Lab-Research Distributed Hydrologic Model (HL-RDHM). Discharge information from HL-RDHM served as upstream boundary conditions for the ADvanced CIRCulation (ADCIRC) hydrodynamic model to incorporate freshwater contributions into coastal water level simulations. Real-time simulations of coastal water levels are available every six hours on the Coastal Emergency Risks Assessment (http://nc-cera.renci.org/) web site.

The Sea Grant Weather & Climate Extension Specialist actively participates in NOAA's Storm Surge Roadmap Team and the FACETs (Forecasting A Continuum of Environmental Threats) Science and Technology Integration (STI) Team. As part of the FACETs STI Team, the Sea Grant Extension Specialist is leading the development of a video to educate NWS forecasters on how the FACETs warning paradigm will impact

their role as a forecaster. Interview questions were developed and NWS forecasters and emergency managers were interviewed during several HWT projects.

Publications

Nemunaitis-Berry, K. L., P. M. Klein, J. B. Basara, and E. Fedorovich, 2017: Sensitivity of predictions of the urban surface energy balance and heat island to variations of urban canopy parameters in simulations with the WRF Model. *Journal of Applied Meteorology and Climatololgy*, **56**, 573-595.

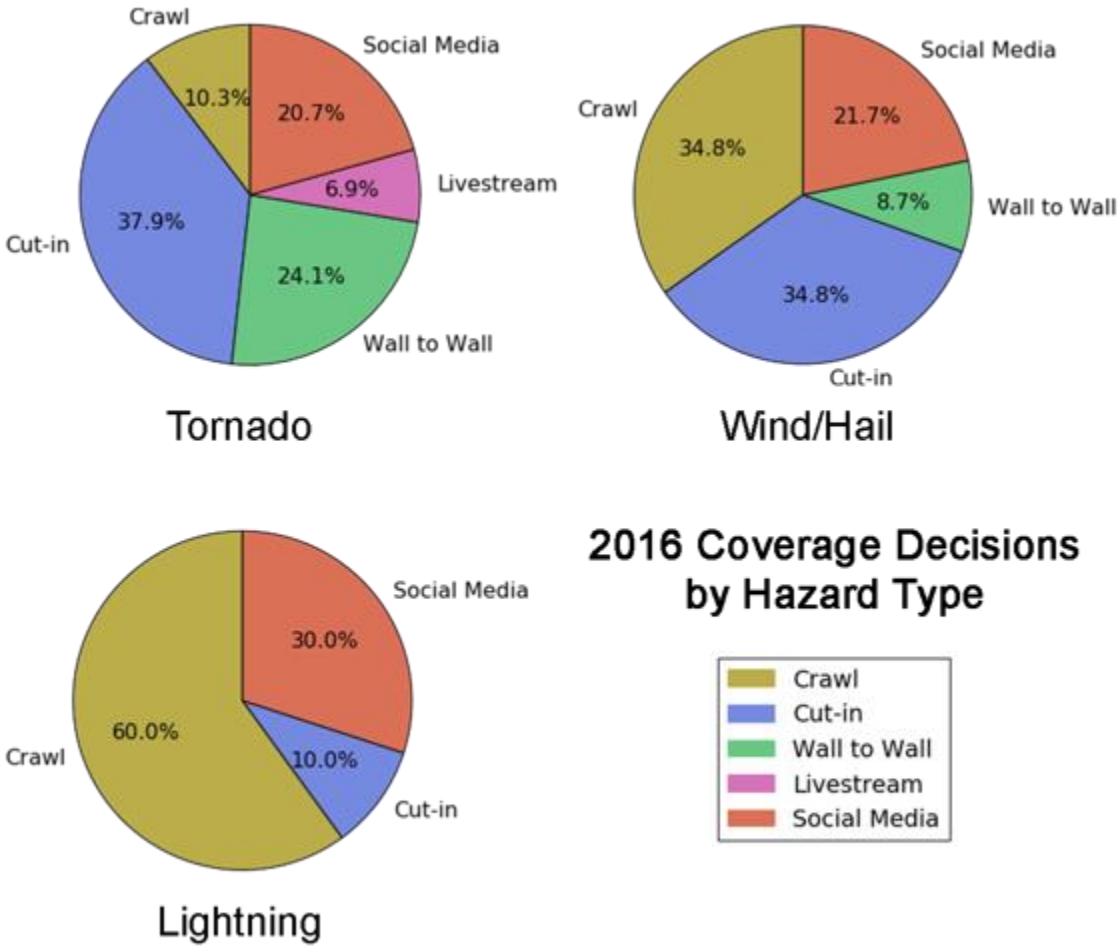

Breakdown of television coverage decisions by hazard type over the three week project. Participants had the option of choosing between five different forms of coverage, including cut-ins and continuous (wall-to-wall) coverage over commercials and/or programming.

CIMMS Task III Project – Prototyping and Evaluating Key Network-of-Networks Technologies

Keith Brewster (CAPS), and Fred Carr, Nickolas Gasperoni, Andrew Osborne, and Matthew Morris (OU School of Meteorology)

NOAA Technical Lead: Curtis Marshall (NOAA OST)

NOAA Strategic Goal 2 – *Weather Ready Nation: Society is Prepared for and Responds to Weather-Related Events*

Funding Type: CIMMS Task III

Objectives
Conduct Observation System Experiments (OSEs) using data denial and other methods to assess the relative impacts of conventional and new observation sources for high-impact mesoscale and storm-scale weather forecasting. The Dallas-Fort Worth Urban Testbed, which is home to several novel data sources, including the CASA X-band radar network, is used for this testing.

Accomplishments
Three high impact weather events in the Dallas-Ft Worth area have been studied.

1. 26-Dec-2015 Rowlett-Garland Tornado

The 3DVAR with Complex Cloud Analysis and Incremental Analysis Updating with Variable-Dependent Timing (IAU-VDT) data assimilation is used to initialize WRF-ARW model forecasts at 1-km resolution to perform data denial experiments focusing on the prediction of the parent vortices of the tornadoes that tracked from Northeast Dallas County across Rockwall County to Collin County. Forecasts of reflectivity (verified via fractions skill score (FSS)) and low-level rotation (0-1 km updraft helicity tracks verified via object-based track error algorithm) were able to accurately capture the storm evolution and locations (first figure below) but only when the WSR-88D radar data was included. The Rowlett storm is on the edge of the shorter-range CASA and TDWR networks and so these radars are not able to provide sufficient observations to initialize the storm properly in the model. A noticeable increase in rotational intensity in the forecasted storm, possibly to unrealistic values, is found when CASA radar data is denied from the control experiment. A separate experiment focus on surface observation impact found substantial positive impact of non-conventional surface observations on frontal placement southwest of the DFW metropolitan area. Comparison of model quantitative precipitation forecast (QPF) output with observed rainfall estimates indicate a wet bias with the single-moment Lin microphysics scheme used here which made the precipitation forecasts less useful than the rotational forecasts for verification, so future work will utilize a double-moment scheme prior to formal publication.

2. 11-April-2015 North Texas Hailstorm

In this case, a prolific hail-producing supercell thunderstorm affected north-central Texas, including the northern portion of the Dallas/Fort Worth metropolitan area. Severe hail was produced from 2000 UTC to 0030 UTC, along a track from just south of Wichita Falls, TX, through the northern Dallas/Ft. Worth metro area to Alba, TX, about 100 km east of Dallas. Hail up to 13.3 cm (5.25 in) diameter was observed, with the maximum near Wylie, Texas where 80% of homes were damaged and over $300 M in damage reported.

The 3DVAR with Complex Cloud Analysis and IAU-VDT is used with the ARPS model run with Milbrandt & Yau double-moment microphysics at 1-km resolution. The analysis includes qualitative comparisons of the forecast reflectivity fields, quantitative comparisons of model-derived hail with radar-observed hail, and surface-level verification of the temperature and dew point forecasts. The CASA radial velocity data offer positive benefit to the forecasted storm structure as noted in the simulated reflectivity, along with model-derived hail, as indicated in the forecast performance diagram (second figure below). The CASA radial velocity data were found to have a positive benefit to the storm structure as noted in the simulated reflectivity, along with forecast performance diagram of model-derived hail (third figure below). Variations in the radar data used had a small impact on the surface verification results, but the use of all data (control) had the best result, particularly in the temperature verification, though including dew point temperature measurements from the non-conventional Earth Networks and CWOP networks resulted in a degradation in the forecasted dew point field in this case.

3. 3-April-2014 North Texas Hail & Tornadic Thunderstorms

For this case, the GSI-based EnKF was used with the WRF ARW model. Experiments were conducted on a two-way nested grid with horizontal resolutions of 12 km and 2.4 km on the outer and inner domains, respectively. Conventional DA was performed on the outer grid in 3-hourly cycles, with the inner grid initialized at 15 Z. High-frequency 5-min cycling was performed after a 1-hour spin-up period on the inner domain for 2 hours total, between 16 and 18 Z using all conventional, nonconventional, and radar observations. Radar observations helped suppress spurious cells and captured ongoing convection that occurred during the cycling period. Data denial experiments with surface observations were performed during this 2-hour cycling on the inner domain, with emphasis on how the ensemble captures the convection initiation (CI) timing, location, and evolution of the storms for the 3-hour forecast initialized at 18 Z. Two supercells initiate between 18 and 19Z in SW Wise County, producing upwards of softball size hail in Denton, TX around 2045.

Since the case results in many hail reports in Wise and Denton Counties, we examined the output of maximum hail size from the model using neighborhood ensemble probability with a 12 km radius. The fourth figure below shows the ensemble probability of hail exceeding 25 mm in size, which is approximately the severe threshold used for

severe thunderstorm warnings. The CNTL experiment (all observations assimilated) shows two distinct maxima of probability exceeding 50%, similar to the two storms that occurred in nature. One important result here is that denying amateur surface stations (CWOP) limits the northern extent of severe hail while maintaining relatively high probabilities in the similar locations to CNTL. The fifth figure below shows difference fields that diagnose effects of moisture from different observations on the resulting CI and hail forecasts. We found that ASOS had a more large-scale effect on the placement of CI, with nonconventional observations from CWOP and Earth Networks (ERNET) having more of a cumulative effect of localizing and converging moisture within the eventual CI location.

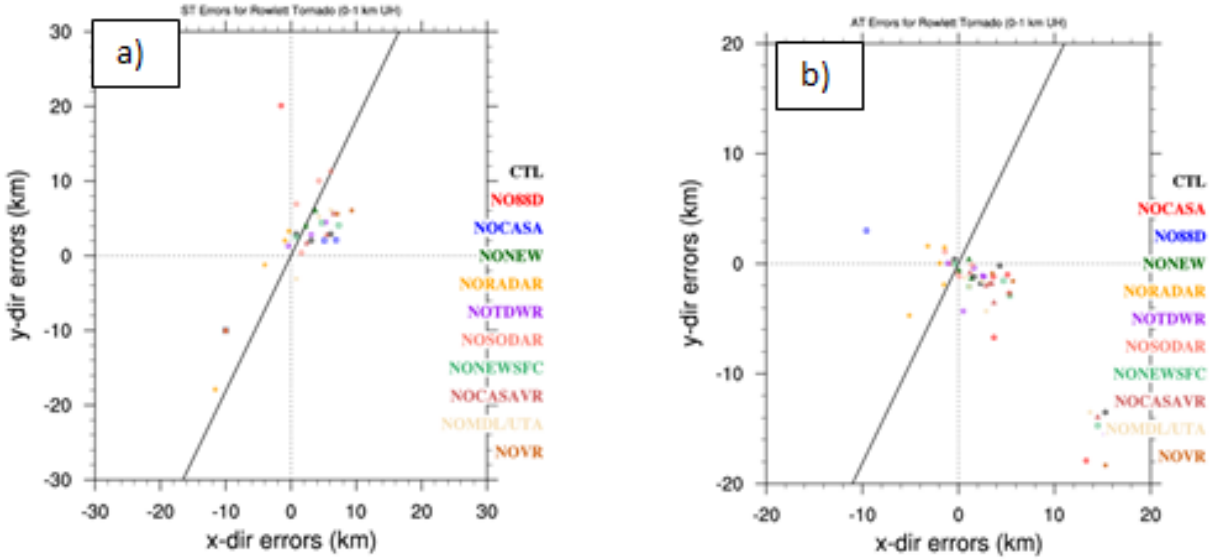

Vector difference between maximum UH center in forecasts and closest observed tornado point. a) at the same time; b) at any time for each 5-minute forecast interval from 0035 UTC to 0100 UTC.

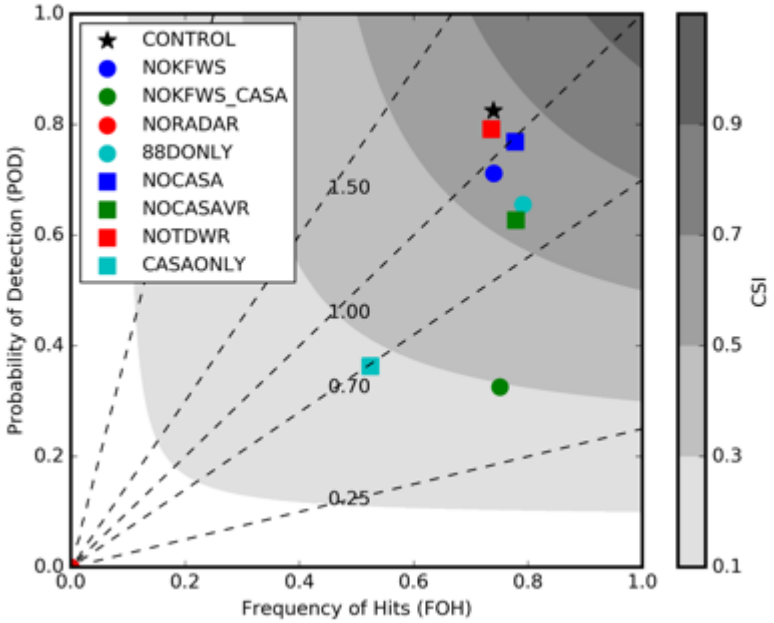

Performance diagram for radar denial experiments using a hail size of 25 mm and neighborhood threshold of 20 km. CONTROL: All radar data used. NOKFWS: omits KFWS data, NOKFWS_CASA: Omits KFWS and CASA, NO RADAR: all radar data omitted, 88DONLY: Only WSR-88D NEXRAD data used, NO CASA: omits CASA X-band radars, NOCASAVR: Omits CASA radial velocity data, NOTDWR: omits TDWR radars, CASAONLY: only used CASA X-band radars.

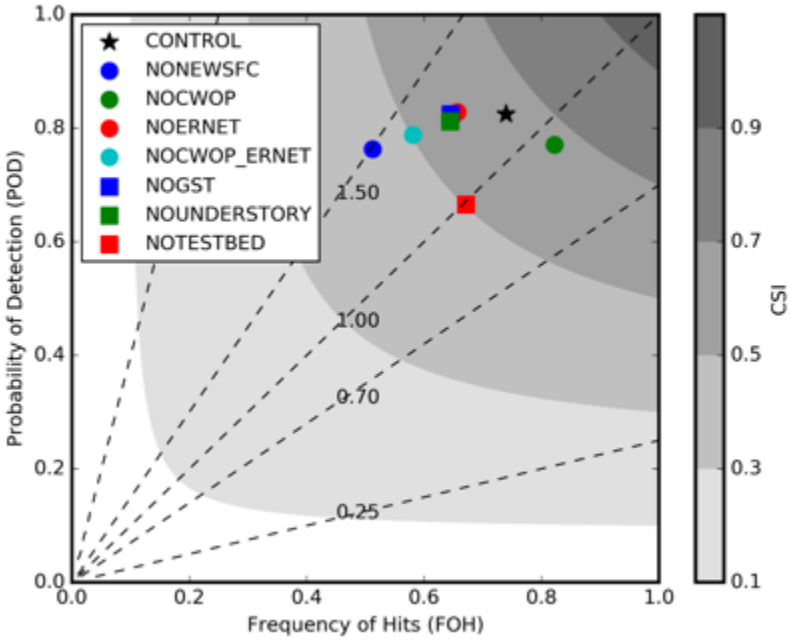

As in the previous figure, but for the surface denial experiments.

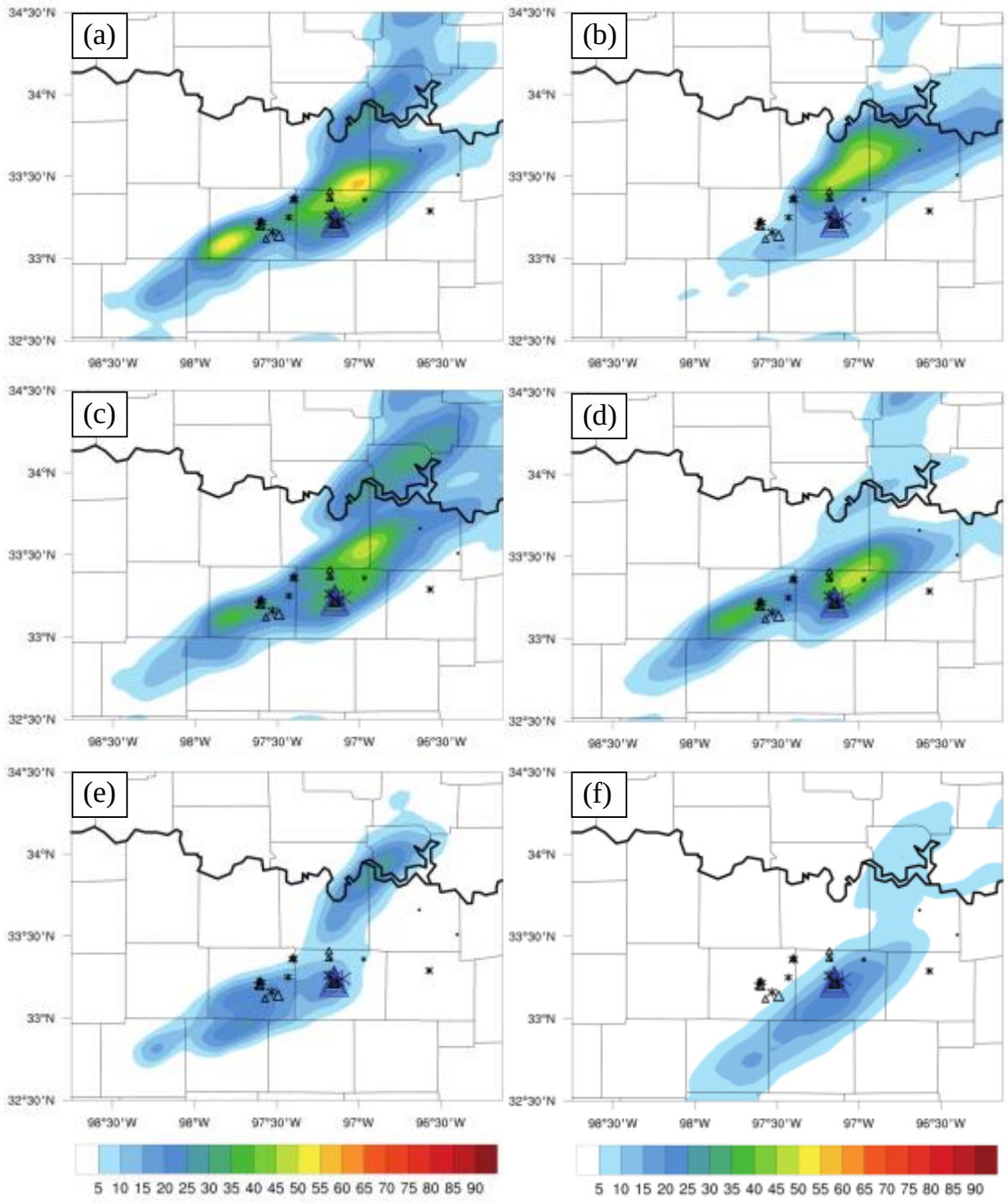

Neighborhood ensemble probability of maximum hail size in the entire column exceeding 25 mm for the entire 3-hour period (1800-2100 UTC), using a neighborhood radius of 9.6 km. Triangles indicate SPC hail reports, and asterisks indicate mPING hail reports, sized according size of the hail reported. Experiments plotted are (a) CNTL, (b) denyASOS, (c) denyERNET, (d) denyCWOP, (e) NONEWSFC, and (f) NOSFC.

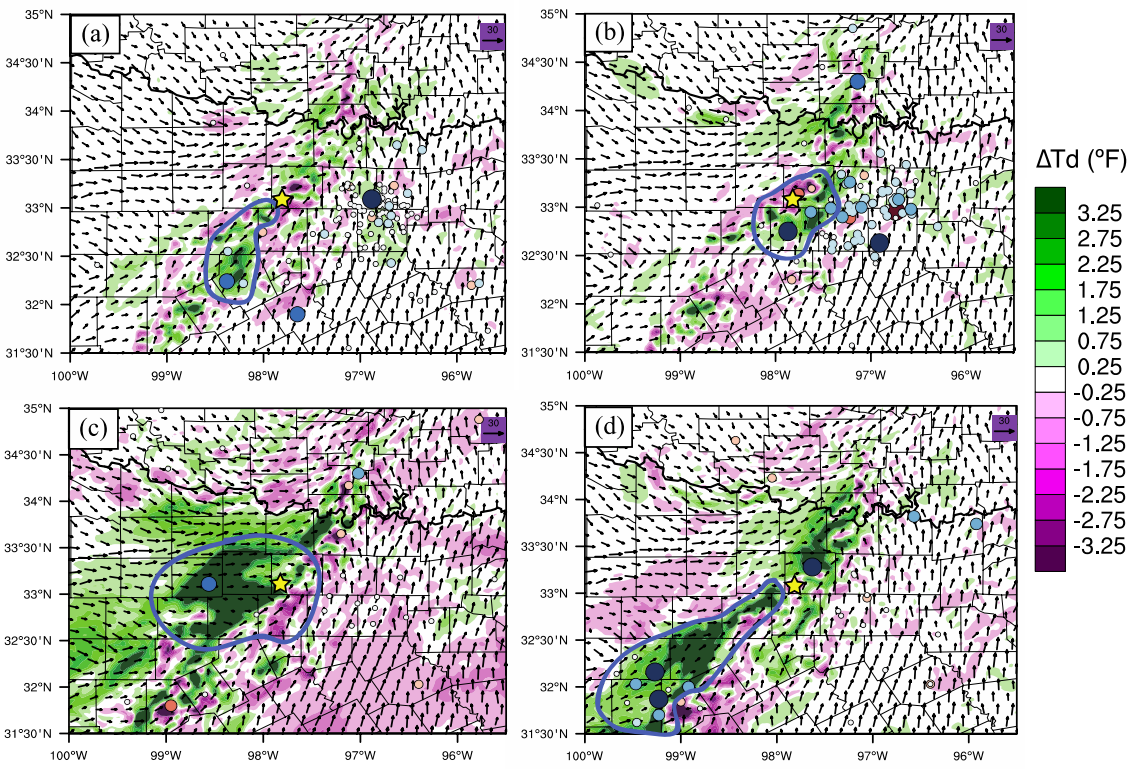

Difference fields for ensemble mean 2-m dewpoint temperature (color fill) and 10-m wind (vectors) for final analysis time 18 UTC 3 April 2014: (a) denyERNET minus CNTL, (b) denyCWOP minus CNTL, (c) denyASOS minus CNTL, (d) denyMISC minus CNTL. Color-fill dots indicate respective observations from each denial experiment for each plot, with colors and sizes indicating the O-A values for each denial dataset (i.e. what the observation innovations would have been if denied observations were assimilated). Yellow star indicates approximate CI location in SW Wise County, and blue outlines highlight relevant observations influencing the CI forecast

Theme 4 – Impacts of Climate Change Related to Extreme Weather Events

CIMMS Task III Project – The Assimilation, Analysis, and Dissemination of Pacific Rain Gauge Data (PACRAIN)

Scott Greene (OU Department of Geography and Environmental Sustainability), and Mark Morrissey, Susan Postawko, and Ethan Cook (OU School of Meteorology)

NOAA Technical Lead: Howard Diamond (NOAA NCEI)

NOAA Strategic Goal 1 – *Climate Adaptation and Mitigation: An Informed Society Anticipating and Responding to Climate and its Impacts*

Funding Type: CIMMS Task III

Objectives

Our overall objective for this proposal continues to seek to support all programs that require rainfall data to assess vulnerability to weather and climates extremes (OCO objective #1). This project continues to support the effort to "build and sustain the global climate observing system that is needed to satisfy the long-term observational requirements of the operational forecast centers, international research programs, and major scientific assessments". Our current and future efforts include expanding our mission to collect, analyze, verify and disseminate rainfall data sets and products deemed useful for Operational Forecast Centers, International Research Programs and individual researchers in their scientific endeavors. Housed at the University of Oklahoma, this project has built upon work from past NOAA-supported projects to become a unique location for scientists to obtain scarce rain gauge data and to conduct research into verification activities. These data are continually analyzed to produce error-assessed rainfall products and are easily assessable via our web page (http://pacrain.ou.edu/). We are also actively involved in research of the tropical rainfall process using data obtained from this project (e.g., Morrissey 2009, and many others).

Accomplishments

Our major accomplishment this year is a gridded sea-level rainfall product, derived solely from atoll station observations, which was developed and published on the PACRAIN website. An iterative version of universal kriging with linear drift was used to produce the gridded estimates. The procedure involved determining non-negative, local rainfall field from which best, unbiased estimates of current observations in the spatial neighborhood could be produced via universal kriging. Variogram parameters were determined using a direct fit to squared differences in rainfall between reports in a spatial neighborhood of a particular grid point. A poster describing the gridding process was presented at the 2017 AMS annual meeting.

The gridding procedure has since been updated and the latest grids using the new procedure are posted each month. The new method employs monthly Variogram model parameters that produce the most internally consistent and unbiased estimate of

historical rains relative to the chosen estimation method, ordinary kriging with positive weights.

The new estimation method and its cross-validation are the subject of a forthcoming paper submitted in the Journal of Atmospheric and Oceanic Technology. Monthly rainfall grids for the period of 1930-2017 are available on the PACRAIN website as a single zipped NetCDF file containing estimated accumulations and standard errors derived via cross-validation of kriging variance. These grids are updated on a monthly basis. In addition to this new product, we continue to expand the PACRAIN database through the incorporation every month of additional observations.

Publications

Cook, W. E., and J. S. Greene, 2017: Gridded historical sea-level rainfall for the Tropical Pacific. Submitted to *Journal of Atmospheric and Oceanic Technology.*

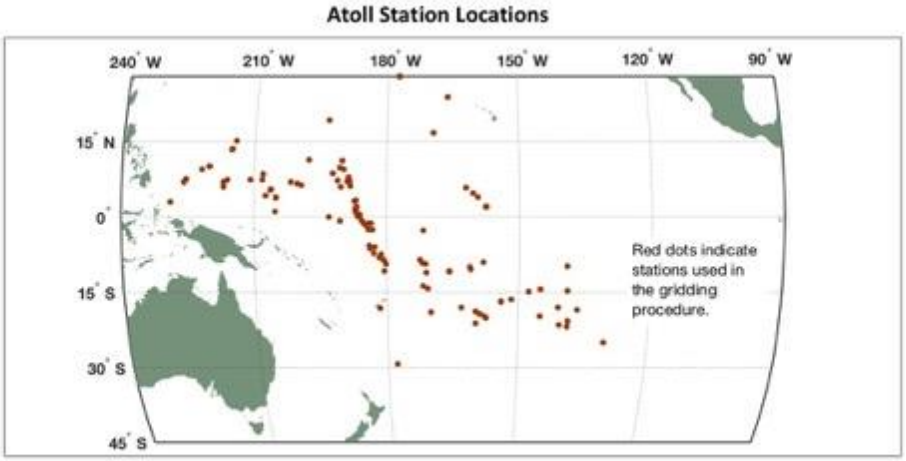

Atoll rainfall stations used in analysis

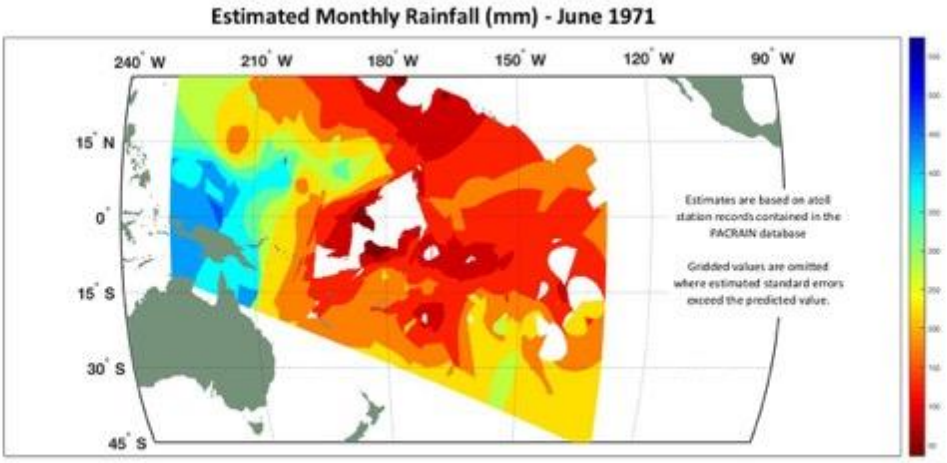

Estimated monthly rainfall.

Theme 5 – Societal and Socioeconomic Impacts of High Impact Weather Systems

NSSL Project 8 – Warning Process Evolution and Effective Communication to the Public

Chris Karstens (CIMMS at NSSL), James Correia, Jr. (CIMMS at SPC), and Gabe Garfield (CIMMS at OUN)

NOAA Technical Lead: Pamela Heinselman (NSSL)

NOAA Strategic Goal 2 – *Weather-Ready Nation: Society is Prepared for and Responds to Weather-Related Events*

Funding Type: CIMMS Task II

Overall Objectives
Improve various aspects of weather warnings (guidance, decision-making) both in the short, medium, and long terms.

Accomplishments
The 2017 HWT Probabilistic Hazard Information (PHI) Experiment was conducted during the weeks of May 8-12, May 22-26, and June 5-9. During this experiment, participants worked in an integrated warning team: forecasters were tasked with issuing experimental probabilistic forecasts for real-time and displaced real-time severe convective events, and Emergency Managers (EMs) and broadcasters used this experimental information to make simulated decisions. After each event, researchers brought the three groups together for discussions focused on particular elements of the forecast information relevant to each forecast hazard type (tornadoes, severe thunderstorms, lightning) and how each element could be improved.

In 2014, when NWS forecasters were the only participants, it was learned that manual generation and maintenance of object-based probabilistic forecasts becomes problematic when there are 4-5 or more hazard areas to manage simultaneously, presenting a potential limitation to the amount of information that can be updated and passed along to users. In an ideal framework, information would be passed along to users without obstructive workload constraints. In 2015, automated, object-based guidance was introduced to combat this workload issue for the forecasters while striving to understand and optimize elements of forecast information for EMs. Initially, the goals were to identify various levels of forecaster-automation and to sense whether or not an optimal human-machine mix exists. Additionally, EMs were added in 2015 to explore key decision-maker needs through the usage of PHI, and to begin a co-creation process among researchers, developers, forecasters, and users.

In 2015 it was learned that an ideal human-machine mix is one in which the automated system maintains and updates geographic hazard areas (i.e., objects) while forecasters

override at least one automated, first-guess attribute (e.g., storm motion, forecast duration, probabilities, communication) of the forecast. This strategy gives forecasters the ability to be more productive, with more time to analyze radar and other observations while communicating more quality forecast information. In addition, no warning decisions were made by forecasters in 2015; they only provided probabilistic information regarding the tornado and wind/hail hazards to the EMs. The presence of EMs provided forecasters an audience for their communication, as well as feedback as to what kinds of information about storms were helpful for decision-making.

Through testing and evaluation, a few critical limitations were identified with this work strategy for forecasters. In particular, automated object identification and tracking is not a steady process. Hazard areas are not always immediately identified and maintained, and thus, the tracking is sometimes unjustifiably (and sometimes justifiably) discontinuous. When presented with these situational impasses, forecasters preferentially assumed control of the object as a way to eliminate the error, but the reversion to manual usage resurfaces the aforementioned workload issues, thus limiting information flow. The challenge for 2016 was to develop and test tools that get forecasters through these impasses to maintain operating in the optimal human-machine mix mode. Additionally, EMs and forecasters independently realized the potential of a short forecast discussion to provide critical information needed by the EMs for sense-making, and thus, decision-making. The meaning the forecasters could add by typing a short discussion was critical. Identification of this critical communication element led to an expansion of efforts focusing on the communication (e.g., formatting, colors, wording) of hazardous weather information to key decision-makers in 2016.

For 2016 and 2017, three types of automated guidance were available to forecasters. These included the NOAA/CIMSS ProbSevere model for the occurrence of any severe (tornadoes, wind, and hail) and individual hazards (added in 2017), the NSSL Experimental Warn-on-Forecast System for ensembles (NEWS-e) for tornadoes, and early algorithm development occurring at CIMMS/NSSL for lightning. In addition to having EM participants, Broadcast Meteorologists participated by using PHI to decide whether and when to do simulated cut-ins to programming on an internal TV broadcast. Week one of the experiment began with forecaster tools identical to those from 2015 to re-identify challenges associated with automated object identification and tracking, particularly when the tracking breaks. This breakage occurs when the original object cannot be identified on the successive data layer, and will manifest as one of three potential situations: (1) the original object disappears; (2) the original object is replaced with a new object or set of objects; or (3) the original object is merged with another previously identified object or set of objects.

To address these three tracking issues, a tactic was developed to reintroduce any forecaster-modified object that undergoes a tracking failure back into the spatial display while automatically masking any overlapping object not being maintained by the forecaster. At this juncture, the forecaster is presented with the power to decide how to proceed, depending on which of the three tracking situations have been incurred. In situation #1, the forecaster can take no action or expire the object. In situations #2 and

#3, the forecaster can repair the broken object tracking by transferring attributes from one object (original) to another (new object(s) that automatically replaced the original).

Usage with this new tactic quickly revealed new results and additional challenges. In convective events, particularly those with minimal spatial coverage, where tracking issues happen intermittently, the tactic appears to work well. Forecasters are able overcome the three situational impasses quickly and decisively without interrupting the flow of information to users. However, some convective events appeared to trigger these tracking situations frequently and randomly, leading to additional workload to maintain a coherent geospatial representation of the hazard areas. In 2017 a real-time best-track algorithm was implemented on ProbSevere objects and dramatically reduced the number of unjustified tracking breakages. However, it is clear that tracking discontinuities are an innate predicament of tracking convective hazard areas.

In 2016 it was also identified that the ideal human-machine mix mode is not applicable for all convective modes and evolutions. Forecasters need tools that effectively allow them to transfer between various modes of usage with automated object-based guidance. Tools were developed for the 2017 experiment to facilitate this conditional usage of automation concept. As in previous experiments there appears to be a preference to assume more control of automation as severity of hazard area increases. To combat the aforementioned object maintenance issues arising from more control, forecasters frequently relinquished control of the automated object shape to automation periodically throughout the hazard's lifetime. Additionally forecasters would often update the object shape with the first guess provided by automation, and then make subtle adjustments to the object as a means to quickly update the forecast while maintaining control of the object shape. Forecasters were also observed to detect hazard areas prior to the automated object identification, leading to the generation of a manual object. As the automated system caught up, forecasters would similarly perform a release of control of the object shape (as well as other forecast attributes) to the automated system as previously described.

In addition to fostering insights by working through the conditional use of automation, forecasters were presented with first guess probabilistic trends within the automated object-based guidance. These trends were created from probabilistic predictions from machine learning algorithms, extending through an assumed or predicted duration of predictability. It was hypothesized that these automated predictions would help forecasters in making their probabilistic trend predictions. Usage with this information revealed that forecasters find the automated predictions to be helpful in prioritizing which hazards to engage for generating forecasts for users, with the highest priority given to hazard areas associated the highest predicted probabilistic values. Such hazard areas were typically assigned a warning, whereas hazard areas with lower probabilistic predictions were typically assigned a significant weather advisory.

EMs and broadcast meteorology participants used both severe and sub-severe information in their decision making. EMs carefully watched the trends in probabilities, and depending upon circumstance, they made decisions based first on time, second on

severity. For example, if a dorm at a university requires 18 minutes to get students to safe areas on the lowest floors, that EM might make a decision ahead of a warning because more time is required than a typical warning lead time. Broadcasters primarily used dichotomous information (warnings/advisories), although PHI and sub-severe information helped in preparing for cut-in decisions. The broadcast meteorologists found PHI useful to confirm their own assessments of the storms.

Additionally, forecasters were given the ability to adjust the first guess probabilistic predictions. In 2016 it was found that adjustments were made frequently (greater than 90% of the time) and the probabilistic trends were typically adjusted to higher values that extended through the assigned duration. However, verification efforts performed from the 2014 experiment indicate that such adjustments result in detrimental reliability, drifting into over-forecasting with little or no skill. These adjustments appear linked to the precautionary principle, and were used as a means to reinforce the communication of a warning and drive desired action. Although these actions appear well intentioned with perhaps some communicative merit (discussed later), the intentional distortion of probabilities implies some level of unjustified mistrust of the guidance, and inevitably leads to misunderstanding and misusage of the probabilistic information. An attempt to address this issue was conducted in the 2017 experiment with two approaches.

First, a three-month climatology of automated forecast swaths produced from ProbSevere objects were conditionally verified to address the maximum predictability of the automated system. These conditional swaths show approximately the same predictability (probability of detection as a function of lead-time) as NWS warnings issued during the same three-month period. This result suggests that if forecasters assign warnings to objects associated with storms they would otherwise issue a warning for, they can achieve similar performance. Additionally, conditional verification performed for swaths with increasing buffer distances applied showed substantial increases in probability of detection, suggestive of an opportunity to increase performance if applied selectively. Forecasters participating in the 2017 experiment were informed of this information at the beginning of each week in an effort to improve trust.

Second, the probability trend tool was given a formal definition, defined as the subjective probability (i.e., confidence) of a defined hazard type occurring at 5-minute forecast intervals through an assigned duration. The hazard type definitions are extended from the current warning paradigm (1” hail, 58 mph wind, tornado), and a single cloud-to-ground strike was used for lightning. A paraphrased version of this definition was provided in the title above the probability trend tool to reinforce the intended purpose of the tool. An analysis of all forecast trends issued during each of the previous four years of HWT experiments implies substantial improvement in reliability of the probabilistic information was gained from this effort, particularly at long lead-times.

Efforts are underway to improve forecasters understanding of the automated guidance by assessing its seasonal skill and envisioning new capabilities for visualizing its underlying reasoning and training information.

Forecaster creation and adjustment toward precautionary probabilistic trends was also partially motivated by interaction with users through the integrated warning team. When the dichotomous products were removed in 2015, users (only EMs that year) were presented with a steep learning curve to begin understanding the intention of and using probabilities for informing decisions for severe convective events. In pre-week surveys they clearly expressed an understanding that warnings have a range of likelihood of verifying. They've not had to operationalize and use that understanding, however, and were initially unsure they knew how to apply these likelihoods and how to do it well. As they gained some comfort in thinking about how probability might link to action, they pointed out that they might act on a much lower probability when high-end severe weather was expected than on a marginal day, when it was unclear whether storms would reach severe criteria. Ultimately, they strongly expressed the need for the meteorologists to make the meteorological assessment regarding whether a storm merited a warning.

It is clear that the emergency management community needs warnings. Their standard operating plans have elements (e.g., sounding outdoor warning sirens) based upon those warnings from the NWS. Reinserting traditional warning information into the PHI system in 2016 and 2017 helped forecasters and users re-establish necessary and (apparently) effective elements of the current warning system (i.e., do no harm). Broadcasters, who first participated in 2016, conveyed that warnings are a lowest-common denominator type of information for the public. In recognition of these needs, the system design was re-strategized in 2017 such that generation and consumption of warnings and significant weather advisories was separated and prioritized, with probabilistic information reframed as supplementary within the geospatial confines of the warning/advisory polygon (i.e., relative probability). Thus all locations within a probabilistic swath receive a dichotomous, expert decision, supplemented with the likelihood of occurrence relative to surrounding locations based on forecaster confidence.

Finally, the reinsertion of traditional warning information allowed forecasters and users to focus on new forecast elements associated with the PHI system. Savvy users not only have well-developed plans of action, but, as mentioned earlier, have estimated the amount of time it takes to execute these plans. Thus, time of arrival information, in addition to traditional warning and probabilistic information, meets important needs of this subset of users. However, providing accurate and reliable timing information *requires* a dedication on the part of the forecaster to provide frequent updates to the hazard location, movement, and its various attributes (e.g., severity, intensity, history of reports, forecast information), as well as an increased attention to the geospatial specification of the hazard areas. This critical process of providing frequent updates is a concept we've termed "continuous flow of information," and it is sought out or calculated (if necessary) by our EMs and broadcasters. Because the PHI system

completes some tasks for the forecasters, they are able to use their time to focus on meteorological assessment and communication. In other words, frequent updates are possible. Observations of forecasters working high-impact tornado events show evidence that forecasters can naturally identify and utilize the capability of providing continuous flow of information while using geospatially precise objects within the PHI system. Additionally, the optimal human-machine mix mode directly supports these concepts, but despite efforts to address forecaster trust, more work is needed to better situate the forecaster with the guidance, particularly in the visualization and information extraction arena.

NSSL Project 9 – Evaluating the Impact of New Technologies, Data, and Information in the Operational Forecasting Environment

NOAA Technical Lead: Lans Rothfusz (NSSL)

NOAA Strategic Goal 2 – *Weather-Ready Nation – Society is Prepared for and Responds to Weather-Related Events*

Funding Type: CIMMS Task III

Accomplishments

1. Development of a Thunderstorm Initiation and Longevity Algorithm

Darrel Kingfield and Alexander Ryzhkov (CIMMS at NSSL), and Joseph Picca (SPC)

Thunderstorms impose a large economic burden on the United States, significantly impacting weather sensitive industries such as aviation. Unexpected thunderstorm development over a busy airspace like that of New York can lead to hundreds or thousands of delayed and cancelled flights, cascading across the National Airspace System. These issues necessitate improved radar algorithms that capitalize on the added microphysical information provided with polarimetric radar. One unique polarimetric signature that often signals new convective growth is the size sorting of raindrops. This can be observed within a developing updraft, where larger hydrometeors with a terminal velocity exceeding the updraft speed will fall to the Earth while smaller hydrometeors will be lofted higher in the cloud. This leads to a lower reflectivity at horizontal polarization (Z) collocated with a higher differential reflectivity (Z_{DR}). Yet, such a signature may not be readily distinguishable as Z_{DR} values tend to be higher everywhere below the melting layer.

A single-radar algorithm, named the Thunderstorm Risk Estimation and Nowcasting Development from Size Sorting (TRENDSS), was developed to automate the identification of this signature by creating dynamic Z/Z_{DR} relationship for reflectivity bins in 5 dBZ intervals below, within, and above the melting layer. Each radar bin has its Z_{DR} normalized by the mean and standard deviation of the relevant Z bin and displayed in terms of standard deviations above the mean. This single-radar algorithm was then

integrated into NSSL's Multi-Radar/Multi-Sensor (MRMS) framework fill-the-gaps that occur in single-radar volume coverage patterns.

This algorithm was beta tested at three National Weather Service (NWS) offices in Norman, OK, Upton, NY, and Taunton, MA. This testing was performed through the use of archived case data via the Weather Event Simulator-2 Bridge workstation in addition to a real-time data feed configured for display in each office's operational AWIPS-2 system. Initial forecaster feedback was promising with expected benefits including (1) improved forecaster confidence in anticipating storm propagation trends, (2) an enhancement in convective nowcasting abilities in the 0-1 hour forecast period, and (3) improvements in tactical decision making for aircraft routing at all stages of flight.

This exploratory research was supported in part by the CIMMS Director's Discretionary Research Fund and is ongoing.

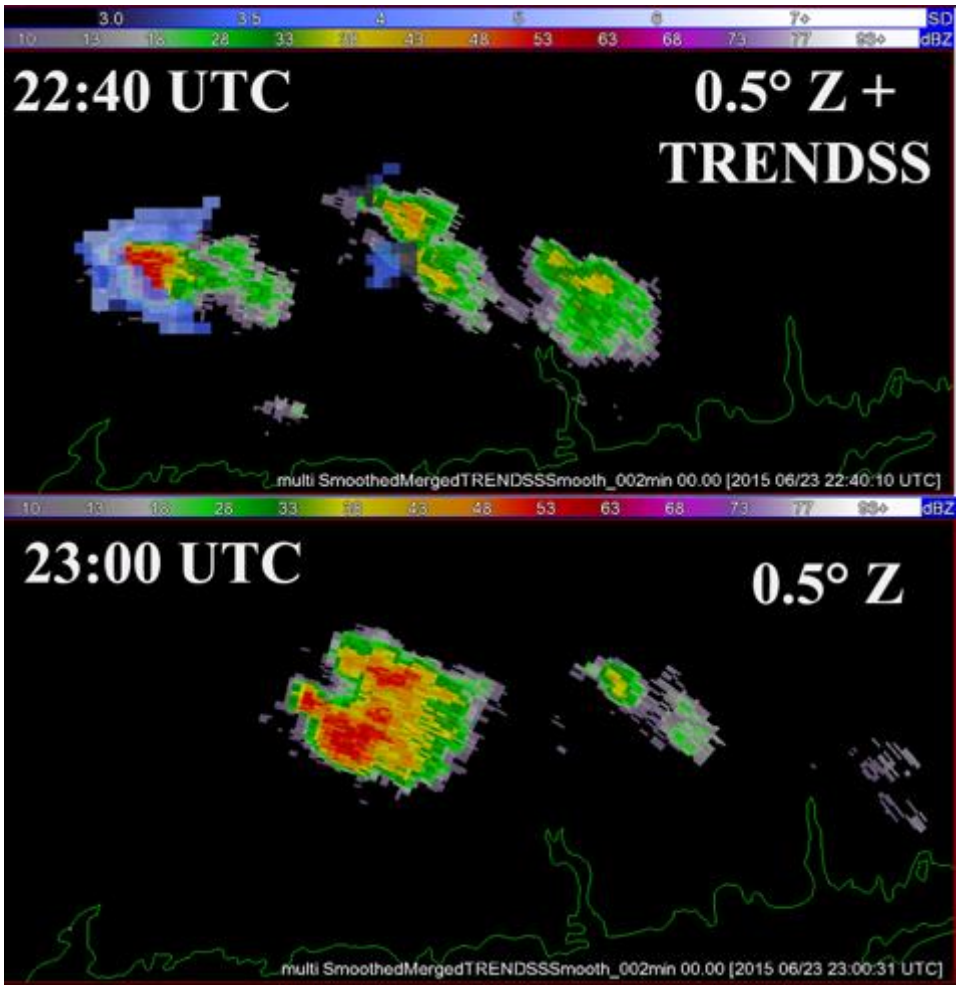

TRENDSS data for the left thunderstorm at 22:40 UTC (top image) reveals a "flared V" shape, indicative of multiple updrafts forming on the rear side. At 23:00 UTC (bottom image) the reflectivity structure reveals the thunderstorm did split with two unique deviant motions.

2. Continuous Testing of Warn-on-Forecast Prototype at the Norman National Weather Service

Gabe Garfield (CIMMS at OUN), and Jessica Choate and Patrick Skinner (CIMMS at NSSL)

In the fall of 2016, the Norman National Weather Service and the National Severe Storms Laboratory began a formal collaboration to test products derived from the NSSL Experimental Warn-on-Forecast System – for Ensembles (NEWS-e). The objectives of this collaboration are (1) to accelerate NEWS-e product feedback from NWS forecasters by creating a continuous feedback channel and (2) to create a group of super-users from which progress of product development can be tracked. Traditionally, feedback for new Experimental Warning Program warning products is received during the annual spring experiments. This joint effort accelerates that process by procuring NWS feedback throughout the year, via the Norman office. It also ensures that the same forecasters are giving feedback on product changes, forming a baseline of product growth.

At the outset, NSSL researchers met with NWS Norman forecasters to give an overview of NEWS-e and its products. It was decided that Norman forecasters would evaluate archive NEWS-e cases from 2016. The evaluation began with a weather briefing to acclimate the forecaster to the environment. Once the forecasters became reacquainted with the atmospheric conditions, they were instructed to grade around 100 system products. After the forecaster feedback was obtained, NSSL researchers used the suggestions to make product changes. Later, researchers and forecasters met again to discuss the evaluations and to determine next steps. Plans were made to continue forecaster evaluations of NEWS-e in 2018.

Additionally, the NEWS-e was used in real-time warning operations. On 16 May 2017, the model was used to great success during a tornado event in western Oklahoma. Before thunderstorms initiated that afternoon, NEWS-e output depicted intense supercells forming and moving toward western Oklahoma. This output was displayed on NWS Norman's situational awareness display, and Patrick Skinner (CIMMS at NSSL) provided a briefing on the guidance in the operations area. Once storms developed, NEWS-e contributed to a high degree of forecast confidence that the storms would become long-lived supercells with a risk of tornadoes. Based on output from NEWS-e, WFO Norman issued an advisory stating "a high probability that tornado warnings will be issued" for parts of four counties in western Oklahoma nearly two hours before the deadly tornado struck Elk City.

```
r
929
WWUS84 KOUN 162216
SPSOUN

SPECIAL WEATHER STATEMENT
NATIONAL WEATHER SERVICE Norman OK
516 PM CDT TUE MAY 16 2017

OKZ014-021-033-034-162245-
Harmon OK-Roger Mills OK-Beckham OK-Greer OK-
516 PM CDT TUE MAY 16 2017

...SIGNIFICANT WEATHER ADVISORY FOR northwestern Harmon...
southwestern Roger Mills...western Beckham and northwestern Greer
Counties Until 545 PM CDT...

Storms capable of producing tornadoes were located in the Texas
panhandle. One storm was located southwest of Wheeler and the other
located northwest of Wellington at 515 pm. The storms were moving
northeast at 35 MPH. These storms will move into western Oklahoma
before 6 PM. Severe weather is likely with these storms as they move
into Oklahoma and there is a high probability that tornado warnings
will be issued.

PRECAUTIONARY/PREPAREDNESS ACTIONS...

Monitor the situation closely. Be ready to act quickly if a warning
is issued or if storms threaten you.

&&

LAT...LON 3573 10000 3584 9984 3496 9976 3489 10000
TIME...MOT...LOC 2214Z 229DEG 32KT 3536 10035 3493 10027

$$

..speg.
```

Significant weather advisory issued for several counties in Oklahoma – including Elk City, which would be struck by a significant tornado 110 minutes later.

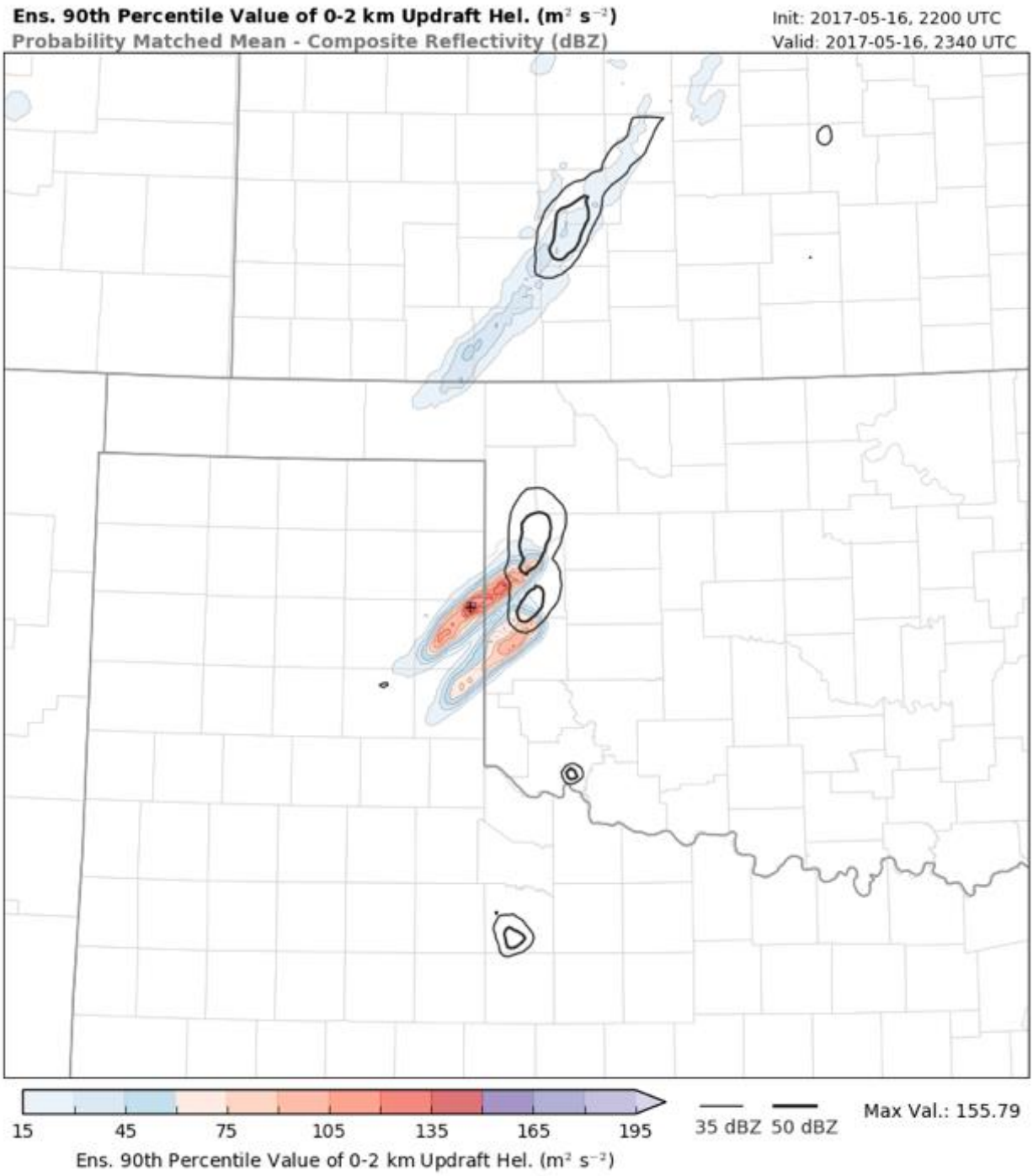

100-minute forecast of the strongest low-level updraft helicity swaths in the NEWS-e. Elk City is located near the end of the southernmost swath. It was hit by a significant tornado 2 hours after this run was initialized.

CIMMS Task III Project – Understanding the Current Flow of Weather Information and Associated Uncertainty, and Their Effect on Emergency Managers and the General Public

Daphne LaDue (CAPS), Jack Friedman (OU Center for Applied Social Research – CASR), Sean Ernst and Tabitha Kloss (OU School of Meteorology), and Melissa Wagner (OU Department of Geography and Environmental Sustainability)

NOAA Technical Lead: Lans Rothfusz (NSSL)

NOAA Strategic Goal 2 – *Weather Ready Nation: Society is Prepared for and Responds to Weather-Related Events*

Funding Type: CIMMS Task III

Objectives

The overall goal of this work is to study how three discrete, but intimately connected types of users of weather data — operational forecasters, emergency managers, and various publics — cope with uncertainty in severe weather forecasts. The aim is to understand both discrete challenges and opportunities for new data generated by the VORTEX SE researchers who are working to better understand physical processes and weather forecast modeling issues.

Accomplishments

Two teams analyzed data from the high numbers of interviews collected: 14 forecasters, 14 emergency managers, 83 pre-post interviews of forecasters, and 20 pre-post interviews of emergency managers. We participated in all Intensive Operations Periods.

1. Team 1: Co-PI Friedman and NWS forecasters

Friedman and his graduate student, Melissa Wagner, completed all coding of all background interviews for all forecasters in the study. In addition, coding was completed for all pre- and post-event interviews. Those latter interviews are shorter (15-20 minutes) and entail interviewing all available forecasters regarding a series of themes related to specific, forecasted events that prompted VORTEX-SE IOPs. Thematically, these interviews examined: (pre- and post-event) overall impressions and expectations for the forecasted event; (pre- and post-event) what will be/was the most difficult aspect of the event to forecast; (pre- and post-event) what information is/was useful or not useful (or not verified) emerging from numerical model guidance; and (only pre-event) what the forecaster felt most and least confident about in the forecast. After coding and analyzing these interviews, they were linked, by interviewee and specific event, into pairwise clusters in order to be able to compare how individual forecasters interpreted guidance before an event with how they interpreted the effectiveness, usefulness, and accuracy of that guidance after the same event. This involved a detailed process of cross-referencing and noting the timing of when each interview occurred in order to account for the influence of different numerical model guidance and other observational

data or interpretive frames that emerged in interactions between forecasters in the WFO. This same method has been used in subsequent VORTEX-SE research (i.e., field work funded for 2017) to great effect.

2. Team 2: Co-PI LaDue and Emergency Managers

LaDue and her undergraduate student finished analyses of emergency manager background interviews and presented the results in September 2016 at the National Weather Association's 41st Annual Meeting in Norfolk, Virginia. Many fruitful discussions took place with operational forecasters and others attending the meeting. LaDue then presented in the spring at the 2017 Tornado Summit in Oklahoma City, Oklahoma, to open a larger discussion with attendees (mostly Oklahoma emergency managers) about some of the emergent themes from this research to see if they resonated for another part of the U.S. and to better understand them. Themes probed at the Tornado Summit were: 1) what lead times emergency managers need for various weather hazards, 2) how their expectations for an event interact with their readiness, 3) what types of NWS products are the most difficult to work with, and 4) what they do to lower their uncertainty about a possible severe weather event.

During this reporting period our next VORTEX SE grant was awarded and the Intensive Observations Periods occurred. LaDue took advantage of the opportunity to add additional background interviews and thus expand the working dataset. Publications in progress will include all data collected.

Southeast U.S. emergency managers consider a great deal of information in making decisions. Two of these key decision factors, the needs of the emergency manager's stakeholders and the logistical needs of other departments, were further explored in the next grant.

No-Notice Event Examples

Event 1: EM chooses stay in the Emergency Operations Center (EOC) after hours because his area was close to a watch and two small cells had appeared on radar.

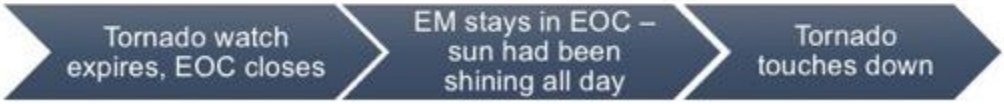

Event 2: EM choses to stay in the Emergency Operations Center (EOC) after a tornado watch expired because the sun had been shining all day.

Southeastern U.S. emergency managers have experienced enough no-notice events to learn to use cues beyond official NWS information to remain alert to changing weather conditions.

Flow of Uncertainty Affecting Severe Weather Action in VORTEX-SE Study Region

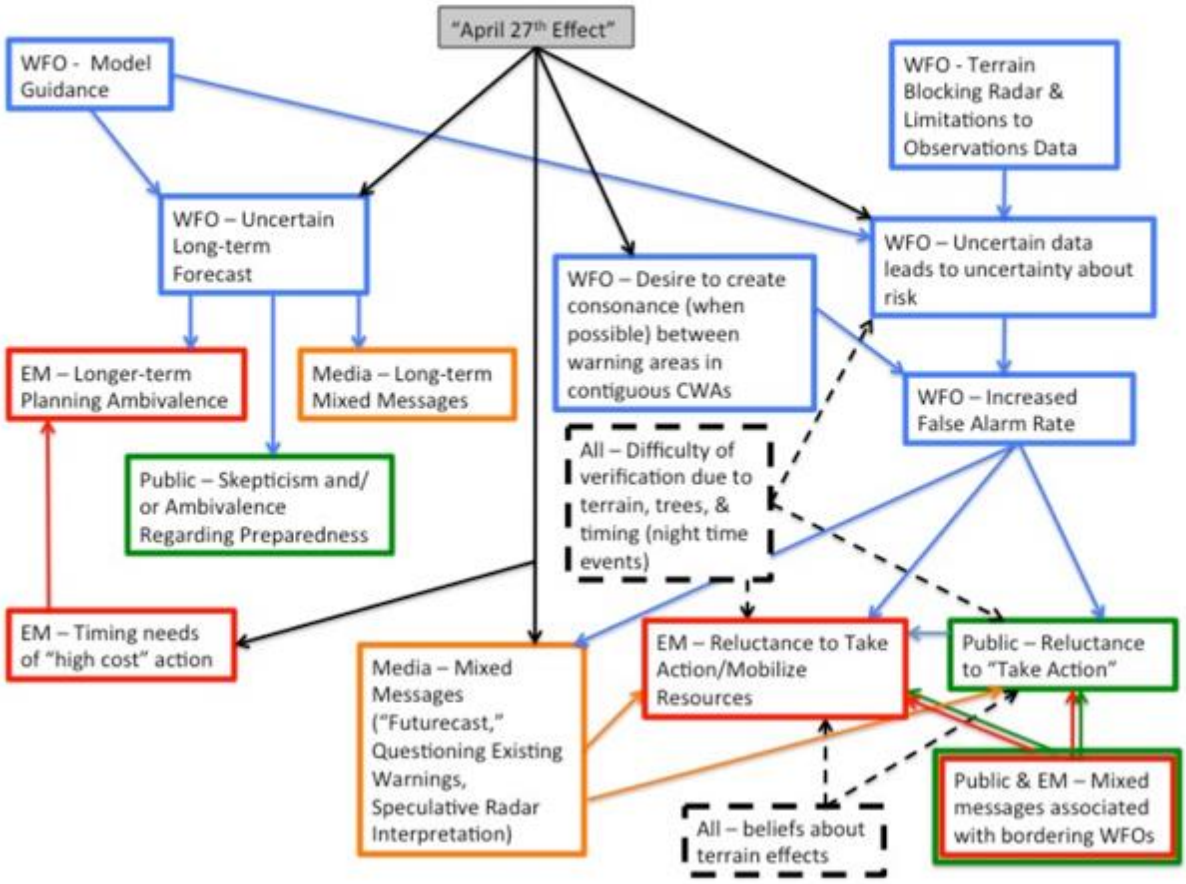

This diagram was developed from our full-team collaboration examining the impacts and influences of multiple factors on the flow of uncertainty that shapes actions or inaction in the VORTEX-SE study region. Each of the actors in the diagram is populated based on directly reported or observed, empirical findings, so, although this diagram might appear to be a "general" diagram that could be the result of deductive reasoning (a diagram constructed a priori), these specific relationships are directly supported by social research conducted by the PIs on this project. ***Key:*** *Blue: NWS WFO; Orange: Media; Red: Emergency Managers; Green: Public; Dashed: All Actors. Shaded Gray: This represents the cascading effects of and uncertainties associated with memories of and experiences with the impacts of the April 27, 2011 super outbreak.*

CIMMS Task III Project – Drought Risk Management for the United States

Mark Shafer (OCS), and Michael Hayes, Mark Svoboda, Cody Knutson, Tsegaye Tadesse, Deborah Bathke, and Brian Fuchs (National Drought Mitigation Center)

NOAA Technical Lead: Veva DeHaza (NOAA NIDIS)

NOAA Strategic Goal 1 – *Climate Adaptation and Mitigation: An Informed Society Anticipating and Responding to Climate and its Impacts*

Funding Type: CIMMS Task III

Objectives
The overall goal of the project is to improve drought risk management across the United States. To accomplish this goal, the project builds upon partnerships between the Southern Climate Impacts Planning Program (SCIPP), National Drought Mitigation Center (NDMC), and National Integrated Drought Information System (NIDIS). The project will develop new tools and procedures and test them in the Southern Plains Drought Early Warning System being developed by NIDIS. Specific objectives of the project include: (1) Improving and expanding drought monitoring activities; (2) Engaging the NIDIS Preparedness Community Technical Working Group activities; (3) Examining drought planning assistance; (4) Continued development of Regional Drought Early Warning System assistance; (5) Conducting a regional drought event assessment; and (6) Communication and dissemination activities.

Accomplishments
The project was on a no-cost extension during this fiscal year. All work at the National Drought Mitigation Center was completed in the previous year. The remaining work was conducted at SCIPP on Objectives 3, 4 and 6:

3. Drought Planning Strategies: SCIPP continued work with the Arkansas Natural Resources Commission (ANRC) on a state drought planning effort in Arkansas. SCIPP summarized notes from the meeting and breakout, held in Little Rock, AR, in June 2016, and delivered a summary report to ANRC to guide further actions as the state develops its drought plan.

4. Regional Drought Early Warning Systems: SCIPP continued collaboration on the Southern Plains Regional Drought Early Warning System (RDEWS), which included developing a strategic plan.

6. Communication and Dissemination Activities: SCIPP and Weather Decisions Technologies (WDT) are collaborating on developing a mobile drought app for the iPhone. The app is currently in prototype stage and should go to a limited group for beta testing in Fall 2017. A companion app for Android and Google platforms is being developed under a separate project.

CIMMS Task III Project – Implementation of a Drought App for Mobile Devices

Mark Shafer (OCS) and Michael Wolfinbarger (Weather Decision Technologies, Inc.)

NOAA Technical Lead: Claudia Nierenberg (NOAA CPO)

NOAA Strategic Goal 1 – *Climate Adaptation and Mitigation: An Informed Society Anticipating and Responding to Climate and its Impacts*

Funding Type: CIMMS Task III

Objectives

A mobile drought app is being developed by Weather Decision Technologies, a private firm located in Norman, Oklahoma, under funding previously provided on a project, *Drought Risk Management for the United States* (described next). This project is to complete development of the app, including iPhone and Android platforms, and make it freely available for download.

Accomplishments

Prototypes for both iPhone (from previous grant) and Android have been completed. Amazon Web Services (AWS) were set up to manage the back-end data requirements (delivery of products to the mobile app and collection of drought condition reports via the app). Developer accounts for Google Play and Apple are currently being established in order to move from the prototype stage to beta testing (Fall 2017).

Public Affairs and Outreach

NOAA Partners Communications, Public Affairs, and Outreach

NOAA Technical Lead: Keli Pirtle (NOAA Public Affairs)

NOAA Engagement Enterprise – *An Engaged and Educated Public with an Improved Capacity to Make Scientifically Informed Environmental Decisions*

Funding Type: CIMMS Task II

Objectives
Communicate CIMMS and NSSL research and news to OU, OAR, NOAA, and Department of Commerce leadership, the U.S. Congress, decision makers, partners, collaborators, and the public.

Accomplishments

1. Data Calls and Monthly Updates – Emily Summars (CIMMS at NSSL)

- Report significant papers: Alert NOAA leadership to published papers determined to be significant by NSSL and CIMMS leadership, add such papers to the OAR Weekly Report and publish in OAR Hot Items. Reports include a summary of each significant paper.
    - CIMMS reported **54** significant papers in FY2017.
- Provide report numbers for Quarterly Education performance taskers to NSSL leadership and CIMMS leadership as needed.
- Provide monthly social media updates, story progress updates and project updates via email and the weekly NSSL Managers Meetings.

2. NOAA and OAR Communications – Emily Summars (CIMMS at NSSL)

- OAR Hot Items: Describe new research, activities and publications. Hot items are posted on the OAR Hub, where the OAR Communications team reviews and chooses significant topics to be added in the Department of Commerce Secretary's Weekly Report. **Twelve** Hot Items were submitted on behalf of NSSL and CIMMS in FY2017, including several topics like VORTEX-SE and CLEAN-AP.
    - Department of Commerce Secretary's Weekly Report: Significant OAR Hot Items are condensed into a few sentences to be included into the Department of Commerce Secretary's Weekly Report. Work with HQ to ensure the accuracy of these items, add details and other items as requested by OAR leadership. CIMMS items featured in the report include publications, VORTEX-SE, participation in EPIC and RiVorS.

3. Research Projects – James Murnan (ACE) and Emily Summars (CIMMS at NSSL)

- Accompany researchers to video, conduct interviews, and take photos during research projects. Examples included VORTEX-SE, EPIC and Hazardous Weather Testbed experiments. Provide social media updates while in the field to provide an "in-that-moment" view for followers. The final result from time in the field includes story(s), video, social media updates, and/or a Flickr album.

4. Project Fact Sheets – Emily Summars (CIMMS at NSSL)

- Fact Sheets are 1-2 page handouts on NSSL/CIMMS projects used to give visitors and guests a "take-away" message. **Seven** Fact Sheets involving CIMMS were designed, written, edited and updated in FY2017, including fact sheets for VORTEX-SE media day, and Congressional fact sheets for MRMS, MPAR and more.

5. CIMMS on Social Media – Emily Summars (CIMMS at NSSL)

- CIMMS's Facebook and Twitter accounts are growing in popularity. New content is published daily based on monthly or daily themes. Partner posts are shared as appropriate. Project photos from researchers, days in the field and media days are shared on NSSL's also has Flickr, Instagram and Pinterest accounts. Updated Facebook and Twitter photos and headers as appropriate. Monitor comments and remove comments using inappropriate language or targeting other individuals.
    - **CIMMS Facebook "likes"**
        - **2017: 780**
        - **2016: 613**
        - **2015: 375**
    - **CIMMS Twitter "follows"**
        - **2017: 642**
        - **2016: 512**
        - **2015: 282**

6. CIMMS Outreach Emails – Emily Summars (CIMMS at NSSL)

- The public submits questions to CIMMS via the CIMMS Outreach email account. The account existed before FY2017 but was added to OU CIMMS website and social media in FY2017.
- Staff outreach:
    - Send reminders about NSSL and OU CIMMS internal Gab at the Lab.
    - Work closely with the College of Atmospheric and Geographic Sciences to ensure all students, faculty and staff are recognized properly in CIMMS related publications and releases.
    - Share stories and social media posts involving students with the College to ensure collaborative efforts.

7. CIMMS Website – Vicki Farmer (ACE) and Emily Summars (CIMMS at NSSL)

- Review, update and post content to the CIMMS website at least once a week.

- Redesign certain products to create a cohesive brand.
- Track awards, accomplishments and publications then post items considered of interest.

8. Back-up NOAA Weather Partners Public Affairs – Keli Pirtle (NOAA Weather Partners) and Emily Summars (CIMMS at NSSL)

- Help Keli Pirtle and other NOAA partners field media calls pertaining to CIMMS.
- Provide additional information on projects involving CIMMS researchers.
- Ensure CIMMS researchers are mentioned properly in news and other media articles.

9. Public Education and Outreach – Patrick Hyland (OU College of Atmospheric and Geographic Sciences)

- Lead tour program of the National Weather Center, including NOAA.
- Plan and organize National Weather Festival activities.
- Facilitate educational outreach opportunities.
- Collaborate with NOAA and CIMMS public relations office on requests that require crossover into both the university and NOAA.

Appendix A

AWARDS AND HONORS

The following awards or other notable achievements occurred during the fiscal year. CIMMS staff (present and past) in **bold**:

Presidential Early Career Award for Scientists and Engineers (PECASE), 2016: **Corey Potvin**

AMS 2016 17th Conference on Mountain Meteorology "Service to the Society" Award: **Heather Reeves**

OU School of Meteorology 2016 Yoshi Sasaki Award for Best M.S. Publication: **Katie Wilson**

National Weather Association 2016 Roderick Scofield Scholarship: **Katie Wilson**

National Weather Association 2016 Larry R. Johnson Special Award: **Travis Smith, Valliappa Lakshmanan, Gregory Stumpf, Kiel Ortega, Kurt Hondl, Karen Cooper, Kristin Calhoun, Darrel Kingfield, Kevin Manross, Robert Toomey, Jeff Brogden, Tiffany Meyer, Kevin Scharfenberg, Tony Reinhart, Brandon Smith, Chris Karstens, Holly Obermeier, Matt Mahalik, Clark Payne, Alyssa Bates, Jill Hardy, Chris Spannagle, Matt Taraldsen, Andy Wood**, James LaDue, Robert Prentice, **Matthew Elliot**

OU College of Atmospheric and Geographic Sciences 2016 Dean's Award for Outstanding Service: **Sebastian Torres**

Named Associate Editor for AMS *Journal of Atmospheric and Oceanic Technology* 2017: **Sebastian Torres**

AMS 2017 7th Conference on Transition of Research to Operations Student Competition Poster Presentation Winners: **Katie Wilson** and **Makenzie Krocak**

AMS 2017 17th Conference on Mesoscale Processes Second Place Oral Presentation Winner: **Hristo Chipilski**

Association for Talent Development's 2017 *One to Watch* Program Honoree: **Megan Taylor**

Named 2017 Emerging Training Leader by *Training* Magazine: **Megan Taylor**

Elected AMS Fellow in 2017: **Alexander Ryzhkov**

Named 2017 OU Student Government Association Outstanding Faculty Member: **Randy Peppler**

Bulletin of the American Meteorological Society Paper of Note: **Randy Peppler**, published in *Weather, Climate, and Society*, April 2017

American Geophysical Union Research Spotlight Article: **Darrel Kingfield**, **Kristin Calhoun**, and Kirsten de Beurs, published in *EOS*, 26 May 2017

Bulletin of the American Meteorological Society Paper of Note: **Darrel Kingfield** and Kirsten de Beurs, published in *Journal of Applied Meteorology and Climatology*, June 2017

Appendix B

PUBLICATION SUMMARY*

	CIMMS Lead Author				NOAA Lead Author				Other Lead Author			
	2009-10	2010-11	2011-12	2012-13	2009-10	2010-11	2011-12	2012-13	2009-10	2010-11	2011-12	2012-13
Peer Reviewed	32	28	31	32	28	32	13	8	40	44	35	45

	CIMMS Lead Author				NOAA Lead Author				Other Lead Author			
	2013-14	2014-15	2015-16	2016-17	2013-14	2014-15	2015-16	2016-17	2013-14	2014-15	2015-16	2016-17
Peer Reviewed	57	60	62	***45***	9	7	5	***5***	44	40	52	***44***

**Publication numbers are approximate. Numbers are slightly lower this year as they are strictly fiscal year.*

Appendix C

PERSONNEL SUMMARY – NOAA FUNDED RESEARCH ONLY

Category	**Number**	**B.S.**	**M.S.**	**Ph.D.**
Research Scientist	82	2	46	34
Visiting Scientist	2		2	
Postdoctoral Fellow	13			13
Research Support Staff	15	6	9	
Administrative	3	2	1	
Total (>50% support)	**115**	**10**	**58**	**47**
Undergraduate Students	27			
Graduate Students (current degree)	43	14	29	
Employees that receive <50% NOAA Funding (not including students)	**43**	**6**	**14**	**21**
Located at Lab	NSSL-92, WDTD-18, SPC-10, ROC-9, NWSTC-6, OUN-1			
Obtained NOAA employment within the last year	**5**			

Appendix D

COMPILATION OF CIMMS-RELATED PUBLICATION – FY 2017

Publications compiled here were reported for projects funded under Cooperative Agreement NA11OAR4320072.

Peer-Reviewed Journal Articles, Books, and Book Chapters *Published*

July 2016

Karstens, C. D., K. Shourd, D. Speheger, A. Anderson, R. Smith, D. Andra, T. M. Smith, and V. Lakshmanan, 2016: Evaluation of near real-time preliminary tornado damage paths, *Journal of Operational Meteorology,* **4**, 132-141. http://dx.doi.org/10.15191/nwajom.2016.0410.

August 2016

Borowska, L., G. Zhang, and D. S. Zrnic, 2016: Spectral processing for step scanning Phased Array Radars. *IEEE Trans. on Geoscience and Remote Sensing*, **54**, 4534-4543. https://doi.org/10.1109/TGRS.2016.2543724.

Carlin, J., A. Ryzhkov, J. Snyder, and A. Khain, 2016: Hydrometeor mixing ratio retrievals for storm-scale radar data assimilation: Utility of current equations and potential benefits of polarimetry. *Monthly Weather Review,* **144**, 2981-3001. https://doi.org/10.1175/MWR-D-15-0423.1.

Gravelle, C. M., K. J. Runk, K. L. Crandall, and D. W. Snyder, 2016: Forecaster evaluations of high temporal satellite imagery for the GOES-R era at the NWS Operations Proving Ground. *Weather and Forecasting*, **31**, 1157-1177. https://doi.org/10.1175/WAF-D-15-0133.1.

Reeves, H., A. Ryzhkov, and J. Krause, 2016: Discrimination between winter precipitation types based on spectral-bin microphysical modeling. *Journal of Applied Meteorology and Climatology,* **55**, 1747-1761. https://doi.org/10.1175/JAMC-D-16-0044.1.

Xie, X., R. Evaristo, S. Troemel, P. Saavedra, C. Simmer, and A. Ryzhkov, 2016: Radar observation of evaporation and implications for quantitative precipitation and cooling rate estimation. *Journal of Atmospheric and Oceanic Technology*, **33**, 1779-1792. https://doi.org/10.1175/JTECH-D-15-0244.1.

Zhang, G. 2016: *Weather Radar Polarimetry*, CRC Press, 322 pp.

September 2016

Cintineo, R., J. Otkin, T. A. Jones, S. Koch, and D. Stensrud, 2016: Assimilation of synthetic GOES-R ABI infrared brightness temperatures and WSR-88D radar observations in a high-resolution OSSE. *Monthly Weather Review,* **144**, 3159-3180. https://doi.org/10.1175/MWR-D-15-0366.1

Krause, J., 2016: A simple algorithm to discriminate between meteorological and non-meteorological radar echoes. *Journal of Atmospheric and Oceanic Technology*, **33**, 1875-1885. https://doi.org/10.1175/JTECH-D-15-0239.1.

Smith, T. M., V. Lakshmanan, G. J. Stumpf, K. L. Ortega, K. Hondl, K. Cooper, K. M. Calhoun, D. M. Kingfield, K. L. Manross, R. Toomey, and J. Brogden, 2016: Multi-Radar Multi-Sensor (MRMS) severe weather and aviation products: Initial operating capabilities. *Bulletin of the American Meteorological Society*, **97**, 1617-1630. https://doi.org/10.1175/BAMS-D-14-00173.1.

Wang, Y., J. Zhang, P. Chang, C. Langston, B. Kaney, L. Tang, 2016: Operational C-Band Dual-Polarization radar QPE for the subtropical complex terrain of Taiwan. *Advances in Meteorology*, 1-15. http://dx.doi.org/10.1155/2016/4294271.

Yu, X., Y. Zhang, A. Patel, A. Zahari and M. Weber, 2016: An implementation of real-time phased array radar fundamental functions on a DSP-focused, high-performance, embedded computing platform. *Aerospace*, **3**, 28. http://dx.doi.org/10.3390/aerospace3030028.

October 2016

Coniglio, M. C., S. M. Hitchcock, and K. H. Knopfmeier, 2016: Impact of Assimilating Preconvective Upsonde Observations on Short-Term Forecasts of Convection Observed during MPEX. *Monthly Weather Review*, **144**, 4301–4325, doi:10.1175/MWR-D-16-0091.1.

Fierro, A. O., J. Gao, C. Ziegler, K. Calhoun, E. Mansell, and D. MacGorman, 2016: Assimilation of flash extent data in the variational framework at convection-allowing scales: Proof-of-concept and evaluation for the short term forecast of the 24 May 2011 tornado outbreak. *Monthly Weather Review*, **144**, 4373–4393, doi:10.1175/MWR-D-16-0053.1.

Grams, H. M., P. E. Kirstetter, and J. J. Gourley, 2016: Naïve Bayesian precipitation type retrieval from satellite using a cloud-top and ground-radar matched climatology. *Journal of Hydrometeorology*, **17**, 2649–2665, doi:10.1175/JHM-D-16-0058.1.

Hardy, J., J. J. Gourley, P. Kirstetter, Y. Hong, F. Kong, and Z. Flamig, 2016: A method for probabilistic flash flood forecasting. *Journal of Hydrology*, **541**, 480–494, doi:10.1016/j.jhydrol.2016.04.007.

He, X., Y. Hong, H. Vergara, K. Zhang, P. E. Kirstetter, J. J. Gourley, Y. Zhang, G. Qiao, and C. Liu, 2016: Development of a coupled hydrological-geotechnical framework for rainfall-induced landslides prediction. *Journal of Hydrology*, **543**, 395–405, doi:10.1016/j.jhydrol.2016.10.016.

Ivic, I. R., 2016: A Technique to Improve Copolar Correlation Coefficient Estimation. *IEEE Transactions on Geoscience and Remote Sensing*, **54**, 5776–5800, doi:10.1109/TGRS.2016.2572185.

Nai, F., S. M. Torres, and R. D. Palmer, 2016: Adaptive beamspace processing for phased-array weather radars. *IEEE Transactions on Geoscience and Remote Sensing*, **54**, 5688-5698. https://doi.org/10.1109/TGRS.2016.2570138.

Schroeder, A. J., J. J. Gourley, J. Hardy, J. J. Henderson, P. Parhi, V. Rahmani, K. A. Reed, R. S. Schumacher, B. K. Smith, and M. J. Taraldsen, 2016: The development of a flash flood severity index. *Journal of Hydrology*, **541**, 523-532. https://doi.org/10.1016/j.jhydrol.2016.04.005.

Vergara, H., P. E. Kirstetter, J. J. Gourley, Z. F. Flamig, Y. Hong, A. Arthur, and R. L. Kolar, 2016: Estimating a-priori kinematic wave model parameters based on regionalization for flash flood forecasting in the Conterminous United States. *Journal of Hydrology*, **541**, 421–433. https://doi.org/10.1016/j.jhydrol.2016.06.011.

November 2016

Fierro A. O., 2016: “Present State of Knowledge of Electrification and Lightning within Tropical Cyclones and Their Relationships to Microphysics and Storm Intensity.” Chapter 7 in *Advanced Numerical Modeling and Data Assimilation Techniques for Tropical Cyclone Predictions*, U. C. Mohanty and

S. Gopalakrishnan, eds. Co-published by Springer International Publishing, Cham, Switzerland, with Capital Publishing Company, New Delhi, India, pp. 197-220.

Houser, J. B., H. B. Bluestein, and J. C. Snyder, 2016: A finescale radar examination of the tornadic debris signatures and weak reflectivity band associated with a large, violent tornado. *Monthly Weather Review*, **144**, 4101-4130. https://doi.org/10.1175/MWR-D-15-0408.1.

Jones, T. A., S. Koch, and Z. Li, 2017: Assimilating synthetic hyperspectral sounder temperature and humidity retrievals to improve severe weather forecasts. *Atmospheric Research,* **186**, 9-25. http://dx.doi.org/10.1016/j.atmosres.2016.11.004.

Stepanian, P. M., K. L. Horton, V. M. Melnikov, D. S. Zrnic, and S. A. Gauthreaux Jr., 2016: Dual-polarization radar products for biological applications. *Ecosphere*, **7**, 1–27. http://dx.doi.org/10.1002/ecs2.1539.

Wilson, T. B., C. B. Baker, T. P. Meyers, J. Kochendorfer, M. E. Hall, J. E. Bell, H. J. Diamond, and M. A. Palecki, 2016: Site-specific soil properties of the US climate reference network soil moisture. *Vadose Zone Journal*, **15**, doi:10.2136/vzj2016.05.0047.

December 2016

DiGangi, E. A., D. R. MacGorman, C. L. Ziegler, D. Betten, M. Biggerstaff, M. Bowlan, and C. K. Potvin, 2016: An overview of the 29 May 2012 Kingfisher supercell during DC3. *Journal of Geophysical Research*, **121**, 14316-14343, doi:10.1002/2016JD025690.

Harrison, D. R., and C. D. Karstens, 2017: A climatology of operational storm-based warnings: A geospatial analysis. *Weather and Forecasting*, **32**, 47–60, doi:10.1175/WAF-D-15-0146.1.

Hwang, Y., T-Y Yu, V. Lakshmanan, D. M. Kingfield, D-I Lee, and C-H You, 2017: Neuro-Fuzzy Gust Front Detection Algorithm With S-Band Polarimetric Radar. *IEEE Transactions on Geoscience and Remote Sensing*, **55**, 1618-1628. doi:org/10.1109/TGRS.2016.2628520.

Murphy, A. M., R. M. Rauber, G. M. McFarquhar, J. A. Finlon, D. M. Plummer, A. A. Rosenow, and B. F. Jewett, 2017: A Microphysical Analysis of Elevated Convection in the Comma Head Region of Continental Winter Cyclones. *Journal of the Atmospheric Sciences*, **74**, 69–91, doi:10.1175/JAS-D-16-0204.1.

Peppler, R. A., 2016: “They could tell what the weather was to be in advance.” Native Oklahoma weather and climate insights from the archive. *The Chronicles of Oklahoma*, **94-4**, 414-431.

Potvin, C. K., E. M. Murillo, M. L. Flora, and D. M. Wheatley, 2017: Sensitivity of Supercell Simulations to Initial-Condition Resolution. *Journal of the Atmospheric Sciences*, **74**, 5–26, doi:10.1175/JAS-D-16-0098.1.

Reeves, H. D., 2016: The Uncertainty of Precipitation-Type Observations and Its Effect on the Validation of Forecast Precipitation Type. *Weather and Forecasting*, **31**, 1961–1971, doi:10.1175/WAF-D-16-0068.1.

Torres, S. M., and D. A. Warde, 2017: Staggered-PRT Sequences for Doppler Weather Radars. Part I: Spectral Analysis Using the Autocorrelation Spectral Density. *Journal of Atmospheric and Oceanic Technology*, **34**, 51–63, doi:10.1175/JTECH-D-16-0071.1.

Wilson, K. A., P. L. Heinselman, and Z. Kang, 2016: Exploring Applications of Eye Tracking in Operational Meteorology Research. *Bulletin of the American Meteorological Society*, **97**, 2019–2025, doi:10.1175/BAMS-D-15-00148.1.

Zhang, K., X. Xue, Y. Hong, J. J. Gourley, N. Lu, Z. Wan, Z. Hong, and R. Wooten, 2016: iCRESTRIGRS: a coupled modeling system for cascading flood-landslide disaster forecasting. *Hydrology and Earth System Sciences*, **20**, 5035–5048, doi:10.5194/hess-20-5035-2016.

January 2017

Cao, Q., M. Knight, A. Ryzhkov, P. Zhang, and N. Lawrence, 2017: Differential phase calibration of linearly polarized radars with simultaneous transmission/reception for estimation of circular depolarization ratio. *IEEE Transactions on Geoscience and Remote Sensing*, **55**, 491–501. https://doi.org/10.1109/TGRS.2016.2609421.

Martinaitis, S. M., 2017: Radar observations of tornado-warned convection associated with tropical cyclones over Florida. *Weather and Forecasting*, **32**, 165–186, doi:10.1175/WAF-D-16-0105.1.

Saeidi-Manesh, H., and G. Zhang, 2017: Characterization and optimization of cylindrical polarimetric array antenna patterns for multi-mission applications. *Progress in Electromagnetic Research B*, **158**, 49-61.

Saharia, M., P. E. Kirstetter, H. Vergara, J. J. Gourley, Y. Hong, and M. Giroud, 2017: Mapping flash flood severity in the United States. *Journal of Hydrometeorology*, **18**, 397–411, doi:10.1175/JHM-D-16-0082.1.

Schvartzman, D., S. Torres, and T. Y. Yu, 2017: Weather Radar Spatiotemporal Saliency: A First Look at an Information Theory–Based Human Attention Model Adapted to Reflectivity Images. *Journal of Atmospheric and Oceanic Technology*, **34**, 137–151, doi:10.1175/JTECH-D-16-0092.1.

Trömel, S., A. V. Ryzhkov, M. Diederich, K. Mühlbauer, S. Kneifel, J. C. Snyder, and C. Simmer, 2017: Multisensor characterization of mammatus. *Monthly Weather Review*, **145**, 235–251, doi:10.1175/MWR-D-16-0187.1.

Umeyama, A., S. Torres, and B. Cheong, 2017: Bootstrap Dual-Polarimetric Spectral Density Estimator. *IEEE Transactions on Geoscience and Remote Sensing*, **55**, 2299-2312. https://doi.org/10.1109/TGRS.2016.2641385.

Wilson, K. A., P. L. Heinselman, C. M. Kuster, D. M. Kingfield, and Z. Kang, 2017: Forecaster Performance and Workload: Does Radar Update Time Matter? *Weather and Forecasting*, **32**, 253–274, doi:10.1175/WAF-D-16-0157.1.

February 2017

Cheong, B., B. David, C. Fulton, S. Torres, T. Maruyama, and R. Palmer, 2017: SimRadar: A Polarimetric Radar Time-Series Simulator for Tornadic Debris Studies. *IEEE Transactions on Geoscience and Remote Sensing*, **55**, 2858-2870. https://doi.org/10.1109/TGRS.2017.2655363.

Kerr, C. A., D. J. Stensrud, and X. Wang, 2017: Verification of Convection-Allowing Model Ensemble Analyses of Near-Storm Environments Using MPEX Upsonde Observations. *Monthly Weather Review*, **145**, 857–875, doi:10.1175/MWR-D-16-0287.1.

Nemunaitis-Berry, K. L., P. M. Klein, J. B. Basara, and E. Fedorovich, 2017: Sensitivity of Predictions of the Urban Surface Energy Balance and Heat Island to Variations of Urban Canopy Parameters in Simulations with the WRF Model. *Journal of Applied Meteorology and Climatology*, **56**, 573–595, doi:10.1175/JAMC-D-16-0157.1.

Perera, S., Y. Zhang, D. S. Zrnic and R. J. Doviak, 2017: Electromagnetic (EM) simulation and alignment of dual-polarized array antennas in multi-mission phased array radars. *Aerospace*, **4**, 7. http://dx.doi.org/10.3390/aerospace4010007.

Richardson, L. M., J. G. Cunningham, W. D. Zittel, R. R. Lee, R. L. Ice, V. M. Melnikov, N. P. Hoban, and J. G. Gebauer, 2017: Bragg Scatter Detection by the WSR-88D. Part I: Algorithm Development. *Journal of Atmospheric and Oceanic Technology*, **34**, 465–478, doi:10.1175/JTECH-D-16-0030.1.

Richardson, L. M., W. D. Zittel, R. R. Lee, V. M. Melnikov, R. L. Ice, and J. G. Cunningham, 2017: Bragg Scatter Detection by the WSR-88D. Part II: Assessment of ZDR Bias Estimation. *Journal of Atmospheric and Oceanic Technology*, **24**, 479–493, doi:10.1175/JTECH-D-16-0031.1.

March 2017

Argyle, E. M., J. J. Gourley, Z. L. Flamig, T. Hansen, and K. Manross, 2017: Towards a user-centered design of a weather forecasting decision support tool. *Bulletin of the American Meteorological Society*, **98**, 373–382, doi:10.1175/BAMS-D-16-0031.1.

Argyle, E. M., J. J. Gourley, C. Ling, R. L. Shehab, and Z. Kang, 2017: Effects of display design on signal detection in flash flood forecasting. *International Journal of Human-Computer Studies*, **99**, 48–56, doi:10.1016/j.ijhcs.2016.11.004.

Cocks, S. B., J. Zhang, S. M. Martinaitis, Y. Qi, B. Kaney, and K. Howard, 2017: MRMS QPE Performance East of the Rockies during the 2014 Warm Season. *Journal of Hydrometeorology*, **18**, 761–775, doi:10.1175/JHM-D-16-0179.1.

Gourley, J. J., Z. Flamig, H. Vergara, P. Kirstetter, R. Clark, E. Argyle, A. Arthur, S. Martinaitis, G. Terti, J. Erlingis, Y. Hong, and K. Howard, 2017: The Flooded Locations And Simulated Hydrographs (FLASH) project: improving the tools for flash flood monitoring and prediction across the United States. *Bulletin of the American Meteorological Society*, **98**, 361–372, doi:10.1175/BAMS-D-15-00247.1.

Kingfield, D. M., and K. M. de Beurs, 2017: Landsat Identification of Tornado Damage by Land Cover and an Evaluation of Damage Recovery in Forests. *Journal of Applied Meteorology and Climatology*, **56**, 965–987, doi:10.1175/JAMC-D-16-0228.1.

MacGorman, D. R., M. S. Elliott, and E. DiGangi, 2017: Electrical discharges in the overshooting tops of thunderstorms. *Journal of Geophysical Research*, **122**, 2929–2957, doi:10.1002/2016JD025933.

Martinaitis, S. M., J. J. Gourley, Z. L. Flamig, E. M. Argyle, R. A. Clark, A. Arthur, B. R. Smith, J. M. Erlingis, S. Perfater, and B. Albright, 2017: The HMT Multi-Radar Multi-Sensor Hydro Experiment. *Bulletin of the American Meteorological Society*, **98**, 347–359, doi:10.1175/BAMS-D-15-00283.1.

McGovern, A., K. L. Elmore, D. J. Gagne, II, S. E. Haupt, C. D. Karstens, R. Lagerquist, T. M. Smith, and J. K. Williams, 2017: Using artificial intelligence to improve real-time decision making for high-impact weather. *Bulletin of the American Meteorological Society,* Early Online Release. https://doi.org/10.1175/BAMS-D-16-0123.1.

Melnikov, V. M., 2017: Parameters of Cloud Ice Particles Retrieved from Radar Data. *Journal of Atmospheric and Oceanic Technology*, **34**, 717–728, doi:10.1175/JTECH-D-16-0123.1.

Mirmozafari, M., G. Zhang, S. Saeedi, and R. J. Doviak, 2017: A dual-linear polarized highly isolated crossed dipole antenna for MPAR application. *IEEE Antennas and Wireless Propagation Letters*, **16**, 1879-1882. https://doi.org/10.1109/LAWP.2017.2684538.

Terti, G., I. Ruin, S. Anqeutin, and J. J. Gourley, 2017: A situation-based analysis of flash flood fatalities in the United States. *Bulletin of the American Meteorological Society*, **98**, 333–345, doi:10.1175/BAMS-D-15-00276.1.

Warde, D. A., and S. M. Torres, 2017: Staggered-PRT Sequences for Doppler Weather Radars. Part II: Ground Clutter Mitigation on the NEXRAD Network Using the CLEAN-AP Filter. *Journal of Atmospheric and Oceanic Technology*, **34**, 703–716, doi:10.1175/JTECH-D-16-0072.1.

April 2017

Biederman, J. A., R. L. Scott, T. W. Bell, D. R. Bowling, S. Dore, J. Garatuza-Payan, T. Kolb, P. Krishnan, D. J. Krofcheck, M. E. Litvak, G. E. Maurer, T. P. Meyers, W. C. Oechel, S. A. Papuga, G. E. Ponce-Campos, J. C. Rodriguez, W. K. Smith, R. Vargas, C. J. Watts, E. A. Yepez, and M. L. Goulden, 2017: CO_2 exchange and evapotranspiration across dryland ecosystems of southwestern North America. Wiley Online in *Global Change Biology* 1-8. doi:org/10.1111/gcb.13686.

Burg, T., K. L. Elmore, and H. Grams, 2017: Assessing the Skill of Updated Precipitation-Type Diagnostics for the Rapid Refresh with mPING. *Weather and Forecasting*, **32**, 725–732. https://doi.org/10.1175/WAF-D-16-0132.1.

Ivić, I. R., 2017: Phase code to mitigate the copolar correlation coefficient bias in PPAR weather radar. *IEEE Transactions on Geoscience and Remote Sensing*, **55**, 2144–2166. https://doi.org/10.1109/TGRS.2016.2637720.

Kaltenboeck, R., and A. Ryzhkov, 2017: A freezing rain storm explored with a C-band polarimetric weather radar using the QVP methodology. *Meteorologische Zeitschrift*, **26**, 207–222. https://dx.doi.org/10.1127/metz/2016/0807.

Kochendorfer, J., R. Rasmussen, M. Wolff, B. Baker, M. E. Hall, T. Meyers, S. Landolt, A. Jachcik, K. Isaksen, R. Brækkan, and R. Leeper, 2017: The quantification and correction of wind-induced precipitation measurement errors. *Hydrology and Earth System Sciences*, **21**, 1973-1989, doi:org/10.5194/hess-21-1973-2017.

Peppler, R. A., 2017: "It's not balancing out like it should be." Perceptions of local climate variability in Native Oklahoma. *Weather, Climate, and Society*, **9**, 317-329. https://doi.org/10.1175/WCAS-D-16-0081.1.

Tromel, S., A. Ryzhkov, T. Bick, K. Muhlbauer, and C. Simmer, 2017: Towards nowcasting of winter precipitation: The Black Ice event in Berlin 2014. *Meteorologische Zeitschrift*, **26**, 147–160. https://dx.doi.org/10.1127/metz/2016/0778.

Wang, Y. and X. Wang, 2017: Direct Assimilation of Radar Reflectivity without Tangent Linear and Adjoint of the Nonlinear Observation Operator in GSI-Based EnVar System: Methodology and Experiment with the 8 May 2003 Oklahoma City Tornadic Supercell. *Monthly Weather Review*, **145**, 1447-1471. https://doi.org/10.1175/MWR-D-16-0231.1.

Xu, Q., and K. Nai, 2017: Mesocyclone-targeted Doppler velocity dealiasing. *Journal of Atmospheric and Oceanic Technology*, **34**, 841–853. https://doi.org/10.1175/JTECH-D-16-0170.1.

May 2017

Bukovčić, P., Z. Dušan, and G. Zhang, 2017: Winter Precipitation Liquid-Ice Phase Transitions Revealed with Polarimetric Radar and 2DVD Observations in Central Oklahoma. *Journal of Applied Meteorology and Climatology*, **56**, 1345-1363. https://doi.org/10.1175/JAMC-D-16-0239.1.

Fridlind, A., X. Li, D. Wu, M. van Lier-Walqui, A. Ackerman, W. Tao, G. McFarquhar, W. Wu, X. Dong, J. Wang, A. Ryzhkov, P. Zhang, M. Poellot, A. Neumann, and J. Tomlinson, 2017: Derivation of aerosol profiles for MC3E convection studies and use in simulations of the 20 May squall line case. *Atmospheric Chemistry and Physics*, **17**, 5947–5972. doi:10.5194/acp-17-5947-2017.

Kain, J. S., S. Willington, A. J. Clark, S. J. Weiss, I. L. Jirak, M. C. Coniglio, N. M. Roberts, C. D. Karstens, J. M. Wilkinson, K. H. Knopfmeier, H. W. Lean, L. Ellam, K. Hanley, R. North, and D. Suri, 2017: Collaborative Efforts between the United States and United Kingdom to Advance Prediction of High-Impact Weather. *Bulletin of the American Meteorological Society*, **98**, 937–948, doi:10.1175/BAMS-D-15-00199.1.

Kingfield, D. M., K. M. Calhoun, and K. M. de Beurs, 2017: Antenna structures and cloud-to-ground lightning location:1995–2015. *Geophysical Research Letters*, **44**, 5203–5212, doi:10.1002/2017GL073449.

Nelson, A. J., S. Koloutsou-Vakakis, M. J. Rood, L. Myles, C. Lehmann, C. Bernacchi, S. Balasubramanian, E, Joo, M. Heuer, M. Vieira-Filho, and J. Lin, 2017. Season-long ammonia flux measurements above fertilized corn in central Illinois, USA, using relaxed eddy accumulation. *Agricultural and Forest Meteorology*, **239**, 202-212. http://dx.doi.org/10.1016/j.agrformet.2017.03.010.

Qi, Y., and J. Zhang, 2017: A Physically Based Two-Dimensional Seamless Reflectivity Mosaic for Radar QPE in the MRMS System. *Journal of Hydrometeorology*, **18**, 1327-1340. https://doi.org/10.1175/JHM-D-16-0197.1.

Saeidi-Manesh, H., and G. Zhang, 2017: Cross-polarization suppression in cylindrical array antenna. *IET Electronics Letters*, **53**, 577-578. doi:org/10.1049/el.2017.0439.

June 2017

Fierro, A. O., and E. R. Mansell, 2017: Electrification and lightning in idealized simulations of a hurricane-like vortex subject to wind shear and sea surface temperature cooling. *Journal of the Atmospheric Sciences,* **74**, 2023-2041. doi:org/10.1175/JAS-D-16-0270.1.

Lang, T. J., S. Pédeboy, W. Rison, R. S. Cerveny, J. Montanyà, S. Chauzy, D. R. MacGorman, R. L. Holle, E. E. Ávila, Y. Zhang, G. Carbin, E. R. Mansell, Y. Kuleshov, T. C. Peterson, M. Brunet, F. Driouech, and D. Krahenbuhl, 2017: WMO World Record Lightning Extremes: Longest reported flash distance and longest reported flash duration. *Bulletin of the American Meteorological Society,* **98**, 1153-1168. https://doi.org/10.1175/BAMS-D-16-0061.1.

Ryzhkov, A., S. Matrosov, V. Melnikov, D. Zrnic, P. Zhang, Q. Cao, M. Knight, C. Simmer, and S. Troemel, 2017: Estimation of depolarization ratio using weather radars with simultaneous transmission / reception. *Journal of Applied Meteorology and Climatology*, **56**, 1797–1816. https://doi.org/10.1175/JAMC-D-16-0098.1.

Snyder, J. C., H. B. Bluestein, D. T. Dawson, and Y. Jung, 2017: Simulations of polarimetric, X-band radar signatures in supercells. Part I: Description of experiment and simulated ρhv rings. *Journal of Applied Meteorology and Climatology*, **56**, 1977–1999, doi:10.1175/JAMC-D-16-0138.1.

Snyder, J. C., H. B. Bluestein, D. T. Dawson, and Y. Jung, 2017: Simulations of polarimetric, X-band radar signatures in supercells. Part II: ZDR columns and rings and KDP columns. *Journal of Applied Meteorology and Climatology*, **56**, 2001–2026, doi:10.1175/JAMC-D-16-0139.1.

Torres, S., C. Curtis, and D. Schvartzman, 2017: Requirement-Driven Design of Pulse Compression Waveforms for Weather Radars. *Journal of Atmospheric and Oceanic Technology*, **34**, 1351–1369, doi:10.1175/JTECH-D-16-0231.1.

Wen, Y., P. Kirstetter, J. Gourley, Y. Hong, A. Behrangi, and Z. Flamig, 2017: Evaluation of MRMS Snowfall Products over the Western United States. *Journal of Hydrometeorology*, **18**, 1707-1713. https://doi.org/10.1175/JHM-D-16-0266.1.

Reported in the Text as Work Conducted during the FY but Published Just After the FY

July 2017

Li Y., K. E. Pickering, D. Allen, M. C. Barth, M. M. Bela, K. A. Cummings, L. Carey, R. Mecikalski, A. O. Fierro, T. Campos, A. Weinheimer, T. Ryerson and G. S. Diskin, 2017: Evaluation of deep convective transport in storms of different scales during the DC3 field campaign using WRF-Chem with lightning data assimilation. *Journal of Geophysical Research-Atmospheres*, **122**, doi:10.1002/2017JD026461.

Melnikov, V, and D. Zrnic, 2017: Observations of Convective thermals with weather radar. *Journal of Atmospheric and Oceanic Technol*ogy, **34**, 1585-1590. doi:org/10.1175/JTECH-D-17-0068.1.

Sayres, D. S., R. Dobosy, C. Healy, E. Dumas, J. Kochendorfer, J. Munster, J. Wilkerson, B. Baker, and J. Anderson, 2017: Arctic regional methane fluxes by ecotope as derived using eddy covariance from a low-flying aircraft. *Atmospheric Chemistry and Physics*, **17**, https://doi.org/10.5194/acp-2016-862.

Saeidi-Manesh, H., M. Mirmozafari, G. Zhang, 2017: Low cross-polarisation high-isolation frequency scanning aperture coupled microstrip patch antenna array with matched dual-polarisation radiation patterns. *Electronics Letters*, **53**, 901-902. doi:org/10.1049/el.2017.1282.

August 2017

Dobosy, R., D. Sayres, C. Healy, E. Dumas, M. Heuer**,** J. Kochendorfer, B. Baker, and J. Anderson, 2017: Estimating random uncertainty in airborne flux measurements over Alaskan tundra: Update on the Flux Fragment Method. *Journal of Atmospheric and Oceanic Technology*, Early Online Release, doi.org/10.1175/JTECH-D-16-0187.1.

Gallo, B. T., A. J. Clark, I. Jirak, J. S. Kain, S. J. Weiss, M. Coniglio, K. Knopfmeier, J. Correia Jr., C. J. Melick, C. D. Karstens, E. Iver, A. R. Dean, M. Xue, F. Kong, Y. Jung, F. Shen, K. W. Thomas, K. Brewster, D. Stratman, G. W. Carbin, W. Line, R. Adams-Selin, and S. Willington, 2017: Breaking New Ground in Severe Weather Prediction: The 2015 NOAA/Hazardous Weather Testbe**d** Spring Forecasting Experiment. *Weather and Forecasting,* **32,** 1541-1568. https://doi.org/10.1175/WAF-D-16-0178.1**.**

North, K. W., M. Oue, P. Kollias, S. M. Collis, S. E. Giangrande, and C. K. Potvin, 2017: Vertical air motion retrievals in deep convective clouds using the ARM scanning radar network in Oklahoma during MC3E. *Atmospheric Measurement Technology,* **10**, 2785-2806. https://doi.org/10.5194/amt-10-2785-2017, 2017.

Supinie, T. A., N. Yussouf, Y. Jung, M. Xue, J. Cheng, and S. Wang, 2017: Comparison of the analyses and forecasts of a tornadic supercell storm from assimilating phased-array radar and WSR-88D observations. *Weather and Forecasting*, **32**, 1379-1401. doi:org/10.1175/WAF-D-16-0159.1.

Warde, D. A., and S. M. Torres, 2017: Spectrum Width Estimation Using Matched Autocorrelations. *IEEE GRSL*, 1-4. https://doi.org/10.1109/LGRS.2017.2726898.

September 2017

Jones, T. A., and C. Nixon 2017: Short-term forecasts of left-moving supercells from an experimental Warn-on-Forecast system. *Journal of Operational Meteorology*, **5**, 151-160. http://nwafiles.nwas.org/jom/articles/2017/2017-JOM13/2017-JOM13.pdf.

Appendix E

NOAA COMPETITIVE AWARD RECIPIENT REPORTS

and

NOAA HURRICANE SANDY COMPETITIVE AWARD RECIPIENT REPORTS

These reports are presented in the format provided by the respective PIs directly to their NOAA Program Managers. ***They appear in a separate document.***